



Università degli Studi di Milano  
Facoltà di Scienze Matematiche, Fisiche e Naturali  
Dipartimento di Chimica Inorganica, Metallorganica e Analitica "L. Malatesta"

DOCTORATE SCHOOL IN CHEMICAL SCIENCES AND TECHNOLOGIES  
PhD course - CHEMICAL SCIENCES (XXIV cycle)

DOCTORAL THESIS

**MULTIANALYTICAL APPROACH  
FOR THE STUDY OF  
BRONZE AND GILDED BRONZE ARTEFACTS**

CHIM/01 - CHIM/12

Doctoral candidate:  
Laura BRAMBILLA  
R08426

Tutor:  
Dr. Paola Fermo

Co-tutor:  
Dr. Sara Goidanich

PhD course coordinator:  
Prof. Silvia Ardizzone

Doctorate school director:  
Prof. Franco Cozzi

Academic Year 2010/2011

*A mia madre Lietta e a mio fratello  
Andrea che mi hanno sempre sostenuta*

*A mio padre Luciano che da lassù mi  
ha sempre guidata e che sarebbe stato  
molto orgoglioso di questo risultato*

*To Christophe, for his support,  
help... and love*

*Più di ogni altro elemento antico, l'oro è sempre stato associato ad un fascino senza tempo.  
Nessuno degli elementi scoperti dalla scienza moderna è stato in grado di sfidare la sua supremazia.*

*Il rame è l'unico metallo rosso, cosa che lo pone in una relazione particolare con l'oro, l'unico altro  
metallo colorato.*

*Hugh Aldersey-William, Favole Periodiche*

*Per me si va nella città dolente,  
per me si va nell'eterno dolore,  
per me si va tra la perduta gente.  
Giustizia mosse il mio alto fattore:  
fecemi la divina potestate,  
la somma sapienza e 'l primo amore.  
Dinanzi a me non fuor cose create  
se non eterne, e io eterno duro.  
Lasciate ogni speranza voi ch'entrate.*

*Dante Alighieri, Divina Commedia- Inferno*

# Table of the contents

Abstract

## 1. State of the art

### 1.1 Gilding techniques

1.1.1 Gold foil and gold leaf

1.1.2 Fire gilding and mercury gilding

### 1.2 Patinas

1.2.1 Natural patinas

1.2.1.1 Atmospheric corrosion

1.2.1.2 Corrosion in soil

1.2.1.3 Marine corrosion

1.2.2 Artificial patinas

1.2.2.1 Techniques of patination

### 1.3 First approaches to the monitoring of gilded bronzes

1.3.1 Development of galvanic sensors in the 70's

1.3.2 Application of galvanic sensors to the study of the "Porta del Paradiso" in the 70's

### 1.4 Case study: the Porta del Paradiso by Lorenzo Ghiberti

1.4.1 Restoration and conservation intervention

1.4.2 Diagnostic campaign of the 80's

1.4.3 Degradation mechanisms

1.4.4 The last restoration

## 2. Aims of the thesis

## 3. Experimental

### 3.1 Preparation of artificial patinas

3.1.1 Chemical patination

3.1.1.1 Cuprite patina

3.1.1.2 Atacamite patina

3.1.1.3 Brochantite

3.1.2 Electrochemical patination

3.1.2.1 Beldjoudi – Constantinides method

3.1.2.2 Vernon method

3.1.3 Applied paste

### 3.2 Analytical techniques for the characterization of patinas

### 3.3 Accelerate electrochemical artificial ageing of gilded bronze specimens

3.3.1 Bronze alloy replica of the Baptistery doors

3.3.2 Gilding replica

3.3.3 Realization of the artificial patina

3.3.3.1 The electrochemical method

### 3.4 Preparation of galvanic sensors

3.4.1 The sensor for the Porta del Paradiso

3.4.2 Gold leaf sensors: chlorides rich patina

3.4.2.1 Set up of the gold leaf sensors with chloride rich patina

3.4.3 Gold leaf sensors: brochantite patina

### 3.5 Display conditions for the case study of the “Porta del Paradiso”

3.5.1 Sealed boxes

3.5.2 Open showcase

3.5.3 Thermo-hygro-metric monitoring inside the three showcases

3.5.4 Characterisation of the three sections from the Porta del Paradiso

3.5.5 Monitoring by means of galvanic sensors

## 4. Results and discussion

### 4.1 Accelerate electrochemical artificial ageing of gilded bronzes – Results

4.1.1 Series I

4.1.2 Series II

4.1.3 Series III

4.1.4 Series IV

4.1.5 Series V

4.1.6 Conclusions

### 4.2 The case study of the “Porta del Paradiso”

4.2.1 Closed showcases

4.2.2 Open showcase

4.2.3 Final considerations for the choice of the best display solution

4.2.4 Considerations about the performances of the galvanic sensors realised for the study of the Porta del Paradiso

### 4.3 Evaluation of the performance of the Gold leaf galvanic sensors

4.3.1 Preliminary gold-leaf galvanic sensors with chloride rich patina

4.3.2 Gold leaf sensors with chloride rich and brochantite patina

### 4.4 Characteristic and stability of the patinas

4.4.1 Stability tests on “Gold leaf sensors”

4.4.2 Stability tests on powders of the patinas and of Nantokite

5. Conclusions

Acknowledgements

# Abstract

This work focuses on one of the most common metal alloy used in the field of art: bronze.

Bronze was discovered about 3500 years BC and was used in the antiquity to create tools, weapons, armour, and later coins, medals, sculptures and other works of art. Bronze objects were harder and more durable than stone or copper ones and easier to work than the iron ones. These characteristics contributed to render bronze a material largely widespread through millenniums.

Of great interest are also the colourings that outdoor bronze exhibit. In fact, when exposed to atmosphere, copper and its alloys form a thin layer of corrosion products, called patina. The naturally formed patinas have different colours depending on the surrounding environment and its chemical composition: urban, rural, marine. A patina on a bronze artwork not only protects the metallic substrate, but also enhances the aesthetic of the artistic objects. Coloured patinas form spontaneously on copper alloys by very slow controlled corrosion either in the presence of moisture, carbon dioxide, and oxygen, or other chemical species present in the atmosphere. Patinas may also be created artificially by artists for aesthetic and protective reasons. Investigation of the corrosion behaviour of copper patinas is of utmost importance for understanding the atmospheric deterioration of bronze monuments as well as objects of cultural heritage. During this work, a multidisciplinary approach has been applied in order to thoroughly understand the degradation mechanisms of the patinas of corrosion products that naturally form over bronzes surface. Particular attention has been paid to the transformations connected to relative humidity variations.

To further adorn and make more precious the artefacts, bronze statue were also gilded. The gilding of a bronze statue allows to obtain an object that has the same aspect of a statue made of pure gold, but that is less expensive and simultaneously presents certain resistance characteristics. Examples of gilded bronze artworks can be found in the Italian artistic patrimony, such as, for example, the horses of St. Mark in Venice, the statue of Marcus Aurelius in Rome and the Porta del Paradiso, the eastern portal of the Baptistery in Florence.

The latter has been the starting point of this work. This important gilded bronze of the Italian Renaissance was damaged during the flood that devastated Florence in 1966 and since then a long process of restoration and characterization of the artwork started and it is still going on.

The study of gilded bronze artworks is a difficult topic in the field of cultural heritage due to the complex structure (tri-layer) of the material. The structure, in fact, is composed by a metallic substrate (bronze), the gold and, between the two metals, a layer of corrosion products formed during time as a consequence of degradation processes. The presence of hygroscopic salts between

the gilding and the bronze may lead to the detachment of the gold layer as a consequence of volume variation related to changes in the crystalline forms of the copper salts composing the patina.

At the beginning of this work, the “Porta del Paradiso” was at the last stage of a long process of restoration carried out by the Opificio delle Pietre Dure and the door was almost ready to be finally unveiled to the public. At that stage of the research it was necessary to identify the best exposure option for this precious and unfortunately very unstable masterpiece of the Renaissance. The optimal display option for the “Porta del Paradiso” had to take into account two important factors: first, it was necessary to choose an environment that could assure the best preservation condition for the restored artwork and therefore able to block corrosion; second, a solution that could provide an enjoyable viewing experience for the public was also expected.

To fulfil these requirements, three different showcases were tested: a) a closed showcase purged by nitrogen; b) a closed showcase with low and controlled relative humidity; c) an open showcase with controlled microclimate that should create the same local environmental conditions as the showcase with low RH, with the big advantage of avoiding a glass panel between the object and the visitor.

To evaluate the resulting conditions of conservation imposed by the three different showcases, qualitative and quantitative studies were necessary. Unfortunately the techniques commonly used to obtain quantitative data regarding corrosion phenomenon from metallic artefacts (i.e. polarization resistance and electrochemical impedance spectroscopy) are not suitable for bimetallic artefacts such as the “Porta del Paradiso”.

Initially some replicas of the “Porta del Paradiso”, with the same bronze alloy and the same gilding technique of the door, were produced by the OPD. It was then necessary to age these samples in order to obtain a system that reproduces the actual condition of the artwork. For this reason a new methodology was developed during this work for the electrochemical artificial ageing of gilded bronze specimens. Unfortunately, due to the unavoidable short circuit between gold and bronze, these aged samples were not suitable to obtain quantitative data concerning the corrosion rate of the door. An alternative solution appeared to be the realisation of galvanic sensors, used as replicas of corroded gilded bronzes, that were developed and used to measure the macrocouple current of the system “Bronze-Patina-Gold”, that is directly correlated to the corrosion rate by Faraday’s law.

The most critical steps during the development of the galvanic sensors are: a) the preparation of an artificial patina of corrosion products and b) the gilding methodology. The realisation of an artificial patina proved to be a very crucial point, because the patina has to fulfil a series of important and specific requirements, such as: 1 – composition similar to the real cases, 2 – adequate thickness, 3 – good homogeneity, 4 – good adhesion to the substrate, 5 – adequate electrical resistance.



The main constituents of natural patinas have been identified after a thorough literature review. Then a procedure for the realisation of artificial patinas with similar composition was developed. Different kind of patination techniques available in literature (such as chemical and electrochemical patination) have been tested to obtain the artificial layer of corrosion products. Unfortunately none of them allowed to obtain a patina with all the required characteristics. A new methodology was then developed for the patina used to realise the galvanic sensors. This method is inspired by the so-called “applied paste” and consists in spreading on the metallic surface a specific mixture of copper salts and water. This procedure allows to control precisely all the parameters previously mentioned.

Concerning the second critical step, i.e. the gilding procedure, two different methodologies have been tested: sputtering and gold leaf application. The best one revealed to be the application of a gold leaf.

A first set of galvanic sensors was realised and used for the solution of the “Porta del Paradiso” case. In that occasion they proved to be a very powerful tool and allowed the identification of the best display option for the doors. However these sensors presented some evident problems of durability and reproducibility. The methodology of preparations of the galvanic sensors has subsequently been completely revised and improved leading to the obtainment of new galvanic sensors, named “gold leaf galvanic sensors”, that proved to be much more durable and reproducible. The galvanic sensors can be used both for monitoring the corrosion rate of real objects and for testing new conservation or cleaning procedures.

---

STATE OF THE ART

## 1.1 Gilding techniques

With the term *gilding* it's usually indicated the covering –with the application of a gold layer – of a less precious material surface. In the various examples of gilding that can be found from the antiquity there are substrates of metals, but also wood and stones. As gold was always considered a precious material, the thickness of the gold layer has been lowered with technological progress in centuries, with the aim to economize this precious metal. The first gilded objects that are known, were created around 3000 BC in Mesopotamia [1] where the thick gold foil is held in its position by mechanical fixing. The invention of gilding by means of a gold leaf fixed with an adhesive or heated, to induce interdiffusion, was developed in the Middle East about 1000 years later, and then slowly spread to the Mediterranean and the Far East [2]. During the 4<sup>th</sup> century BC the Chinese discovered the fire gilding method that consist in the preparation of an amalgam of mercury and gold, deposited on the surface of the object and then heated to allow the evaporation of the mercury. It is not sure yet when this technique reached the Roman Empire, but once adopted it remained the most commonly used technique until the invention of the electroplating in the 19<sup>th</sup> century [1].

Concerning the gilding of metals, gold is usually applied to copper, silver and their alloys. Among these an important role is given to bronze, especially for the case of large statuary works, as some well-known Italian artworks such as the Horses of the St Mark's Basilica in Venice, the Marcus Aurelius and Hercules in Rome and the Porta del Paradiso of the Baptistery in Florence (Figures 1) [3-6].



**Figure 1: Porta del Paradiso in Florence, example of gilded bronze artwork (left). Particular of Miriam's Frieze (a) and Noah's panel.**

Several techniques for gilding, which lead to very different results especially in terms of conservation, have been developed within millenniums. It is important to note that different gilding techniques lead to different defects of the surface, and if the gold layer is not uniformly continuous and efficiently adherent its protective action against corrosion of the substrate is lacking. With the evolution of different techniques the thickness of the gold layer passed from the fractions of millimeters of the gold leaf to the nanometers scale of the modern techniques.

### **1.1.1 Gold foil and gold leaf**

The first gilding technique developed was the use of gold foil: in this method a consistent layer of gold that is called “foil” is placed around the object and held in its position by folding it over the edges of the object or into some specifically designed grooves on the surface, or again with the help of some rivets. This technique is based not on the use of a physical or chemical bond between the gold foil and the substrate, but merely on the mechanical effect. The use of mechanical forces was the first technical solution developed, as it was the easiest to realize [2].

Some variations of these techniques can be found in literature. In the case of the gold foil, for example, when the object is completely covered by gold, the overlapping edges of the foil can be burnished together, as in some objects of the Oxus treasure [7]. On the contrary the insertion of gold foil edges into grooves, although described by Pliny, concerning the statue of Alexander the Great that emperor Nero decided to cover with gold [8], has not been found very often and only some examples are known, such as the statue of Karomama at the Louvre museum [9].

#### *The production of the gold leaf*

The natural evolution of the foil gilding appeared when the processes were precise enough to allow the production of thinner layers, called gold “leaves”. In this case the gold layer has a dimensional order thinner than the tens of microns. For this reason it cannot oppose to any mechanical force applied, not even to its own weight. To prepare gold leaves, a prerequisite was the competence to hammer gold in very thin layers.

Thus, achieving thinner layers relies on a technique called “gold-beating”; an improved implementation of simple hammering. It consists in hammering a so-called “cutch” (superimposed sheets) of alternated gold and another material, “the goldbeater’s skin”. The latter, being used to avoid plastic unification of gold, was originally made of calf’s intestine, material selected for its elasticity.

Using gold leaves present the advantage not only of requiring less raw material, but also of allowing a better fitting to the shape of the coated parts, thus exhibiting more details of the original surface.

Additionally, adherence to the substrate is also a key issue that is improved by applying gold leaves. However, a major drawback of this method resides in the fact that in order to obtain a drastic reduction of the thickness it is necessary to increase the purity of the gold used.

In literature, there is not only one definition of “gold leaf”. On the one side, considering exclusively the thickness parameter, the gold leaf can be defined as a gold layer thinner than one micron [10]. On the other side, a “mechanical” approach can be used, considering that a leaf can be defined as a layer that cannot oppose any resistance to tangential flexion not even to its own weight [11]. Another definition, based on the process used to produce the thin layers, i.e. the beating of multilayers gold sheets samples to achieve the thickness of interest, might be relevant as well.

### *The fixation of the gold leaf*

A mechanical fixing of gold leaves cannot obviously be considered, whatever the substrate, due to the very small thickness of the gold layer. This issue led the ancient Egyptian manufacturers to develop a technique based on the application of an adhesive to fix the gold leaf to different supports (wood, stone and even bronze, sometimes) prepared with ground<sup>1</sup> [11].

The technique used for fixing the leaves most probably varied depending on period, location and even manufacturer. Oddy [11] and Eluere [12] propose that the adhesive could be the white of an egg as mentioned by Pliny [8]. Additionally, it was proposed that the gilding “adhesive” could be also applied directly on the surface of the substrate, as observed typically in the case of the coating of bronzes.

Another important technique developed to fix gold leaves, mainly on silver substrates is the so-called “interdiffusion” or “diffusion bonding” [1]. The method relies on the heating of the gold applied directly on the surface: the energy transferred by heat to the metal accelerates sufficiently the interdiffusion to make it suitable for a fabrication process.

Whereas this method is relevant for gold-silver and gold-copper interfaces, as these metal systems are known to be highly soluble in solid state, some doubts are still persisting concerning the feasibility with bronzes and other alloys [11]. Indeed, a rough calculation leads to a required temperature higher than 500-600°C for accelerated interdiffusion to occur. This temperature does not sound realistic for finished and shaped bronze statues and, as Vittori [13] suggests, the existence itself of this method has to be confirmed with experimental evidence.

---

<sup>1</sup>The ground is a preparatory layer, mainly composed of gypsum or calcite mixed with an organic adhesive (possibly animal glue) [1].

### **1.1.1.2 Fire gilding and cold mercury gilding**

Fire gilding, i.e. the mercury-gold amalgam process, is one of the progresses of utmost importance made in the ancient times concerning gilding. The method is based on a spreading–evaporation process of a Mercury–Gold mixture [11]. First the amalgam is spread on the surface to be gilded, and then an external heat source is used to evaporate the mercury, thus allowing the formation of really thin gold layers. Thicker layers may be produced using an overlaying procedure.

Main drawbacks of the fire-gilding technique are the high porosity of the coating, due to the evaporation process, as well as the presence in the film of remaining mercury. The presence of unevaporated mercury, nevertheless, allows an easy identification of this process when used.

This technique was most probably elaborated in China during the Warring States period (468 – 221 BC) before spreading towards west, reaching the Roman civilization around the 1st century BC. For example, Vitruvius (I BC), as well as Pliny (I AD), both mention mercury while describing the gilding of copper alloys and silver [11].

The method became widely used in the 2nd century AD, and, from then on, remained the predominant method during the whole Middle Age [1].

Surprisingly, Pliny mentions the role of mercury as an adhesive. On one hand, even if the description made in *Naturalis Historiae* is very precise, it has been admitted that Pliny could have misunderstood the role of mercury in the gilding process, as he was neither an artisan nor an expert in the domain [11]. On the other hand, one may also consider the existence of an additional technique in which mercury could actually be used in the role of adhesive [14]. This technique would then be based on the preliminary spreading of a thin layer of mercury before the application of a gold leaf. The mercury evaporate spontaneously in the days following the coating, without requirement for any special heat treatment. Therefore, this alternative method is called “Cold Mercury Gilding”, however it is not proven to be the one used by the Romans. This technique is used nowadays for the gilding of copper domes on the Bavarian churches [2].

More recently, in other geographical areas, other gilding techniques were developed, such as depletion gilding in South America (not tackled in the present work) as well as electrochemical gilding in the XIX century. Electrochemical gilding, also known as immersion or replacement gilding, involves immersion of the copper or the silver in a solution containing a soluble salt of gold. An electrolytic reaction takes place at the surface of the base metal, which undergoes simultaneous anodic dissolution and deposition of gold. This technique will only deposit a very thin layer of gold because as soon as the base metal is completely covered the process stop [11].

## References

- [1] A. Oddy, **Gilding of metals in the Old World**, in “Metal Plating and Patination”, Butterworth Heinemann, 1993
- [2] A. Oddy, **Gilding through the ages**, *Gold Bulletin*, 14, 2 (1981), 75–79
- [3] M. Marabelli, **The monument of Marcus Aurelius: Research and conservation**, in *Ancient & Historic Metals*, 1991, 1–19
- [4] V. Alunno-Rossetti, M. Marabelli, **Analyses of the patinas of a gilded horse of St. Mark’s Basilica in Venice: Corrosion, Mechanisms and Conservation Problems**, *Studies in Conservation* 21, 4 (1976), 161–170
- [5] A. Giusti, M. Matteini, **The gilded bronze Paradise Doors by Ghiberti in the Florence Baptistery – Scientific investigation and problems of restoration**, *Proceedings of the International Conference on Metal Restoration*, German National Committee of ICOMOS, Munich, 1997, 47–51
- [6] G. Alessandrini, G. Dassù, P. Pedeferra, G. Re, **On the conservation of the baptistery doors in Florence**, *Studies in Conservation*, 24 (1979), 108–124
- [7] O.M. Dalton, **The treasure of Oxus**, British Museum, London, 1964
- [8] Pliny, **Natural History**, Rackham 1968, vol 9
- [9] E. Delange, M.E. Meyohas, M. Aucouturier, **The statue of Karomama, a testimony of the skill of Egyptian metallurgists in polychrome bronze statuary**, *Journal of Cultural Heritage* 6 (2005) 99–113
- [10] Lechtman K.N., **Ancient methods of gilding silver: examples from the Old and New Worlds**, *Science and archaeology*, 1973
- [11] A. Oddy, **A history of gilding with particular reference to statuary**, in “Gilded metals: history, technology and conservation”, London, Archetype, 2000
- [12] C. Eluere, **Les secrets de l’or antique**, La Bibliotheque des Arts, 1989
- [13] O. Vittori, **Interpreting Pliny’s gilding: archeological implications**, *Rivista di Archeologia* 2 (1978), 71–81,
- [14] A. Oddy, **The gilding of Roman silver plate**, in “Argenterie Romaine et Byzantine”, de Boccard, Paris, 1988

## 1.2 Patinas

When exposed to the Earth's atmosphere, copper and its alloys react with oxygen to form a thin layer of corrosion products that is named patina. For this reason the bronze artefacts of cultural heritage are often covered with a patina which confers, and often enhances, their aesthetic as well as protects the metallic substrate. For example, it is well known coloured patinas form spontaneously on copper alloys by very slow controlled corrosion either in the presence of moisture, carbon dioxide, and oxygen, or in seawater [1].

The term patina is a word commonly used that can have different meaning and it could refer not exclusively to metals. The Webster dictionary define the term patina, concerning the formation over a metallic substrate as “a thin usually green film that forms naturally on copper and bronze by exposure to the air for a long time or artificially and often valued aesthetically for its colour” [2]

Thus, it is not an easy task to define exactly the term “patina”, nevertheless in this work, the term patina will be used to describe both naturally and artificially formed layers of corrosion compounds on copper alloys.

Unlike most metal corrosion phenomena, the formation of a coloured surface on bronze due to atmospheric chemical composition is regarded as an attractive feature. As above-mentioned such colorations on bronze and other metals are termed “patinas” [3-5].

Since antiquity, the copper patinas have always given rise to great interest. Plutarch already mentioned it in *Moralia*, about some statues of the Temple of Apollo in Delphi (Greece) that are covered by a polish layer of bright blue compact patina [6, 7].

The importance attributed to the patinas derived mostly from the particularity of copper to react with atmospheric agents. Different environmental conditions, generally, forming corrosion products of various colour and appearance. This led the men since antiquity to address the problem of creating artificial patinas, aesthetically pleasing as well as able to preserve the statues and artefacts from corrosion.

The main constituents of “alteration layers” on bronze, reported in the literature, are copper based compounds. As a consequence, bronze patinas have often been thought to be very similar to pure copper patinas. In the case of a Cu-Sn alloy, it is generally admitted that the surface layer consists of copper (II) salts, e.g. malachite (in soil) as well as brochantite (in the atmosphere) or atacamite (in seawater), which covers a red cuprous oxide layer that is in contact with the metal core [8].

Patinas of copper corrosion products can also be prepared artificially, using different techniques [9], either by the artist to confer particular aesthetic features to an artwork as well as for protective



reasons or by the scientist to study the composition and the behaviour of patinas themselves varying the environmental conditions.

Patinas, alongside their aesthetic interest, may also have precious protective role as mentioned above. But they can also present serious drawbacks and cause destructive phenomena on bronze, on its surface as well as in the bulk material . For example, it is well known that the presence of chloride in patina is the cause of “bronze disease” [1, 10-12].

## **1.2.1 Natural patinas**

The natural patinas generally do not present a smooth and uniform but a rather heterogeneous aspect. The surface is highly porous and this can easily be attributed to their great ability to absorb large amounts of water [13]. Natural patinas form on the metal surface in different way modifying the surrounding environment of the metallic surface of the artefact.

### ***1.2.1.1. Atmospheric corrosion***

Copper and bronze exposed to outdoor environment gradually turn to red-brown. The corrosion layer that is formed will exhibit various shades of green, and possibly black, over longer exposure periods, such as typically 30 to 70 years [3, 14-24].

The earliest studies of patinas were performed in the 19<sup>th</sup> century and led to the conclusion that the patina formed on outdoor copper roofs or bronze statues consisted primarily of copper carbonate. However, at the end of the 19<sup>th</sup> century, accelerated rates of green patina formation were observed in urban and industrial area. These environments presenting an increased concentration of sulphur containing pollutants, copper sulphates were finally suggested to be the main corrosion products [25-27].

The first scientific studies of atmospherically corroded copper were led by W.H.J. Vernon in 1932 [28]. This research included the analysis of various naturally corroded samples as well as the testing of metallic samples by exposing them either to specific concentrations of gases, or to various outdoor atmospheres [28].

Vernon established different steps in the corrosion progress throughout time:

- formation of an initial red brown film of the copper oxide cuprite,
- development of crystals of copper sulphates,
- finally, after several years exposition, stabilization of the green patina on the surface.

The external layer was identified as deposited coarse particles such as soot.

In the few decades after Vernon’s work, the importance of electrochemical reactions in atmospheric corrosion was evidenced. Consequently, electrochemical methods were applied to the study of

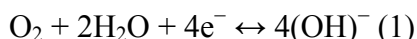
corrosion. However, progress remained limited due to the difficulty to mimic atmospheric exposure conditions in an electrochemical cell.

In the 60's and 70's, the progress in surface sensitive analytical techniques allowed investigating not only corrosion rates, but also relationships between air pollutants and patina characteristics such as morphology and chemical composition. Several corrosion studies were performed between 1980 and 1990, some of them also in the field of cultural heritage. In 1987, on the occasion of the centennial restoration works of the Statue of Liberty in New York Graedel et al. [29] performed the first extensive study of copper patinas, using several surface analysis methods.

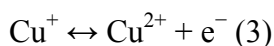
The phenomenon of corrosion due to atmospheric components is complex and several chemical species composing the pollutants are involved. Oxidation is the first process that takes place, as it occurs as soon as the copper metal enters in contact with oxygen. Besides oxygen, various other chemical groups can influence the corrosion, such as, for example,  $S^{2-}$ ,  $SO_4^{2-}$ ,  $Cl^-$ ,  $CO_3^{2-}$ ,  $NO^{-3}$  or  $O_3$ .

- ***Oxidation phenomenon:***

When exposed to a humid atmosphere, a thin water layer acting as an electrolyte, is deposited on the copper surface [10, 30]. The metal becomes oxidized, while the oxygen dissolved in the water is reduced, according to equation 1:



The simultaneous anodic reaction dissolves the metal and cuprous and cupric ions are formed, according to equations 2 and 3, respectively:



Depending on the conditions of potential, and pH, of the surrounding environment of copper, this one can remain in its original metallic state, or be converted into different compounds.

One of these compounds is cuprous oxide or cuprite  $Cu_2O$  [25, 27, 31]. This product may exhibit a wide range of colours, depending on the presence of impurities as well as on particle size. Cuprite is a “good” corrosion product. Indeed, this kind of corrosion layers usually preserve the original shape of the object, thanks to the similarities in the crystal lattice of copper and cuprite [25]. On the

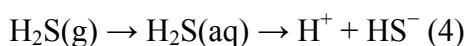
opposite lattice defects make the crystal non stoichiometric and this makes cuprite act as a semiconductor. This characteristic results in the conductivity of the oxide layer and the possibility to transport different anions and cations thus enhancing the corrosion process.

Another corrosion products is cupric oxide, i.e. tenorite (CuO), that is usually dull black. Although tenorite should be stable in the water stability domain, kinetics will limit the mineral's formation to a few specific conditions making tenorite a rare component of natural patinas. As a consequence, when tenorite is present as a patina constituent, it usually indicates that the object has been the subject of additional heating [3, 32].

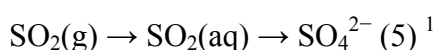
#### - *Presence of Sulphur in the atmosphere*

Sulphur can enter water as a gas (hydrogen sulphide, carbonyl sulphide and sulphur dioxide) or as a solid particle (for example from ammonium sulphate) [29, 30, 33].

On the one hand, carbonyl sulphide is hydrolyzed and forms hydrogen sulphide that is slightly soluble in water. After dissolution into an aqueous surface film, it dissociates, and the resulting HS<sup>-</sup> ions play the role of the active corrosion agent while the formed protons provoke an acidification:



Sulphur dioxide on the other hand is moderately soluble in water so that a significant amount is absorbed into aerosol particles. Dissolved sulphur dioxide oxidizes to bisulphate ions, which are subsequently converted to sulphate ions by ozone or hydrogen peroxide.



If the sulphide concentration is sufficiently important in the aqueous layer, copper sulphides (for example chalcocite Cu<sub>2</sub>S) can be formed. These products are expected to form more easily in reducing, such as marine, environments.

When sulphate ions are present the formation of copper hydroxysulphates can begin. The different steps involved in the formation of these compounds on the surface include dissolution, ion pairing as well as precipitation.

As soon as the copper surface is in contact with moist air, it is hydroxylated [27].

---

<sup>1</sup> Different steps are required to transform aqueous sulphur dioxide in sulphate ions

Copper hydroxide,  $\text{Cu}(\text{OH})_2$ , forms through ion pairing of  $\text{Cu}^{2+}$  and  $(\text{OH})^-$  ions. The ions are produced by cathodic and anodic reactions.

Some of the hydroxyl ligands are replaced by  $\text{SO}_4^{2-}$  ligands and amorphous copper sulphate is formed. This phase is necessary as a transition between the cubic lattice of cuprite and the crystal lattice of copper sulphates, which can be remarkably different (orthorhombic, monoclinic, triclinic, etc.). After a few months of exposure, the solid surface rearranges into one of different possible basic copper sulphates, listed below, depending on the degree of humidity and local sulphur pollution.

A variety of copper sulphates forms more easily through contact of cuprite and sulphate ions [25, 27]. Which compound is most likely to be formed, depends on the relative amounts of sulphate, cupric and hydroxyl ions.

Posnjakite,  $\text{Cu}_4(\text{OH})_6\text{SO}_4 \cdot \text{H}_2\text{O}$ , is formed in the less polluted and relatively dry environments, while langite,  $\text{Cu}_4(\text{OH})_6\text{SO}_4 \cdot 2\text{H}_2\text{O}$ , is most likely to be observed in humid climates.

Both are precursors to the formation of brochantite  $\text{Cu}_4(\text{OH})_6\text{SO}_4$ , which occurs after longer exposure times.

In more polluted, more acidic areas, strandbergite  $\text{Cu}_{2.5}(\text{OH})_3\text{SO}_4 \cdot 2\text{H}_2\text{O}$  will be the intermediate compound preceding the formation of antlerite  $\text{Cu}_3(\text{OH})_4\text{SO}_4$  [25, 27].

All five copper hydroxy sulphates present a structural resemblance. They consist of corrugated planes of copper atoms each surrounded by 6 oxygen atoms. Adjacent planes are held together by sulphate groups, hydrogen bonds and weak copper–oxygen bonds [27].

The structural similarity suggests that one phase can be transformed into another and that the sequence of formation can change from the more to the less sulphur–containing sequence and vice-versa.

Different theories are available in the literature to understand which compounds formation is thermodynamically favoured. According to Pollard and co-workers [34] antlerite is stable at slightly more acidic conditions than brochantite. Similarly, chalcantite will only occur at very low pH values ( $\text{pH} < 4$ ) [34].

In reality, the Earth's atmosphere contains more than one gaseous pollutant [35] and then not only sulphates,  $\text{SO}_4^{2-}$ , but also chloride,  $\text{Cl}^-$ , and carbonate,  $\text{CO}_3^{2-}$ , are present [25]. Consequently, besides copper oxides (cuprite, tenorite) and sulphates (antlerite, brochantite), also carbonates (malachite) and chlorides (nantokite) can be formed.

In order to determine which compound will form, for the sake of scientific study, it is often more easy to work with *stability diagrams* where the concentration of one specific pollutant is plotted as a function of the pH.

These stability diagrams then indicate which compound is the most stable in specific conditions of pH and pollutant concentration. For example one may notice in Figure 1 that antlerite and brochantite form during outdoor exposure in the presence of a large range of sulphate concentrations. Additionally, compared to brochantite, antlerite is stable in a narrower pH domain as well as more acidic conditions [17, 25, 36].

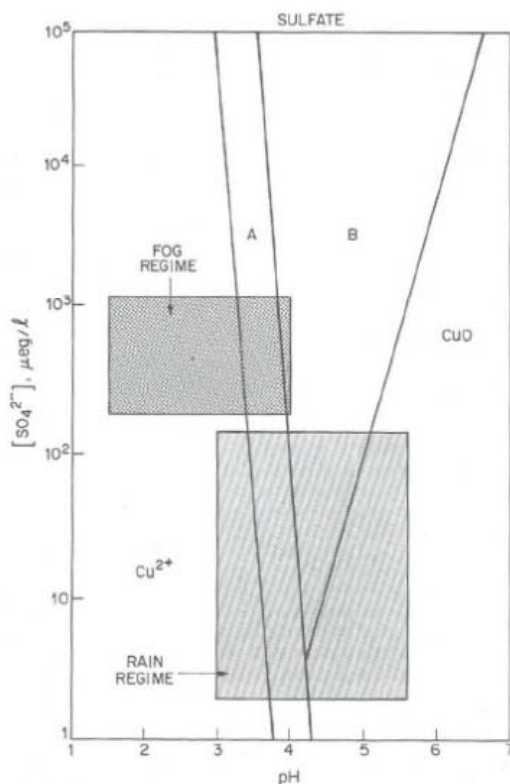
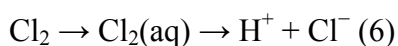


**Figure 1: Stability diagram of the system Cu-SO<sub>4</sub>-H<sub>2</sub>O with fog and rain areas shown for urban atmospheres. A = antlerite stability, B = brochantite stability. Concentration of sulfate (μeq/l) as a function of pH [25]**

Different stability diagrams may be combined when several pollutants are present, in order to express the pH condition in terms of concentration of hydroxyl. The stability of the compounds is represented as a function of two concentrations of influencing elements (e.g. pollutant gases).

**- Presence of Chlorine in the atmosphere**

Chloride ion, Cl<sup>-</sup>, enters the liquid phase through the deposition of sea salt particles, precipitation or by incorporation of gaseous Cl<sub>2</sub>. Gaseous Cl<sub>2</sub> dissolves promptly in atmospheric water droplets and dissociates to form Cl<sup>-</sup> ions in solution, according to reaction 6.



Once chloride ion-the oxidizing agent- is present, it may reach the cuprite oxide layer and dissolve it thus producing cuprous ions [25].  $\text{Cu}^+$  and  $\text{Cl}^-$  ions then combine to form nantokite,  $\text{CuCl}$ , which acts as a seed crystal for the formation of one of the polymorph copper trihydroxy chlorides  $\text{Cu}_2(\text{OH})_3\text{Cl}$ . Atacamite, clinoatacamite as well as botallackite may be formed through many subsequent “dissolution-ion pairing-precipitation” steps. Nantokite,  $\text{CuCl}$ , or one of the polymorphs  $\text{Cu}_2(\text{OH})_3\text{Cl}$  will be the final product, depending on kinetics and thermodynamic conditions.

The stability diagram of a system consisting of  $\text{Cu}-\text{Cl}-\text{H}_2\text{O}$ , Figure 2, shows that atacamite is stable only at  $\text{Cl}^-$  ions concentrations near the maximum of the range of concentrations measurable in rain [25]. Evaporation increase the stability of atacamite, since higher concentrations of  $\text{Cl}^-$  move the system into the stability domain. Atacamite is soluble in weak acids and is consequently not easily found in polluted areas, but it is a common corrosion product by the sea [37-39].

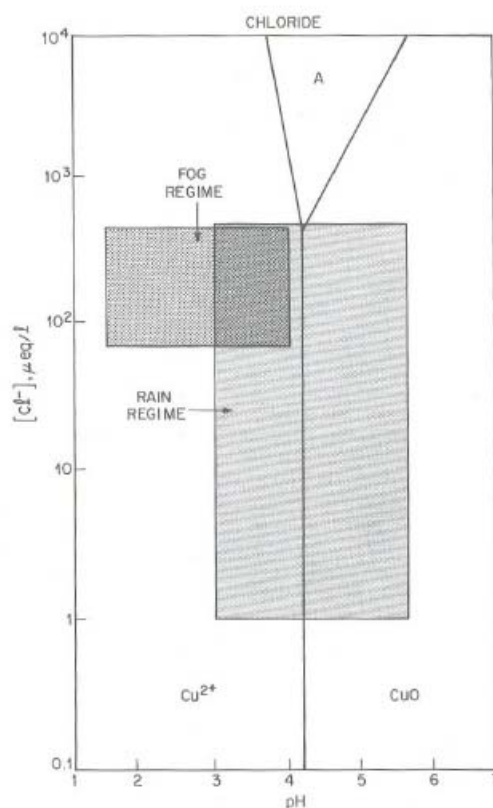


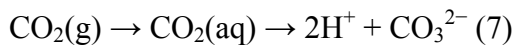
**Figure 2: Stability diagram for the system  $\text{Cu}-\text{Cl}-\text{H}_2\text{O}$ . A indicates the region where atacamite is stable.  $\text{Cl}^-$  ( $\mu\text{eq/l}$ ) concentration as a function of pH. [25]**

Presence of chlorides and more particularly nantokite may lead to bronze disease [25, 40]. This progressive deterioration of copper alloys is probably due to the transformation of nantokite under the influence of humidity and oxygen into one of the copper trihydroxy chlorides. This conversion involves an expansion in volume, which creates physical stress inside the object. As nantokite is

present underneath the cuprite which is in turn covered by other cupric salts, it is often invisible until the expansion results in cracking and/or fragmentation of the object.

- ***Presence of Carbon in the atmosphere***

Carbon dioxide is naturally present in the atmosphere but is also produced by anthropogenic activities [35]. CO<sub>2</sub> is weakly soluble in water and may be readily absorbed by a surface water layer. A portion of the dissolved gas transforms into the carbonate ion CO<sub>3</sub><sup>2-</sup> and protons H<sup>+</sup> according to equation 7:



Other sources of carbon species present in the atmosphere as well as in precipitations, such as aldehydes and organic acids, lead to the formation of copper oxalates [35].

Although the formation of malachite Cu<sub>2</sub>(OH)<sub>2</sub>CO<sub>3</sub> has to be the predominant in the stability domain of water, the concentrations of dissolved gaseous CO<sub>2</sub> (of about 300-600 ppmv – parts per million volume ) are too low for malachite to be stable in atmospheric system [25, 31].

- ***Presence of Nitrogen in the atmosphere***

The normal concentrations of NO<sub>2</sub> in the atmosphere (150-300 ppbv – parts per billion volume) are too low for copper nitrates such as gerhardtite Cu<sub>2</sub>(OH)<sub>3</sub>NO<sub>3</sub> to form [25, 31].

However, NO<sub>2</sub> is considered to be an important oxidizing agent, considerably increasing the corrosion rate of many metals in combination with SO<sub>2</sub>.

Furthermore, NO<sub>2</sub> can be photolyzed under visible and ultraviolet light, to form NO and O, which will recombine with oxygen gas to form ozone O<sub>3</sub>. Ozone is chemically active as an oxidizer. It is sensitive to ultraviolet radiation, generating O<sub>2</sub> and O, which will recombine with water to obtain two hydroxyl radicals. Hydroxyl radicals react with a very wide variety of atmospheric gases. Ammonia NH<sub>3</sub> is highly soluble, and it is readily recombined with water and sulphur dioxide to form ammonium sulphate (NH<sub>4</sub>)<sub>2</sub>SO<sub>4</sub> [35].

- ***Influence of the cover and the orientation***

The formation of corrosion compounds is principally influenced by atmospheric constituents [27]. However, within one type of atmosphere, it is even possible to obtain other products than those foreseen only considering the level of pollutants [27, 41]. The determining factor will then be the orientation of the metal in the atmosphere. Corrosion will be different for copper alloys which are

protected from, or on the contrary, directly exposed to the aggressive action of precipitation or wind.

In the case of covered exposure, coarse aerosol particles, such as soil dust, are prevented from reaching the corroding surface which is not exposed to direct precipitation. Surface retention of water will occur. During drying the pH will decrease while the copper ions concentration increases. When evaporation is slow, a highly concentrated and acid solution will be present on the surface, allowing the formation of antlerite, to the disadvantage of brochantite.

On the contrary, uncovered areas are sensitive to the run-off effect of precipitation which prevents the surface retention of air constituents and dissolves water soluble compounds. Patinas form more slowly and display fewer compounds than in sheltered areas. Precipitation can wash away corrosion stimulators and decrease the corrosion effect but also add corrosion enhancing ions to the liquid layer and increase the corrosion effect. Exposed surfaces are sensitive to evaporation and do not allow the surface water to obtain a sufficiently low pH and high copper ion concentrations in order to form antlerite. The surface will thus present brochantite as principal final corrosion product. Other phases are only present as traces or not present at all.

In the case of  $\text{Cl}^-$  dominated environments, on partially sheltered surfaces chloride compounds are formed more rapidly than on exposed surfaces, which may be washed free of wind blown sea salt by rain.

#### ***1.2.1.2. Corrosion in soil***

The soil is composed of numerous chemical species. Some of them have a greater influence than the others on corrosion processes concerning copper alloys.

Burial in soil, barrows, tombs or cemeteries is a common event in the life of most archaeological copper alloy artefacts. Soil is a medium distinguished by the complex nature of its composition and of its interactions with other environmental factors. Organic matter, but also dissolved species, such as  $\text{O}_2$ ,  $\text{SiO}_2$ ,  $\text{F}^-$ ,  $\text{Na}^+$ ,  $\text{Ca}^{2+}$ ,  $\text{Cl}^-$ ,  $\text{SO}_4^{2-}$ ,  $\text{CO}_3^{2-}$ ,  $\text{Fe}^{2+}$ ,  $\text{Al}^{3+}$ ,  $\text{NO}_3^-$  or  $\text{PO}_4^{3-}$  are present in varying proportions in each soil. Granulometry, resistivity, wetness and pH, that are parameters of utmost importance when dealing with corrosion process, will also differ so that not two soils are alike, and extremes of structure, composition, and corrosive activity are found in different soils. This makes the study of soil corrosion extremely difficult and multivariate statistical analysis [42-44] is often used to try to correlate variables with observed effects.

On the basis of the classification of Robbiola and co-workers, a buried bronze can display one of two categories (called type I and II in the following lines) of corrosion patterns, according to



whether the original surface boundary is still observable or not [42]. Both structures may coexist on a same object.

In the Type I (Figure 3), the original shape of the artefact has been left intact: macroscopic traces of polishing or use may subsist. The surface layers display different colours, depending on the incorporated soil elements, ranging from grey to blue and green. Corrosion originates from a process of selective dissolution of the alloy, affecting principally the copper, followed by the diffusion of ionic species through the thin corrosion layer, from the alloy to outwards. The corrosion layers have grown up from the original surface towards the alloy without apparent volume change and proved to have excellent corrosion resistance properties. The external layer contains soil elements and the internal layer oxides or hydroxides. The bilayered structure is generally between 10 and 100  $\mu\text{m}$  thick, although in some cases thickness can range up to several millimetres. The structure contains high Sn and low Cu amounts.

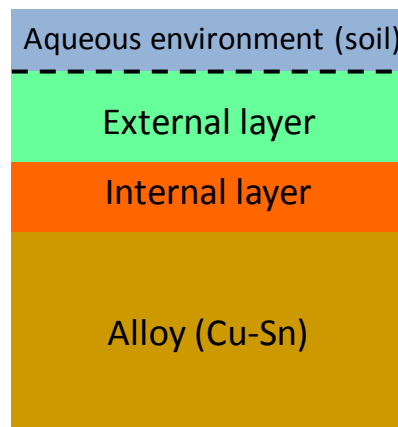


**Figure 3: Schematic illustration of a type I corrosion on a Cu-Sn alloy. The dashed line represents the limit of the original surface [42]**

In the Type II structures, the original surface has been damaged (Figure 4). Structures are rough and colours may be red, brown or green. Localized corrosion phenomena as well as generalized attacks due to a high dissolution rate occurred, but the same corrosion steps are observed as in type I structures. The external layer contains green Cu(II) compounds such as carbonates, chlorides, silicates and/or phosphates. The middle layer is a disrupted and fragmented red cuprite layer. Finally, the composition of the internal layer has been characterized by a structure containing soil elements and noticeable amounts of  $\text{Cl}^-$ . The structure displays lower Cu and higher Sn contents than in the alloy [3, 42].

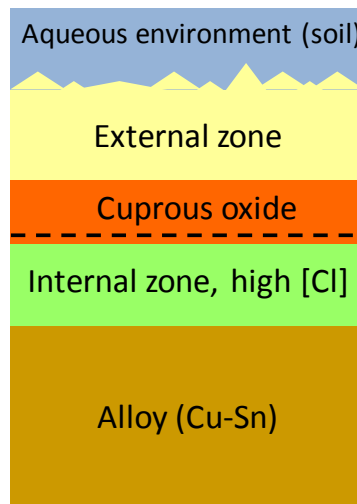


**Figure 4: Schematic illustration of a type II corrosion on a Cu-Sn alloy. The dashed line represents the hypothetical limit of the original surface [42]**

### **1.2.1.3 Marine corrosion**

The most common components of seawater are  $\text{Cl}^-$ ,  $\text{Na}^+$ ,  $\text{SO}_4^{2-}$ ,  $\text{Mg}^{2+}$ ,  $\text{Ca}^{2+}$  and  $\text{K}^+$  ions [25]. The principal dissolved gases are oxygen and carbon dioxide. Part of the reason why copper alloys do not corrode quickly when immersed in the sea is that a cuprite film tends to develop over the surface. In general, the oxygen content of a marine environment is a significant factor in the corrosion of copper.

The corrosion products in oxygenated water range from cuprite to cuprous chloride and include the isomers of the copper trihydroxy chlorides. Relatively uncommon are the carbonates and sulphates. Many artefacts recovered from the sea are associated with shipwrecks. At such sites, marine life, algae or coral, may strongly influence the local “chemical” environments of submerged bronzes; as a result such artefacts may be heavily covered with concretions.

In natural environments, bacteria attach to solids, including metals, where they colonize the surface and produce a biofilm. The sulphate reducing bacteria are a particularly important group in the corrosion of metals, since the production of the sulphide ion and hydrogen sulphide is usually damaging to metal surfaces as these species react with the cupric ions, whereby reaction  $\text{Cu}^+ \leftrightarrow \text{Cu}^{2+} + \text{e}^-$  is enhanced. Consequently, a number of corrosion events can be initiated at the metal surface in absence of oxygen. On objects buried in seawater sediments, removed from oxygenated conditions, copper sulphides are a common corrosion product since hydrogen sulphide is commonly available as a product of plant decay [3].

## 1.2.2. Artificial patinas

By both artistic and scientific point of view, the possibility of creating artificial patinas on copper alloy surfaces is really useful.

From the artistic point of view, these procedures allow to obtain the aesthetic results that require many years in a natural uncontrolled process. Moreover effects that cannot be created naturally on the metallic surfaces, can be created artificially.

From the scientific point of view, since tests can rarely be made directly on real artefacts, for the sake of conservation, obtaining artificial patinas allows the preparation of a nearly infinite number of samples available to perform analysis or test new procedures and products.

Patinas may be used to ‘antique finishing’ objects, as a part of the design or decoration of art and furniture. After a sculpture has been cast, for example, it is ready for the last finishing. Some artists choose the natural colour and natural ageing, but others choose to apply a patinated finishing. The light and shadows of an artificial patina can give good definition to the curves and texture, as well as special artistic effects [45].

A wide range of chemicals, both household and commercial, can create a large variety of patinas [46] and hundreds of recipes for patina preparation and application technique are known [9]. Artists often use patination as creative act, which unites skill and spirit, on surface improvement either for colour, texture, or both, but also aesthetic dimension and artistic expression [1]. Patina composition varies with the elements that react together and these will determine the colour of the final layer. Exposure to chlorides, for example, leads to green, while sulphur compounds tend to brown. For artworks, patination is deliberately accelerated by heat. Colours range from matte sandstone yellow to deep blues, reds and various blacks, sometimes with the surface sheen enhanced by waxing for artwork displayed indoors [46].

The ancient use of artificial patination as a deliberate aesthetic effect is uncertain. Even though the natural patination on bronze artefacts generally evokes a desirable sense of age and quality [5]. As a result, these coloration has long been mimicked by Modern, Renaissance, and Medieval artisans (especially in Europe and China), by direct application of chemical agents to the bronze surface in order to imitate the natural coloration of ancient and classical bronze artefacts [9, 47]. The recipes for bronze patinas found in literature generally involve the exposure of the bronze to some combination of solutions of sulphide, sulphate, acetate, and ammonium salts, producing the blacks, browns, and various greens associated with copper sulphides and sulphates [5, 9].

Several historical references exist, mentioning methods to intentionally alter the surface appearance [3, 9, 48]. Since antiquity, craftsmen tried to imitate minerals (such as cuprite, malachite and azurite) on the metal objects they were producing. Techniques of metal coloration were applied

since the 4<sup>th</sup> – 3<sup>rd</sup> pre-Christian millennium. Indeed, the ancients were confronted with the effect that certain manufacturing techniques (such as casting, hammering, annealing, etc.) had on the colour of the surfaces of cast and forged bronzes. Craftsmen were able to produce two basic colours, red and black, as well as many variations, through simple oxidation of the surface. Furthermore, the minerals themselves were often used as inlay material. The most ancient literature sources mentioning artificial patination, date back from Plutarch and Pliny as mentioned before. The ancient Greeks put all their efforts to maintain their bronzes as a bright metal so as to resemble expensive gold. However, black and brown patination recipes have also been mentioned at this period. For the following centuries, chemical treatment of copper on bronze surfaces and the use of chemically reacting solutions, were tried out by metalworkers. Through their experiences they achieved a wide range of colours [3].

Later, in the Renaissance, thin transparent oxides of red and brown became the most desired patinas. Green verdigris-like coatings were also present but did not really come into vogue in Europe before the 19<sup>th</sup> century. In the 19<sup>th</sup> century, the development of colouring was accompanied by the increased use of superficial pigments which were bound to the surface with waxes, varnishes and lacquers. The possibility of colouring by immersion was investigated in the late 19<sup>th</sup> and begin 20<sup>th</sup> century. The growing application of new techniques led to radical changes in sculpture, resulting in the production of large quantities of domestic articles and small decorative items. This rendered in most cases the use of traditional colouring techniques, which required considerable skill, not appropriate anymore and metal colouring became a rather neglected area. In the early part of the 20<sup>th</sup> century, opaque, dark green and black layers were popular as they formed naturally on bronzes by exposure to modern atmospheres, especially those containing high amounts of sulphur. Since the mid 20<sup>th</sup> century, there has been a renewed interest in the potential of the decorative use of color in metalwork. Currently, a variety of both browns and greens, and even other colours not appearing in nature are appreciated along with a translucent effect, as had been preferred in the mid-19<sup>th</sup> century [3, 4].

Artificial patinas are nowadays considered as a surface treatment, aiming at colouring the metallic support and at giving a protection to the metal.

The increasing pollution levels in modern's world lead to the necessity of understanding and controlling the patination process that was formerly left to the action of nature. The pollutants introduced in the atmosphere due to industrial activities in 19<sup>th</sup> and 20<sup>th</sup> century, for example, led to the formation of patinas that had never formed before on outdoor metallic artefacts. Artificially created patina can undergo to the same processes and the final aspect created by an artist can change completely.

One of the problems the modern conservator is facing, is determining whether a patina is the result of natural corrosion, or if it was obtained through deliberate manipulation such as, for example, patination [25, 48, 49]. The difficulty to differentiate natural and artificial patinas is due, in part, to the fact that bronzes artefacts, are almost never available in the conditions in which they have been found in archaeological sites. As soon as they are discovered on excavations, they are decalcified and washed. Materials that pass through the hands of art dealers have usually undergone a similar or even worse treatment. Handling, corrosive mechanisms, repeated cleaning and conservation through the centuries by museums and art dealers make it thus almost impossible to if the patinas were at the origin artificially added or if they have been created naturally. Additionally, the lack of documentation has made it difficult to reconstruct which exactly has been the “story” of the objects in the past. Although traces of artificial patination are still visible, it is almost impossible to identify them as such. This difficulty arises because analysis can only reveal minerals that could also have originated through natural processes. In some cases, though, brush strokes from the treatment can confirm an ancient artificially applied patina. Furthermore, a number of surface compounds are extremely unlikely to have been produced by natural processes on copper and bronze objects, whilst others are unlikely to have been produced artificially [9, 27].

#### ***1.2.2.1 Techniques of patination***

Copper is an especially satisfying metal to colour, because its hue can easily be changed into one of many possible colours [9, 48, 50]. Copper is really reactive and it is quite easy to obtain on its surface several coloured compounds. In copper alloys, the colour is almost entirely due to the copper, while the alloying elements (zinc, tin or lead), contribute little to the colouring of the metal. Two are the most common methods of colouring a metal, besides the use of paints and varnishes. The fast way is to coat the metal with another, by the plating technique, especially used on industrial scale. The second way is to convert the metal surface into an oxide or salt which is coloured or capable of absorbing colouring materials, or that produces colour by interference. Therefore, chemical conversion or deposition, thermal oxidation, electrolytic deposition and conversion processes, as well as paints and metallic lacquers can be used. The chemical conversion methods is the most common, due to the ease of realization as no or little instrumentation is required and usually a brief contact between metal and a chemical solution is sufficient to obtain a large variety of colours. A large number of chemical conversion recipes can be found in the literature [9, 50]. The majority of the recipes was built up empirically and they were rarely written down exactly by patination ateliers, eager to keep their best recipes secret. Therefore, those recipes do not always provide satisfactory results without the know-how of skilled craftsmen.

### Patination by solutions

Within the chemical conversion methods, the solution is applied to the metallic surface into various ways, such as immersion, dipping, vapour or torch technique [9]. The produced coloured films are most of the time extremely thin and tenuous. They display a rather poor resistance to the atmosphere and to handling. This is due to the fact that, once a continuous layer of corrosion compounds is produced in immersion, it forms a barrier for the underlying metal and the action ceases. The poor resistance and adherence makes a continuous maintenance necessary to maintain the original colour of the artificial patina.

Different shades and even colours can be obtained by immersion in a solution, or brushing the liquid on the metallic surface. The final result depends on the density of the solution and its temperature. A prolonged immersion will most of the time only lead to a superficially powdery and poorly adherent layer.

Many traditional finishes, particularly those associated with the production of a green patina on bronze sculpture, are produced by the direct application of solutions to the surface of an object. The method of applications of the solution directly on the surface are: brushing, dabbing and wiping, spraying and dipping. This colouring method is seldom accomplished in one application, but characteristically involves a cycle of sparing applications and periods of drying, for a matter of days or even weeks, until the desired colour has developed. This technique is of particular relevance in the colouring of large sculptures, which it would be impractical to colour by immersion [9], but, due to the long time required to obtain a satisfactory results is not the best option for scientific purposes. Since most of the recipes for artificial patination are classified on the basis of the colour of the final layer, little is known about the final corrosion compound which is formed on the metal. Without an extensive study of the patination techniques, it is hard to obtain specific compounds using these recipes. Patination remains a contentious issue because there is no certainty that the treatment will improve the preservation and aesthetic appearance of the bronze in the long term unless continued maintenance is provided [25]. Before being used in restoration, it is thus necessary to study the patinas behaviour in time and in contact with specific compounds. The necessity to study patination techniques in a more scientific approach has then become an evidence [4, 51].

### Patination using applied paste

Of particular interest for the purpose of this work is the method of application of a paste of copper salts is described in literature for the artificial patination by Hughes and Rowe [2]. The authors report that *a restricted range of chemicals have traditionally been used in the form of paste, to colour objects on a variety of scales. The most commonly used are the statuary pastes based in*

sulphides, which are used to produce bronze finishing. The remainder tend to produce variegated surfaces of various colours, which often include the development of some green or blue-green patina. The applied paste method was developed as alternative technique in cases where the direct application of solutions failed to wet the surface of the metal. Two basic approaches were tried:

- patinating solutions were thickened into pastes, using inter media such as clays, gelatin or flour to provide the "body"
- the ingredients of patinating solution were taken and only very small quantities of water were added

The first methods usually failed to produce patinas, probably because the resulting pastes tended to exclude air from the surface. With the second method, instead, concentrated thick pastes were produced [2].

For the obtaining of the paste solid ingredients should be ground to a fine consistency using a pestle and mortar. The liquid components are then added, with continued grinding. The addition of liquids must be very gradual as the paste can easily become too thin. A thick creamy consistency is the most suitable [2] for the expected patinas.

Concerning the methodology of application of the paste, Hughes and Rowe suggest that *there are two basic approaches to the application of pastes, which tend to give rise to slightly different results. They can be applied sparingly by wiping with a soft cloth and allowed to dry; the applications being repeated a number of times as necessary until the surface has developed. The depth of colour and precise surface quality obtained will depend on the period of treatment. Alternatively, the paste can be applied thickly by brushing, and left for a longer period to dry out completely. Variations in the surface quality obtained can be made by altering the method of application slightly. The paste can be stippled into place, applied locally in patches so that the surface is gradually built up, or the applied paste can be 'raked' so that lines are produced that nearly break through to the metal surface* [2].

#### Other technique of patination

Although lots of studies introduce the notion of “artificial” patina, few are based on artists traditional recipes. They rather obtain the patina layers through application of artificial ageing methods [52], contact with corrosive species [53, 54] or electrochemistry [28, 55]. A few projects studied patinas realized according to traditional recipes. Balta [51] deepened especially recipes producing black and dark brown patinas, obtained using mainly potassium sulphide,  $K_2S$ . The effect of the concentration and temperature on the chemical composition and morphology of the resulting patina was also investigated. Most of the studies concern black and brown patinas, which are

relatively easy to produce while, in order to obtain a satisfactory green-blue patina, such that naturally formed by outdoor exposition of metal, much more knowledge and practical skills are required [3].

The electrochemical techniques for the creation of artificial patinas [28, 55] are suitable in particular for laboratory applications. They consist in the immersion of metallic specimens in a salt solution and in the application of an appropriate current density. Usually the procedures are divided in steps and different current densities are applied. The duration of these methods can vary according to the desired result, but they required at least few days to obtain satisfactory results.

The recipes chosen and used in this work to obtain artificial patinas will be explain in the chapter 3.1 “Preparation of artificial patinas”.



## References

- [1] K. Marušić, H. Otmačić-Ćurković, Š. Horvat-Kurbegović, H. Takenouti, E. Stupnišek-Lisaca, **Comparative studies of chemical and electrochemical preparation of artificial bronze patinas and their protection by corrosion inhibitor**, *Electrochimica Acta* 54 (2009) 7106–7113
- [2] <http://www.merriam-webster.com/>
- [3] Valérie Hayez, **Use of micro-Raman spectroscopy for the study of the atmospheric corrosion of copper alloys of cultural heritage**, PhD Thesis, Vrije Universiteit Brussel, Department of Metallurgy, Electrochemistry and Materials Science (2006)
- [4] Valérie Hayez, Virginia Costa, Joseph Guillaume, Herman Terryna, Annick Hubina, **Micro Raman spectroscopy used for the study of corrosion products on copper alloys: study of the chemical composition of artificial patinas used for restoration purposes**, *Analyst*, 2005, 130, 550–556
- [5] Ashley E. Devantier, Susan J. Murch, W. Stephen McNeil, **Exploration and characterisation of novel bronze patinas derived from simple coordination complexes**, *Dalton Trans.*, 2011, 40, 614
- [6] Walter A. Franke and Magda Mircea, **Plutarch's report on the blue patina of bronze statues at Delphi: a scientific explanation**, *Journal of the American Institute for Conservation*, 44, 2 (2005), 103–116
- [7] <http://penelope.uchicago.edu/misctracts/plutarchVerses.html> – Why the Pythia does not now give oracles in verse, (1918) trans. A. O. Prickard, adapted by J. Eason.
- [8] Constatinides, I., A. Adriaens, F. Adams, **Surface characterization of artificial corrosion layers on copper alloy reference materials**, *Applied Surface Science*, 189 (2002) 90–101
- [9] R. Hughes, M. Rowe, **The colouring bronzing and patination of metals**, Thames & Hudson, London (GB), 1991
- [10] I. Odnevall Wallinder, C. Leygraf, **Seasonal variations in corrosion rate and runoff rate of copper roofs in an urban and a rural atmospheric environment**, *Corrosion Science*, 43, 12 (2001) 2379–2396
- [11] A.M. Pollard, R.G. Thomas, P.A. Williams, **The copper Chloride System and corrosion: a complex interplay of kinetics and thermodynamic factors**, *Dialogue/89 – The conservation of bronze sculpture in the outdoor environment: A dialogue among conservators, curators, environmental scientists, and corrosion engineers*, Terry Drayman-Weisser (1992), 123
- [12] R. Organ, **Aspects of bronze patina and its treatment**, *Studies in Conservation*, 8, 1 (1963), 1–9

- [13] T.E. Graedel, K. Nassau, J.P. Franey, **Copper patinas formed in the atmosphere – I. Introduction**, Corrosion Science, 27, 7 (1987), 639–657
- [14] K. Nassau, P.K. Gallagher, A.E. Miller, T.E. Graedel, **The characterization of patina components by X-ray diffraction and evolved gas analysis**, Corrosion Science 27 (1987) 669–684
- [15] Nassau, K., Miller, A. E. and Graedel, T. E., **The reaction of simulated rain with copper, copper patina and some copper compounds**, Corrosion Science 27 (1987), 703–719
- [16] Strandberg H., **Reactions of copper patina Compounds – 1. Influence of some air pollutants**, Atmospheric Environment 32 (1997), 6719–6733
- [17] T.E. Graedel. **Copper patinas formed in the atmosphere – II. A qualitative assessment of mechanisms**, Corrosion Science, 27, 7 (1987), 721–740
- [18] A. J. Muller and C. McCrory-Joy, **Chromatographic analysis of copper patinas formed in the atmosphere**, Corrosion Science, 27 (1987), 695–701
- [19] R. L. Opila, **Copper patinas: an investigation by Auger electron spectroscopy**, Corrosion Science, 27, (1987), 685–694
- [20] A. Atrens, K. FitzGerald, G. Skennerton, and J. Nairn, Paper 42, in Proceedings of the 13th International Corrosion Congress, International Corrosion Council, Nov 25-29, 1996
- [21] A. Atrens, J. Nairn, H. Fernee, K. FitzGerald, G. Skennerton, and A. Olofinjana, Mater. Forum, 21, 57 (1997)
- [22] D.P. Fitzgerald, J. Nairn, A. Atrens, **The chemistry of copper patination**, Corrosion Science, 40 (1998), 2029–2050
- [23] G.P. Cicileo, M.A. Crespo, B.M. Rosales, **Comparative study of patinas formed on statuary alloys by means of electrochemical and surface analysis techniques**, Corrosion Science, 46 (2004) 929–953
- [24] J.P. Franey, M.E. Davis, **Metallographic studies of the copper patina formed in the atmosphere**, Corrosion Science, 27 (1987) 659–668
- [25] Scott, David A., **Copper and bronze in art**, The Getty Conservation Institute (2002)
- [26] L.L. Schreir and R.A. Jarman. **Corrosion. Metal/environments reactions, volume 1**. Butterword Heineman, 3rd edition, 1994
- [27] C. Leygraf and T.E. Graedel, **Atmospheric Corrosion**. The Electrochemical Society Series, 2000
- [28] W.H.J. Vernon, **The Open-air corrosion of copper. Part III. Artificial production of green patina**, J. Inst. of Metals, 49 (1932), 153–167

- [29] T.E. Graedel, **Copper patinas formed in the atmosphere – III. A semi-quantitative assessment of rates and constraints in the greater New York metropolitan area**, *Corrosion Science*, 27, 7 (1987), 741–769
- [30] A. Krätschmer, I. Odnevall Wallinder, C. Leygraf, **The evolution of outdoor copper patina**. *Corrosion Science*, 44 (2002), 425–450
- [31] D.A. Scott, **Copper compounds in metal and colorants: oxides and hydroxides**, *Studies in conservation*, 42 (1997), 93–100,
- [32] J.M. Cronyn, **The elements of archaeological conservation**, Routledge, London and New York, 1990
- [33] Odnevall I, Leygraf C., **Atmospheric corrosion of copper in rural atmosphere**, *J. Electrochem. Soc.*, 142 (1995), 3682
- [34] A.M. Pollard, R.G. Thomas, and P.A. Williams. **The stabilities of antlerite and  $\text{Cu}_3\text{SO}_4(\text{OH})_4 \cdot 2\text{H}_2\text{O}$ : their formation and relationships to other copper(II) sulfate minerals**, *Mineralogical Magazine*, 56 (1992), 359–365,
- [35] B. J. Finlayson-Pitts, Jr. J. N. Pitts, **Chemistry of the upper and lower atmosphere: theory, experiments, and applications**, Academic Press Inc (1999)
- [36] R. Schlesinger, H. Klewe-Nebenius, M. Bruns, **Characterization of artificially produced copper and bronze patina by XPS**, *Surf. Interface Anal.* 30 (2000), 135–139
- [37] C. Chiavari, K. Rahmouni, H. Takenouti, S. Joiret, P. Vermaut, L. Robbiola, **Composition and electrochemical properties of natural patinas of outdoor bronze monuments**, *Electrochimica Acta*, 52 (2007), 7760–7769.
- [38] A. Lins and T. Power, in *Ancient and Historic Metals: Conservation and Scientific Research*. ed. D.A. Scott, J. Podany and B.B. Considine, Getty Conservation Institute (1994), 119-151
- [39] P.L. Cavallotti, L. Nobili, *Rame notizie*, 23, Istituto Italiano del Rame, Consedit (1997)
- [40] J.B. Sharkey and S.Z. Lewin, **Conditions governing the formation of atacamite and paratacamite**, *The American Mineralogist*, 56:179–192, 1971
- [41] L. Robbiola and L.P. Hurtel. **New contribution to the study of corrosion mechanisms of outdoor bronzes: characterization of the corroding surfaces of Rodin's bronzes**. *Mémoires et études scientifiques de la revue de métallurgie*, 88(12):809–823, 1991
- [42] L. Robbiola, J.M. Blengino, C. Fiaud, **Morphology and mechanisms of formation of natural patinas on archaeological Cu-Sn alloys**, *Corrosion Science* 40, 12 (1998) 2083-2111
- [43] A.G. Nord, E. Mattsson, and K. Tronner. **Mineral phases on corroded archaeological bronze artefacts excavated in Sweden**. *Neues Jahrbuch für Mineralogie*, (6): 265–277, 1998

- [44] A.G. Nord, E. Mattsson, and K. Tronner. **Factors influencing the long-term corrosion of bronze artefacts in soil.** *Protection of metals*, 41(4): 309–316, 2005
- [45] Tadeja Koseca, Helena Otmačić Čurković, Andraž Legata, **Investigation of the corrosion protection of chemically and electrochemically formed patinas on recent bronze,** *Electrochimica Acta* 56 (2010) 722–731
- [46] P. Dillmann, G. Beranger, P. Piccardo, H. Matthiessen, **Corrosion of metallic heritage artefacts, investigation, conservation and prediction for long-term behaviour,** Woodhead Pub., Cambridge (GB), 2007 (EFC publications (EFC48)).
- [47] R. J. Gettens, **Patina: noble and vile,** in *Art and Technology: A Symposium on Classical Bronzes*, ed. S. Doeringer, D. G. Mitten and A. Steinberg, MIT Press, 1970, Cambridge MA, 57–72
- [48] H. Born. **Patinated and painted bronzes: Exotic technique or ancient tradition?** In *The J. Paul Getty Museum, editor, Small Bronze sculptures from the Ancient World*, pages 179–196, 1990
- [49] M. Schreiner. **Microanalysis for the study of materials and objects of art and archaeology.** *Fresenius Journal of Analytical Chemistry*, 337:715–720, 1990
- [50] D. Fishlock. **Metal Colouring.** Robert Draper Ltd, 1962
- [51] I.Z. Balta and L. Robbiola. **Study of black patinas on copper and bronze obtained by using 19-th century western traditional techniques of artificial patination.** In *Proceedings of the 8th International Conference on non-destructive investigations and microanalysis for the diagnostics and conservation of the cultural and environmental heritage*, 2005
- [52] F. Noli, P. Misaelides, A. Hatzidimitriou, E. Pavlidou, and M. Kokkoris, **Investigation of artificially produced and natural copper patina layers,** *Journal of Materials Chemistry*, 13 (2003), 114–120
- [53] B. Rosales, R. Vera, G. Moriena, **Evaluation of the protective properties of natural and artificial patinas on copper. Part I: patinas formed by immersion.** *Corrosion Science*, 41:625–661, 1999
- [54] M. Watanabe, Y. Higashi, M. Tomita, T. Ichino, **Microstructural analysis of artificially formed patinas on copper,** *Electrochemical and Solid-State Letters*, 5 (8) B28-B31 (2002)
- [55] I. Constantinides, A. Adriaens, and F. Adams, **Surface characterization of artificial corrosion layers on copper alloy reference materials,** *Applied Surface Science*, 189 (2002), 90–101

## 1.3 First approaches to the monitoring of gilded bronzes

The study of gilded bronzes is a particularly complex topic. The characterization of the corrosion products developed between gold and bronze is not easy without inducing damage to the gilding. In fact, it is rarely allowed to take samples from the precious gilded bronzes and even more to obtain cross section to understand the stratigraphy of the artefact. Moreover, quantitative data about the corrosion rates are not easily obtainable. In fact traditional electrochemical techniques, such as Linear Polarisation Resistance ( $R_p$ ) or Electrochemical Impedance Spectroscopy (EIS), that allow to collect quantitative data on corroded metallic artefacts [1-10], cannot be applied to a bimetallic object due to the difficulties on the interpretation of results. A promising alternative is the use of electrochemical cells simulating the stratigraphy of a corroded gilded bronze and allowing the continuous monitoring of the macrocouple current that is directly proportional to corrosion rate.

### 1.3.1 Development of galvanic sensors in the 70's

The galvanic sensors, simulating corroded gilded bronzes were first developed in the late 70's by Professor Bruno Mazza of Politecnico di Milano and co-workers [11]. The sensors were defined like "corrosion system simulating the behaviour of gold plated bronzes" [11] and were used to study the corrosion of such complex systems under different environmental conditions.

The system prepared in 1977 consisted of a "sandwich" formed of bronze covered by its artificially obtained corrosion products, on which a high porosity gold film is finally applied. The schematic representation of the sensors prepared by Mazza and co-workers is presented in Figure 1.

This system form a galvanic cell which may be short-circuited so as to reproduce the corrosion phenomenon of gilded bronzes artefacts. The current thus measured by a zero resistance ammeter provides instantaneous and continuous information on the corrosion rate of the bronze.

The short-circuit current of the system of Figure 1 may be assumed to equal the dissolution rate of the bronze, the "local processes" on the bronze itself being negligible also in consequence of the coupling with the gold (positive differential effect).

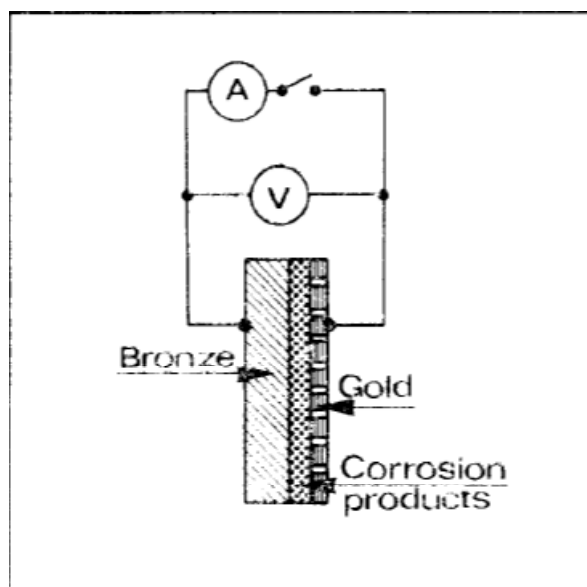
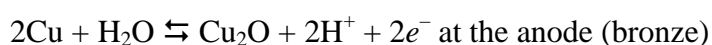


**Figure 1: Schematic representation of the galvanic cell simulating gilded bronzes set up by Mazza and co-workers [1]**

The electrochemical reactions corresponding to the operation of the galvanic cell of Figure 1, may be represented schematically as follow:



With these galvanic sensors it was possible to measure currents from  $\sim 10^{-9}\text{A}$  upwards, the corresponding corrosion rate is about 1mm/million years on a specimen whose exposed area is  $10\text{ cm}^2$ .

Thus, the system set up is a rationalized model of the real systems and it is possible to achieve the following aims:

- measure the corrosion rate in different conditions, identifying in particular the influence of some factors, such as relative humidity, condensed water on the surface, pollutants in the air and so on.
- check the effectiveness of the proposed methods for the protection of gold plated bronze works of art, such as in particular: control of the relative humidity, use of inhibitors, heating, and so on.
- define the electrochemical aspects of the behaviour of the real systems, so as to determine, on the one hand, the driving force available for the occurrence of the corrosion process, and, on the other hand, the type of kinetic control (anodic, cathodic or ohmic) of the process

itself, thus throwing light on phenomena which are also of general interest in the field of atmospheric corrosion.

#### *Composition of the galvanic cells set up by Mazza and co-workers*

The artificial patina deposited on the bronze substrate was obtained by Vernon electrochemical method [12]. The artificial patina (approximately 70  $\mu\text{m}$  in thickness) consists of basic copper sulphates which have a composition similar to those that formed in natural processes. The gold plates (approximately 20  $\mu\text{m}$  in thickness) were deposited on an inert support by vacuum evaporation technique. The gold plates were fixed on the patinas of corrosion products with glue spread around their edges. A very large number of pores whose diameter was smaller than 1  $\mu\text{m}$  was found, as well as small holes with diameter of approximately 10  $\mu\text{m}$ .

The authors underlined that the data obtained using their sensors are merely qualitative and may differ from one specimen to another up to one order of magnitude, even if the working conditions remained unchanged, due to the following reasons, presented by order of importance:

- Differences in the composition of the artificial patina of corrosion products as regard the presence of hygroscopic salts, ascribable to the preparation procedure (such as rinsing).
- Differences in the contact area between the gold plate and the patina underneath.
- Differences in the porosity of the gold plate.

### **1.3.2 Application of galvanic sensors to the study of the “Porta del Paradiso” in the 70’s**

Galvanic sensors similar to those described above were used few years later by the same research group to understand the corrosion behaviour of the “Porta del Paradiso” [13]. In particular the researchers wanted to test a heating system created for the door to avoid the condensation of water on the metallic surface.

In fact, the chemical reactions that occur during corrosion processes requires liquid water (generally produced by condensation of atmospheric humidity) to proceed at an appreciable rate. Water condensation takes place on a solid surface through several mechanisms: as a consequence of the cooling of the object caused by thermal radiation, or due to a lowering of vapour pressure inside surface porosities. The dangerous chemical condensation takes place in the presence of solutions which have a water-vapour pressure considerably lower than that of pure water. These solutions are formed if the surrounding atmosphere contains soluble compounds (e.g. sulphur dioxide) or if the

patina contains hygroscopic salts which absorb water when the partial water-pressure in the air is higher than the vapour pressure of the saturated solution. The chemical condensation always occurs at a relative humidity lower than 100 % and often at a very low humidity in the presence of chlorides and ammonium compounds, which are common in the sea and in rural environments, respectively. The solutions formed are often very conductive and enriched with ions which may induce an acceleration of electrode reactions. Besides, the gold layer on gilded bronze has the effect of priming a corrosion process by bimetallic contact.

These considerations led the authors to propose a protection method based on the thermal control of the “Porta del Paradiso”. In fact, they guessed that if the door was kept a few degrees warmer than the surrounding atmospheric air, by using a suitable heating system, the relative humidity of the air layer near the patina might become lower, water condensation might be prevented and consequently chemical reactions and corrosion processes could also be reduced. Moreover, assuming that the proposed conditions of the thermal control could be quite moderate, it seemed very unlikely that they would cause damage to the doors even if heating always increases chemical and electrochemical reaction rates [13].

The tests with the galvanic sensors were carried out both at environmental temperature and at 4°C above it, and the following was observed :

- the corrosion rate increases with the hygroscopicity of the corrosion products.
- The heating has a positive effect, because it lowers the corrosion rate in proportion to the local diminution of the relative humidity. The diminution of the local relative humidity was calculated assuming that the environmental absolute humidity is constant.

To evaluate the influence of the different composition of salts, similar tests were performed by replacing the salts of different hygroscopicity, with salts of different anions involving different influence on the electrode reactions (e.g. sulphate and chloride). It was found that the sulphate ion tends to stop more quickly the operation of the macrocouple, whereas when chloride is present, the corrosion rate is much greater and decreases slowly with time.

On the basis of these observations the authors could conclude that:

- except in the presence of a liquid film on the gilded surface, the corrosion rate of samples exposed to a polluted atmosphere and heated was lower than the corrosion rate of identical samples kept at the environmental temperature. The extent of this effect could be estimated as about 50-70 % of the value obtained without any thermal protection.
- This effect was pronounced on the samples kept at a temperature 4°C higher than the environment, but no significant difference between 4 or 8°C over-temperature was noted.



- The positive effect the heating decrease with time.
- The electrochemical model verifies the effect also in the presence of hygroscopic products.

A negative effect was also noted: on heated samples the patina becomes more fragile and, consequently, less adherent and protective and it splinter easily.

On the basis of these preliminary and promising results, in the framework of this project, new and improved galvanic sensors have been developed and used for the monitoring of corrosion rate in different environments. The set up of the new galvanic sensors and the results of their monitoring will be described thoroughly in the following chapters.

## References

- [1] ASTM G 59-97 (2009) **Standard Test Method for Conducting Potentiodynamic Polarization Resistance Measurements**
- [2] ASTM G 106-89 (2010) **Standard Practice for Verification of Algorithm and Equipment for Electrochemical Impedance Measurements**
- [3] ASTM G 102-89(2010) **Standard Practice for Calculation of Corrosion Rates and Related Information from Electrochemical Measurements**
- [4] Letardi P., Beccaria A., Marabelli M., D'Ercoli G., Application of electrochemical impedance measurements as a tool for the characterization of the conservation and the protection state of bronze works of art, Metal98 – International Conference on Metal Conservation, Draguignan, France 26–29 May 1998, 303–308
- [5] C. Bartuli, R. Cigna, O. Fumei, **Prediction of durability for outdoor exposed bronzes: estimation of the corrosivity of the atmospheric environment of the Capitoline Hill in Rome**, Studies in conservation, 44, 4 (1999), 245–252
- [6] G. D'Ercoli, M. Marabelli, **La resistenza di polarizzazione: indagine non distruttiva per la caratterizzazione di patine e protettivi di un monumento bronzeo**, in Monumenti in bronzo all'aperto. Esperienze di conservazione a confronto, Nardini Editore, Firenze, 2004, 135–142
- [7] K. Leyssens, A. Adriens, E. Pantos, C. Degryny, **Study of corrosion potential measurements as a means to monitor the storage and stabilisation processes of archeological copper artefacts**, Metal 04. – International Conference on Metal Conservation, National Museum of Australia, Canberra, 4–8 October 2004, 332–343
- [8] E. Angelini, S. Grassini, S. Corbellini, G. M. Ingo, T. de Caro, P. Plescia, C. Riccucci, A. Bianco, S. Agostini, **Potentialities of XRF and EIS portable instruments for the characterisation of ancient artefacts**, Applied Physics A, 83 (2006), 643–649
- [9] P. Letardi, G. Luciano, **Survey of EIS measurements on copper and bronze patinas**, Metal07 – International Conference on Metal Conservation, Amsterdam (The Netherlands), Rijksmuseum, 17–21 September 2007, vol. 3, 44–50
- [10] D. M. Bastidas, M. Criado, S. Fajardo, V. M. la Iglesia, E. Cano, J. M. Bastidas, **Copper deterioration: causes, diagnosis and risk minimisation**, International Materials Reviews, 55, 2 (2010), 99–127
- [11] B. Mazza, P. Pedferri, G. Re, D. Sinigaglia, **Behaviour of a galvanic cell simulating the atmospheric corrosion conditions of gold plated bronzes**, Corrosion Science 17 (1977), 535–541
- [12] W.H.J. Vernon, **The Open-air corrosion of copper. Part III. Artificial production of green patina**, J. Inst. of Metals, 49 (1932), 153–167

[13] G. Alessandrini, G. Dassù, P. Pedefferri, G. Re, **On the Conservation of the Baptistery Doors in Florence**, *Studies in Conservation*, 24, 3 (1979), 108–124

## 1.4 Case study: the Porta del Paradiso by Lorenzo Ghiberti

The Porta del Paradiso is a masterpiece of Italian Renaissance, created by Lorenzo Ghiberti, goldsmith and sculptor, between 1425 and 1452. It's a gilded bronze artwork made using the technique of indirect lost-wax casting [1] and then gilded using the fire gilding technique (or mercury amalgam).

The Porta del Paradiso was the main entrance of the Baptistery of Florence and was located in front of the Duomo of Santa Maria del Fiore, in the east cardinal direction. The artwork is constituted by 10 panels representing different episodes of the Bible, 24 friezes in which are situated small statues of biblical personages and 24 medallions with heads and small busts in which appears also a self portrait of the artist himself. Figure 1 presents the Porta del Paradiso with the position and the description of the ten panels [2].



### Scenes on the Porta del Paradiso:

1. Adam and Eve
2. Cain and Abel
3. Noah
4. Abraham
5. Isaac with Esau and Jacob
6. Joseph
7. Moses
8. Joshua
9. David
10. Solomon and the Queen of Sheba

Figure 1: Porta del Paradiso: distribution and description of the 10 panels.

The metal used for the casting is a quaternary alloy constituted by copper, zinc, tin and lead [2]. In table 1, the average chemical composition of three panels (Moses, Adam and Eve as well David) is

reported [1] . The single parts of the artwork (panels, friezes and medallions), after fire gilding, were assembled on a bronze substrate that constitute the “skeleton” of the door.

**Table 1:Percentage composition of alloy of three panels of Porta del Paradiso [1].**

<b>SAMPLE</b>	<b>Cu wt%</b>	<b>Sn wt%</b>	<b>Pb wt%</b>	<b>Zn wt%</b>	<b>Fe wt%</b>	<b>Ni wt%</b>	<b>Ag wt%</b>	<b>Mn wt%</b>	<b>Au wt%</b>	<b>Co wt%</b>	<b>Sb wt%</b>
<i>VII (Moses)</i>	93.51	0.13	1.14	3.78	0.13	0.14	0.06	0.00	0.00	0.00	0.13
<i>I (Adam and Eve)</i>	91.12	2.09	1.37	3.43	0.47	0.22	0.05	0.00	0.00	0.03	0.44
<i>IX (David)</i>	95.19	0.70	0.84	1.10	0.38	0.17	0.05	0.00	0.00	0.02	0.50

Alloys of similar composition were often used in the past for the creation of artworks, thanks to their good mechanical properties and their high resistance to atmospheric corrosion determined by thin layer of oxides that forms on the surface [3]. A special feature of the alloy forming the portal is the low percentage of alloy elements, in particular the low amount of lead, which means a low fluidity in the liquid state. This justifies the high melting temperatures and the complex pattern of melting channels used to understand the fusion technique used by Ghiberti [1].

### **1.4.1 Restoration and conservation intervention**

In the past, the door was kept shining and bright, which is the reason why it was sometime cleaned in aggressive ways. Signs of these cleaning intervention, scratches and abrasions, can be observed in few points of the surface of the gilding [4]. During a period of the XVIII century the Porta del Paradiso was intentionally covered by a dark patina: the painter Raffaello Mengs, in the second half of 1700, describes this patina and asked for the authorization to remove it, but his request was rejected [4]. However, the photographic documentation of XX century shows that the gilding was back in view and the artwork was again maintained bright, by the mean of different cleaning interventions, including one just at the end of the Second World War [4]. The most traumatic event in the history of this artwork was the flood that devastated Florence in 1966. The heavy wings were flung open and swung, leading to the expulsion from the frame of six of the ten bronze panels, which fortunately did not receive serious damages in the fall. To reinstall them easily at their original location, the wings were pierced in several places, and the panels 'screwed' in their bed with bronze through pins [4].

## 1.4.2 Diagnostic campaign of the 80's

The intervention with the through pins, even if not really respectful of the integrity of the door although "practical", has offered facilities when the diagnostic campaign started in the 80's, allowing to unscrew and remove from the frame the panels fallen during the flood.

The studies were performed using different techniques that, over the years, provided more thorough answers about the state of degradation of the artworks and about the deterioration of the materials.

The first investigations, dating from 1981-1982, were performed on the panels depicting the stories of Joseph, the sacrifice of Isaac, Adam and Eve as well as Cain and Abel [2].

Through a preliminary observation using an optical microscope, and subsequent investigations with a spectrophotometer as well as X-ray diffraction, several different kind of products and phenomena of surface alteration were determined. The distribution of the products that were found is represented schematically in Figure 2 taken from [5].



Figure 2: Schematic representation of the degradation products distribution and the deposited materials on the surface of the Porta del Paradiso [5].

The thin layer of gold was only partially visible, due to the thick layer of heterogeneous materials of various origins that covered it.

In particular, it was identified (Figure 2):

- Greyish-black deposited materials, characterized by X-ray diffraction and infrared spectrophotometric analysis, consisting of stratified particulate matter with a predominance of gypsum, sand and coal concretionary with bituminous materials and copper salts coming from the corrosion of the alloy.

- Dark-brown areas corresponding to abrasion of the gold layer, characterized by the presence of gypsum, carbonaceous particles and copper sulphates. These spots appear as patinas of bronze corrosion products, on which is, then, deposited the particulate matter.
- Micro-lifting and lacks in the gilding (small bubbles, with an average diameter of few tenths of millimeter).
- Greenish thin layer on the gold surface, in areas where the metallic layer is not hidden by other materials. This is due to the presence of corrosion products of the alloy, that migrated to the surface through fractures and liftings.
- Punctiform gray-green and green-blue aggregates, that, analysed by X-ray diffraction, revealed to be basic copper sulphates and basic copper nitrate. These salts, slightly soluble in water, resulted from the electrochemical corrosion of the alloy, from the interaction between corrosion products and air pollutants as well as from gradual processes of solubilisation and re-crystallization of the reaction products. The gilding was present beneath these formations, but partially affected by micro-lifting caused by crystallization of salts.

The study of these phenomena was analysed in depth by Mello and Parrini in 1982, thanks to the sampling of a micro sample [6].

The analysis, carried out using scanning electron microscopy coupled with microprobe, showed that for the corrosion phenomenology there are two different evidences:

- formation of pustules, i.e. micro-lifting and breaking of the gold layer, related to the processes of sulphatation and nitrification.
- Subsurface processes in the form of pitting, i.e. a compact layer of corrosion products, mainly composed by oxides and chlorides; this layer does not cause volume changes provoking detachment of the gilding which instead maintains a high adhesion to the underneath bronze.

With the same technique, combined with Auger and photoelectron spectroscopy, the material present on the gold layer was also characterized. This was composed partly of copper corrosion products (mainly chlorides and sulphates) and partly by depositing material (silica, silicates, calcium sulphate, smog particles).

### **1.4.3 Degradation mechanisms**

On the basis of the results obtained by the different diagnostic campaigns, some hypothesis about the degradation mechanisms occurring on the door were formulated [7-12]. In particular, Fiorentino et al. in 1982 [10] as well as Matteini and Moles in 1982 [11] and 1997 [12] highlighted that two

different degradation processes can be distinguished: one due to corrosion phenomenon and one due to deposition phenomenon. For the first case, one can assume that the beginning of the process may be due to the electrochemical attack created by the couple gold/copper in which the copper works as the cathode and the gold as the anode: if an electrolyte is present (for example the water due to the condensation of the humidity present in the atmosphere), the oxidation of copper and of the other components of the bronze occurs, forming copper oxides and other oxidation products of the metals composing the alloy. These compounds accumulate at the gold/alloy interface forming a primary patina. Subsequently, due to water condensation phenomenon that favour the contact between the patina and the aggressive nitrogen and sulphur oxides present in the urban atmosphere, primary copper oxides transform in more soluble sulphates and nitrates. The beginning of the process occur in presence of discontinuities in the gilding, where the salt crystallization and the subsequent volume growth determines micro-lifting of the gold layer, and, in many case the breaking of the gilding itself. Due to that, a small crater, pustule, in which accumulates corrosion products is formed. Finally, the continuous and periodical phenomena of solubilisation and migration of copper salts through the gold porosities and the crystallization on top of the gold surface, cause the formation of crystalline aggregates and of the greenish thin layer.

In parallel with the corrosion processes, deposit and accumulation of particulate matter occur, favoured both by the condensation of humidity and by the presence of corrosion products on the surface. The surface become more reactive, and then more porous and rough.

These degradation phenomena result in the fact that the gold layer is no longer completely adherent to the bronze surface. Instead, it adheres to the new layer of oxides and salts products. This situation is extremely delicate and fragile because the salt crystallization determines both the lifting of the gilding, in form of bubble, and, as consequence of salt crystals expulsion, the opening of very small, but numerous, craters in the gold layer. This phenomenon, that cannot be controlled without restoration and preservation of the door, could lead to , during the time, the gradual and total loss of the gilding.

#### **1.3.4. The last restoration**

The results of the scientific investigations highlighted that the mechanical cleaning was to be avoided because the gold surface could be seriously and irremediably scratched and damaged. From another point of view, the removal of the deposited products was necessary both to satisfy the esthetical request as well as to save and preserve the artwork. Initially it was chosen to use chemical methods, that respect the integrity of the original surface, and, at the same time,



decontaminate the surface in a selective way, without altering the oxide and salts layer that acted as a support for the gold layer.

Fiorentino and co-workers in 1982 [10] reported a series of comparative tests of cleaning done initially on samples taken from the back of the panel of Joseph, to evaluate the effect of the procedure on the bronze surface, and then on three areas (7x7 cm<sup>2</sup>) of the gilding. The tests were performed using ionic exchange resins, trisodium EDTA and Rochelle salt (potassium sodium tartrate). The experiment, controlled by checking the cupric ion content, conductivity and pH of the washing solutions, showed that the three products removed selectively the superficial concretions without altering the metallic layer. Kinetic studies performed in the meanwhile by Matteini and Moles [13] highlighted that, while trisodium EDTA and ionic exchange resins showed a certain aggressiveness on copper oxides, that had to be preserved, the Rochelle salt had nearly no drawback, both in neutral and alkaline solution. After further tests a protocol for the cleaning had been set up; this protocol included baths with acetone, distilled water and neutral solution of Rochelle salt. This procedure was applied to the six panels detached during the flood.

After the restoration of these first 6 panels [14], in 1990 the whole door was removed from the Baptistery and replaced by a bronze copy: new alteration phenomena of the system gold/oxides/bronze manifested, with the formation of a thin greenish thin layer above the gold layer. The atmospheric humidity was sufficient to reactivate the process of galvanic corrosion. It was therefore decided to keep the artefact in a confined environment, i.e. in an inert atmosphere (nitrogen), protected from oxygen, and under controlled relative humidity levels using silica gel.

The restoration was resumed in 1996 when it was decided to remove the other gilded reliefs in order to perform the complete washing of the latter.

Between 1996 and 2000, some investigations were carried out [15] in order to determine the conservation state of some panels (Noah, Jacob's stories, and Moses) which included: identification of the deposits as well as the corrosion products on the gilding by XRD and FTIR techniques, analysis of the alloy and of the black crusts present on the gilding. The results, in agreement with those obtained in the 80's on the first panels analyzed (Joseph, Tales of Creation), show the presence of deposit products, such as cementing gypsum, and many phases attributable to corrosion of the bronze including those, dangerous, consisting of chlorides (nantokite, atacamite). Since 2000 a series of cleaning tests was started, according to a new approach that involved the use of the laser technology. After the unsatisfactory initial results due to the use of an instrument [16] that was not adapted, the HELEN CO<sub>2</sub> laser, that caused the partial melting of the deposit and corrosion products, the tests went on and the procedure was modified using a tool that would allow a better control of the heat: the QS-Nd: YAG laser [17, 18]. Several experiments were then performed on

the panel with the stories of Noah, combining compresses of Rochelle salts at different concentrations with the use of the laser [19]. The evaluation of the results, performed by microscopy and control of the washing solutions by ion chromatography, showed the effectiveness of the laser in the removal of deposits, promoting the adoption of an integrated procedure.

Currently, the cleaning of the artwork is finished and the restorers of the OPD are making the delicate reassembly of the door. Due to the not eliminable, highly destabilizing presence of corrosion products between gold and bronze, the door remains extremely sensitive to relative humidity and air pollutants and, if not protected in an adequate way, a rapid degradation might occur. For this reason an experimental plan which aims to investigate the possible methods of preservation of the door for exhibition to the public has been started in collaboration with the Politecnico di Milano. It aims principally at o guaranteeing at the same time safeguarding and good visibility of this so precious artwork.

## References

- [1] S. Siano, P. Bertelli, M. Miccio, F. Marinelli, **Studio sulla tecnica di fusione dei rilievi della Porta del Paradiso**, 2005
- [2] Salvadori Barbara (OPD), **Relazione sulla ricerca bibliografica preliminare nell'ambito del progetto "bronzi dorati"**
- [3] Walter Nicodemi, **Acciai e leghe non ferrose**, Zanichelli (2000)
- [4] Anna Maria Giusti (OPD), **Settore restauro Bronzi e Armi Antiche – Porta del Paradiso, bronzo e bronzo dorato**
- [5] M. Matteini, A. Moles, **Baptistry Panels degradation and cleaning procedure**, Proceedings of the International Conference of Digital Signal Processing – Part 3, Florence 2–5 September 1981, 52–61
- [6] E. Mello, P. Parrini, **Lorenzo Ghiberti, Storia di Giuseppe e di Beniamino, Storie di Adamo ed Eva – Stato di conservazione: esame di una microcarota**, Metodo e Scienza Operatività e Ricerca nel Restauro, Catalogo della Mostra Firenze 23 giugno 1982 – 6 gennaio 1983, Sansoni Editore, Firenze, 1982, 176–180
- [7] C. Panseri, M. Leoni, **Relazione delle indagini metallografiche effettuate sulla Porta del Paradiso di L. Ghiberti del Battistero di Firenze danneggiata dall'alluvione del 4 novembre 1966**, Istituto Sperimentale dei Metalli Leggeri, Milano, rapporto n. 17918 del 5 aprile 1968
- [8] G. Dassù, G. Piazzesi, G. Alessandrini, **Problemi di conservazione delle Porte del Battistero di Firenze**, Atti del XXIX Congresso Nazionale A.T.I., Firenze, Settembre 1974
- [9] G. Alessandrini, G. Dassù, P. Pedeferra, G. Re, **On the conservation of the baptistry doors in Florence**, Studies in Conservation, 24 (1979), 108–124
- [10] P. Fiorentino, M. Marabelli, M. Matteini, A. Moles, **The condition of the "Door of Paradise" by L. Ghiberti. Tests and proposals for cleaning**, Studies in Conservation, 27 (1982), 145–153
- [11] M. Matteini, A. Moles, **Bassorilievi in Bronzo dorato della Porta del Paradiso. Firenze Battistero**, Catalogo della Mostra Firenze 23 giugno 1982 – 6 gennaio 1983, Sansoni Editore, Firenze, 1982, 168–198
- [12] A. Giusti, M. Matteini, **The gilded bronze Paradise Doors by Ghiberti in the Florence Baptistry – Scientific investigation and problems of restoration**, Proceedings of the International Conference on Metal Restoration, German National Committee of ICOMOS, Munich, 1997, 47–51
- [13] M. Matteini, A. Moles, **Kinetic control of the reactivity of some formulations utilized for the cleaning of bronze works of art**, ICOM Committee for Conservation 6<sup>th</sup> Triennial Meeting, Ottawa 1981, 81/23/4

[14] Archivio OPD: schede S74.6 – 10

[15] Archivio OPD: schede S74.11 – 15

[16] Archivio OPD: schede S74.16

[17] M. Matteini, C. Lalli, I. Tosini, A. Giusti, S. Siano, **Laser and chemical cleaning tests for the conservation of the Porta del Paradiso by Lorenzo Ghiberti**, *Journal of Cultural Heritage*, 4 (2003), 147s–151s

[18] S. Siano, R. Salimbeni, R. Pini, A. Giusti, M. Matteini, **Laser cleaning methodology for the preservation of the Porta del Paradiso by Lorenzo Ghiberti**, *Journal of Cultural Heritage*, 4 (2003), 140s–146s

[19] Archivio OPD: schede S74.17 – 20

---

AIM OF THE THESIS

## 2 Aim of the thesis

The main goals of this work were to investigate thoroughly some aspects related to the corrosion of copper alloys artefacts, such as the stability of the patina under different environmental conditions, as well as to develop a tool for the monitoring of the corrosion rate of gilded bronzes. To study a quite complex system, such as corroded gilded bronze artefacts, a multi-analytical and pluridisciplinary approach is necessary. Different analytical techniques are required to characterize the corrosion products that develop between the gold and the bronze as well as their modifications while varying the environmental conditions and more particularly, the relative humidity.

Even if a prerequisite, the complete characterization of the corrosion products is not sufficient to understand the corrosion processes. It is also fundamental to be able to quantitatively evaluate the corrosion rate and the influence that the main environmental parameters have on it.

In the field of cultural heritage, it is of utmost importance to be able to monitor the state of conservation of an artwork in-situ and with non-destructive methodology. Electrochemical techniques such as linear polarization resistance and electrochemical impedance spectroscopy have been developed in the last decades for the in situ monitoring of metallic artefacts. Although the results obtained with these techniques are promising, they cannot be applied to the case of a bimetallic system, such as a gilded bronze, due to the complexity of the interpretation of the results. Therefore alternative solutions, such as galvanic sensors simulating corroded gilded bronzes, were chosen. The galvanic sensors can be exposed together with real gilded bronze artefacts under different environmental conditions and provide an estimation of the corrosion rate of the process occurring on real artwork.

The main goals of this work can be summarised as follows:

- Individuation of the best display solution for the “Porta del Paradiso” by Lorenzo Ghiberti.
- Development of a methodology for the accelerated artificial ageing of gilded bronze.
- Realisation of a tool for the monitoring of corrosion rate of gilded bronzes, such as galvanic sensors.
- Development of new methodologies for the preparation of artificial patinas.
- Evaluation of the stability of the artificial patina in different environmental.

---

EXPERIMENTAL

## 3.1 Preparation of artificial patinas

In order to prepare galvanic sensors able to simulate gilded bronzes and to be used for the measurement of the corrosion rate (Chapter 3.4), it was first of all necessary to develop an artificial patina of corrosion products on the bronze surface.

The techniques for artificial patination, although used since ancient times, are not easily accessible because many producers, both in industrial and handicraft field, are reluctant to reveal the secrets of their findings and methods of production. Then, even if the chemicals required are easily available, the method of application, such as timing, surface preparation, and so on, is often vague or even missing in the literature.

The principal methodologies of patination available in literature have been tested in a previous master thesis work [1] and the stability of the obtained patinas studied in different environments.

Some of these methodologies [2-4] have been tested for the preparation of the galvanic sensors presented in this work. The methodologies were chosen considering that the patina used for the preparation of galvanic sensors must have some specific characteristics, listed below:

- **Composition:** it has to be similar to the one that can be found on real objects. Due to the high variability of compositions that could be met on real object, during the first stage of the research, the main focus was to obtain a patina with a composition similar to the corrosion products found on the surface of the Porta del Paradiso [5] (Paragraph 1.4.2) (copper chlorides and sulphates). Subsequently also patinas of different composition, such as brochantite ( $\text{Cu}_4\text{SO}_4(\text{OH})_6$ ), mimicking other type of corrosion have been prepared.
- **Thickness:** the patina used for the galvanic sensors must be thick enough to avoid any short circuit between gold and bronze layers. The thickness of the patina, however, influences the durability of the galvanic sensors and the macrocouple current that can be supplied by the sensors. A thin layer of patina is preferable to achieve both durable sensors and an high macrocouple current.
- **Homogeneity:** the patina has to be homogeneous on the whole surface of the sample. This allows to obtain more reproducible sensors and to avoid holes that can be the cause of short-circuits between gold and bronze
- **Adhesion to the substrate:** the patina must have a good adhesion to the substrate. This in order to obtain more durable and reproducible sensors.
- **Resistance:** to allow the measurement of the macrocouple current the patina must offer a quite high resistance to the current flow. This will assure that just a negligible part of the



macrocouple current flows through the patina; therefore all the macrocouple current can flow through the zero resistance ammeter used for the monitoring. In the other hand, if the resistance is too high (e.g. too thick patina or too dry), the galvanic coupling could not work properly.

In the following part all the methodologies that have been tested and used for the realisation of the artificial patinas will be described in detail.

### 3.1.1 Chemical patination

The chemical method is one of the simplest methods to obtain patinas on metal surfaces. It consists of the reaction of the metal in appropriate solutions containing chemical species that are selected depending on the desired patina.

This method has been used during this research project to produce a cuprite ( $\text{Cu}_2\text{O}$ ) layer on the surface of the metal.

Other recipes were also tested in order to verify if with this methodology patinas constituted by atacamite ( $\text{Cu}_2(\text{OH})_3\text{Cl}$ ) and brochantite ( $\text{Cu}_4\text{SO}_4(\text{OH})_6$ ) and with the previously described characteristics could be obtained.

#### 3.1.1.1 Cuprite patina

Two different recipes were taken from “*The colouring, bronzing and patination of metals*” of Hughes and Rowe [2]. They were used to obtain a thin and adherent layer of cuprite on copper and bronze.

- Cuprite on bronze – Recipe 1.3 [2]: dipping of the samples, previously degreased using ethanol, in a boiling solution of copper sulphate pentahydrate ( $\text{CuSO}_4 \cdot 5\text{H}_2\text{O}$ ), 25 g/L, followed by rinsing in boiling demineralised water and drying in air.
- Cuprite on copper – Recipe 3.3 [2]: dipping of the samples, previously degreased using ethanol, in a boiling solution of copper sulphate pentahydrate ( $\text{CuSO}_4 \cdot 5\text{H}_2\text{O}$ ), 6.25 g/L, copper acetate monohydrate ( $\text{Cu}(\text{CH}_3\text{COO})_2 \cdot \text{H}_2\text{O}$ ), 1.25 g/L, sodium chloride ( $\text{NaCl}$ ), 2 g/L and potassium nitrate ( $\text{KNO}_3$ ), 1.25 g/L, followed by rinsing in boiling demineralised water and drying in air.

The obtained patinas are quite stable and adhere well to the metallic surface. The patina looks uniform over the surface of the sample as it can be observed in Figure 1.



**Figure 1: Layer of cuprite on copper prepared following recipe 3.3 [2].**

### **3.1.1.2 Atacamite patina**

To obtain a layer of atacamite ( $\text{Cu}_2(\text{OH})_3\text{Cl}$ ), a common corrosion product that, in marine environment, spontaneously forms on copper alloys artefacts, a solution of sodium chloride, 35 g/L has been used.

Three specimens of copper,  $4 \times 2 \text{ cm}^2$ , previously covered by a layer of cuprite, have been left immerse for one, two and three weeks, respectively, in the 3.5% sodium chloride solution. After the period of immersion the samples were examined by optical microscopy and FTIR spectroscopy. The final aspect of all the three samples was similar: numerous and densely well distributed crystals could be observed on all the surface (Figure 2). However their quantity is not sufficient to create an homogeneous and compact layer suitable for the preparation of galvanic sensors, i.e. that can separate in an appropriate way the gold and the copper alloy to avoid short circuit.

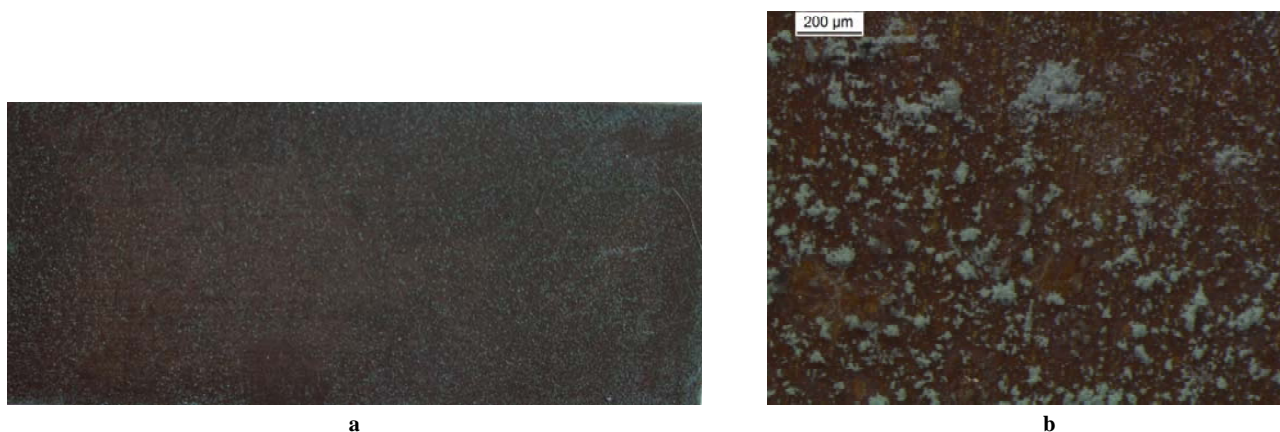


**Figure 2: Atacamite crystals observed using stereo-microscopy.**

The crystals formed on the surface were removed using a scalpel and analysed by FTIR: the resulting spectra were similar for all the three samples as presented on Figure 3.

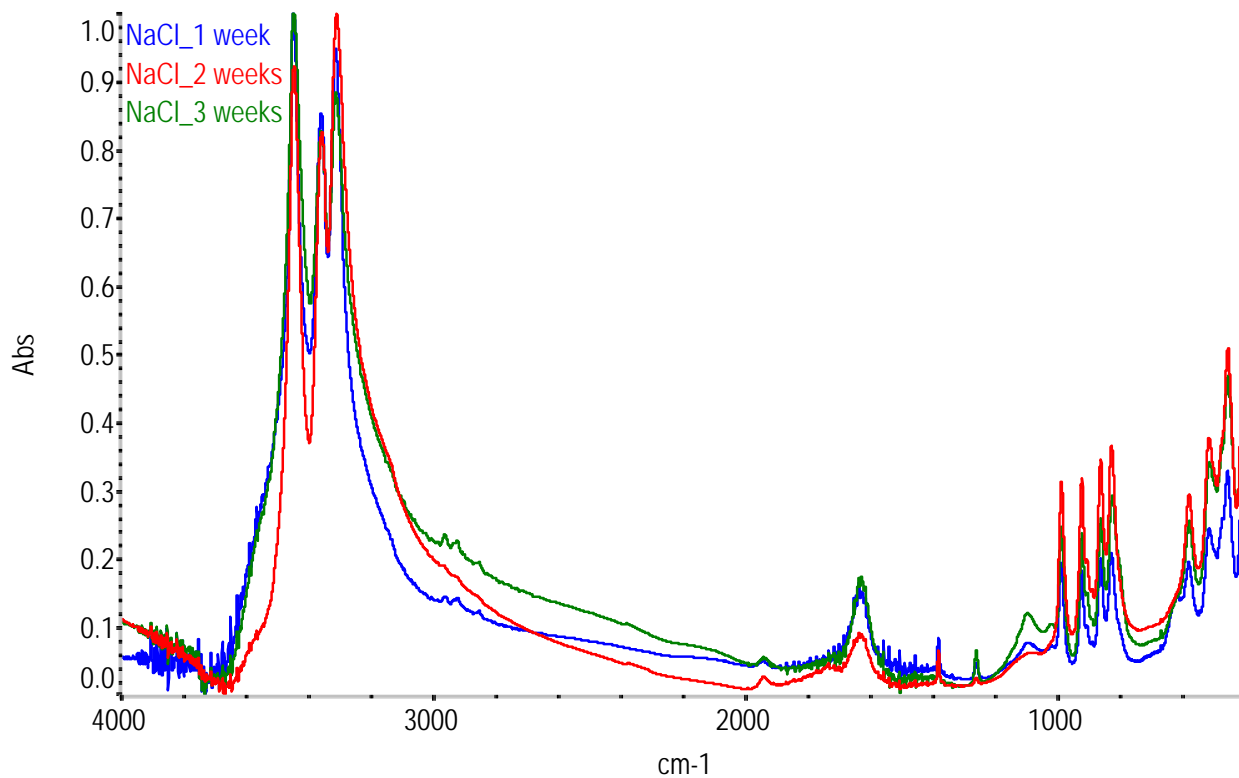


**Figure 3: Comparison of the FTIR spectra obtained for the crystals collected on the three samples immersed in 3.5% NaCl solution.**

The spectra were then compared with the atacamite and paratacamite standard references: the best matches were found with the paratacamite ( $\text{Cu}_2(\text{OH})_3\text{Cl}$ ) reference spectrum (Figure 4). Atacamite and paratacamite differ only in their respective crystalline lattice.

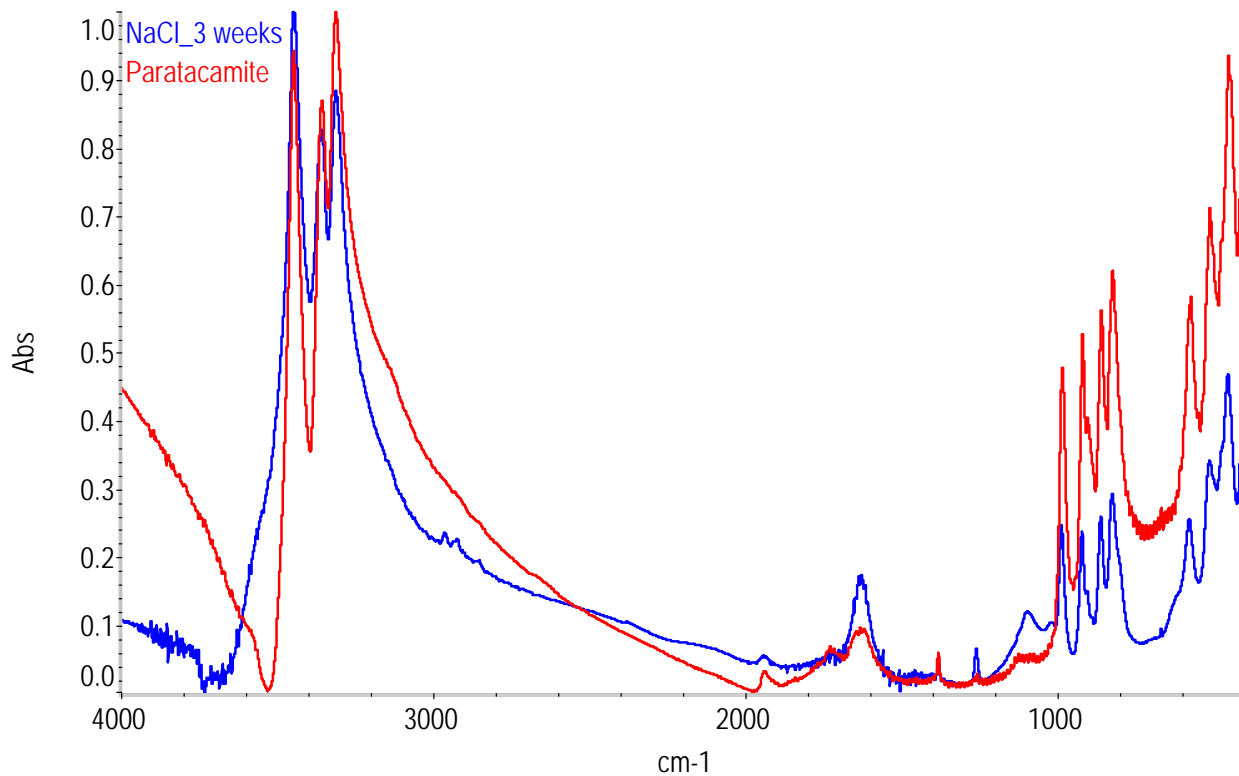


**Figure 4: Comparison between the FTIR spectrum of the sample and the paratacamite reference spectrum.**

This method allows to obtain a basic chloride patina, mainly constituted by paratacamite. However it is not suitable to develop galvanic sensors due to the fact that the patina layer is not uniform enough and too thin. It's possible that, with longer immersion time, the patina could reach the required thickness. This option was not further investigated because the time required for the realization of the patina was not considered as acceptable in the context of the present research project.

### 3.1.1.3 Brochantite patina

To obtain a layer of brochantite, which is the most common corrosion product on the copper alloys artefacts in urban environment, a solution of artificial rain has been used. The composition of the artificial rain corresponds to the atmosphere of Bologna, and the components taken from Reference [6] are reported in Table 1.

**Table 1: Composition of the artificial rain used for the preparation of brochantite patina [6]**

CaSO <sub>4</sub> ·5H <sub>2</sub> O	1.443·10 <sup>-3</sup> g/L
(NH <sub>4</sub> ) <sub>2</sub> SO <sub>4</sub>	1.504·10 <sup>-3</sup> g/L
NH <sub>4</sub> Cl	1.915·10 <sup>-3</sup> g/L
NaNO <sub>3</sub>	1.513·10 <sup>-3</sup> g/L
HNO <sub>3</sub> 65%	3.93 μL/L
CH <sub>3</sub> COONa	0.319·10 <sup>-3</sup> g/L
HCOONa	0.083·10 <sup>-3</sup> g/L

Six specimens of copper, 4x2 cm<sup>2</sup>, previously covered by a layer of cuprite, have been used for the testing this procedure, with two different methodologies: three of them have been left immerse for one, two or three weeks respectively in artificial rain solution, while the other three samples underwent to a “wet and dry” procedure. The latter consisted in extracting the samples twice a day and letting them dry for one hour each time, before re-dipping them. The samples have been observed using a stereomicroscope and analysed by FTIR spectroscopy after one, two and three weeks of treatment.

The aspect of the samples was different depending on the treatment and the duration of application. The samples immersed continuously presented on the surface some powdery compounds and few crystals, as observed in Figure 5. The quantity and the thickness of the compounds grown on the surface increase during the weeks, but not the distribution on the surface. Some areas of the samples remained nearly uncovered.

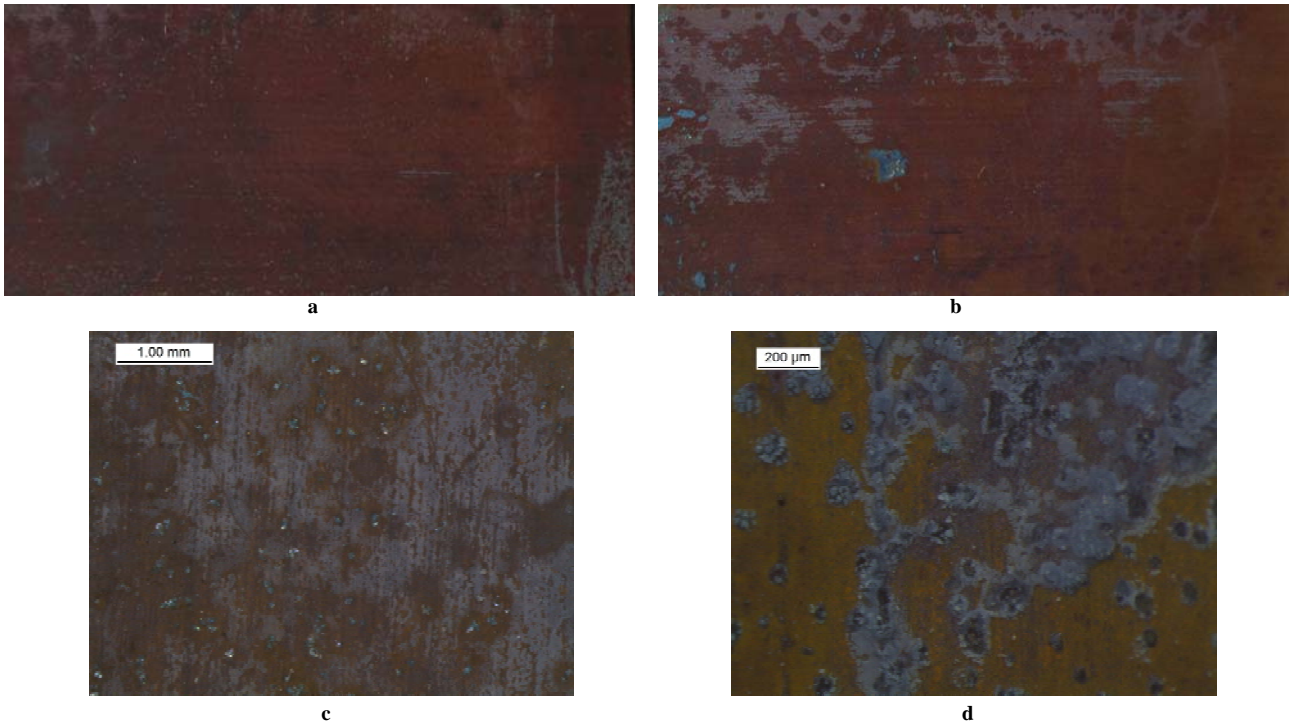


**Figure 5: Macro and stereomicroscope images of the surface of the sample immersed for one week (a) (c) and for three weeks (b) (d).**

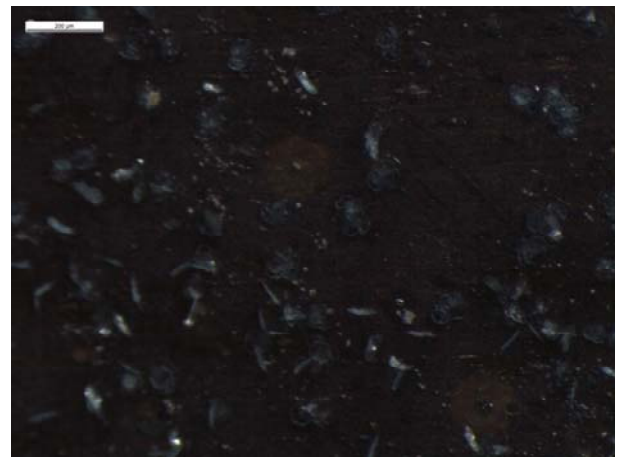
On the contrary, the samples treated with the “wet and dry” procedure developed numerous green crystals, nucleated on the whole surface. In the case of the samples treated for 2 and 3 weeks, also a dark patina developed in some areas of the surface, as observed in Figure 6.



a



b



c

**Figure 6: Macro (a) and stereomicroscope (b) (c) images of the dark patina formed on the sample treated with “wet and dry” procedure in artificial rain for 3 weeks.**

After one, two and three weeks of “wet and dry” or continuous procedure, the crystals formed on the surface of the samples have been removed and analyzed by FTIR spectroscopy: no differences have been observed on the spectra of the different samples, despite the different methodology and duration of treatment, as revealed by the spectra in Figures 7 to 9.

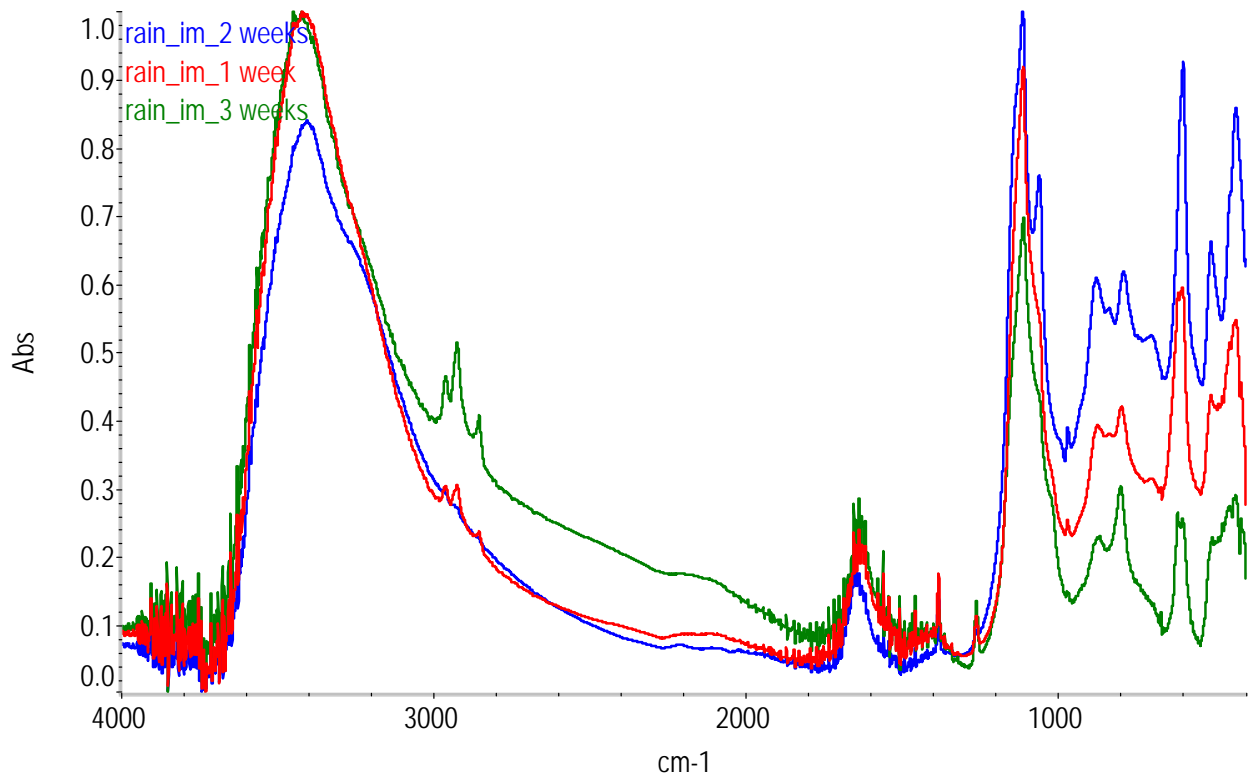


**Figure 7: Comparison between FTIR spectra of the three samples immersed in artificial rain solution.**

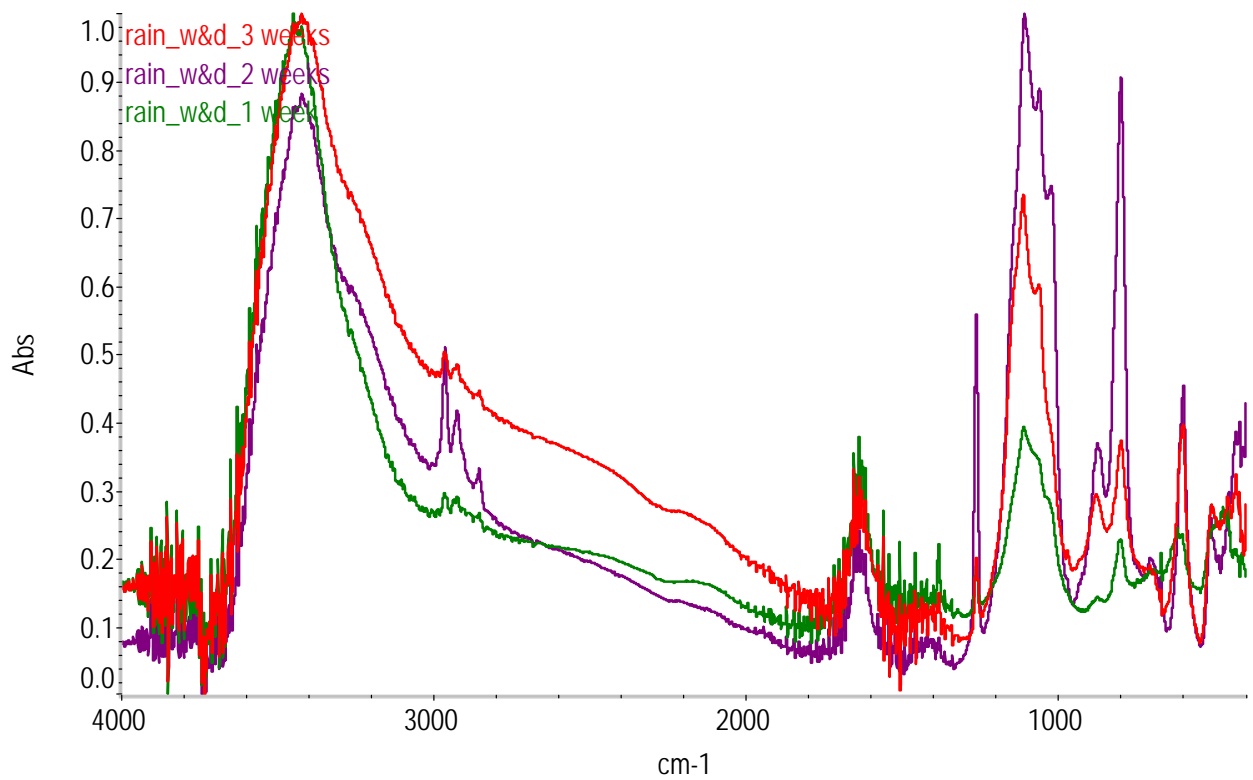


**Figure 8: Comparison between FTIR spectra of the three samples treated with “wet and dry” procedure in artificial rain solution.**

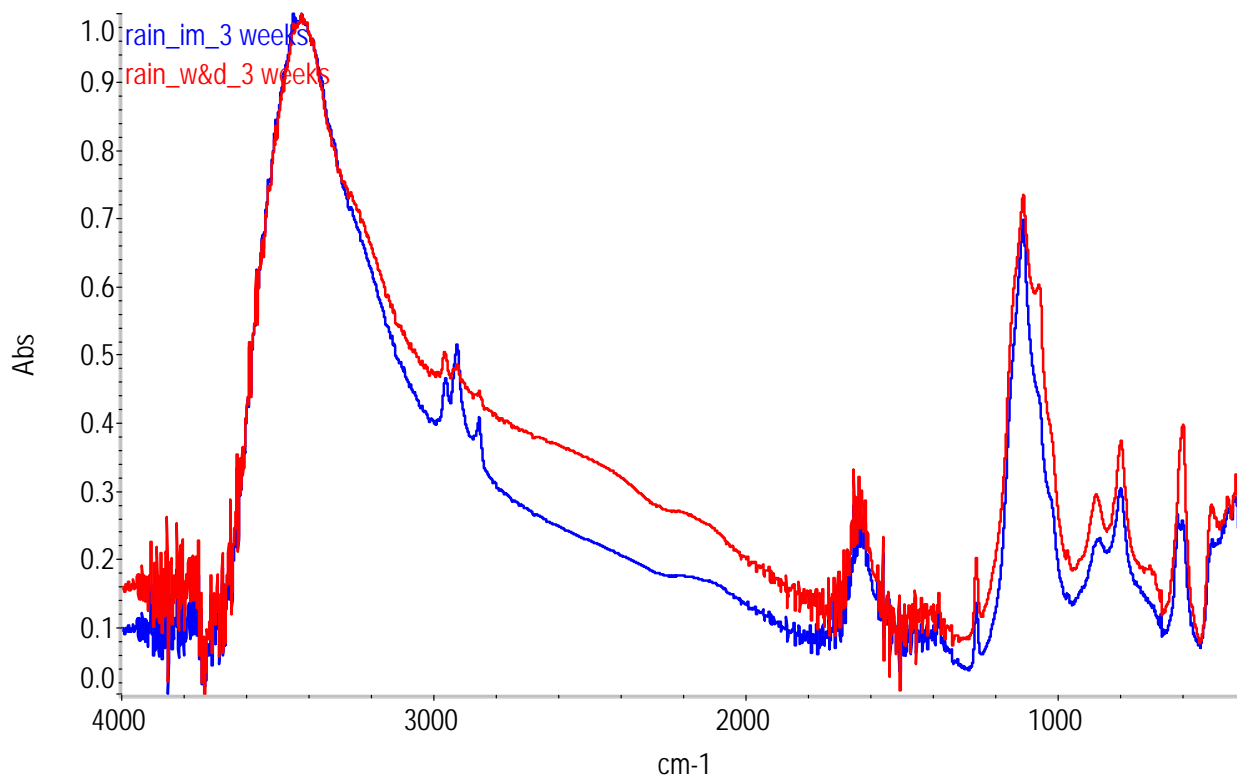


**Figure 9: Comparison between FTIR spectra of the samples treated with immersion and “wet and dry” procedure in artificial rain solution.**

The presence of brochantite was identified in the spectra of the samples obtained using the two procedure as can be observed in Figures 10 and 11. In particular the strong peak of sulphates around 1100 cm<sup>-1</sup> is clearly visible. The spectra exhibit some peaks that have not been attributed to identified species yet.

No evidence of the growth of chloride salts can be deduced by the FTIR spectra, even if chlorides are present in the artificial rain solution.



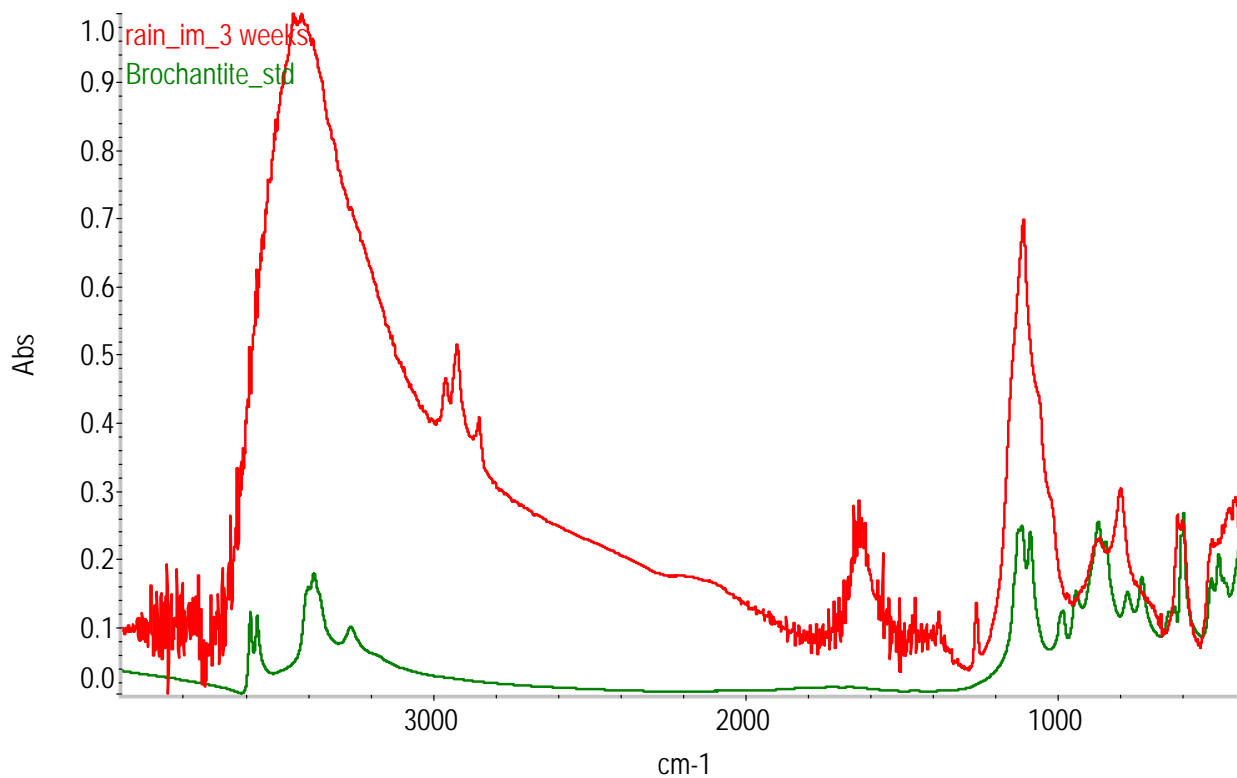


**Figure 10: Comparison between the FTIR spectrum of the sample immersed in artificial rain for 3 weeks and the standard reference spectra of brochantite.**

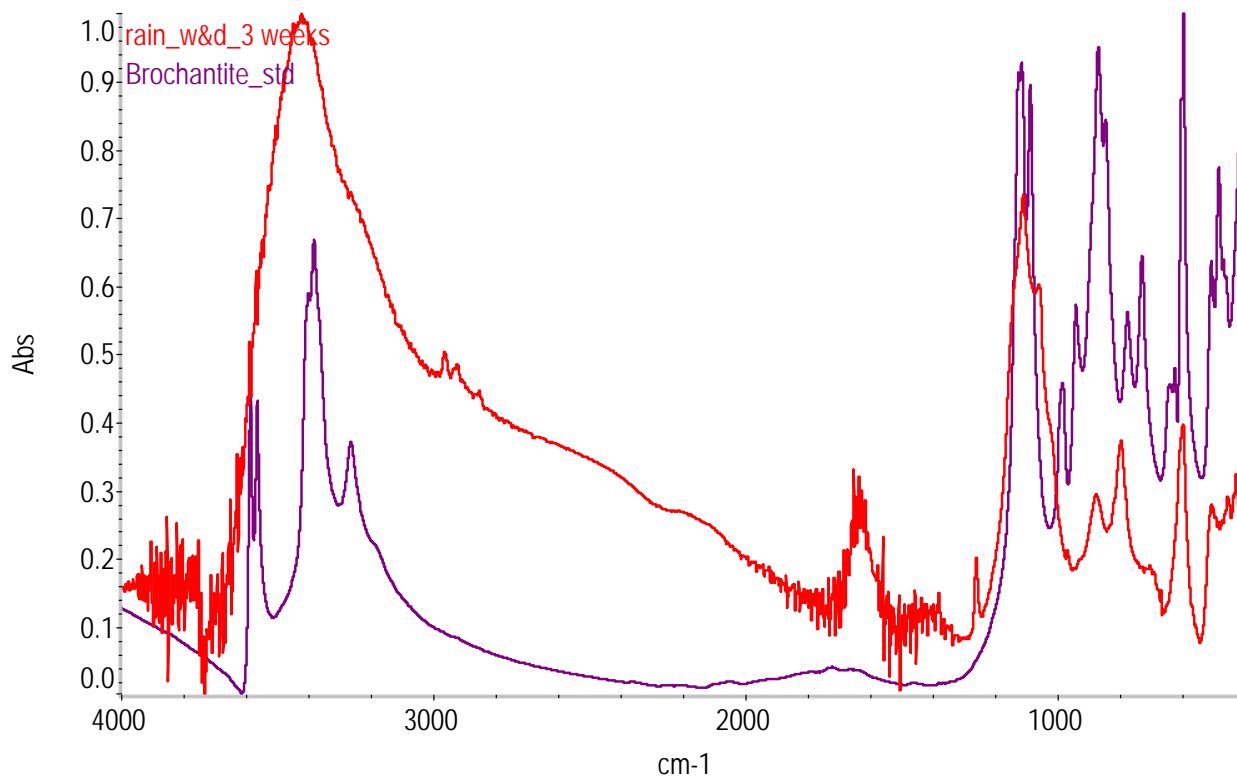


**Figure 11: Comparison between the FTIR spectrum of the sample treated with the wet and dry procedure in artificial rain for 3 weeks and the standard reference spectra of brochantite.**

The chemical patination revealed to be an appropriate method for the realisation of galvanic sensors only in the case of the preparation of the cuprite patina, that was used, as it will be described in Paragraph 3.4.2, as preparation layer for the realisation of the “gold leaf sensors”. Indeed, for the preparation of copper chloride and copper sulphate patinas the results are not satisfactory because the obtained patinas are not homogeneous and too thin.

### **3.1.2 Electrochemical patination**

In order to obtain, in a shorten time, thicker layers of artificial corrosion products it is possible to accelerate the process by carrying out an electrochemical artificial patination. In this case, the patina is achieved by imposing a difference of potential between an anode and a cathode. The use of an electrolytic solution containing specific chemical species allows to obtain patinas of different chemical composition.

There are many recipes for the production of patinas by using electrochemical method. In the context of this research project, the purpose was to obtain a patina of chemical composition similar to the one that formed on the bronze surface of the “Porta del Paradiso”.

#### ***3.1.2.1 Beldjoudi – Constantinides method***

On the basis of the results obtained in a previous master thesis work [1], a technique has been used that allows to obtain on bronze the same compounds present in the patina of the abovementioned door: copper oxide (cuprite), copper hydroxi-sulphate (brochantite) and copper chlorides (nantokite, atacamite, paracatamite). Therefore it was decided to test this technique on samples of quaternary bronze with composition similar to the one of the Porta del Paradiso.

This method was developed by Beldjoudi, Constantinides et al. [3, 7] and is called in this text “Beldjoudi – Constantinides method”. The authors discovered that a solution containing the species known as corrosion responsible (chloride, sulphate and hydrogenocarbonate) was created by the American Society for the Testing of Materials and it is referenced as ASTM D 1384. Moreover, it was proved that a ten times concentrated ASTM D1384 solution develops ionic activity and corrosion phenomena. Beldjoudi – Constantinides drawn up an experimental protocol, divided into the following two stages:

1. *Phase A*: 0.1 M Na<sub>2</sub>SO<sub>4</sub> solution, anodic potential 40 mV/SCE polarization for 7 days.
2. Drying in air.
3. *Phase B*: ASTM D1348 solution with added carbonates (0.01 M Na<sub>2</sub>SO<sub>4</sub>, 2.8·10<sup>-2</sup> M NaCl, 16.1·10<sup>-2</sup> M NaHCO<sub>3</sub>), anodic potential of 350 mV/SCE for 8 days.

4. *Phase C*: ASTM D1348 solution with added carbonates (0.01 M Na<sub>2</sub>SO<sub>4</sub>, 2.8·10<sup>-2</sup> M NaCl, 16.1·10<sup>-2</sup> M NaHCO<sub>3</sub>), anodic potential of 850 mV/SCE for 3 days.
5. Rinse in deionised water to remove corrosion products not adhering to the substrate.
6. Drying in air.

The first stage corresponds to the selective formation of cuprite (Cu<sub>2</sub>O). The second stage allows the formation of more complex compounds, including chlorides, carbonates and sulphates.

### Morphology

The patina obtained at the end of the treatment is thick and green. However, its aspect is highly inhomogeneous. The surface of each sample shows significant morphological differences that are due to the formation of overlapped layers of corrosion products and to the resulting different adhesion conditions between them.

By stereo-microscopy three different layers of corrosion products can be distinguished (Figure 12):

- *Layer A*: layer of cuprite in contact with the metallic surface, visible to the naked eye only in a limited number of samples.
- *Layer B*: white-green layer, above the cuprite, with features ranging from compact to powdery depending on the degree of the corrosion process (Figure 13).
- *Layer C*: thick, continuous, homogeneous, hard but brittle, superficial layer which can be considered the last step in the evolution of the previous layer. This layer has two different colours, green or red, depending on the sample (Figure 14).

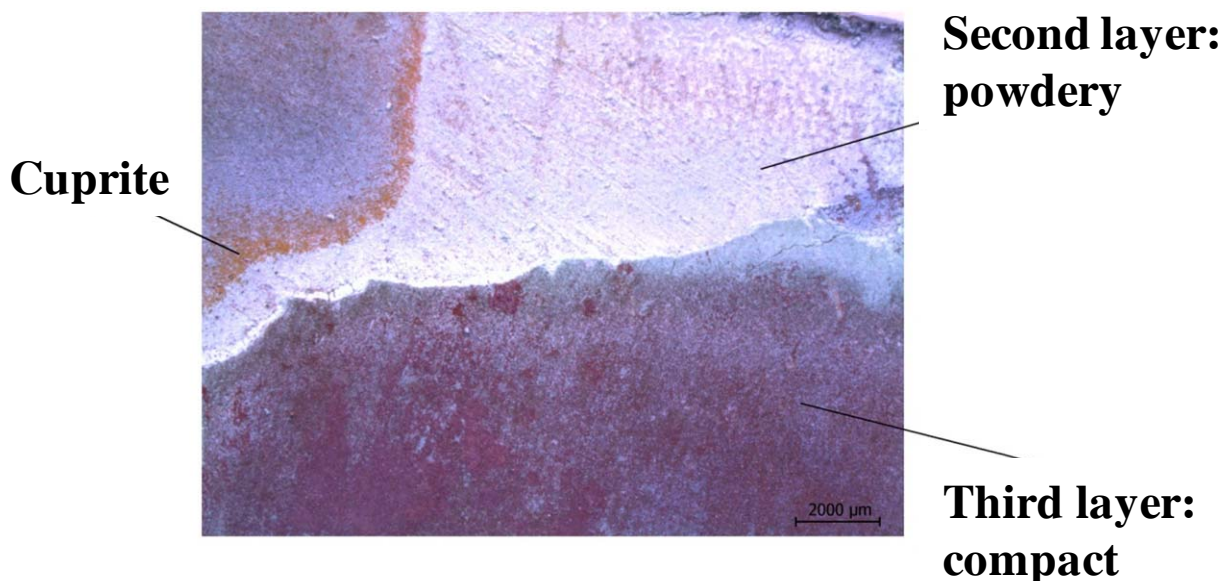


**Figure 12: Microscopic appearance of three different layers of the patina obtained by Beldjoudi – Constantinides electrochemical method: the reddish bottom layer of cuprite, white - green powdery middle layer, red and/or green compact layer on the top.**



**Figure 13: Evolution of the growth of the second layer of corrosion products: compact layer on the top and powdery part (circumscribed by a red line).**

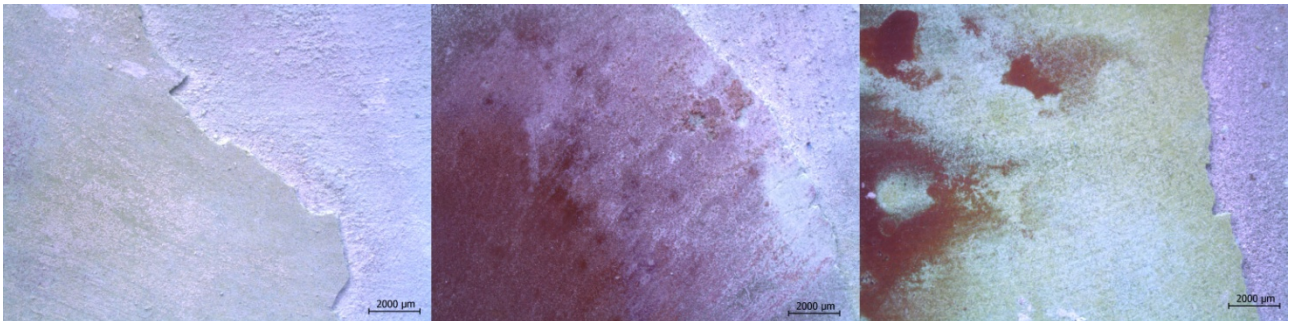


**Figure 14: Different superficial layer of patina: green (left), red (centre), mixed green - red (right).**

It is obvious that the corrosion products may grow in complete different ways, as shown in Figure 15.

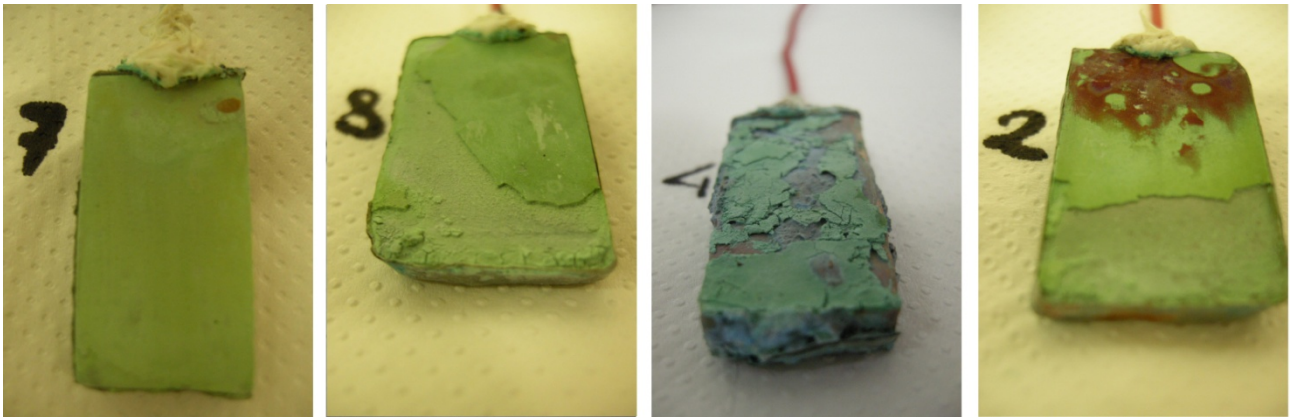


**Figure 15: Morphological inhomogeneities of the patina in some samples obtained by electrochemical patination.**

Analysis of the chemical composition of the patina

XRD analysis of the patina obtained by the Beldjoudi – Constantinides electrochemical method (Figure 16) shows that this technique allows to obtain a patina with a chemical composition similar to the one expected.

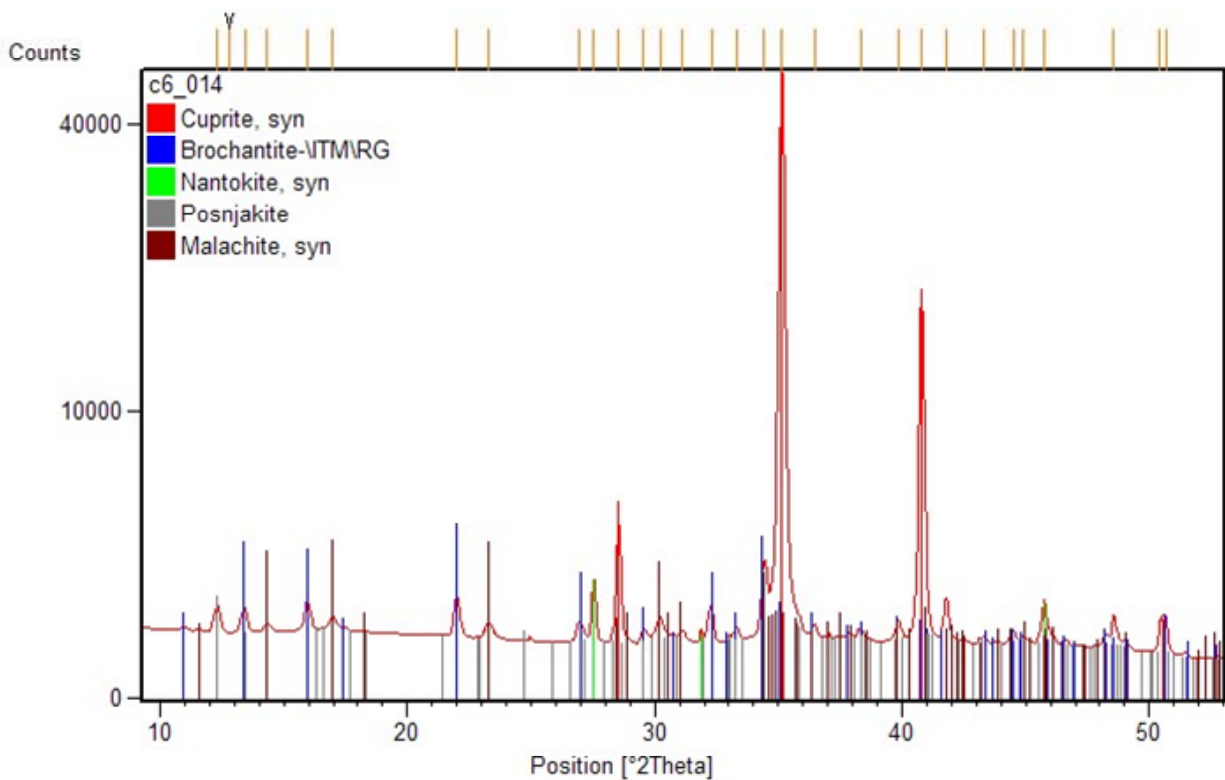


**Figure 16: XRD diffractogram of the patina obtained with the Beldjoudi – Constantinides method.**

At the end of the procedure, a thick layer of copper mineral can be obtained. The solution used for the patination contains carbonates, sulphates and chlorides, and allows the formation of brochantite,

posnjakite, malachite and nantokite over a layer of cuprite, obtained in the Phase A. This procedure, however, as a drawback, leads to a certain deterioration of the sample.

### **3.1.2.2 Vernon method**

Another electrochemical patination technique tested was the one proposed by Vernon [4]. This method was also the one used by Professor Pietro Pedferri to obtain artificial patinas on the galvanic sensors used in the studies of the Porta del Paradiso in the late 70's [8, 9]. This technique consists in imposing a current of  $2.7 \text{ A/cm}^2$  in a  $0.5 \text{ M Na}_2\text{SO}_4$  solution. The samples used for these tests, made of the quaternary bronze alloy (Paragraph 1.4.2), with a surface of  $9 \text{ cm}^2$  ( $2 \text{ cm} \times 4.5\text{cm}$ ). That corresponds to the following electrical parameters:

- current: 0.3 A
- potential: 1.2 V vs. SCE

#### Morphology

Figure 17 shows the aspect of the patina obtained with the Vernon method. The surface is not homogeneous at all; in the same way, the other required characteristics for the realisation of galvanic sensors are not fulfilled and the reproducibility is even lower compared to the Beldjoudi – Constantinides electrochemical method. Sometimes thicker and compact, sometimes thinner patinas are obtained. In all the cases, however, the patinas appear to be really fragile. This last characteristic is particularly negative and the present method has been rejected as a candidate for patination technique of the galvanic sensors.



**Figure 17: Superficial appearance of the patinas obtained with the Vernon method.**

### Analysis of the chemical composition of the patina

The spectrum collected by FTIR spectroscopy (Figure 18) shows that with the Vernon method there is a possibility to obtain copper sulphates. The exhibited peaks at 1633, 1113 and 619  $\text{cm}^{-1}$  are characteristic of these chemical species.

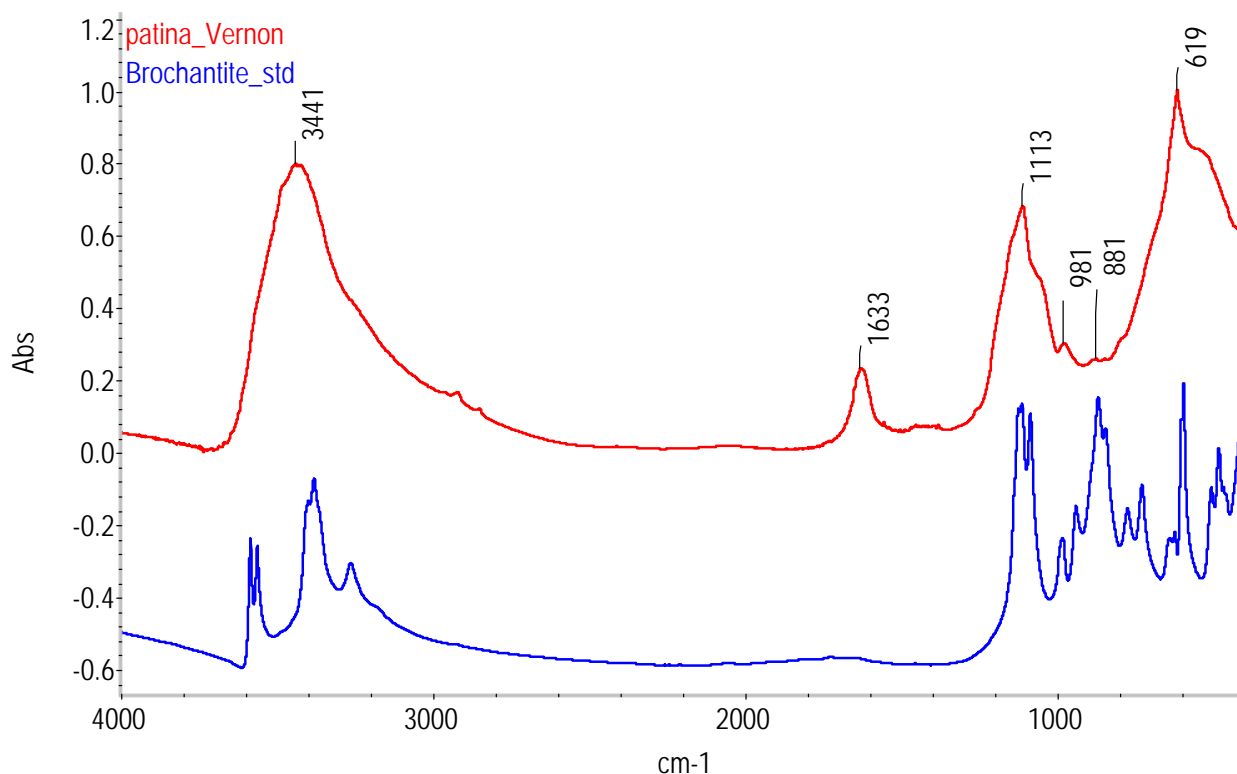


**Figure 18: FTIR spectrum of the patina obtained with Vernon method compared to the one of brochantite mineral standard reference.**

As in the case of chemical patination, both the tested electrochemical methods are not suitable for the realisation of galvanic sensors. The patina obtained with these methods, in fact, are not adherent enough to the metallic substrate and quite often inhomogeneous. Furthermore they proved to be too conductive. Few sensors were realised with the samples that presented a thick and adherent patina: for most of them the resistance of the patina layer was too low (about 10  $\Omega$ ).

### **3.1.3 Applied paste**

The method of application of a paste of copper salts is described in literature for the artificial patination by Hughes and Rowe [2].

For the preparation of the applied paste, the steps reported in literature have been followed thoroughly. The solid ingredients should be ground to a fine consistency using a pestle and mortar. The liquid components are then added, with continued grinding. The addition of liquids must be very gradual as the paste can easily become too thin. A thick creamy consistency is the most suitable [2] for the expected patinas.

Initially the composition that would be reproduced was that of the corrosion products found on the surface of the “Porta del Paradiso” (atacamite and brochantite). For this reason copper chlorides and sulphates were mixed together. Concerning the chlorides component, both cuprous and cupric chlorides were added. The nantokite ( $\text{CuCl}$ ) has been added because is the most instable and is suspected to be responsible of the corrosion phenomenon called “bronze disease”. The eriochalcite ( $\text{CuCl}_2 \cdot 2\text{H}_2\text{O}$ ) was added, in lower quantity, to favour the formation of atacamite ( $\text{Cu}_2(\text{OH})_3\text{Cl}$ ), which is a copper (II) mineral. Subsequently, also patinas with different composition, i.e. brochantite ( $\text{Cu}_4\text{SO}_4(\text{OH})_6$ ), have been prepared.

The recipes reported in literature [2] involve the use of chemical substances that react with the metallic surface to create the corrosion products. In this work, at the contrary, the corrosion products have been mixed together or synthesized on purpose *a priori* and only subsequently spread on the surface of metal. For the chloride rich patina, the starting products react with water to produce other chemical species, as revealed by the analytical characterization. In the case of brochantite patina, the corrosion product is synthesized before the mixture with water. In this way it is possible to completely control the composition of the patina applied on the metallic surface.

For the chloride rich patina, the ratio between the total amount of chlorides and the total amount of sulphates (in mass) has been kept constant, even if the absolute weight of these species was varied. Then a mixture  $\text{CuCl} - \text{CuCl}_2 \cdot 2\text{H}_2\text{O} - \text{CuSO}_4 \cdot 5\text{H}_2\text{O}$  (3:1:4) was finely ground in a mortar and mixed with water.

Different powder/water ration have been tested:

- 6 for the sensors used for the “Porta del Paradiso” monitoring. This P/W ratio allowed to obtain a thick patina. However the surface was too rough and the patina revealed to be too inhomogeneous and too reactive to RH variations due to its thickness.
- 4 for the preliminary “gold leaf sensors”.
- 1 for the final version of “gold leaf sensors”, that allow the production of a thinner and smoother patina.

Concerning the methodology of application of the paste, Hughes and Rowe suggest two different method. The sparingly application, repeated several times, using a soft cloth or the application using a brush [2]. However, the two methods proposed by the authors were not suitable for the purpose of this research project, i.e. patina for galvanic sensors, because the final thickness of the patina was not large enough to avoid the short circuit between bronze and gold.

After the mixing with the water the patina was then spread on the surface of the metal with a spatula and worked with the spatula to obtain a surface as smooth as possible.



Varying the quantity of powder per cm<sup>2</sup>, the water/powder ratio and the spreading on the surface, it's possible to obtain patinas with different thickness, depending of the foreseen use. The final aspect of the artificial patinas obtained with the applied paste method can be observed in Figure 19.

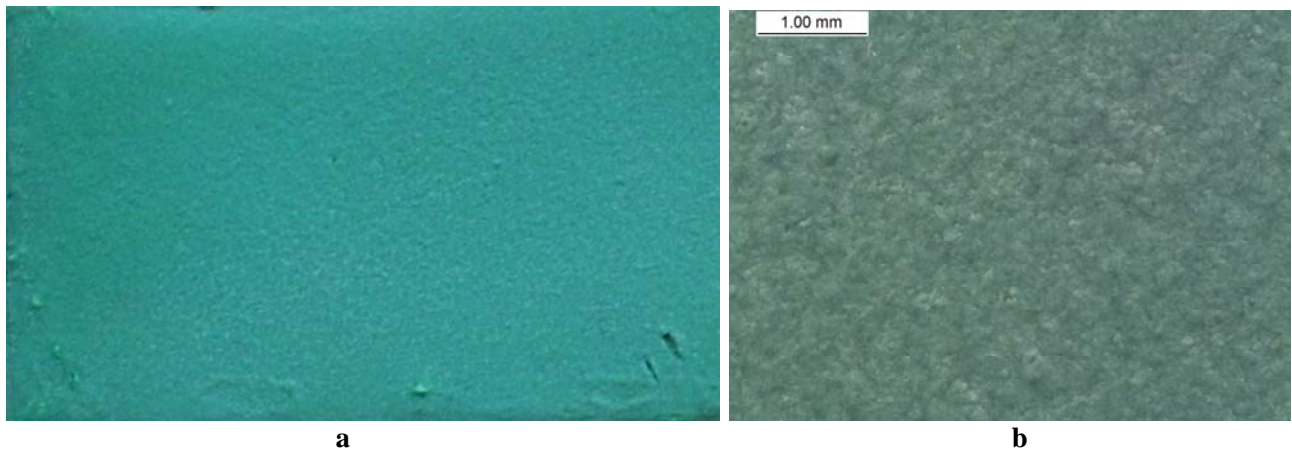


**Figure 19: Macro images of a brochantite patina (a) and stereomicroscope images of the chloride rich patina (b), both obtained with the applied paste method.**

The different patina that were obtained with this methodology were characterized using different analytical techniques to define their precise composition.

In Figure 20 and 21 the FTIR spectrum and the XRD pattern are reported of the patina obtained by mixing chlorides and sulphates, respectively. It can be observed by both techniques, that the copper sulphate doesn't react with water, while chlorides transform in atacamite (basic copper chlorides). Unreacted nantokite is found by XRD and makes the patina more reactive to the variations of relative humidity.

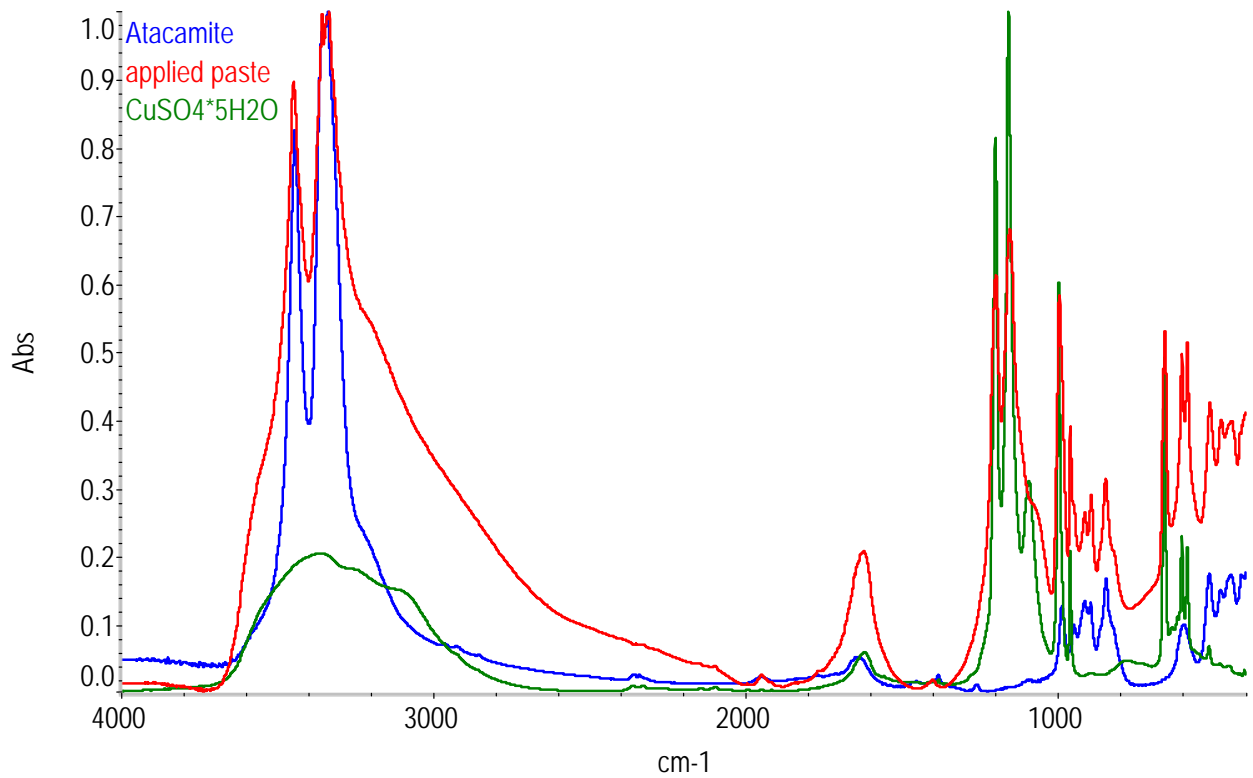


Figure 20: FTIR spectrum of the patina obtained by mixing copper chlorides and sulphate.

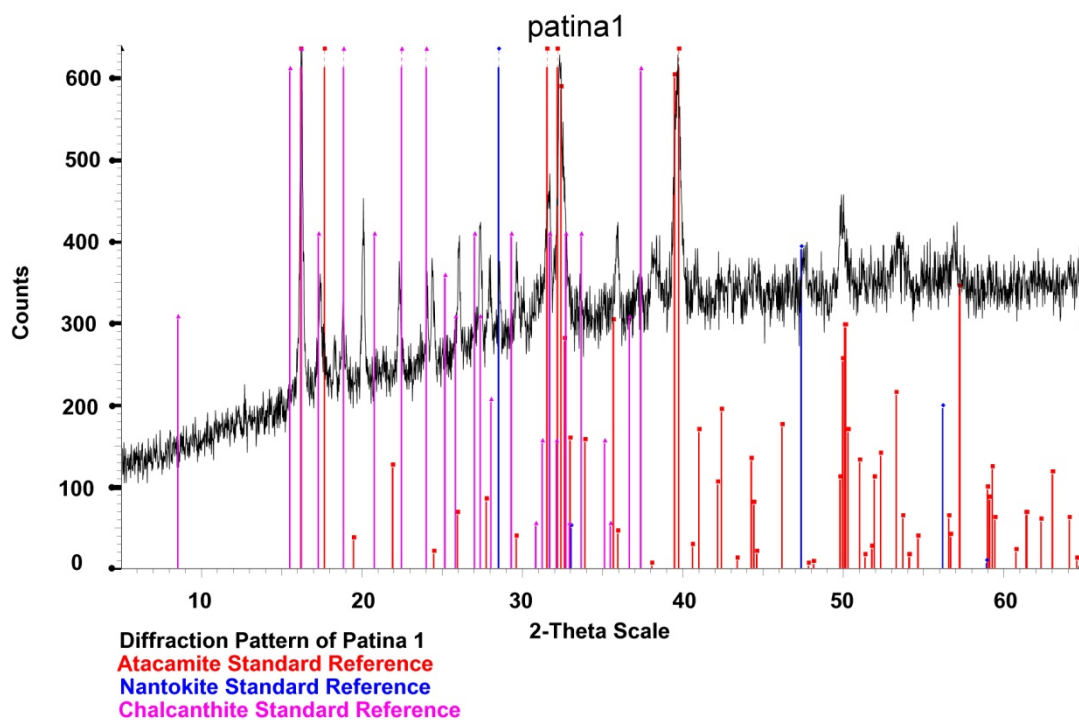
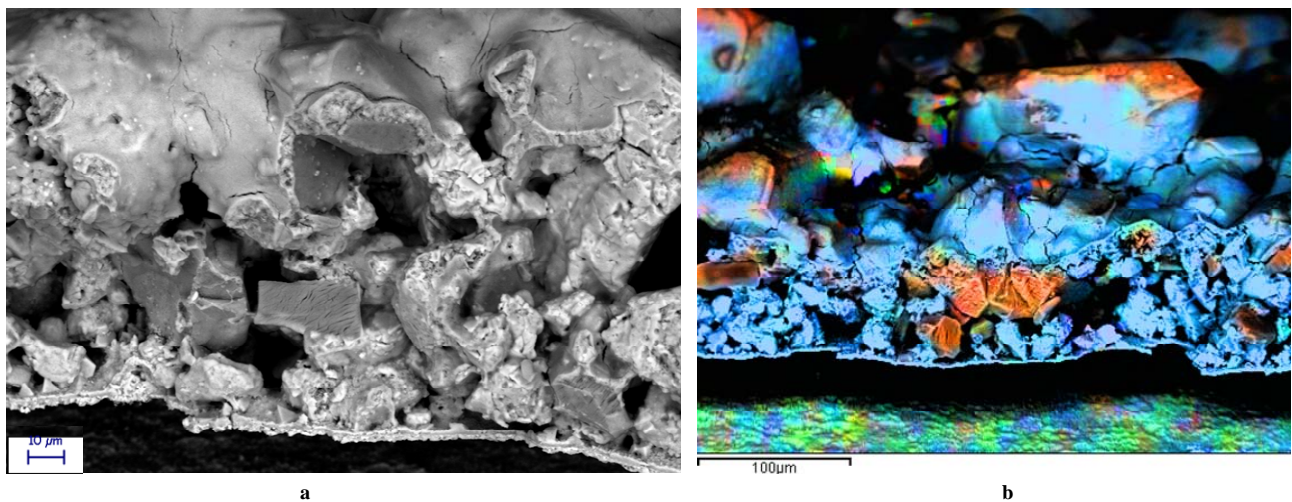


Figure 21: XRD pattern of the patina obtained mixing copper chlorides and sulphate.

The patina has been also characterized by SEM-EDX and it was possible to observe that the distribution in the depth of the patina is not homogeneous: copper sulphate tend to form bigger

crystals surrounded by copper chlorides (Figure 22). In Figure 22b, the SEM mapping of the patina is reported: in light blue the chlorides can be observed, while in orange are presented the sulphates.



**Figure 22: SEM image (a) and mapping of the patina obtained mixing copper chlorides and sulphate.**

The patina composition chosen for the first tests with applied paste represents the worst possible scenario for a corroded bronze artefact. Unfortunately this is the case of the Porta del Paradiso. In general there are many other bronzes and gilded bronzes that present other more stable corrosion layers. In particular, in urban environments, the brochantite is a very common compound of the patina on bronze artworks exposed to the atmosphere.

For these reason a patina composed by brochantite prepared. The first tests were performed mixing together copper sulphate and copper hydroxide with water. The chemical composition obtained was the one searched but the patina was powdery and not adherent to the substrate.

Subsequently, the brochantite was synthesised by using a recipe found in the literature [10]. Brochantite was precipitated by adding a 0.5 M copper sulphate solution (50 mL) at 60°C to a solution 0.1 M of sodium hydroxide (100 mL) at the same temperature. The mixture was stirred continuously and its pH was kept constant throughout the precipitation. The precipitate was aged in its solution overnight and washed with distilled water until the washing had a pH<7.0 [10]. The sample was then dried at 60°C. The obtained powder was mixed with water (powder/water ratio 0.5) and spread on the metallic substrate. In Figure 23 and 24 the FTIR spectrum and the XRD pattern, respectively, of the brochantite patina are reported. As one may notice, the correspondence between the artificial patina and the mineral standard reference is quite perfect.

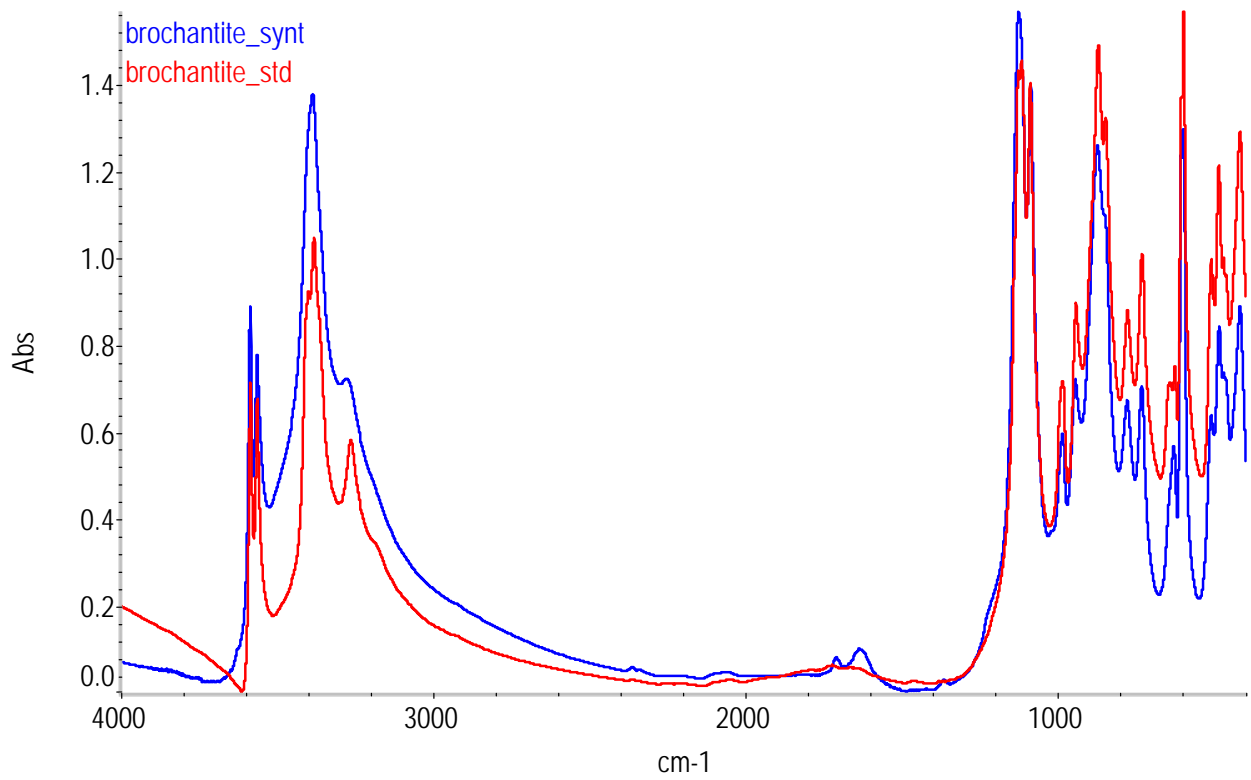


Figure 23: FTIR spectrum of the brochantite patina.

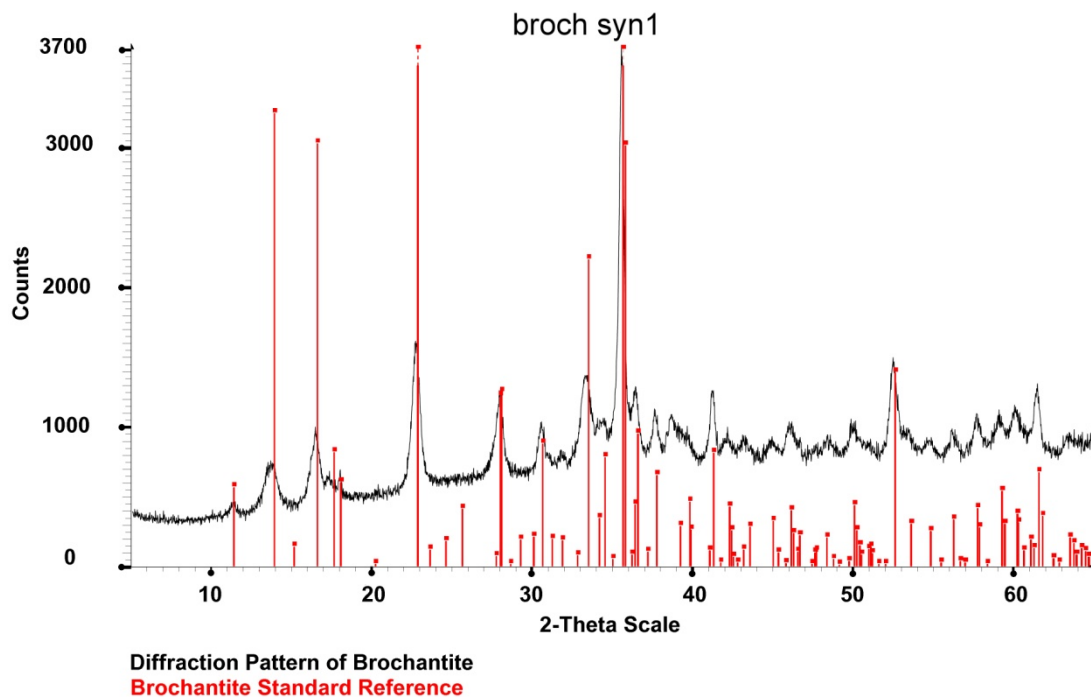


Figure 24: XRD pattern of the brochantite patina.

Among all the tested methodologies for artificial patination (i.e. Chemical, Electrochemical and Applied Paste), the Applied Paste method was the only one that could guarantee the obtainment of a

patina with all the required characteristics for the realisation of galvanic. Indeed, this methods allows the production of a reproducible, continuous and homogeneous patina, with a thickness that can be adjusted as desired. This is a fundamental requirement for the obtainment of reliable galvanic sensors, as it will be discussed in the following chapters of this thesis.

## References

- [1] Pintaudi M., Setti C., **Produzione e caratterizzazione di patine su rame e bronzo**, Politecnico di Milano - Biblioteca Campus Durando, 2005
- [2] Hughes R., Rowe M., **The colouring, bronzing and patination of metals**, Thames & Hudson, London (GB), 1991
- [3] T. Beldjoudi, F. Bardet, N. Lacoudre, S. Andrieu, A. Adriaens, I. Constantinides, P. Brunella, **Surface modification processes on European Union bronze reference materials for analytical studies of cultural artefacts**, La Revue de Métallurgie-CIT/Science et Génie des Matériaux Septembre 2001
- [4] W.H.J. Vernon, **The Open-air corrosion of copper. Part III. Artificial production of green patina**, J. Inst. of Metals, 49 (1932), 153–167
- [5] M. Matteini, A. Moles, **Baptistry Panels degradation and cleaning procedure**, Proceedings of the International Conference of Digital Signal Processing – Part 3, Florence 2–5 September 1981, 52–61
- [6] E. Bernardi, C. Chiavari, C. Martini, L. Morselli, **The atmospheric corrosion of quaternary bronzes: an evaluation of the dissolution rate of the alloying elements**, Applied Physics A, 2008
- [7] Constantinides, I., A. Adriaens, F. Adams, **Surface characterization of artificial corrosion layers on copper alloy reference materials**, Applied Surface Science, 189 (2002) 90-101
- [8] B. Mazza, P. Pedferri, G. Re, D. Sinigaglia, **Behaviour of a galvanic cell simulating the atmospheric corrosion conditions of gold plated bronzes**, Corrosion Sciences 17 (1977), 535-541
- [9] G. Alessandrini, G. Dassù, P. Pedferri, G. Re, **On the conservation of the baptistry doors in Florence**, Studies in Conservation 24 (1979), 108-124
- [10] S.V S. Prasad, V. Sitakara Rao, **Thermal analysis, X-ray diffraction and infrared spectroscopic study of synthetic brochantite**, Journal of Thermal Analysis and Calorimetry 30, 3 (1985) 603-609

## 3.2 Analytical techniques for the characterization of patinas

For the characterization of artificial patinas that were realised with copper and bronze corrosion products, several analytical techniques have been used.

### *FTIR spectroscopy*

The FTIR spectroscopy has been used to characterize the patinas artificially produced with all the methodologies tested in this work. This technique is fast, easy and cheap and allows to recognize the functional groups of copper salts. Thanks to the small amount of sample required for the analysis and to the rapidity of the measurements, this technique is ideal to perform the controls of the composition of the products formed during long time tests. In this work FTIR spectroscopy has been used, for example, to control the growth of corrosion products during chemical patination tests (Chapter 3.1).

FTIR analysis have been performed using a Thermo Scientific Nicolet 6700 spectrophotometer, in the spectral range between 4000 and 400  $\text{cm}^{-1}$ , with 4  $\text{cm}^{-1}$  resolution. 64 scans have been carried out both for the background and for the acquired spectrum.

KBr pellets of the samples of interest have been prepared in order to obtain spectra in transmission mode. The corrosion products have been removed from the metallic surface using a scalpel and then the powder has been finely grinded in an agate mortar with the KBr powder. Thus, the spectra obtained represent an average composition of the sample.

Compounds have been identified by comparison with spectra of pure minerals previously recorded. It has to be noticed that some copper compound, such as nantokite, do not have a FTIR spectrum suitable for our study. The bands of the Cu-Cl stretching modes, in fact are outside the range of the mid-infrared.

Moreover, copper chlorides are really corrosive and then the preparation of KBr pellets using a stainless steel mechanical press can result in destructive effects for the instrumentation itself.

Other kind of FTIR analysis, such as ATR or specular reflectance could be used instead of KBr pellets, to avoid the problem of corrosion of the equipment, and will be taken into account for future development of the work.

### ***Raman spectroscopy***

Micro Raman spectroscopy has been used to identify the composition of the artificial patinas obtained using the applied paste method. Moreover, it has been applied for the study of the chemical modifications induced by different levels of relative humidity on artificial patinas.

This technique revealed to be more suitable for the latter purpose, because it allows the analysis of the compounds without direct contact with the sample. Then, it is a completely non destructive, non invasive technique. Moreover, in the case of nantokite kept at high relative humidity, liquid water is present on the surface of the sample. This may be problematic for the FTIR analysis, because the peaks of the water are really broad in the infrared spectrum and may overlap to the peaks of the other components. By Raman spectroscopy, instead, no particular problem in the acquisition of the spectra has been noticed.

The analyses have been performed with the following equipment:

- Dispersive notch Rayleigh rejection filter Raman spectrometer Horiba Jobin Yvon Labram HR800 UV. Interchangeable gratings with 600, 1800 and 2400 groove/mm for measurement up to 325 nm, Olympus BX41 microscope with 20X and 50X objectives and 1024x256 pixels thermoelectric cooled CCD detector
- Exciting laser sources: Spectra-Physics 2017 Ar+ 514.5 nm
- Power: 20 mWatt or 2 mWatt according to the needing
- Reticule: 1800 nm

The use of a micro-Raman allowed the identification of the different species presents in the samples, thanks to the possibility to acquire spectra on different crystals found on the surface of the artificial patinas. Thus, in the case of Raman spectroscopy, a local composition of the sample is supplied, instead of an average value.

### ***XRD***

X-ray powder diffraction was performed using a Philips PW1830 X-Ray Diffractometer, with a PW3020 goniometer in the Bragg-Brentano geometry and a copper anticathode ( $K\alpha_1$  radiation). Samples were finely grinded and deposited on a dedicated sample holder in order to obtain a surface as smooth as possible. This technique was used to identify mineral phases present in the artificially prepared corrosion compounds. As in the case of FTIR spectroscopy, this technique provide an average composition of the sample.



### ***SEM-EDX***

The instrument used for the SEM–EDX analysis is an Environmental Scanning Electron Microscope (ESEM) Zeiss EVO 50 EP equipped with a LaB6 source and X-ray spectrometer Oxford INCA 200 - Pentafet LZ4.

This technique has been used to study the morphology and the composition in some particular cases such as the characterization of crystals growth on gold surface.

### ***Stereomicroscope***

Observations and images of the samples prepared have been performed on a Leica M205C stereomicroscope, equipped with a Leica DFC 290 digital camera.

### **3.3 Accelerate electrochemical artificial ageing of gilded bronze specimens**

The study of gilded bronze artworks is a very difficult topic in the field of cultural heritage because of the complexity of the structure (tri-layer) of the material. This one is composed by a metallic substrate (bronze), a gold layer and a layer of corrosion products formed during time between gold and bronze, as a consequence of the interaction with the atmosphere. The presence of hygroscopic salts between the gilding and the metallic substrate may lead to the detachment of the gold layer as a consequence of volume variations related to changes in the crystalline forms of the copper salts composing the patina.

In the field of the conservation of cultural heritage, because of the inestimable value of the studied artworks, it is important to be able to create samples, with the maximum similarity possible with the original piece, in order to test conservation techniques.

In order to reproduce artefacts, as faithfully as possible, not only as it was created by the artist, but also in the same way the natural ageing processes has modified it, the Opificio delle Pietre Dure (OPD) studied the materials composing the doors of the Baptistery of St. Maria del Fiore and recreated samples of gilded bronze with the same composition and production method used in the time of Ghiberti [1].

These samples are in the same condition in which the doors were immediately after their completion.

In order to achieve perfectly representative samples, however, it is necessary to age them so as to recreate, between gold and bronze, corrosion products that would have accumulated during natural processes over the centuries, such as copper oxides, chlorides and sulphates.

In this work the process followed by OPD to achieve gilded bronze specimens as well as procedures used during this thesis work for aging the samples are reported.

#### **3.3.1 Bronze alloy replica of the Baptistery doors**

The doors of the Baptistery of Florence are three, placed along the cardinal points, North, East and South. The southern door was created by Andrea Pisano, while the northern and the eastern, also

called the “Porta del Paradiso”, were created by Lorenzo Ghiberti. The doors are made of bronze, which composition vary slightly from one to another.

The OPD has performed a diagnostic campaign on the doors by studying cores taken in different parts of each portal and performing EDX and ICP-OES analysis in order to understand the metallographic structure and chemical composition of the alloy [2, 3]. It was concluded that the quantity and quality of alloy elements varies not only from door to door, but also depending on the areas from which the samples have been taken: as an example the bottom and the decoration of the panels contain different amounts of tin.

The average of the measured values (Figure 1) was subsequently used to reproduce the samples E (East) , N (North), S (South), whose composition reflects that of the east, north and south doors respectively; the main differences are noted in the level of zinc and tin, which vary inversely one to another.

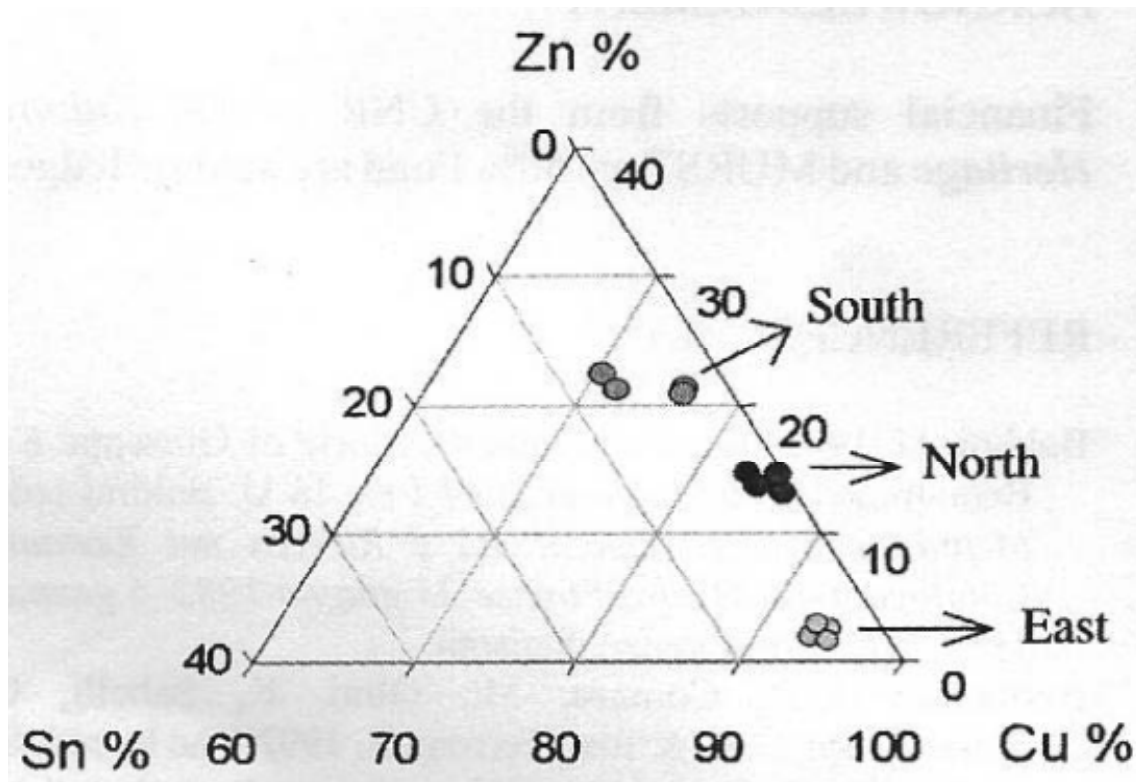


Figure 1: Elemental composition of metal alloys composing the doors of the Baptistery.

### 3.3.2 Gilding replica

Through treaties and documents from the same period as Ghiberti, such as "De Artibus diversis" of Theophilus [4], and thanks to in thorough microscopic analysis [5], the technique used for the gilding of the door could be understood. Subsequently, some replicas of gilded bronzes could be obtained with a good approximation. The technique used by Ghiberti is the mercury amalgam one,

in which the capability of this element to form a viscous solution, consisting of complex  $Au_2Hg$  dispersed in a liquid phase of metallic mercury, is utilized. The resulting dispersion, a kind of paste, is deposited on the substrate to be gilded, which is afterwards heated to  $300^{\circ}C$  in order to vaporize the mercury and leave only the gold on surface.

This method of gilding ensures the formation of thick final layer ( $2 - 10 \mu m$ ), especially if compared to other techniques such as electro-deposition, sputtering or the gold leaf [6] that barely reach the micrometer thickness.

The final result is not homogeneous, however, because the evaporation of mercury leaves the gold surface very porous, as observed in Figure 2 taken from reference [7].

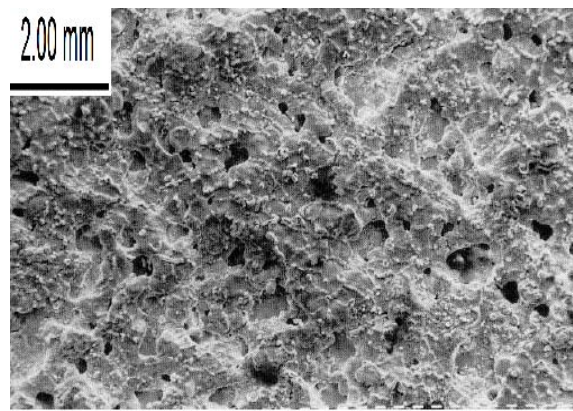


Figure 2: Porosity of the gilding obtained by the mercury amalgam technique.

To try to close the pores and obtain a brighter gold (Figure 3a), a mechanical treatment, called burnishing, was used to flatten the surface (Figure 3b).

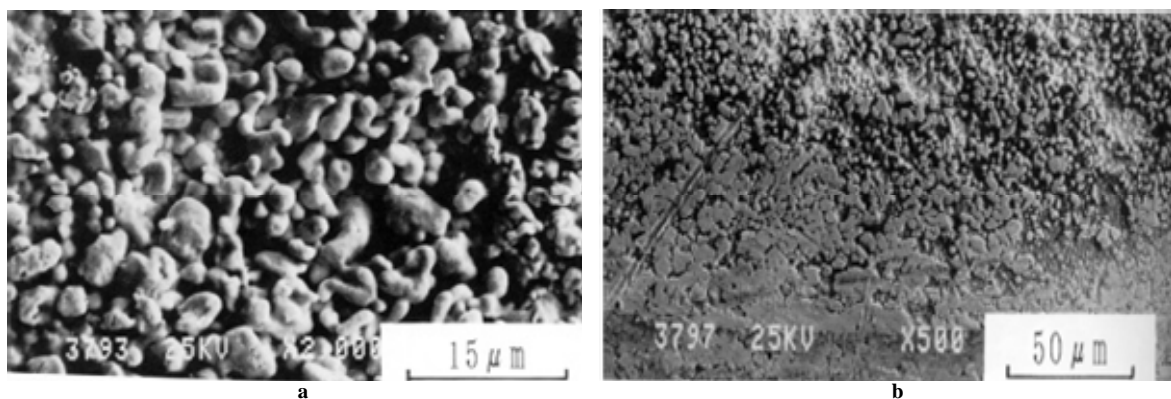


Figure 3: Surface morphology of gold after the evaporation of mercury amalgam (a) and after the burnishing (b).

### 3.3.3 Realization of the artificial patina

Being able to recreate the alloy and the gilding of the door is essential, but not enough, to obtain a realistic replica of the Baptistery doors. Indeed, as mentioned above, during the centuries a layer of corrosion products has naturally grown between the two metals (gold and bronze). In order to test new conservation methodologies, it is therefore necessary to be able to re-create also these corrosion products. The chemical analysis carried out on the film of corrosion products of the door [8] showed the presence of copper chlorides and sulphates, in particular atacamite  $\text{Cu}_2\text{Cl}(\text{OH})_3$ , nanokite  $\text{CuCl}$  as well as brochantite  $\text{Cu}_4\text{SO}_4(\text{OH})_3$ . The artificial synthesis of these products is complicated because they have been formed in a very long time. To this purpose an electrochemical method has been developed.

#### 3.3.3.1 The electrochemical method

The electrochemical method chosen to recreate the patina consists of immersing the replicas of gilded bronzes (samples of about 2 or 6  $\text{cm}^2$  each, electrically insulated) in an aqueous solution containing chlorides and sulphates, connecting the samples to an electric generator and imposing a current through them in order to accelerate the growth of copper products, thus simulating and enhancing the processes that take place during natural ageing.

To define the best experimental conditions, such as, composition of the solution, treatment time, and particularly the current density to apply, several series of tests have been carried out and are summarized in Table 1.

The first four series of tests were carried out on small samples (2  $\text{cm}^2$ ) produced by cutting some of the replicas prepared by the OPD staff. These tests were necessary to set up the procedure that has been then applied subsequently on the final series of samples (fifth series). Those nevertheless were significantly larger (6  $\text{cm}^2$ ).

**Table 1: Experimental conditions tested for the electrochemical artificial ageing.**

SERIES	CURRENT DENSITY	TIME
I	variable: from 0.005 to 0.5 A/m <sup>2</sup>	from 7 to 10 days
II	from 0.03 to 1 A/m <sup>2</sup>	from 4 to 9 days
III	from 0.5 to 1 A/m <sup>2</sup>	from 4 to 8 days
IV	1 A/m <sup>2</sup>	3 days
V	1 A/m <sup>2</sup> and 0,1 A/m <sup>2</sup>	5+2 days

The potential of the samples was measured with a reference electrode Ag/AgCl.

Since the first series , the solution used for the ageing, was composed by Na<sub>2</sub>SO<sub>4</sub> (4 g/L) and NaCl (2 g/L) dissolved in deionised water.

Since the IV series the tiny the incisions of the gilding were realised before the electrochemical treatment in order to localize the growth of corrosion in correspondence of the incisions and to obtain a reproducible growth of the corrosion products.

The final procedure can be summarised as follows:

- Incision of the gilding in several points.
- Immersion of the samples in a solution of Na<sub>2</sub>SO<sub>4</sub> (4 g/L) and NaCl (2 g/L).
- Application of a current density of 1 A/m<sup>2</sup> for 5 days, followed by the application of a current density of 0,1 A/m<sup>2</sup> for 2 days.

The results obtained during the development of this electrochemical methodology for the artificial ageing of gilded bronze samples are reported in chapter 4.1.

## References

- [1] S. Goidanich, L. Toniolo, D. Matera, B. Salvadori, S. Porcinai, A. Cagnini, A.M. Giusti, R. Boddi, A. Mencaglia, S. Siano, D. Camuffo, C. Bertolin, R. Mazzeo, S. Prati, A. Addis, D. Prandstraller, M. Matteini, D. Pinna, **Corrosion evaluation of Ghiberti's "Porta Del Paradiso" in three display environments**, Proceedings of Metal 2010, International Conference on Metal Conservation, Interim meeting of the international council of museums committee for conservation metal working group, October 11–15, Charleston, South Carolina, USA, 2010, 151–159
- [2] P. Parrini, **Lorenzo Ghiberti, Storie di Giuseppe e di Beniamino, Storie di Adamo ed Eva – Sulla tecnica di esecuzione**, Metodo e Scienza Operatività e Ricerca nel Restauro, Catalogo della Mostra Firenze 23 giugno 1982 – 6 gennaio 1983, Sansoni Editore, Firenze, 1982, 199–202 [3] G.P. Bernardini, M.C. Squarcialupi, R. Trosti-Ferroni, M. Matteini, C.G. Lalli, G. Lanterna, M. Rizzi, I. Tosini, **The bronze doors of the Baptistery in Florence: a comparative study of the bronze alloys and alteration products**, Protection and Conservation of the Cultural Heritage of the Mediterranean Cities, Galàn and Zezza Eds., Swets & Zeitlinger, Lisse, 2002, 43–47
- [4] J.G. Hawthorne, C.S. Smith, **On divers arts - The Treatise of Theophilus**, Dover Publications, New York, 1979
- [5] Internal report – Relazione OPD, June 2006
- [6] P. Northover, K. Anheuser, **Gilding in Britain: Celtic, Roman and Saxon**, Gilded Metals. History, Technology and Conservation. Terry-Drayman-Weisser (Ed.), London, Archetype Publ. (2000), 109
- [7] R. Murakami, **Archaeological gilded metals excavated in Japan**, Gilded Metals. History, Technology and Conservation. Terry-Drayman-Weisser (Ed.), London, Archetype Publ. (2000), 157
- [8] Internal report – Barbara Salvadori, Relazione OPD bronzi, 2005

## 3.4 Preparation and set up of galvanic sensors

One of the main goal of this experimental work was to realise a tool to measure the corrosion rate of gilded bronzes in the context of cultural heritage. More particularly, concerning the case study of “The Porta del Paradiso”, the aim was to evaluate which was the most suitable display option for the doors. Unfortunately, traditional electrochemical techniques used to gather quantitative data of metallic artefacts, such as Linear Polarisation Resistance ( $R_p$ ) or Electrochemical Impedance Spectroscopy (EIS) [1-10], cannot easily be applied to a bimetallic object like a gilded bronze as it is the “Porta del Paradiso”. A promising alternative is the use of galvanic sensors [11, 12] simulating the stratigraphy of the doors and allowing the continuous monitoring of the macrocouple current that is directly proportional to the corrosion rate. The sensors developed during this work are thoroughly described in the following paragraphs.

### 3.4.1 The sensors for the Porta del Paradiso

The first series of galvanic sensors was realized in this work for the evaluation of the best exposure solution of the “Porta del Paradiso” (Chapter 3.5) [13]. A quaternary bronze alloy, (Cu 93,1%; Zn 3,2%; Sn 2,6%; Pb 1,1%) has been used as metallic substrate. This alloy has been chosen because it is similar to that of the “Porta del Paradiso” (see Chapter 1.4.2) [14-16].

The patination method chosen for the preparation of the galvanic sensors is the applied paste presented in Paragraph 3.1.3. This technique allows to obtain an homogeneous patina, thick enough to avoid short circuit between bronze and gold. Moreover the composition of the patina has been realised with the goal of reproducing the conditions of the most unstable areas of the “Porta del Paradiso”. To this aim, the patina prepared is rich in chlorides and sulphates. A schematic representation of the galvanic sensors realized for the “Porta del Paradiso” is reported in Figure 1.

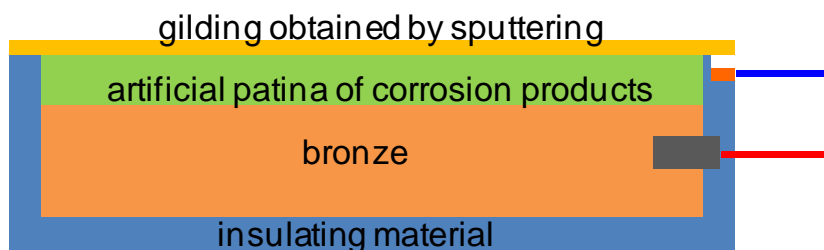


Figure 1: Schematic representation of a galvanic sensor realized for the “Porta del Paradiso” (not in scale).



The procedure used to prepare the samples is the following:

1) *Preparation of the metallic surface*

- Polishing of the surface in order to eliminate the oxidation products and to obtain a plane and reproducible surface.
- Cleaning of the surface with ethanol.
- Riveting of the copper wires to allow the electric contact.

2) *Insulation*

An epoxy resin coating has been applied to the electrical connection, as well as to the four sides and the back of the sensor to ensure a complete electrical insulation of the entire system.

3) *Patination*

An artificial patina of corrosion products has been prepared by grinding together, in an Agate mortar, Nantokite (CuCl), Tolbachite (CuCl<sub>2</sub>) and Chalcantite (CuSO<sub>4</sub>·5H<sub>2</sub>O), in the 2:1:3 proportions and mixing the salts with water (powder/water ratio 6); the resulting paste has been spread directly on bronze surface using the “paste application” method previously described (Paragraph 3.1.3). The powder of copper salts, mixed with water produce a moist, workable paste, easily spreadable on the bronze surface of the sample. The paste, left to dry into air, sets and hardens. The obtained layer of corrosion products is then adherent, hard and resistant.

4) *Gilding*

After the complete drying of the paste, the surface of the artificial patina was covered by a thin gold layer. The gilding was obtained by sputtering, i.e. deposition in the vapour phase under vacuum (at a pressure below 10<sup>-3</sup> Pa). The parameters used for the gilding are as follows:

- Argon pressure: 2 Pa
- Current: 20 mA
- Applied Voltage: ~1 kV
- Time: 12 minutes

5) *Electrical connections*

Each sensor has electrical connections to the bronze substrate and to the gilding for the measurement of the macrocouple current. The electrical connections to bronze substrate were obtained by riveting. The electrical connection with the thin gold layer was obtained by applying a conductive silver-based glue.

The aspect of the patina before and after drying are presented in Figure 2a and 2b respectively, while the aspect of the sensor after the gilding may be observed in Figure 2c.

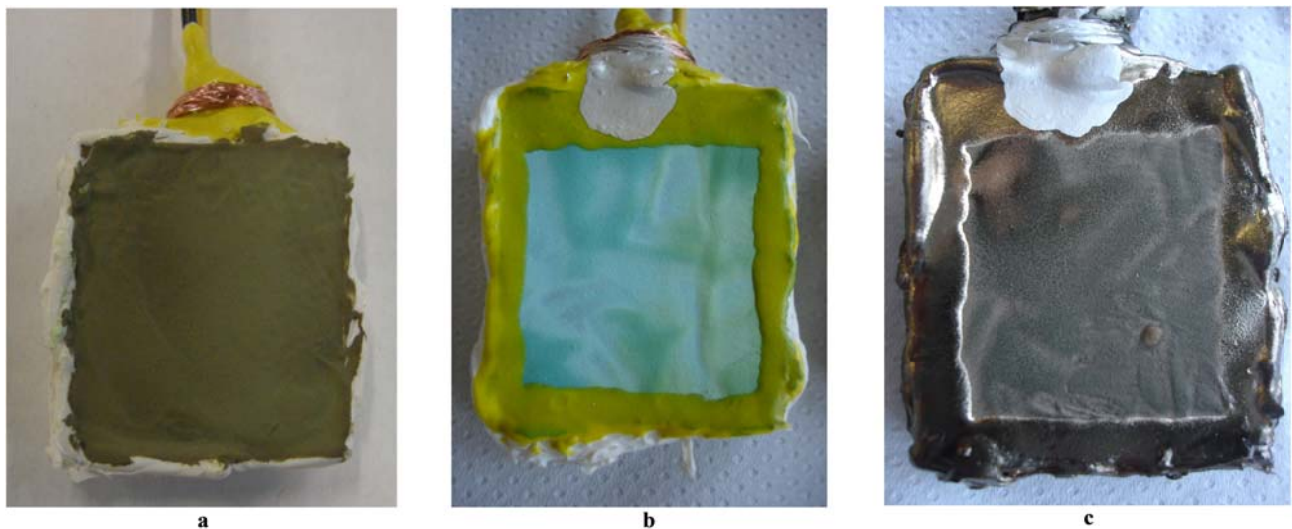


**Figure 2: External aspect of the patina after immediately after application (a) and after drying (b); in (c) aspect of the finished sensor after the gilding.**

The values obtained from the monitoring of the “Sensors for the Porta del Paradiso” are reported in the Results and Discussion Chapter 4.2.

### **3.4.2 Gold leaf sensors: chloride rich patina**

The sensors used for the “Porta del Paradiso” case study revealed to be a powerful tool for the monitoring of the corrosion rate [13]. However, as will be discussed later (Chapter 4.2), they presented the drawback of not being durable and reproducible. New sensors, called “Gold leaf sensors”, were then realized in order to obtain more durable samples with more reproducible and reliable signals [17]. New sensors, named “Gold leaf sensors” have then been developed. The Gold leaf sensors have been prepared using the same bronze used for the “Sensors for the Porta del Paradiso” or copper 99.9% (thickness 0.45 mm) as a substrate.

The procedure to obtain the final series of galvanic sensor, with a chlorides riche patina, is the following:

#### *1) Preparation of the metallic surface*

- Polishing of the surface in order to eliminate the oxidation products and to obtain a plane and reproducible surface (this step is skipped if copper is used as a substrate).
- Cleaning of the surface with ethanol.

- Riveting of the copper wires to allow the electric connection.

## 2) *Insulation*

An epoxy resin coating has been applied to the electrical connection, as well as to the four sides and the back of the.

## 3) *Patination*

- Cuprite: for the realization of these sensors a layer of Cuprite ( $\text{Cu}_2\text{O}$ ) has been interposed between the bronze and the copper salt paste in order to improve the adhesion of the patina to the metallic substrate. Moreover, the cuprite is the first corrosion layer that naturally forms on copper alloys when exposed to the atmosphere [18]. The layer of Cuprite has been obtained by immersing the bronze in a boiling solution of Chalcantite,  $\text{CuSO}_4 \cdot 5\text{H}_2\text{O}$ , (25 g/L) (Paragraph 3.1.1) [19].
- Paste of corrosion products: the composition of the mixture of copper salts has been slightly modified. Eriochalcite ( $\text{CuCl}_2 \cdot 2\text{H}_2\text{O}$ ) has been used instead of Tolbachite ( $\text{CuCl}_2$ ), because it requires a lower quantity of water for the preparation of the paste. Moreover, the proportions of the three constituents (nantokite, eriochalcite and chalcantite) have been changed to 3:1:4: the quantities of  $\text{CuCl}$  and  $\text{CuSO}_4$  have been increased respect to that of  $\text{CuCl}_2$  because the latter is less frequently found as a natural corrosion product. Nevertheless, it has been maintained in the composition because it allows the transformation to atacamite ( $\text{Cu}_2(\text{OH})_3\text{Cl}$ ), a copper (II) hydroxychloride. The ratio between sulphates and chlorides has been kept the same of the first recipe. The powder/water ratio in the copper salt paste has been changed to 1, to obtain a smoother and thinner patina.

After the application of the paste, the patina is left to dry 24 hours in laboratory environment. The influence of relative humidity during the “curing” period of the patina will be discussed in Paragraph 3.4.2.1.

## 4) *Gilding*

The gilding method has been modified, respect to the sputtering, in order to have a more continuous, thick and resistant layer of gold. To this aim, a gold leaf has been used. The use of the gold leaf instead of sputtering of gold introduce another advantage: the patina doesn't undergo to a thermal and vacuum treatment that can alter the patina itself. The gold leaf is applied by wetting the surface of the dry patina with demineralised water, using a water sprayer, and then leaning the wet surface of the patina directly on the gold leaf, previously cut at the right dimensions.

Figure 3a presents the schematic representation of a “Gold leaf sensor” with chlorides rich patina of the final series (Figure 3b).

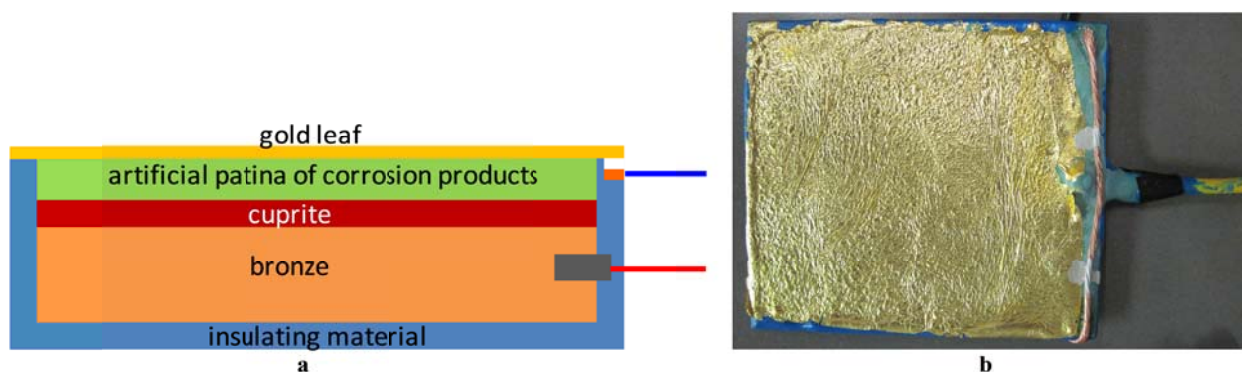


**Figure 3: Schematic representation of a “Gold leaf sensor” with chlorides rich patina (not in scale) (a), and image of a complete sensor of the final series (b).**

The main differences between the sensors for the Porta del Paradiso and the gold-leaf sensors with chloride rich patina are reported in Table 1.

**Table 1: Principal differences between the sensors for the Porta del Paradiso and the gold-leaf Sensors with chloride rich patina.**

	<b>Patina composition</b>	<b>P/W ratio<sup>1</sup></b>	<b>Thickness<sup>2</sup> of the patina: <math>\frac{\text{g}_{\text{powder}}}{\text{cm}^2}</math></b>	<b>Gilding method</b>
<i>Sensors for the Porta del Paradiso</i>	Chloride rich patina: CuCl + CuCl <sub>2</sub> + CuSO <sub>4</sub> ·5H <sub>2</sub> O ratio 2:1:3	6	0.5	Sputtering
<i>Gold leaf sensors</i>	Chloride rich patina: CuCl + CuCl <sub>2</sub> ·2H <sub>2</sub> O + CuSO <sub>4</sub> ·5H <sub>2</sub> O ratio 3:1:4	1	0.025	Gold leaf

In order to obtain the previously described procedure for the realisation of the Gold-Leaf Sensors with chlorides rich patina, several tests were performed to define the following parameters:

- The best powder/water ratio (P/W) for the preparation of the patina;
- Thickness of the patina;
- The best methodology for the application of the gold leaf.

The results of the various tests performed to set-up the definitive procedure as well as the problems related to the relative humidity during the “curing” period are described in the Paragraph 3.4.2.1.

<sup>1</sup> P/W ratio indicate the ratio between the powder of copper salts and the water used for the preparation of the patina  
<sup>2</sup> The thickness of the patina is expressed in terms of powder surface density

The values obtained from the monitoring of the “Gold leaf sensors”, are reported in the Results and Discussion paragraph 4.3.1 and 4.3.2.

### ***3.4.2.1 Setup of the gold-leaf sensor with chloride rich patina***

As previously mentioned, the reproducibility of the gilding obtained by sputtering appears to be rather low due to problems inherent to the technique itself. This method implies an increase of temperature of the substrate that is noxious for the sample and induces mechanical stress for the components of the sensor that can alter the chemical composition of the patina [20]. Moreover, the gold layer is extremely thin and easily damageable.

Unfortunately, the original method of fire gilding could not be applied because it is suitable only for clean metallic surfaces and even if it is possible to properly age bronzes that were gilded with this technique, the unavoidable short circuits between gold and bronze would not allow the measurements of the macrocouple current.

Thus, the method of gold leaf application has been chosen for the gilding of the galvanic sensors.

As previously mentioned in order to define the definitive gilding procedure for the realisation of the “Gold Leaf Sensors” with chlorides rich patina (Paragraph 3.4.2), several tests were required to define the following parameters:

- The best powder/water ratio (P/W) for the preparation of the patina;
- Thickness of the patina;
- The best methodology for the application of the gold leaf.

In the following part of this Paragraph the main tested parameters will be presented and their influence on the final properties of the sensors discussed.

#### *Importance of the powder/water ratio (P/W)*

The P/W ratio for the preparation of the patina proved to be a very important parameter in terms of reproducibility of the sensors. The tested ratios were: 6, 4 and 1; a smaller ratio corresponds to a higher amount of water that allows to obtain a more homogeneous and less rough patina. For this reason the final P/W ratio was set to 1, allowing the realisation of more reproducible sensors.

#### *Importance of the thickness of the patina*

The thickness of the patina will be expressed in terms of powder surface density and the tested values are: 0.5 g/cm<sup>2</sup>, 0.1 g/cm<sup>2</sup> and 0.025 g/cm<sup>2</sup>. It has been observed that the thinner the patina, the more stable it is, faced to the RH variations. Furthermore a thinner patina should also offer a lower resistance to the current flow allowing the realisation of galvanic sensors that can supply a

higher macrocouple current. For this reason the thinnest option (0.025 g/cm<sup>2</sup>) was chosen. It was not possible to further decrease the thickness because otherwise the risk of short circuit between the gold and the metallic substrate would be too high. The sensors prepared with this thinner patina proved to be the most durable.

#### Importance of the methodology for the application of the gold leaf

The choice of the gold leaf gilding instead of the sputtering offered different advantages:

- First, the elimination of the thermal shock due to the PVD process, that can damage both the patina and the whole sensor [20].
- In addition, the morphology of the gilding obtained with this method is more similar to that resulting from the fire gilding, in terms of thickness, porosity and continuity.

The major limitation of this technique is related to the manual ability of the operator that may affect the reproducibility of the final result. For this reason the gilding procedure has been defined and setup in detail.

First of all it was decided to do not use any kind of glue because this is never present in case of fire gilding and it would have significantly reduced the macrocouple current. It was observed that the gold leaf develops a good adhesion over the patina when it is applied on a moist patina.

Initially the gold leaf has been applied when the patina was still wet, before it dried up. The elapsed time between the spreading of the patina paste over the surface and the application of the gold leaf proved to be a crucial point. If the gold leaf was applied too early the finished sensors would present a huge number of white or green crystals over the gold surface as visible in Figure 4, while, in the other hand, if the drying time between the patination and the application of the gold leaf is too long, the gold doesn't adhere completely to the patina (Figure 5). Moreover, the environmental conditions, in terms of temperature and, in particular, of relative humidity, proved to be very important for the definition of the time of "curing" of the sensors before the application of the gold leaf. Different experiments have been performed in different environments, with both low and high RH, and with different curing durations. The different tested conditions, in terms of Relative Humidity, and time of curing are reported in Table 2. All the reported results and consideration refers to the gold-leaf sensors with chloride rich patina.

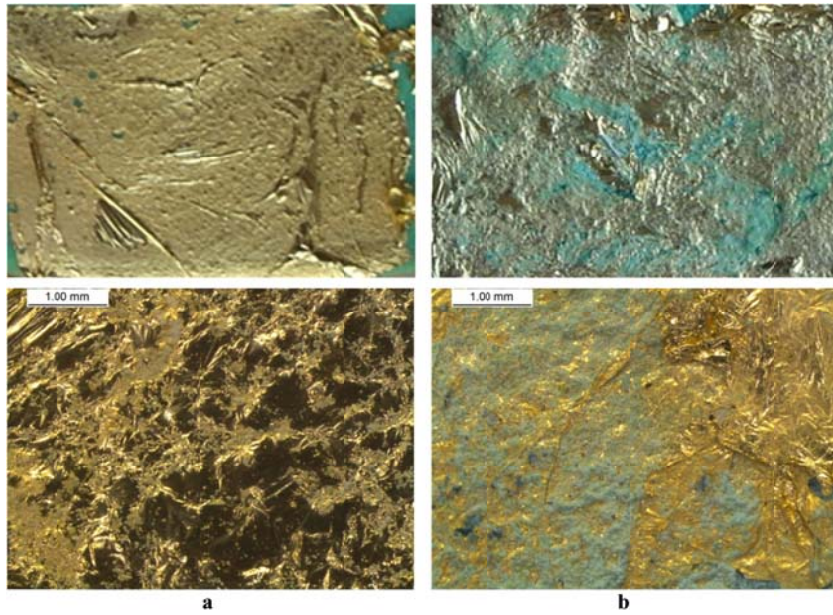


Figure 4: Macro (top) and stereomicroscope (bottom) images of white (a) and green (b) crystals growth on the surface of the gold.

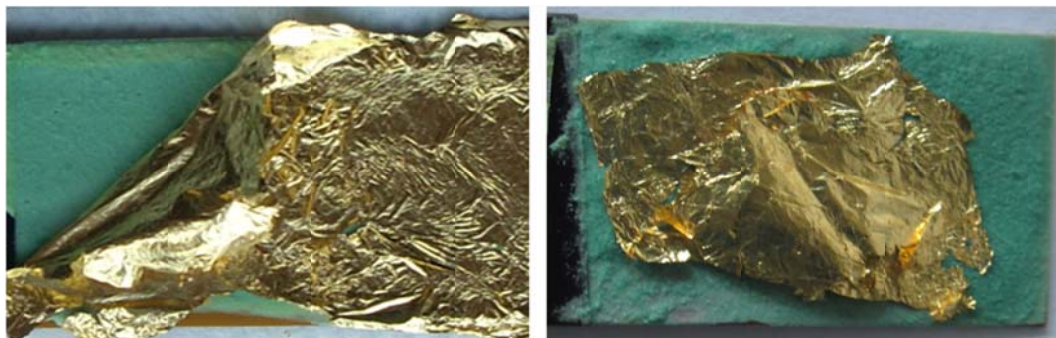
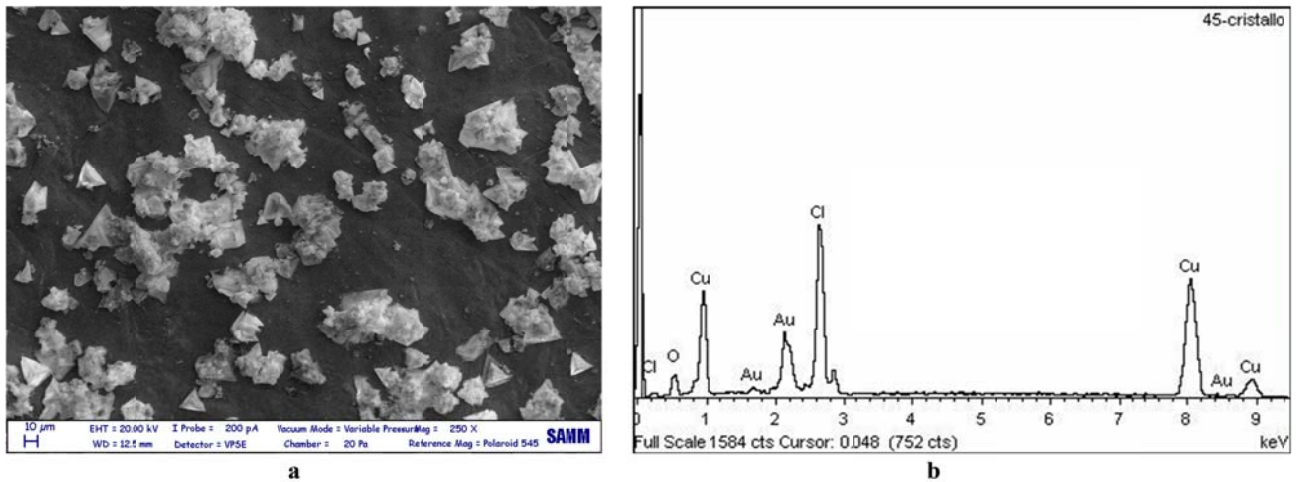


Figure 5: Problems of adhesion of the gold leaf due to the application on a too dry patina.

Table 2: Different environmental conditions and time of curing tested for the definition of the best methodology for the realisation of “Gold leaf sensors”

Time between patination and gilding	Curing environment between patination and gilding
Between 15 and 40 minutes	Sealed box with high relative humidity
Between 35 and 40 minutes	Sealed box
Between 15 and 50 minutes	Desiccator with silica gel
45 minutes	Desiccator with silica gel

The crystals growing on the gold surface have been observed and characterized by SEM-EDX and they were composed only by copper chlorides (Figure 6); no trace of copper sulphates have been found on the surface of the gold.



**Figure 6: SEM image (a) and EDX spectrum (b) of the crystals growth on the surface of the gilding due to a too high relative humidity.**

The method that proved to give the best results was to keep the sensors after the patination in a close desiccator with silica gel for 45 minutes. The gilding was applied by using a “gilding knife” and a soft brush.

Also the curing of the sensors after the gilding proved to be of great importance to avoid the growth of crystals on the surface of gold. Therefore, after the application of the gold leaf the sensors were kept in a sealed box for 24 hours.

This procedure was used for the realisation of the first “Gold leaf sensors”, that will be named in the future “*Preliminary gold-leaf galvanic sensors with chloride rich patina*” (Figure 7a). These sensors were realised with a P/W ratio of 4 and a thickness of  $0.1 \text{ g/cm}^2$ .

However this procedure for the application of the gold leaf was quite complicated and often caused several breaks of the gilding.

A new procedure was then set up, that allowed to solve most of the problems related to the gilding and that was then chosen as the definitive procedure (Paragraph 3.4.2): the gold leaf is applied by wetting the surface of the dry patina with demineralised water, using a water sprayer, and then leaning the wet surface of the patina directly on the gold leaf, previously cut at the right dimensions (Figure 7b). No crystals have been observed on the surface of the gold leaf sensors (Figure 7), both in their preliminary and definitive version.



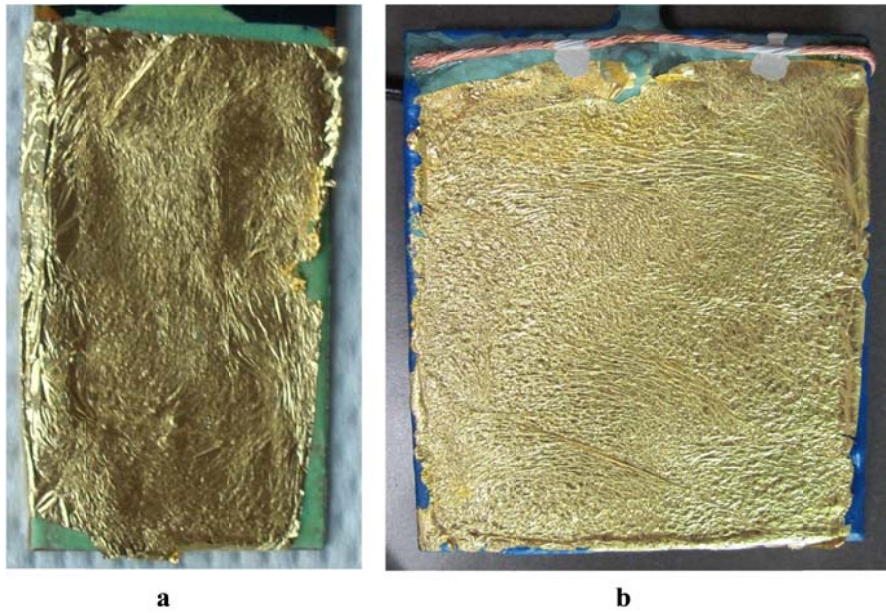


**Figure 7: Gold leaf gilding: differences between the first preliminary gold leaf sensors (a) and the definitive ones (b).**

*Characterisation of the gold leaf before and after the gilding*

The gold leaves were characterized by Scanning Electron Microscopy for a thorough knowledge of their structure, surface and thickness.

One must take into account that the gold leaf is very thin which implies a significant intrinsic fragility. The gold leaves are sold in form of “booklet” of 25 leaves each. Gold leaves used in this work are composed by gold 24 KT (999,9/1000), 80 X 80 mm, thickness 20. The value of the thickness refers to the grams used to produce 1000 leaves of the same dimensions. The procedure to obtain the gold leaves is still craft, and the thickness of each leaf can vary. The average thickness of the gold leaf used in this work is 0.16  $\mu\text{m}$ . The SEM-EDX analysis performed on one gold leaf (Figure 8) revealed a thickness of 0.24  $\mu\text{m}$  on the piece of gold analysed. The analysis of gold leaves were carried out in high vacuum.

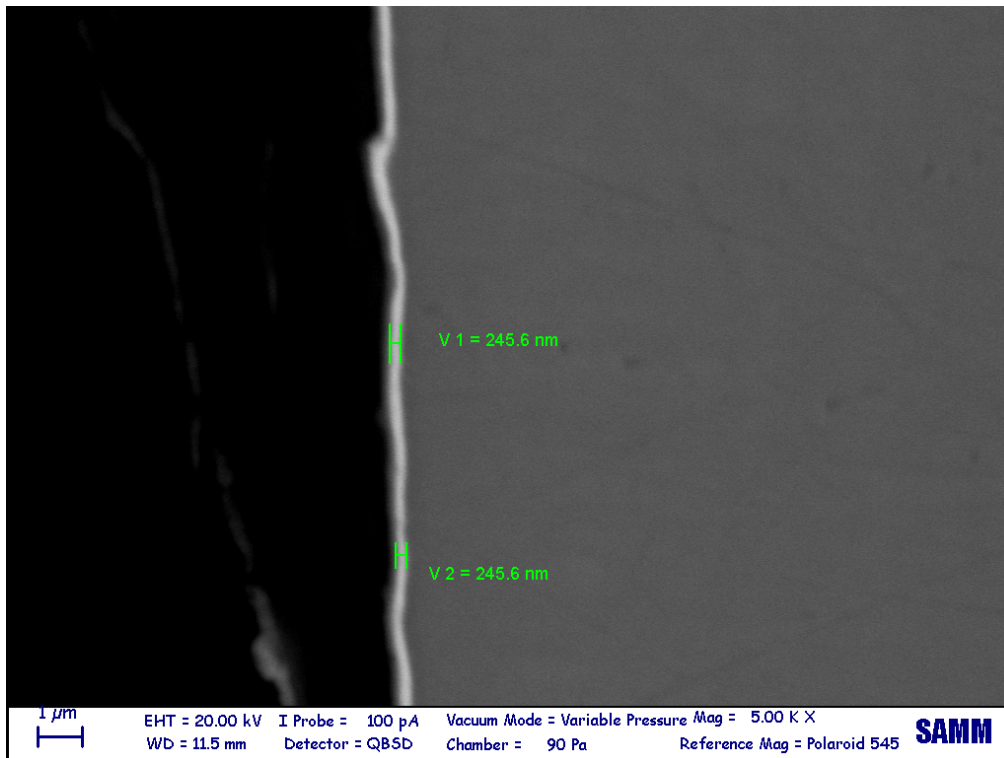


**Figure 8: Measurement of the thickness of one gold leaf by SEM.**

The two parameters of major interest for the purpose of this work are the thickness and the porosity of the gold layer.

The porosity is not distributed evenly on the surface but is concentrated in some areas (Figure 9) and the order of magnitude of the pores is in the range of hundreds of nanometers (Figure 10). The presence of these pores is a desirable characteristics because it allows the permeation of chemical species and relative humidity from the environment to the patina and vice versa. This is what happens in the real objects where the corrosion attacks concentrates at the defects and porosities of the gilding.

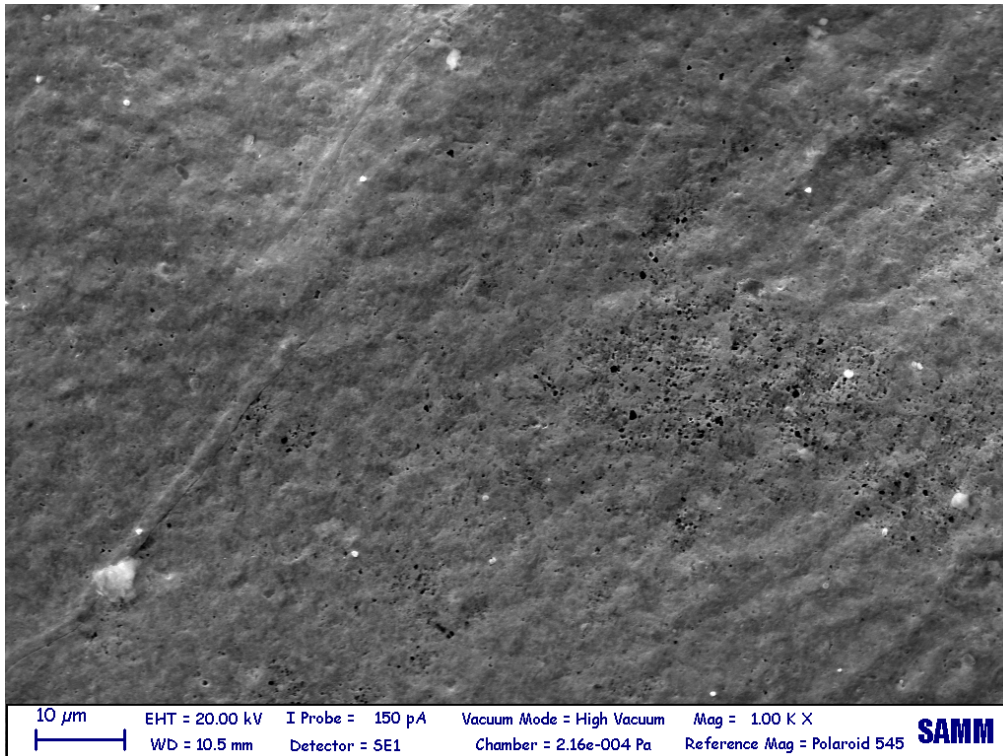


Figure 9: Porosity of the gold leaf by SEM, secondary electrons.

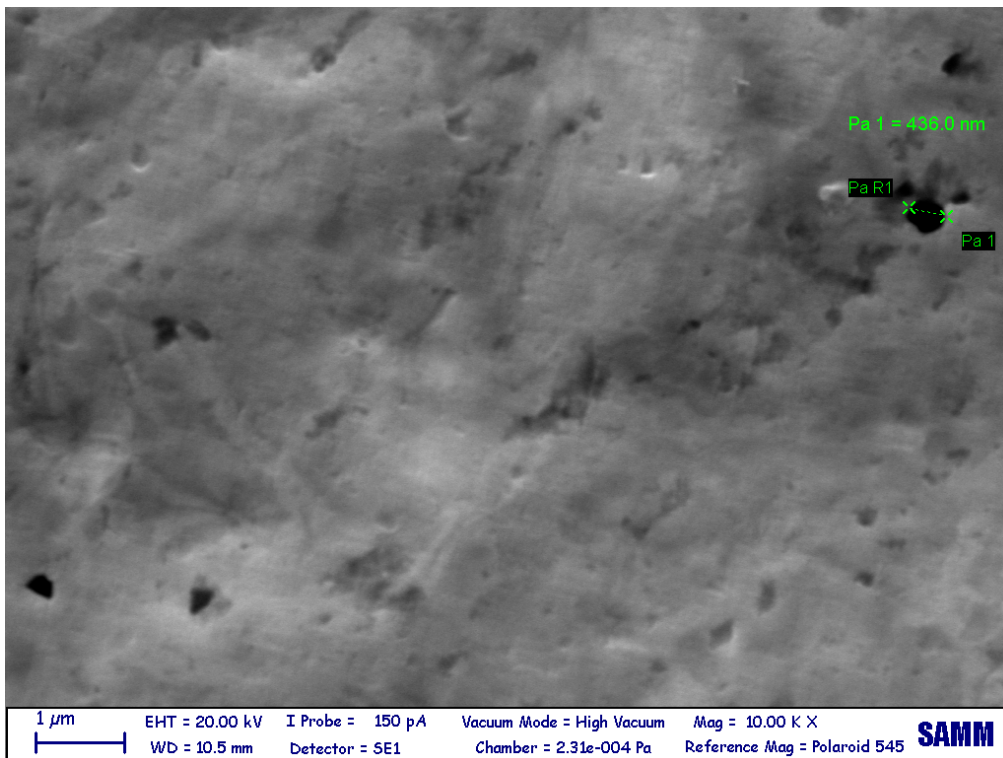


Figure 10: Measurement of a pore by SEM.

The last conditions proved to be the best option and allowed to obtain the so called “*preliminary gold-leaf galvanic sensors with chloride rich patina*”.

### 3.4.3 Gold leaf sensors: brochantite patina

Since brochantite is the most common corrosion product in urban environment (Chapter 1.2) [18, 21], it was considered really important to realise galvanic sensors containing this basic copper sulphate. Different procedures have been tested to obtain brochantite (Chapter 3.1), before selecting the final methodology presented below. The adopted methodology consists in the synthesis of brochantite [22]. Subsequently, the synthesized compound is grinded, mixed with water and applied on the metallic surface using the “applied paste” method used for the chloride rich patina. This method, even if longer compared to the preparation of chlorides rich patina (the synthesis of brochantite requires approximately 48 hours) is still quicker than the other tested methodologies to obtain brochantite (Chapter 3.1), which in addition did not allowed to obtain patinas with the required characteristics.

The procedure for the preparation of the galvanic sensors with brochantite patina is exactly the same as the one used in the case of chloride rich sensors (Paragraph 3.4.2). The only difference is the powder/water ratio that in the case of brochantite is 2 instead of 1. The schematic representation of a galvanic sensor with brochantite patina (picture in Figure 11b) is reported in figure 11a.

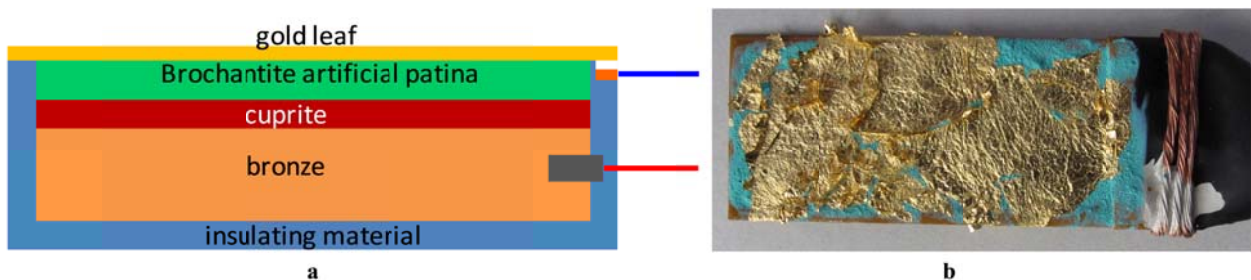


**Fig. 11: Sketch of a “Gold leaf sensor” with brochantite patina (a), and image of the complete sensor (b).**

## References

- [1] ASTM G 59-97 (2009) **Standard Test Method for Conducting Potentiodynamic Polarization Resistance Measurements**
- [2] ASTM G 106-89 (2010) **Standard Practice for Verification of Algorithm and Equipment for Electrochemical Impedance Measurements**
- [3] ASTM G 102-89(2010) **Standard Practice for Calculation of Corrosion Rates and Related Information from Electrochemical Measurements**
- [4] Letardi P., Beccaria A., Marabelli M., D'Ercoli G., **Application of electrochemical impedance measurements as a tool for the characterization of the conservation and the protection state of bronze works of art**, Metal98 – International Conference on Metal Conservation, Draguignan, France 26–29 May 1998, 303–308
- [5] C. Bartuli, R. Cigna, O. Fumei, **Prediction of durability for outdoor exposed bronzes: estimation of the corrosivity of the atmospheric environment of the Capitoline Hill in Rome**, Studies in conservation, 44, 4 (1999), 245–252
- [6] G. D'Ercoli, M. Marabelli, **La resistenza di polarizzazione: indagine non distruttiva per la caratterizzazione di patine e protettivi di un monumento bronzeo**, in Monumenti in bronzo all'aperto. Esperienze di conservazione a confronto, Nardini Editore, Firenze, 2004, 135–142
- [7] K. Leyssens, A. Adriens, E. Pantos, C. Degryny, **Study of corrosion potential measurements as a means to monitor the storage and stabilisation processes of archeological copper artefacts**, Metal 04. – International Conference on Metal Conservation, National Museum of Australia, Canberra, 4–8 October 2004, 332–343
- [8] E. Angelini, S. Grassini, S. Corbellini, G. M. Ingo, T. de Caro, P. Plescia, C. Riccucci, A. Bianco, S. Agostini, **Potentialities of XRF and EIS portable instruments for the characterisation of ancient artefacts**, Applied Physics A, 83 (2006), 643–649
- [9] P. Letardi, G. Luciano, **Survey of EIS measurements on copper and bronze patinas**, Metal07 – International Conference on Metal Conservation, Amsterdam (The Netherlands), Rijksmuseum, 17–21 September 2007, vol. 3, 44–50
- [10] D. M. Bastidas, M. Criado, S. Fajardo, V. M. la Iglesia, E. Cano, J. M. Bastidas, **Copper deterioration: causes, diagnosis and risk minimisation**, International Materials Reviews, 55, 2 (2010), 99–127
- [11] B. Mazza, P. Pedferri, G. Re, D. Sinigaglia, **Behaviour of a galvanic cell simulating the atmospheric corrosion conditions of gold plated bronzes**, Corrosion Sciences 17 (1977), 535-541
- [12] G. Alessandrini, G. Dassù, P. Pedferri, G. Re, **On the conservation of the baptistery doors in Florence**, Studies in Conservation 24 (1979), 108-124

- [13] S. Goidanich, L. Toniolo, D. Matera, B. Salvadori, S. Porcinai, A. Cagnini, A.M. Giusti, R. Boddi, A. Mencaglia, S. Siano, D. Camuffo, C. Bertolin, R. Mazzeo, S. Prati, A. Addis, D. Prandstraller, M. Matteini, D. Pinna, **Corrosion evaluation of Ghiberti's "Porta Del Paradiso" in three display environments**, Proceedings of Metal 2010, International Conference on Metal Conservation, Interim meeting of the international council of museums committee for conservation metal working group, October 11-15, Charleston, South Carolina, USA, 151-159, 2010
- [14] G.P. Bernardini, M.C. Squarcialupi, R. Trosti-Ferroni, M. Matteini, C.G. Lalli, G. Lanterna, M. Rizzi, I. Tosini, **The bronze doors of the Baptistery in Florence: a comparative study of the bronze alloys and alteration products**, Protection and Conservation of the Cultural Heritage of the Mediterranean Cities, Galàn and Zezza Eds., Swets & Zeitlinger, Lisse, 2002, 43-47
- [15] E. Mello, P. Parrini, **Lorenzo Ghiberti: storie di Giuseppe e di Beniamino; bassorilievo in bronzo dorato della Porta del Paradiso. Stato di conservazione: esame di una microcarota**, Metodo e Scienza Operatività e Ricerca nel Restauro, 1982, 176-180
- [16] A. Giusti, M. Matteini, **The gilded bronze Paradise Doors by Ghiberti in the Florence Baptistery – Scientific investigation and problems of restoration**, Proceedings of the International Conference on Metal Restoration, German National Committee of ICOMOS, Munich, 1997, 47-51
- [17] S. Goidanich, L. Brambilla, B. Salvadori, S. Porcinai, A. Cagnini, L. Toniolo, **Galvanic sensors for monitoring corrosion rate of gilded bronzes**, 10<sup>th</sup> International Conference on non-destructive investigations and microanalysis for the diagnostics and conservation of cultural and environmental heritage (Art'11), 13th-15th April 2011, Florence, Italy, E17
- [18] T.E. Graedel, K. Nassau, J.P. Franey, **Copper patinas formed in the atmosphere – I. Introduction**, Corrosion Science, 27, 7 (1987), 639-657
- [19] R. Hughes, M. Rowe, **The colouring, bronzing and patination of metals**, Thames and Hudson (1997)
- [20] R. Schlesinger, H. Klewe-Nebenius, M. Bruns, **Characterization of artificially produced copper and bronze patina by XPS**, Surface and Interface Analysis, 30 (2000), 135–139
- [21] J.P. Franey, M.E. Davis, **Metallographic studies of the copper patina formed in the atmosphere**, Corrosion Science, 27 (1987) 659–668
- [22] S.V.S. Prasad, V. Sitakara Rao, **Thermal analysis, X-ray diffraction and infrared spectroscopic study of synthetic brochantite**, Journal of Thermal Analysis (1985) 30, 603-609

## 3.5 Display conditions for the Porta del Paradiso

At the beginning of this work the “Porta del Paradiso” was at the final stage of the restoration process (Paragraph 1.4.4). The doors had then to be re-assembled and finally unveiled to the public at the Museo dell’Opera del Duomo in Florence. It was then necessary to define a suitable long-term display environment for the door. Due to the presence of highly unstable corrosion products between gold and bronze, that could not be removed during the cleaning procedure, the door was still extremely sensitive to relative humidity and air pollutants. Thus, if not protected in an adequate way, a rapid degradation of the artwork might occur.

For this reason a new phase of research begun with the scope of determine which was the best solution for the exposure of the doors to the public. This phase of the research was coordinated by the OPD and involved several Italian research groups. The tasks assigned to the Politecnico units were: a) the accelerated aging of gilded bronzes with the same characteristic and composition of the door at the time they were realized; b) the development of some tool or methodology for evaluating the impact of the microclimate on the doors, c) to provide quantitative data for the choice of the best option for the display.

In order to choose the best display solution for the “Porta del Paradiso”, two factors have to be taken into account:

- The environmental conditions must guarantee the best preservation for this precious Renaissance masterpiece.
- An enjoyable viewing experience for the public should be provided.

The three display solutions that have been proposed by the team of experts involved are the following:

- Low humidity showcase: a closed showcase with low and constant relative humidity (between 15 and 20%).
- Nitrogen showcase: a closed showcase saturated with nitrogen.
- Open showcase: an open showcase with controlled microclimate where a dynamic flux of air separates the space occupied by the door parts from the surrounding environment.

Three parts of the doors have been included in this study to test the different showcases. They are two friezes and one panel:

- Elia’s frieze (frieze number XV), shown in Figures 1a, was placed in the showcase with low and controlled RH (Figure 2a).

- Miriam's frieze (frieze number XIX), shown in Figures 1b, was placed in the showcase purged with nitrogen (Figure 2b).
- Noah's panel, (panel number 3), shown in Figures 1c, was placed in the open showcase (Figure 2c).



**Figure 1:** The parts of the Porta del Paradiso chosen for testing the three exhibition solution: Elia's frieze (a), Miriam's frieze (b) and Noah's panel (c).

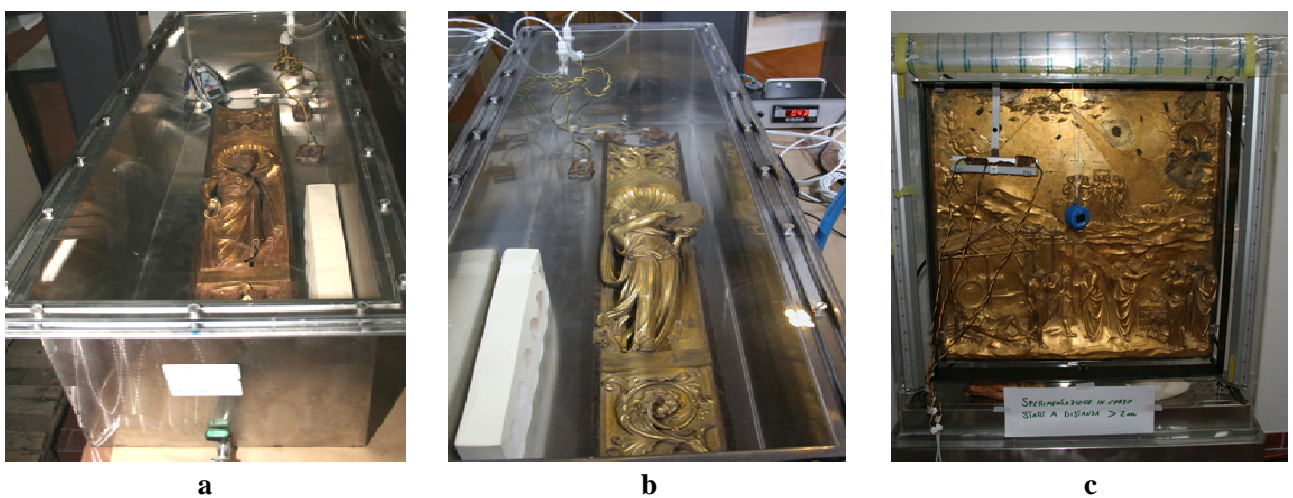


**Figure 2:** The three exhibition solutions tested for the Porta del Paradiso: Elia's frieze in the low RH showcase (a), Miriam's frieze in the nitrogen showcase (b) and Noah's panel in the open showcase (c).



The galvanic sensors previously described (Chapter 3.4) were used for the choice of the best display options proposed by the Opificio delle Pietre Dure.

Due to the complex technology required to set up the open showcase with controlled microclimate, experimentations with the nitrogen-purged and the low RH showcases began earlier (July 2009) than the one of the open showcase (September 2009). For technical reasons, it was not possible to start the planned conditioning of the two showcases at the same time as the two friezes were placed in the cases. In the meantime, low RH (below 20%) was achieved by the use of conditioned silica gel.

### **3.5.1. Closed showcases**

The two closed showcases were realised by the colleagues of the OPD. The volume of the two closed showcases (Figure 2a and 2b) is approximately 80 litres. They are constructed from stainless steel. The lids are made of Plexiglas and are equipped with two taps for the introduction and discharge of gases.

The nitrogen showcase (Figure 2b) was saturated by flushing (3 liters/minute) with pure nitrogen for approximately two hours. The complete removal of oxygen was verified by an oxygen sensor connected to the discharge tap. A box of moisture absorbers calibrated to 0% RH was also introduced into the showcase to maintain a low relative humidity all the time.

In the showcase with low relative humidity (Figure 2a), the latter is kept constant at a value of approximately 20% as follows:

- a) before being introduced inside the showcase, the dry air hose is split into two lines. One line (5 liters/minute) is forced through a water bubbler to provide humid air. The two air lines are then re-joined in an airtight chamber equipped with a sensor measuring relative humidity and temperature.
- b) Two flowmeters are used to adjust the ratio of dry/humid air to obtain the desired conditions of relative humidity. A box of humidity absorbers calibrated to 20% RH is also installed in the showcase.

### **3.5.2 Open showcase**

The open showcase with controlled microclimate was designed and built by the colleagues of the CNR of Sesto Fiorentino. The open showcase should create the same local environmental conditions as the showcase with low RH, but with the additional advantage of avoiding the presence of a glass panel between the object and the visitor. However, this solution is not easy to achieve

compared to the ones with the closed showcases. Significant technical difficulties such as leakage, and the related degree of insulation between the inner and the external environments, are complex to overcome.

The open showcase has the shape of a parallelepiped (Figure 2c), and is  $102 \times 102 \times 21.5 \text{ cm}^3$  (H×W×D) in size. The central area,  $78 \times 79 \text{ cm}^2$  (H×W), of its front surface is open, i.e. only a 10 cm wide *passé-partout* is left. The door panel is placed at the centre of the case. The case is designed so that a volume of dry air surrounds the panel permanently, without any need for a glass cover. The efficiency of the system was investigated, by the colleagues of the CNR of Sesto Fiorentino, with the acquisition of accurate profiles of temperature, air speed, relative humidity and moisture content in front of the door panel. Relative humidity is the most critical parameter for the panel. It is controlled by the air temperature and moisture content, expressed in terms of the Humidity Mixing Ratio. This ratio is expressed as the ratio between the mass of moisture present in the air to the mass of dry air. The air speed and Mixing Ratio profiles show that the protective air layer is approximately 20 cm thick, but the Mixing Ratio profile shows that the airflow includes some 60% of ambient air. This reduces by 40% the ambient relative humidity.

The airflow profile, measured with a hot wire anemometer in front of the panel shows that the air speed ranges from 10 cm to  $20 \text{ cm s}^{-1}$ , and is of the same order of magnitude as the airflows, i.e. up- or downdraughts, that are naturally generated in a room for the small temperature differences generally existing between indoor air and walls.

### **3.5.3 Thermo-hygrometric monitoring inside the three showcases**

The monitoring of thermo-hygrometric conditions started at the time corresponding to the definitive conditioning of the showcases and was carried out using wireless data loggers (Giorgio Bormac, mod. Marconi SPY TH) acquiring data every 30 minutes.

The temperature and RH variations for the different display environments are shown in Figure 3.

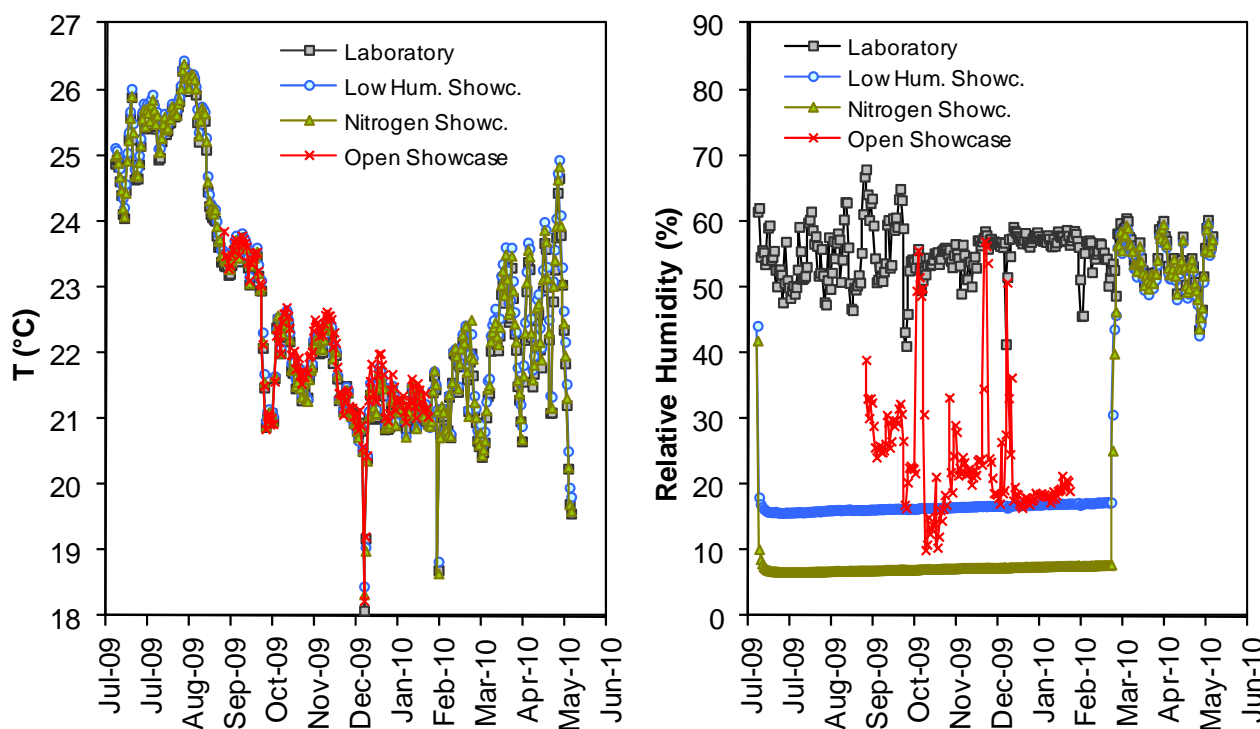


**Figure 3: Temperature and relative humidity variations during the monitoring of the “Porta del Paradiso”.**

The relative humidity (RH) stabilised at around 7% in the nitrogen-purged case, and around 17% in the case with low RH. These results reveal as well that it was not possible to completely stabilise RH at a specific value in the open showcase. Indeed in the open showcase, RH oscillates in the range 16–39%. Nevertheless, this value is considerably lower than the ambient conditions in the surrounding environment (the laboratory), which remained in the range 40–70%.

### 3.5.4 Characterisation of the three sections from the Porta del Paradiso

The three sections from the Porta del Paradiso that were characterised by the colleagues of the OPD.

It has been observed that the surfaces of the two friezes are different, despite their common past conservation history. Corrosion products are visible in several areas on Elia’s frieze (Figure 4a), which appears to be the less stable than Miriam’s frieze, as corroded areas are less frequent over the latter frieze.

$\mu$ -FTIR and SEM-EDS analyses results revealed the typical residual porosity of mercury gilding (see Figure 4b) and a patina of corrosion products mostly composed of cuprite ( $\text{Cu}_2\text{O}$ ), a copper oxide; atacamite,  $\text{Cu}_2(\text{OH})_3\text{Cl}$ , a hydroxychloride; as well as antlerite,  $\text{Cu}_3\text{SO}_4(\text{OH})_4$  and brochantite,  $(\text{Cu}_4\text{SO}_4(\text{OH})_6$ , both hydroxysulphates. Results from analysis of the surface of Noah’s

panel revealed microblistering of the gilded surface (see Figure 4c), as well as minor pitting and extrusion of green corrosion products through the gilding. These minerals were also identified as copper hydroxychlorides and hydroxysulphates mixed with cuprite and tin oxides.

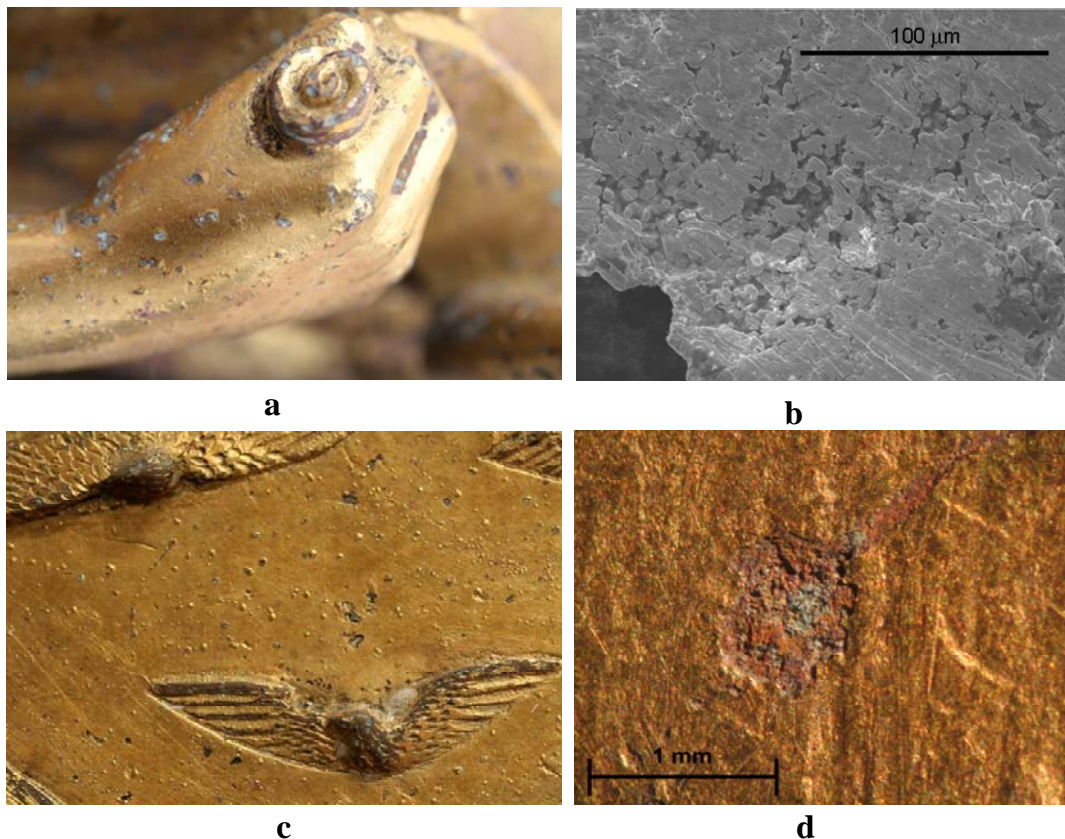


**Figure 4: Detail of Elia’s frieze (a), SEM image of the gilded surface (b), detail of Noah’s panel (c) and microscopic image of a corrosion pustule (d).**

### **3.5.5 Monitoring by means of galvanic sensors**

The monitoring of the electric parameters of the galvanic sensors prepared for for the choice of the best display environment for the “Porta del Paradiso” has been performed using a multi-channel acquisition system KEITHLEY 3706. This instrument allows the monitoring of the electric parameters (current, potential and resistance) of 20 sensors at the same time by the mean of a switch/multimeter system.

The potential and the resistance are measured at open circuit, whereas the current after the closure of the measurement channel that allows the measurement and the flow of the macrocouple current through a zero-resistance system. The macrocouple current is recorded only after 5 minutes of stabilization of the galvanic coupling, and the average of the last ten measurements (1 measurement/sec) is taken as macrocouple value. A Labview® based software has been written to control the KEITHLEY 3706 and the data acquisition.

---

RESULTS AND DISCUSSION

## 4.1 Accelerate electrochemical artificial ageing of gilded bronze specimens – Results

The description of the samples and the methodology used for the electrochemical artificial ageing of gilded bronze specimens are described in the Chapter 3.3 and the results are reported in the following paragraphs.

As a reminder, N labelled samples referred to the sensors mimicking the composition of the North door of the Baptistery, S and E ones to the South and East doors, respectively.

### 4.1.1 Series I

**Table 1: Experimental parameters used for the electrochemical artificial ageing of samples of series I.**

SAMPLE	CURRENT DENSITY	TIME	POTENTIAL	NOTES
N5a	0.0005 A/m <sup>2</sup>	10 days (240 hours)	Never over 240 mV	3 breaking in the gilding.
E6b	0.05 A/m <sup>2</sup>	7 days (178 hours)	over 500 mV	The gold broke in many points.
SM5a	0.05 A/m <sup>2</sup>	7 days (178 hours)	over 500 mV	Pre-treatment by chemical reaction: immersion for 20 minutes in a concentrated boiling solution of CuSO <sub>4</sub> , and 2 g/L of NaCl. At the end of the treatment the surface is covered by crystals

This series was used to confirm the choice of the appropriated solution and to understand the magnitude of the current to be used for artificial ageing. The three trials are different in the procedure itself because the best methodology for the following tests still needed to be evaluated. Treatments performed under low current density, such as in the case of sample labelled N5a, produce corrosion products of rather small size and appearing only in a few locations (Figure 4). Contrarily, increasing the current density and therefore the aggressiveness of the treatment, the layer of salt become thicker. The ageing treatment on samples labelled E6b and SM5a, however, leads to different results: in the first case, E6b (Figure 5), there are only few points of contact between gold and bronze . In the case of SM5a, instead, pits larger than in the case of sample N5a are observed (Figure 6). In

addition, for sample SM5a, it is difficult to evaluate the state of the surface because this one is covered by copper salts. The chemical pre-treatment has been discarded because no specific improvements to the quality of the final result have been noticed.

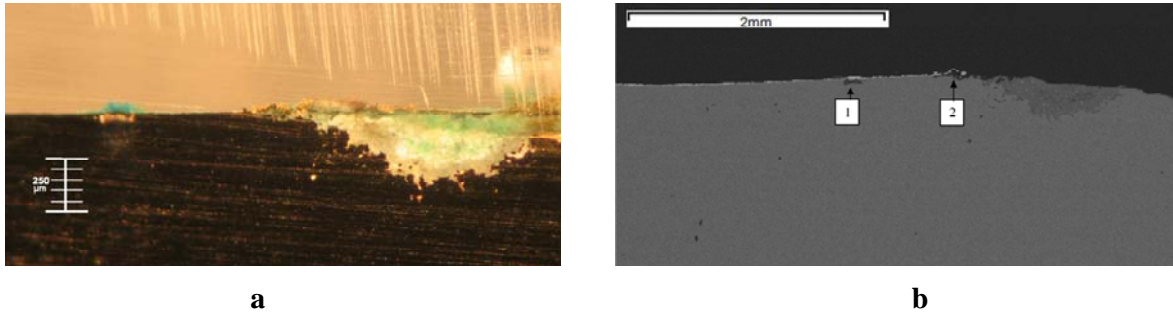


Figure 4: Stereomicroscope (a) and SEM (backscattered electrons) (b) images of sample labeled N5a. Two smaller blister formed near the main one are highlighted.

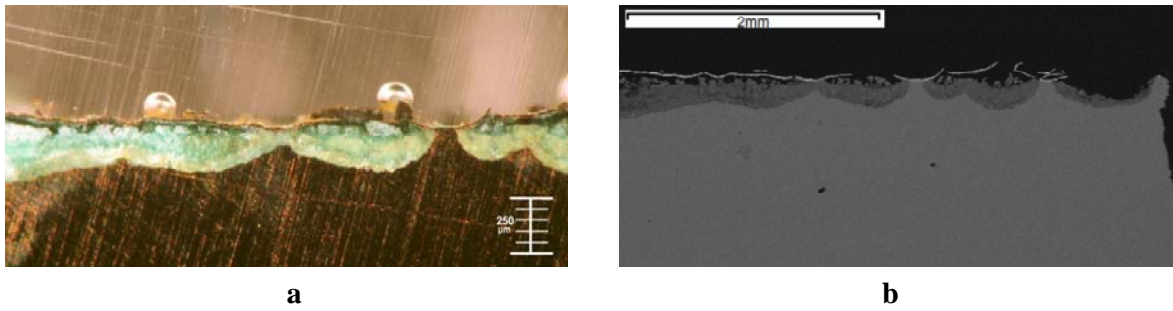


Figure 5: Stereomicroscope (a) and SEM (backscattered electrons) (b) images of sample E6b.

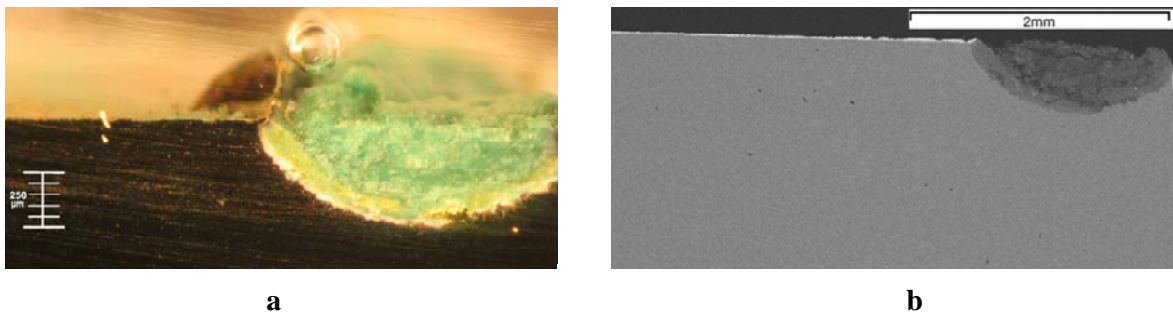


Figure 6: Stereomicroscope (a) and SEM (backscattered electrons) (b) images of sample Sm5a.

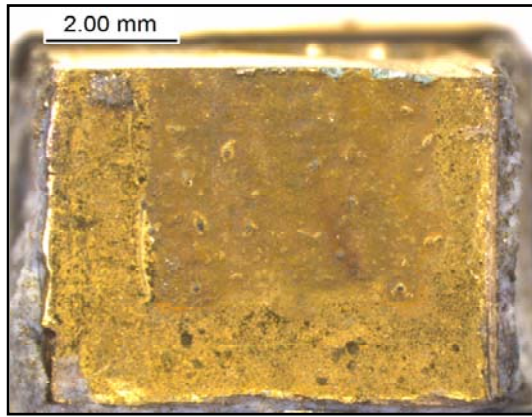
## 4.1.2 Series II

**Table 2: Experimental conditions used for the electrochemical artificial ageing of samples of series II.**

SAMPLE	CURRENT DENSITY	TIME	POTENTIAL	NOTES
N6a	0.05 A/m <sup>2</sup> 0 A/m <sup>2</sup> 0.03 A/m <sup>2</sup>	1 day (24 hours) 1 day (24 hours) 2 days (41 hours)	High (over 1000mV VS SCE)	The sample was treated first with a current of 0.05 A/m <sup>2</sup> , then extracted from the solution, dried, dipped again in the solution and subjected to less intense treatment (only 0.03 A/m <sup>2</sup> ). It has developed products of corrosion.
E8a	0.038 A/m <sup>2</sup>	2 days (41 hours)	High (over 1000mV VS SCE)	The result is similar to that of sample N6a.
N7b	1 A/m <sup>2</sup> 10 A/m <sup>2</sup> 0.058 A/m <sup>2</sup>	3 ½ hours 1 minutes 3 days (68 hours)	Varying from +100 mV (first part of the treatment) and negative values (second part)	The attempt to force growth by increasing the current of one order of magnitude, though for a limited period, has proved to be unsuccessful, since copper salts did not grow at the interface between gold and bronze.
N8b	0.05 A/m <sup>2</sup>	8 days (202 hours)	It keeps at about 50 mV	No corrosion products developed under the gilding.
S5b	0.063 A/m <sup>2</sup>	8 days (202 hours)	It keeps at about 50 mV	No corrosion products developed under the gilding

Only the first two samples have developed substantial deposits of copper as visible in Figures 7a and 8a. At the end of the treatment, the gilding of both samples appeared severely damaged (Figure 7b and Figure 8b). In contrast in samples N7b, N8b and S5b (Figure 9) there is no trace of chloride or sulphate below the gilding. The data reported in Table 3 seem to favour the idea that the success or failure of the treatment depends not on the application of more or less intense current, but on the potential that is reached during ageing.



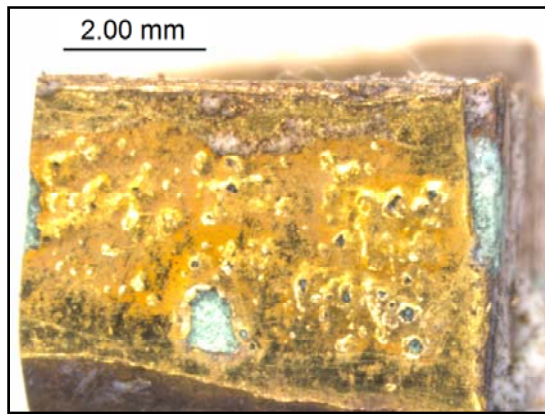


**a**

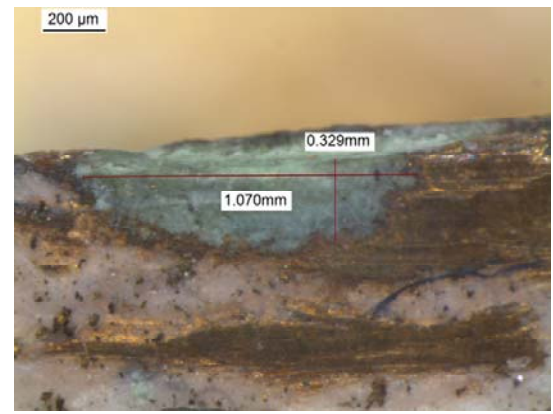


**b**

**Figure 7: Sample N6a – stereomicroscope image of golden surface (a) and of the cross section (b) in which a pit of corrosion products is visible.**

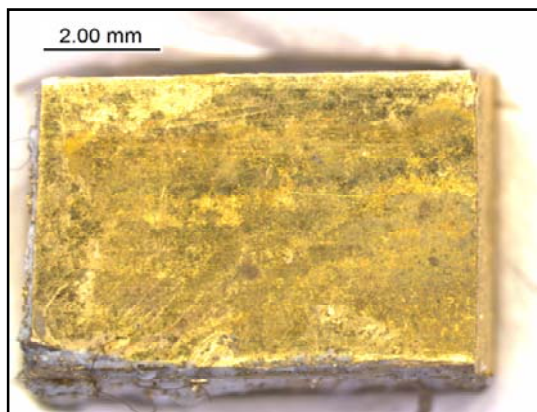


**a**

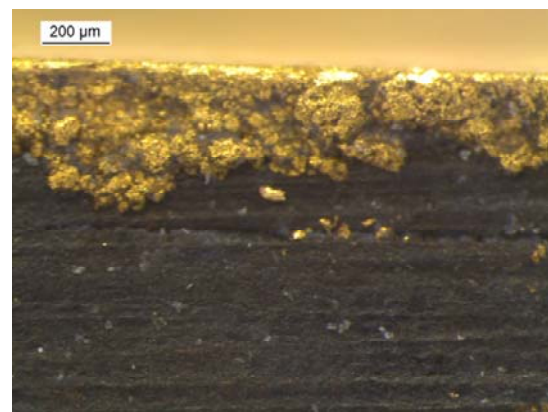


**b**

**Figure 8: Sample E8a – stereomicroscope image of golden surface (a) and of the cross section of the sample (b) in which a pit of corrosion products is visible.**



**a**



**b**

**Figure 9: Sample N7b – stereomicroscope image of golden surface (a) and of the cross section (b). No deposits of corrosion products have been found below the gilding.**

### 4.1.3 Series III

**Table 3: Experimental conditions used for the electrochemical artificial ageing of samples of series III.**

SAMPLE	CURRENT	TIME	POTENTIAL	NOTES
S1, N1, E1	0.04 A/m <sup>2</sup>	6 days (116 hours)	Varying between negative values and 250 mV in the early days, then decrease until 150 mV.	Salts developed over the surface, but not under the gilding.
E2	0.5 A/m <sup>2</sup> 0.005 A/m <sup>2</sup> 0.5 A/m <sup>2</sup>	2 days (49 hours) 3 days (69 hours) 3 days (72 hours)	Hundreds of mV in the first part of the treatment; negative values in the third part.	Presence of cuprite and some pits.
E3	0.995	4 days (100 hours)	Between 100 and 200 mV..	Satisfying treatment: salts developed deep in.

The first three samples (S1, N1 and E1) presented big difference one to each other, despite they underwent the same treatment: while N1 and E1 exhibited , at the end of treatment, points where nucleation of copper crystals, rather large, appeared (Figure 10a, Figure 12a), the surface of sample S1 is exactly as before the electrochemical ageing (Figure 11a). It's important to notice that the areas of "attack" are in correspondence with defects in the gilding. However, by analyzing the samples cross-sections, no traces of corrosion products have been found beneath the gold in any of the cases mentioned above (Figure 10b, 11b as well as 12b).

The treatment of the sample labelled E2 gave unexpected results: although a pit rich in copper chlorides and sulphates has grown (Figure 13a), a layer of reddish compounds, most probably composed by cuprite, grew from gilding surface discontinuities. This phenomenon had never been observed in previous tests and this layer extended quite deep under the surface of gold (Figure 13b).

Sample E3 provided the most encouraging results among all samples analyzed: it has developed pits of considerable size in which the corrosion products of bronze are concentrated. It has to be noticed that the surface crystals are concentrated near the edges of the sample and near the defects of the gold. In the former case, this corresponds to the location where it is expected that the current is more important due to the effect of the geometry. The sample cross – section shows very large deposits of salt right at the interface of the two metals (Figure 14, Figure 15). In such a case, the potential is measured

at values ranging between 100 and 300 mV, far from the 1000 mV of the first series , but nevertheless the results are even better.

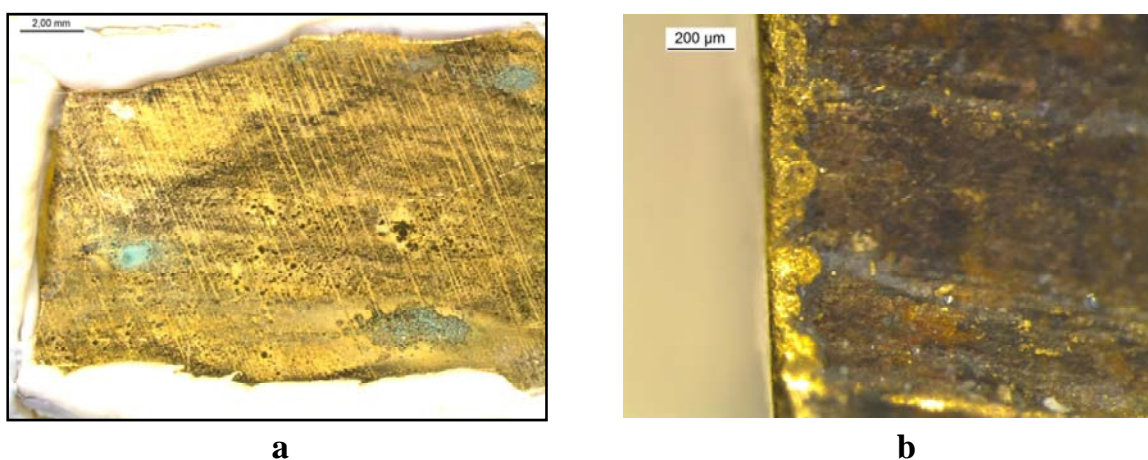


**Figure 10: Sample N1 – stereomicroscope image of golden surface (a) and of the cross section (b). No deposits of corrosion products have been found below the gilding.**

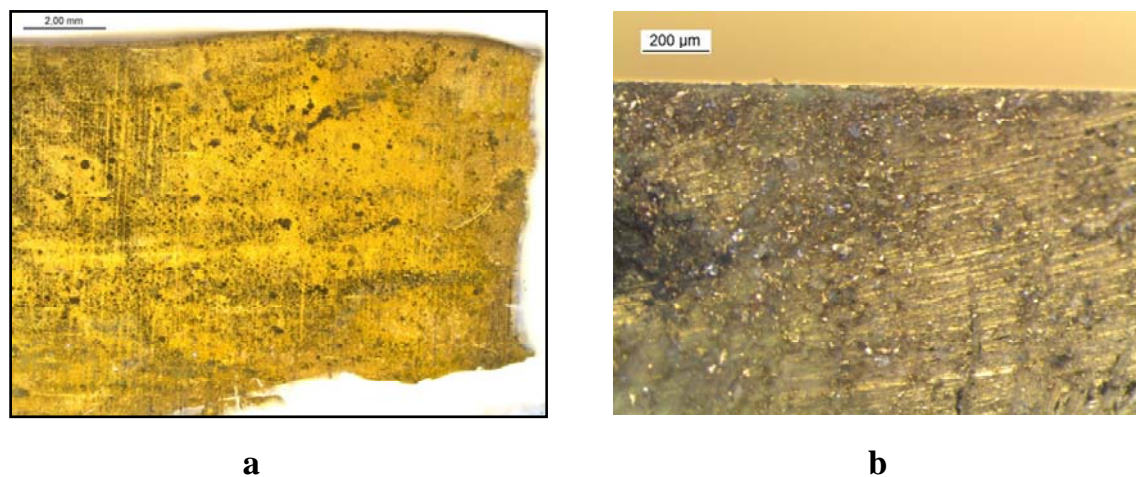
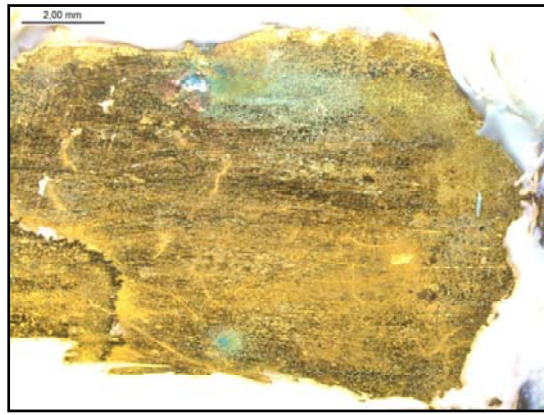
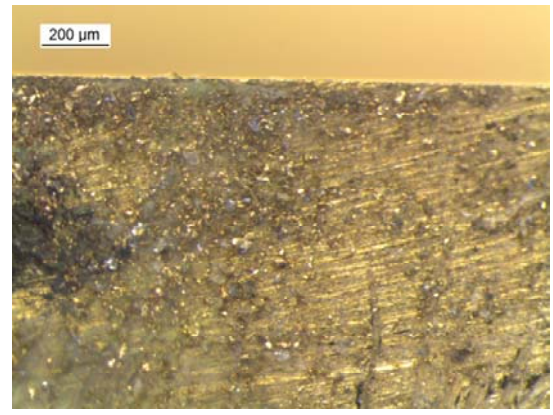


**Figure 11: Sample S1 – stereomicroscope image of golden surface (a) and of the cross section (b). No deposits of corrosion products have been found below the gilding.**



**a**

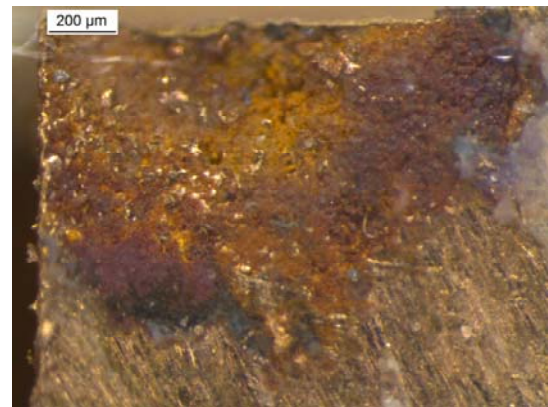


**b**

**Figure 12: Sample E1 – stereomicroscope image of golden surface (a) and of the cross section (b). No deposits of corrosion products have been found below the gilding.**



**a**



**b**

**Figure 13: Sample E2 – stereomicroscope image of a detail of the golden surface (a) and of the cross section (b). A thick reddish layer of cuprite can be observed in deep respect to the surface.**

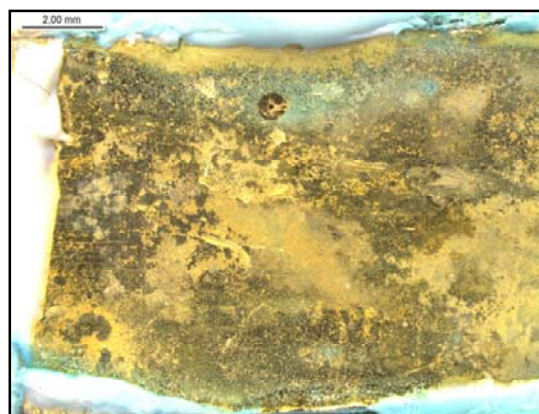


**Figure 14: Stereomicroscope image of golden surface of sample E3.**

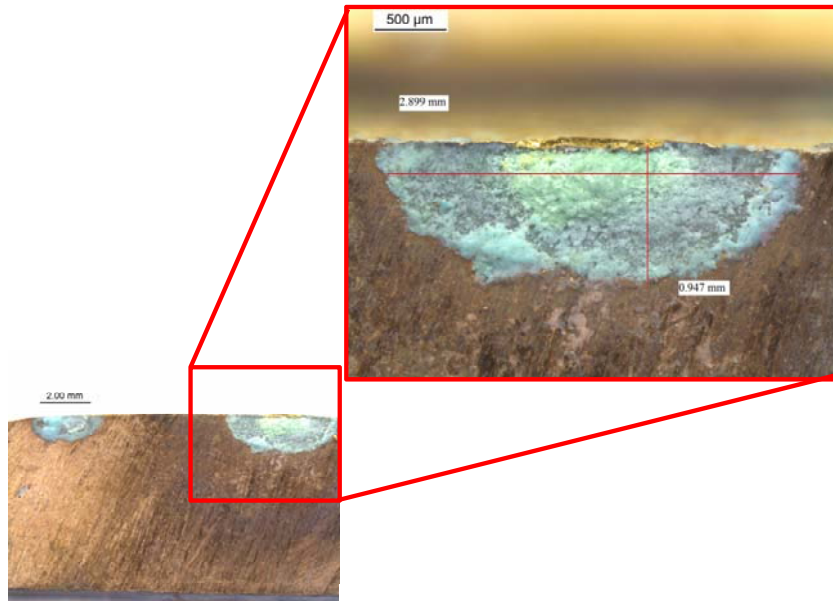


**Figure 15: Cross section stereomicroscope image of sample E3 in which two pits of corrosion products can be observed.**

#### 4.1.4 Series IV

Table 4: Experimental conditions used for the electrochemical artificial ageing of samples of series IV.

SAMPLE	CURRENT DENSITY	TIME	POTENTIAL	NOTES
N2, S2	1 A/m <sup>2</sup>	3 days (76 hours)	Varying between 300 and 200 mV vs SCE	Some cuts have been made on the surface. Expected results have been reached

The very high variability of the obtained results during the first series was probably due to the discontinuities in the gold layer caused by the method used for the gilding. In fact the technique of mercury amalgam is based on the ability of mercury to form complexes with gold and evaporate in the presence of additional heating. However the evaporation process causes the formation of pores that may be more or less large and deep depending on the local composition of the amalgam. Subsequently, it is through these defects that the corrosion attack can start and sulphates and chlorides could pass through the gilding and originate the copper salts that had to be formed.

Since the process of gilding was followed by a “burnishing” process in order to reduce the porosity of the surface, it was possible that, for some samples, the gold film was so thick and compact that corrosion could not start. Since there is no guaranty to control the reproducibility of the porosity, in this last series of tests, the gilding has been carved, in order to locate the beginning of the corrosion processes and facilitate the migration of sulphates and chlorides from the solution to the bronze.

In the case of samples S2 and N2, the incisions were performed delicately, trying to carve only the gold surface and minimize the damage to the bronze alloy below. The incisions were made with a scalpel ("scratch" Figure 16a) or with a tip ("hole" Figure 16b).

At the end of the treatment, the samples surface was covered by crystals (Figure 17a, Figure 18), but, moreover, as could be seen from the cross – sections (Figure 17b, Figure 19), the salt deposits have grown deeply in the alloy. More important, the corrosion attack appeared to be locate only in correspondence of the surface defects that had been artificially created.

As the ageing treatment was successful, these samples were analyzed more thoroughly by scanning electron microscopy.

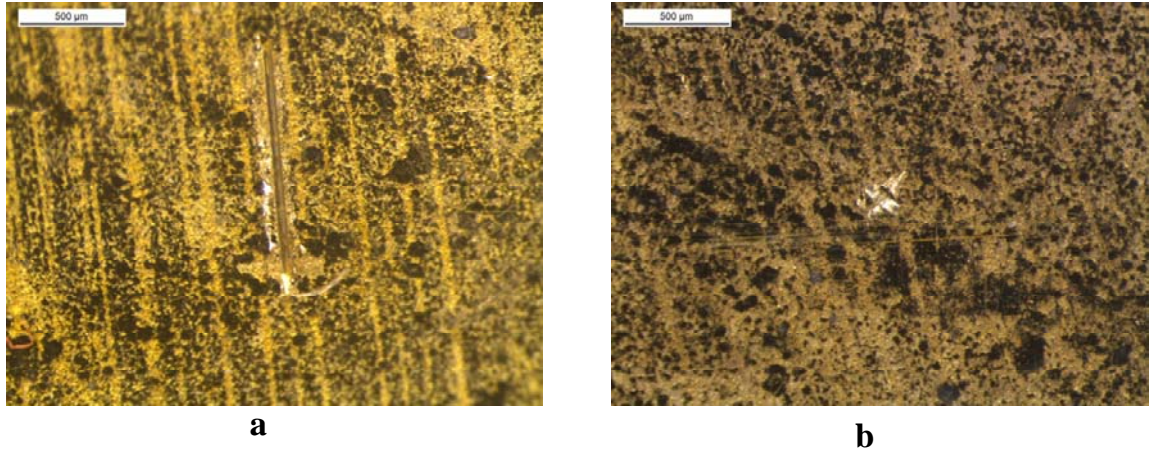


**Figure 16: Stereomicroscope image of a “scratch” (a) and a “hole” (b) on the gilding of sample N2 before the electrochemical treatment.**

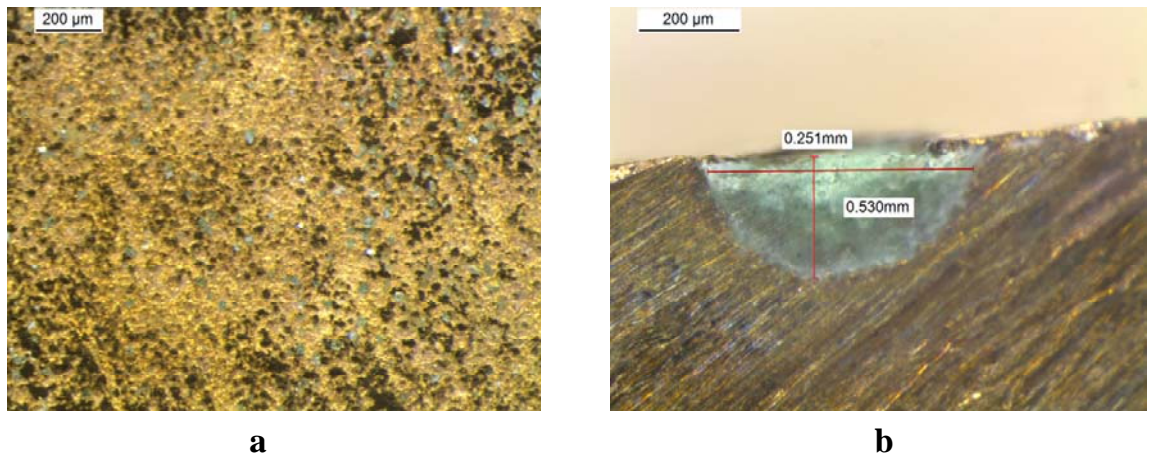


**Figure 17: Stereomicroscope image of gilded surface of sample N2 at the end of the electrochemical treatment (a) and cross section of the same sample, in which a pit of corrosion products is visible.**

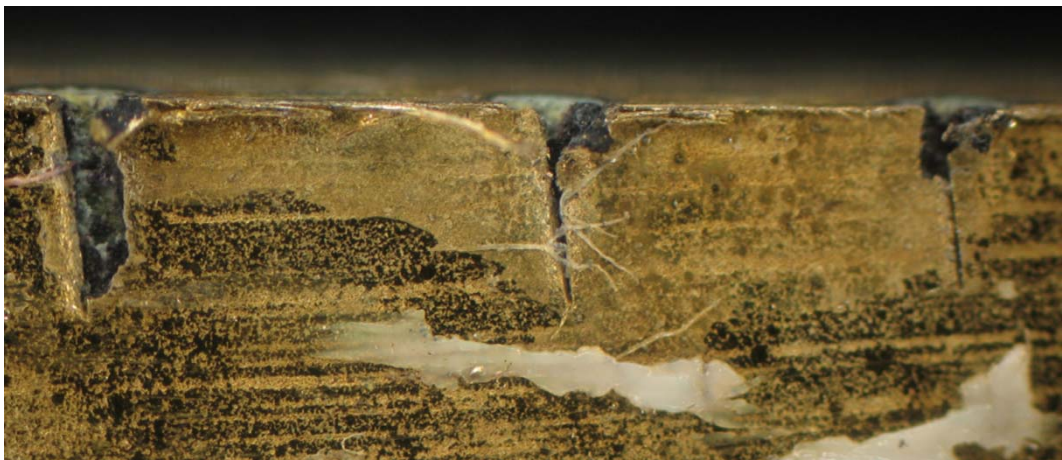


**Figure 18: Stereomicroscope image of golden surface of sample S2 at the end of the electrochemical treatment. In which three scratches made on purpose are visible (2,5X magnitude).**



**Figure 19: Cross section stereomicroscope image of sample S2 in which the scratches of Figure 32 are visible (2,5X magnitude).**

Images obtained by a Scanning Electron Microscope of samples N2 and S2 cross – sections are reported in Figures 20 and 28. Analyses were performed in high vacuum.

### ***Sample S2***

In Figure 24 and Table 6, the results of EDX analysis carried out on the locations indicated by points “Spectrum” in Figure 23 are reported: they confirm the presence of sulphates and chlorides within the pit and consequently the effectiveness of the ageing treatment.

The analyzed area is the one that has been “attacked” by the corrosive treatment: the analysis were focused on the area of the sample that shows 3 pustules nucleated in correspondence with 3 scratches made on purpose (Figure 20).

Focusing on the analysis of a single pustule (Figure 21) it is possible to distinguish 3 areas:

- an outer zone corresponding to the base alloy, where the signs (horizontal lines) left by the blade used to dissect the specimen can be distinguish.
- the area of the incision where the corrosion products has been accumulated below the gilding.
- a transition zone, intermediate between the previous two (Figure 21), where it can be assumed that the alloy is altered but not completely corroded. Higher magnification of the images of this area show a sponge – like structure which could be associated with a phenomenon of selective corrosion, called dezincification (Figure 22).

To confirm these observations and to determine if the ageing process has really led to the electrochemical formation of the desired corrosion products, several qualitative and quantitative analysis were performed using EDX. Moving from an area to another one



(Figure 24), a map of the elements was recorded (Figure 25) and a concentration profile along a line (Figure 26) was made.

It is immediately possible to notice the differences between areas: the chlorine is present mainly in the area immediately adjacent to the crater, while the sulphur is less concentrated in this area than in the centre of the pit. A significant concentration of sulphur is also present on the gold layer or just below it. Oxygen is located mainly in the pit. One element that seems to be absent from both the altered areas near the pustule is zinc, and this confirms what has been observed previously (Figure 34). Since zinc concentration in the corroded area is never higher than in the alloy bulk, it can be assumed that atoms are selectively corroded from the alloy and carried into solution by the passage of current.

The zero on the graph presented in Figure 27 corresponds to the bronze alloy, while the pit is located at 400  $\mu\text{m}$ . Chlorine has a highest concentration in an area of 100 microns, which correspond to the alteration zone at the edge of the crater. The border between this last area and the bronze alloy is underlined by the black line.

The analysis of the other two pits provided results comparable to those listed above.

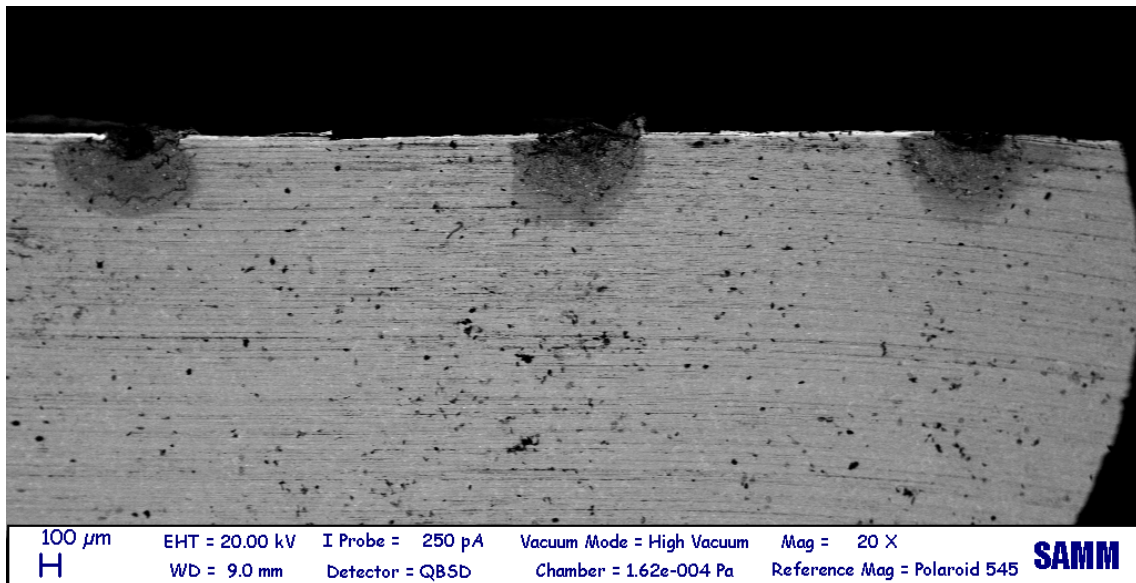


Figure 20: SEM image (backscattered electrons) of sample S2.

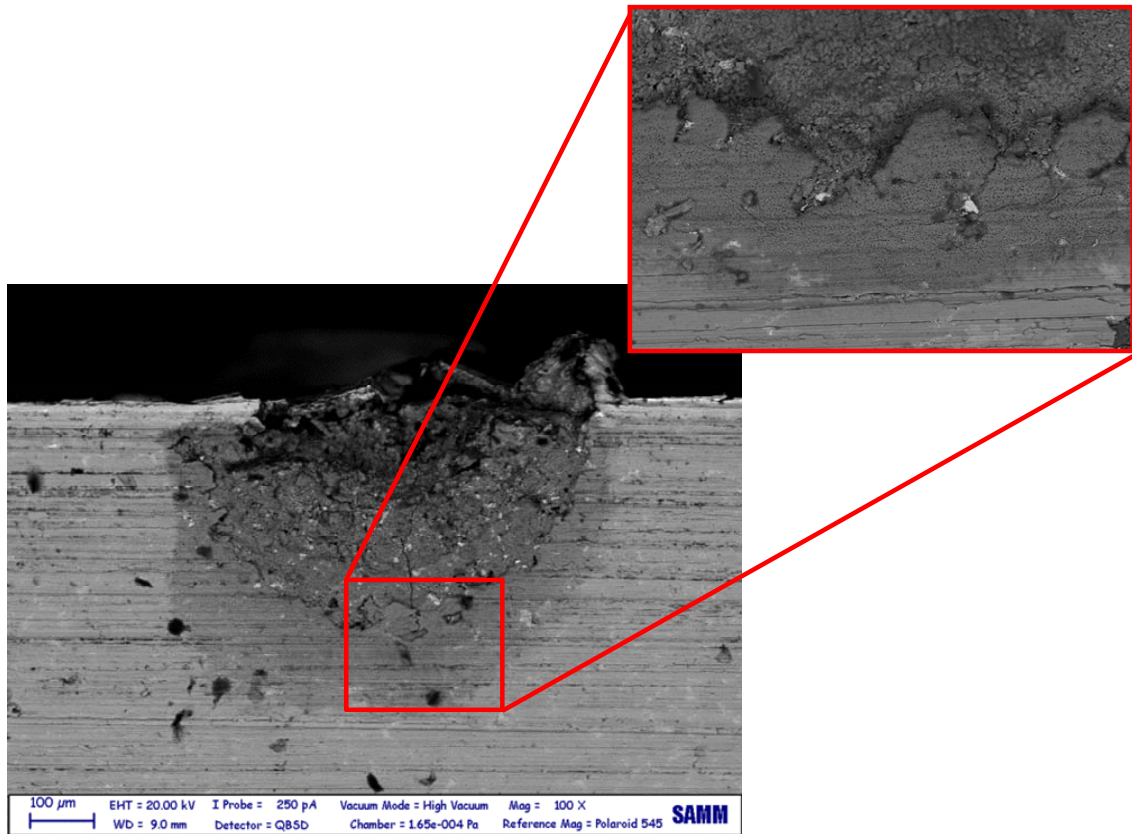


Figure 21: Sample S2 – SEM image (backscattered electrons) of the first pustule, from left, of Figure 19 and enlargement of the area between bronze alloy and pustule.

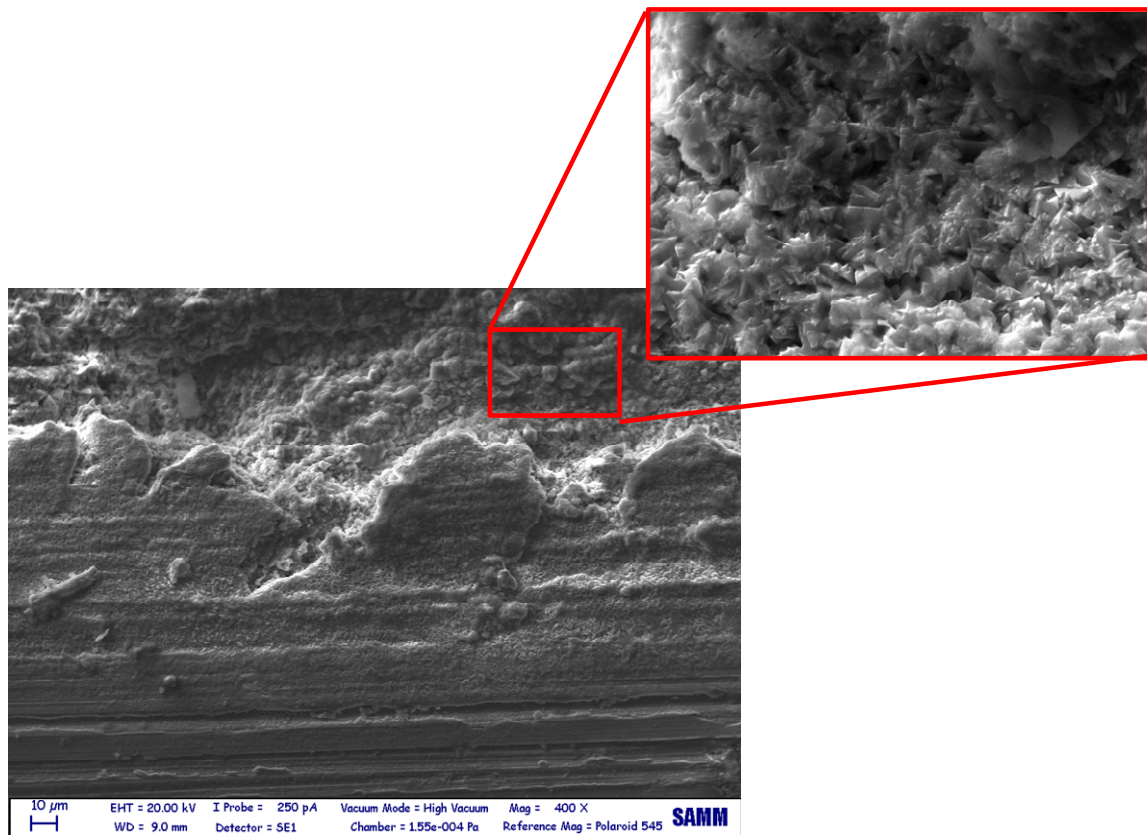


Figure 22: Detail (secondary electrons) of the zone of Figure 36. The sponge – like structure due to the dezincification has been noted.

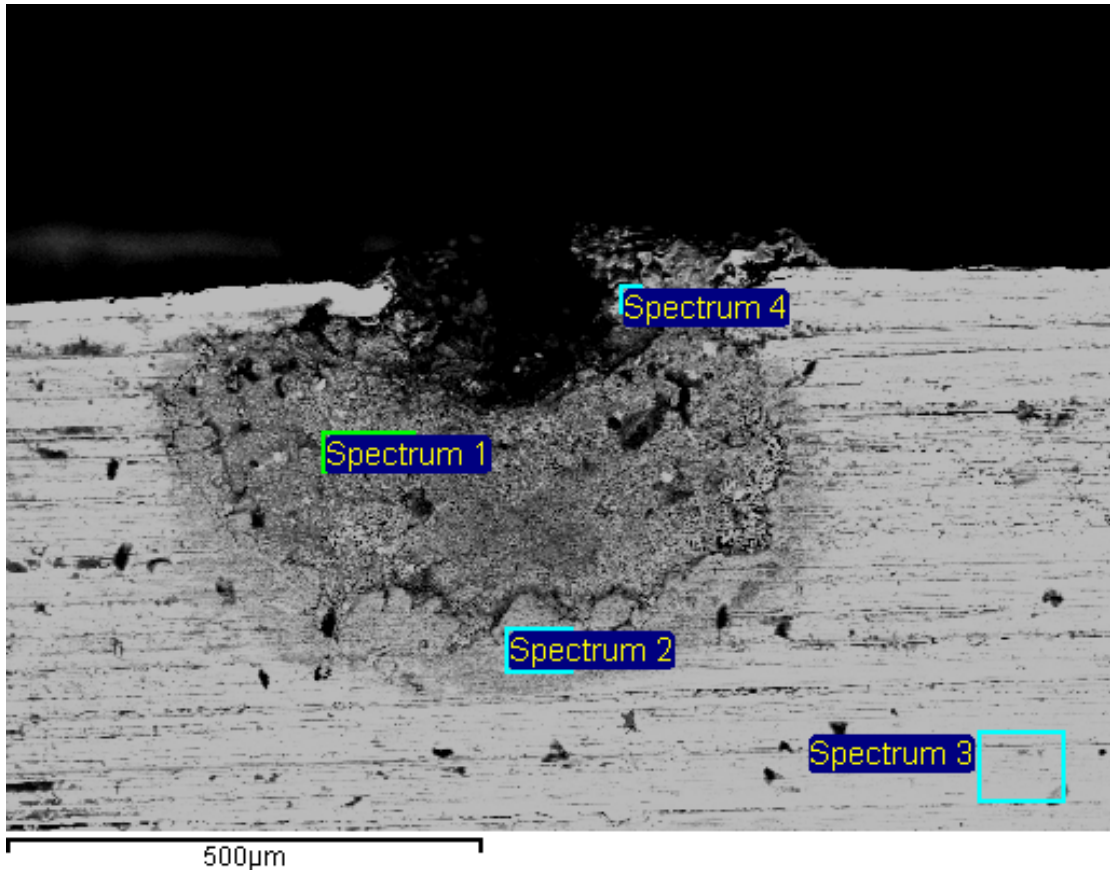


Figure 23: EDX scans areas of sample S2.

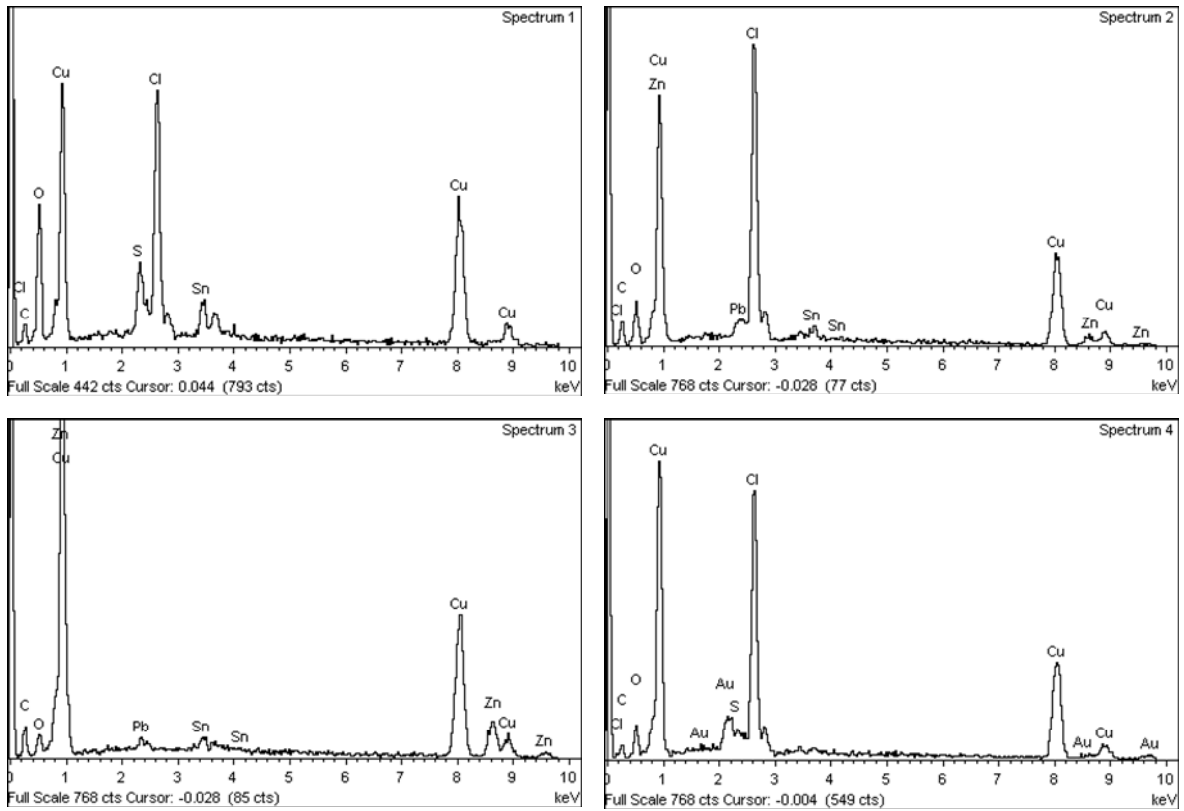
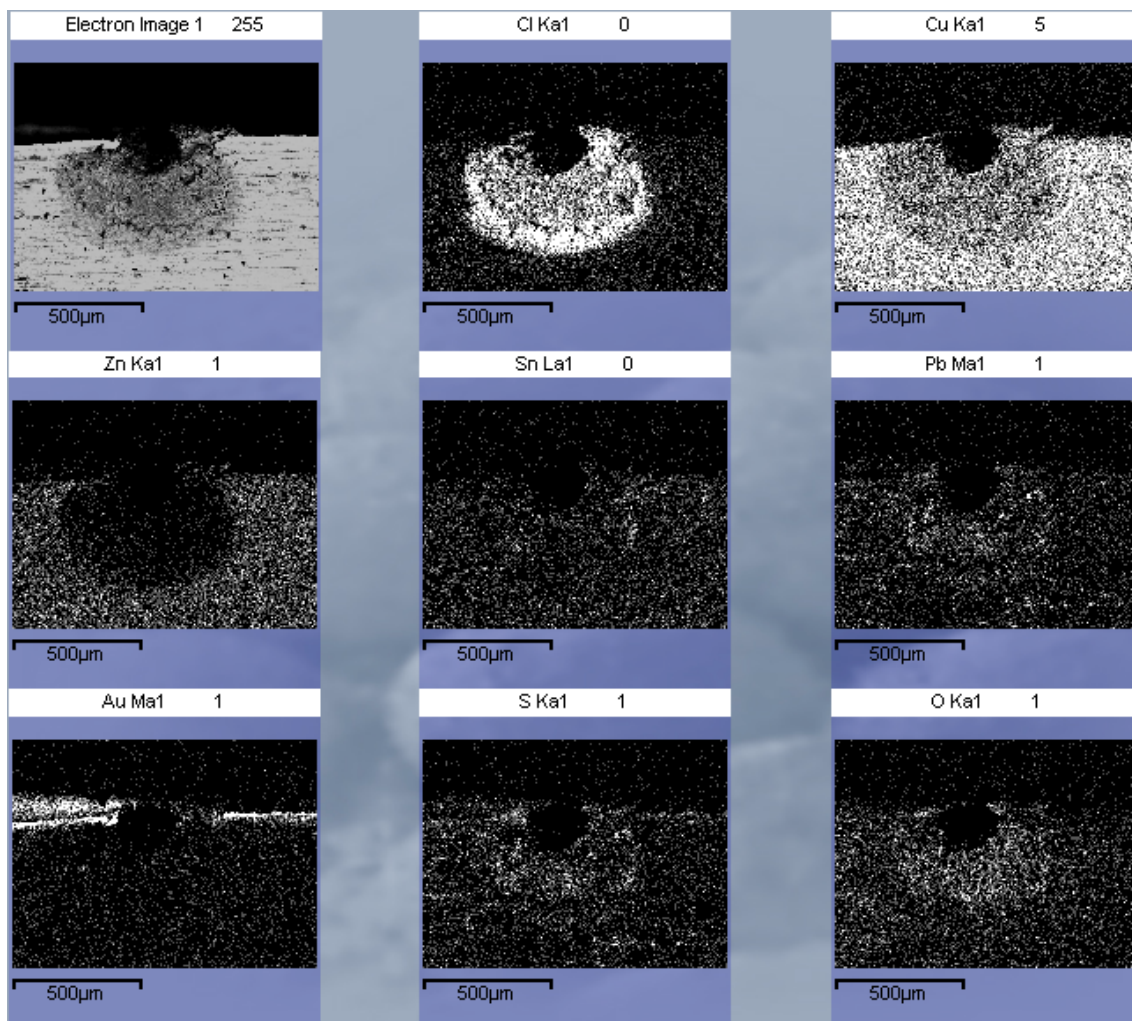


Figure 24: EDX spectra of the four areas of figure 35.

**Table 5: % of elements in each EDX spectrum recorded in the four areas of the pit**

Spectrum	O	S	Cl	Cu	Zn	Sn	Pb
1	26,32	2,10	15,02	43,28	1,56	6,69	5,03
2	12,99	0,11	28,39	47,59	4,18	2,62	4,12
3	4,66	0,31	0	67,47	21,45	3,54	2,64
4	10,58	0,86	27,41	55,83	1,23	2,00	3,80



**Figure 25: EDX mapping of principal elements present in sample S2.**

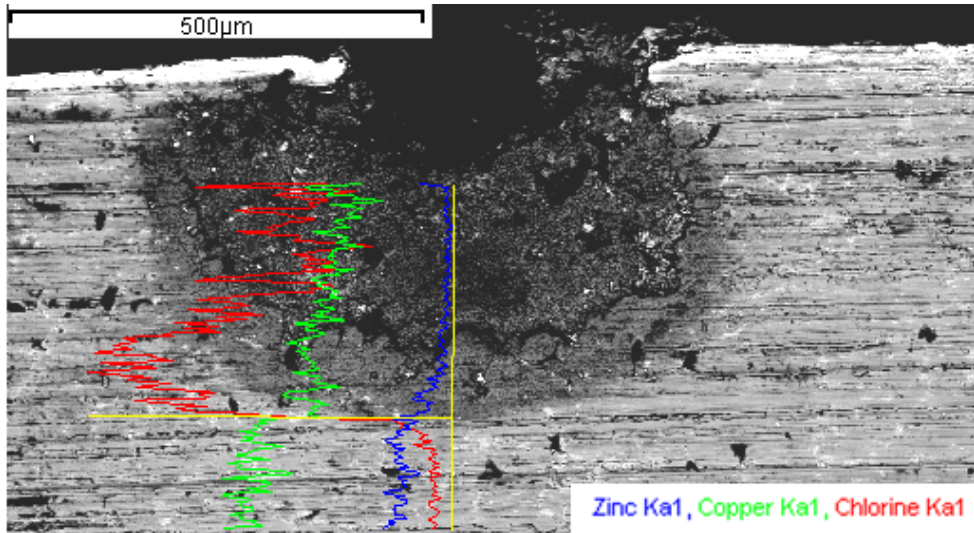


Figure 26: Elements analysis along a line.

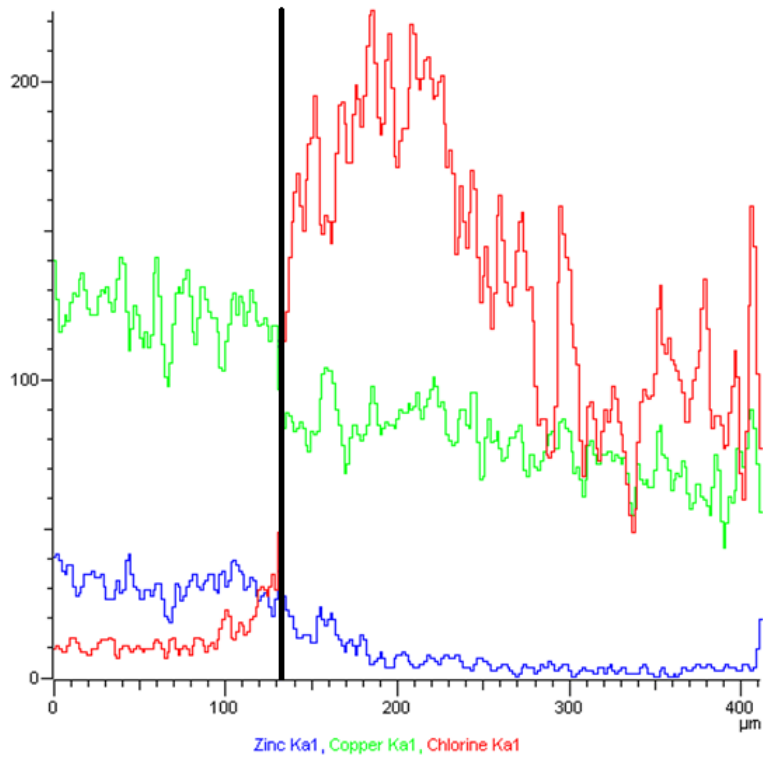
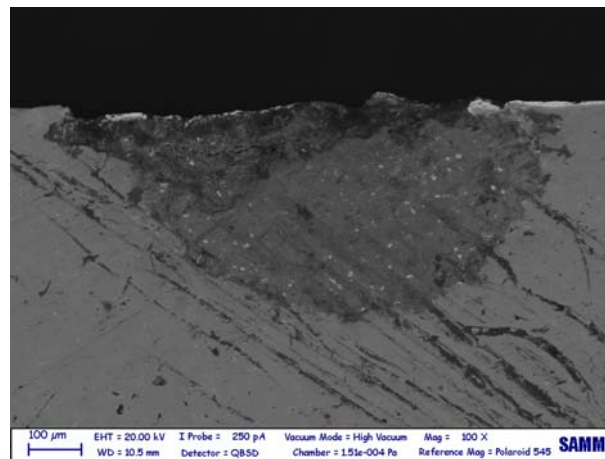


Figure 27: Graph of distribution of the elements (Zn, Cu and Cl) along a line.

### *Sample N2*

It is difficult to distinguish the three areas that were well defined in sample S2, but this is probably due to the fact that the cross – section was not carried out precisely in the middle of the crater, so the pustule remains confined to the top left area of the image (Figure 28). In any case the morphology seems a bit different because the alloy that was used to prepare the two samples was not exactly the same.

The EDX analysis of the three areas substantially coincide with those performed on sample S2. The only differences are a greater percentage of sulphur and oxygen in the transition area compared to the previous case. The presence of some peaks of Ca due to the contamination of the sample during the cut are also visible, here. However the difference is not so pronounced and the most important element remains chlorine.



**Figure 28: SEM image (backscattered electrons) of sample N2.**

### 4.1.5 Series IV

**Table 6: Experimental conditions used for the electrochemical artificial ageing of samples of series V.**

SAMPLE	CURRENT DENSITY	TIME	POTENTIAL	NOTES
E3 E4 E5a E6a E6b E7a E7B EM4 EM1 EM5 E8a E8b	1 A/m <sup>2</sup>  0.1 A/m <sup>2</sup>	5 days (124 hours)  2 days (41 hours)	The values of potential of the various samples are consistent and comparable with those of samples N2 and S2.	Final set of samples. The cuts were deeper than in the previous case

The procedure followed to achieve these samples was very similar to the previous one (Series IV), except for the incisions on the gilding, much deeper, carried out on the samples by the staff of the OPD.

Almost all the samples reacted in same way (Figure 29, Figure 30) and their potential has always shown similar values ranging approximately between 300 mV, at the beginning of the treatment, and 100 mV, at the end. Only one sample, labelled E6b, constantly showed values of 30 to 40 mV lower than the average and in fact its final appearance is slightly different from other samples: in addition to the usual blue-green salts it has developed red products, probably cuprite (Figure 31). Other samples, viewed under a stereomicroscope, also show the presence of the same substance, but only confined to particular areas of the incisions (Figure 32).

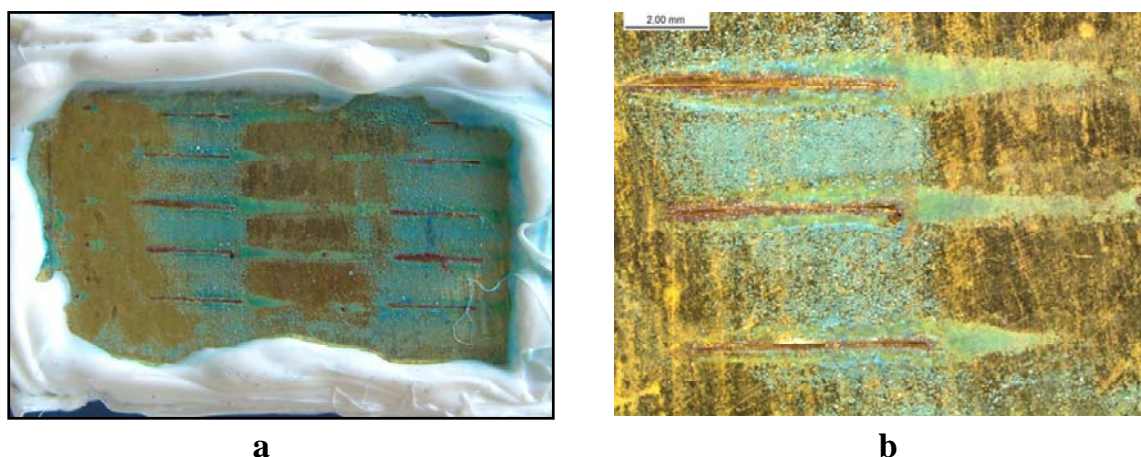
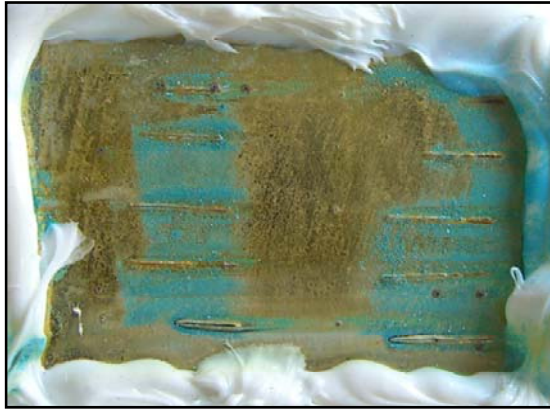
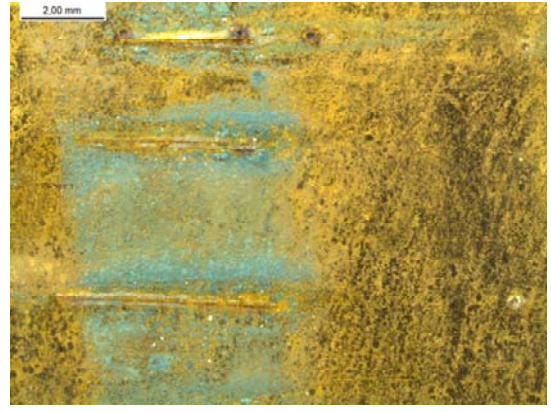


**Figure 29: Macro (a) and stereomicroscope (b) images of sample E8a at the end of the treatment.**



**a**



**b**

**Figure 30: Macro (a) and stereomicroscope (b) images of sample E4m at the end of the treatment.**

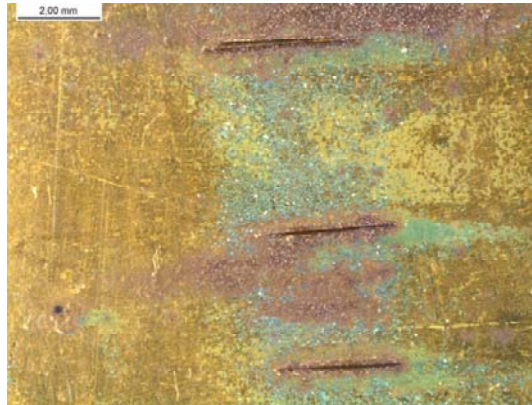


**Figure 31: Stereomicroscope image of sample E6b. The presence of cuprite can be noted also far from cuts.**

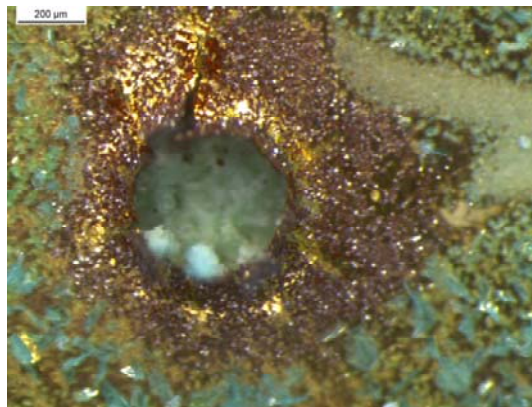


**Figure 32: Stereomicroscope image of sample E3. The cuprite is present only near the hole made on purpose in the gilding.**



## 4.1.6 Conclusions

To summarize the results of the electrochemical artificial ageing performed on specimens of gilded bronze, the following outcomes have been observed:

- Series I: useful to verify the composition of the solution as well as to identify the magnitude of current density to be applied.
- Series II: it was not possible to establish a correlation between ageing time, current density and treatment efficiency. However, a correlation between the success of the treatment and high values of potential versus Ag/AgCl has to be noted. In contrast treatments in which the value of potential is only 50 mV do not give good results.
- Series III: using the same treatment time and current density does not guarantee the reproducibility of results.
- Series IV: the surface of the specimen was carved in order to confine the points of etching. The reproducibility of the treatment is the expected one. It must be noticed that the potentials throughout the treatment were similar in trend and values.
- Series V: final set. In this case as well the surface has been carved to locate the attack. Excellent reproducibility of the treatment was achieved.

The procedure set up for the final set of specimens (series V), that consist in the application of a current density of  $1 \text{ A/m}^2$  for 5 days followed by the application of a current density of  $0.1 \text{ A/m}^2$  for 2 days revealed to be suitable for the purpose of creating artificially aged gilded bronzes. The incision of the gold surface allows the localization of the corrosion process and the growth of corrosion products.

Specimens of gilded bronze artificially aged using this procedure can be used to test cleaning methodology and conservation treatments.

## 4.2 The case study of the Porta del Paradiso

The galvanic sensors that were developed for case study of the Porta del Paradiso, (Paragraph 3.4.1) have been used to record the electric parameters of the corrosion process (macrocouple current, voltage and resistance between gold and bronze) under different environmental conditions. The aim of this part of the research project was to choose the best display option by comparing the values recorded by the galvanic sensors under the three different exposure condition that were proposed for the display of the Porta del Paradiso (Chapter 3.5):

- Low humidity showcase: a closed showcase with low and constant relative humidity (between 15 and 20%)
- Nitrogen showcase: a closed showcase saturated with nitrogen
- Open display case: an open showcase with controlled microclimate. A dynamic flux of air separates the space occupied by the door parts from the surrounding environment.

20 galvanic sensors have been prepared at the Politecnico di Milano laboratories and then transported to Opificio delle Pietre Dure where the three showcases were prepared for the tests.

For the monitoring of the corrosion process parameters, a multi-channel acquisition system KEITHLEY 3706 was used. This instrument allows the monitoring of the parameters of the 20 sensors by the means of a switch/multimeter system.

The macrocouple current, between the gilding and the bronze, is directly correlated to corrosion rate by Faraday's law.

For this study, the following assumptions were made:

- the bronze and the gilding have the same surface area
- the cathodic process (oxygen reduction) occurs mainly over the gold surface
- only copper is oxidised ( $\text{Cu} \rightarrow \text{Cu}^{2+} + 2\text{e}^-$ )
- corrosion is generalised

The galvanic sensors used in this study were acclimated to the partially controlled environment of the laboratory for at least two months before being placed in their test environment (Figure 1). The laboratory had controlled temperature, but no control for RH. The two-month period of preconditioning in the laboratory was necessary for the stabilisation of the sensors and to acquire the average macrocouple current characteristic of each sensor.

After this period of preconditioning, the sensors (three for each exposure solution) were placed alongside three sections from the doors in the three display environments previously described (Chapter 3.5).



Figure 1: Galvanic sensors at the OPD laboratory, during the preconditioning period.

Some sensors had to be removed or changed during the experimentation. The two main problem observed that lead to the removal of some sensors were the presence of short circuit or the lack of a continuous electric contact between the gold and the copper cable.

The values of macrocouple current, potential and resistance of a sensor that had to be removed is reported in Figures 3, 4 and 5 (grey coloured). For comparison in orange are also reported the values of a good sensor.

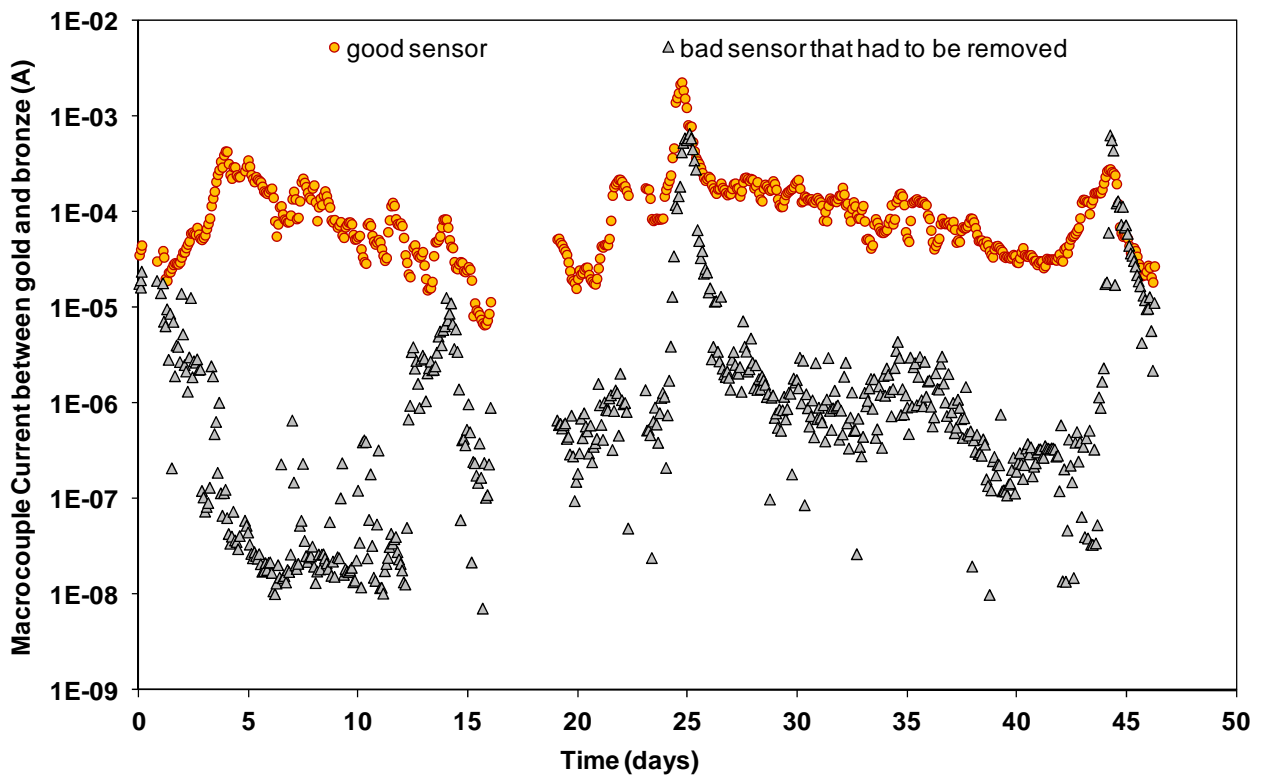
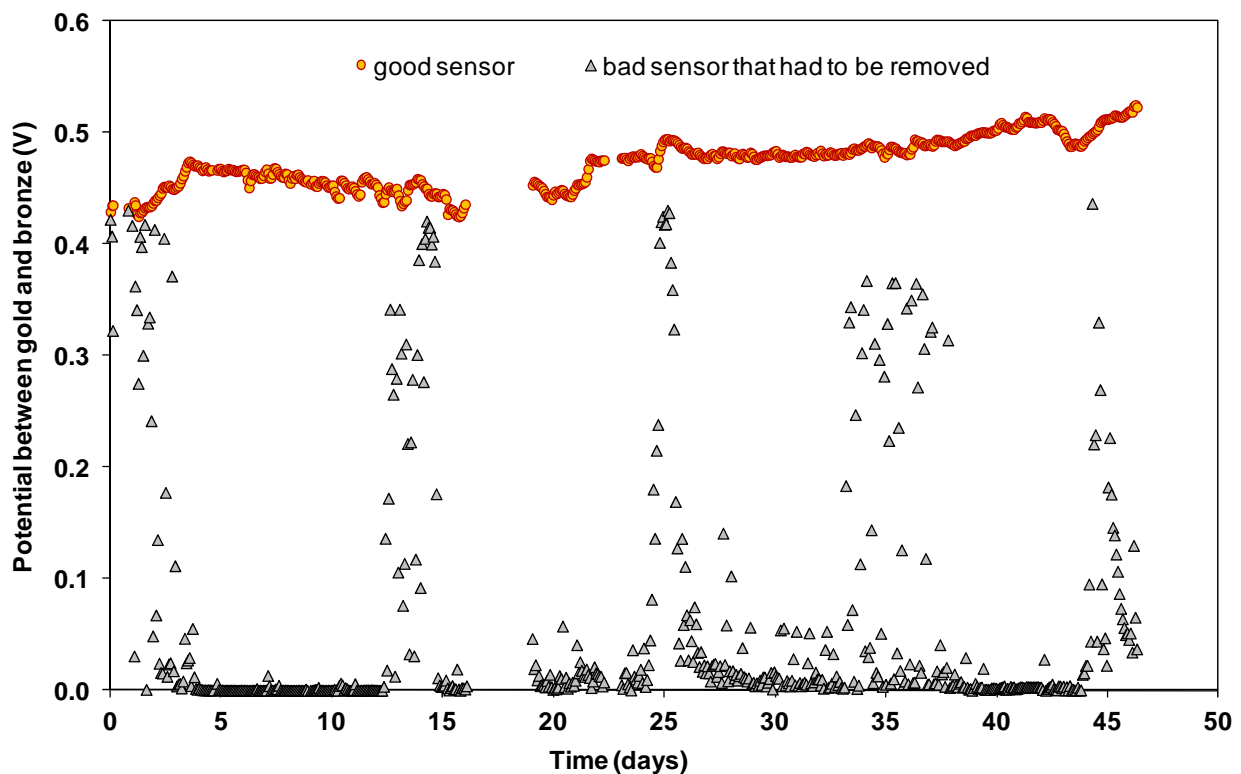


Figure 2: Macrocouple current measurements in OPD laboratory environment for 2 galvanic sensors: in orange a sensors with a good signal, in grey a sensor with a bad signal.

The sensors with a good signal of macrocouple current, such as the one reported in orange in Figure 2, were really reactive from the beginning and all showed very similar trends. The variations with time of the macrocouple current are attributable to the variations of relative humidity. Samples with a bad signal, such as the one reported in grey, definitely presented a more random trend.

The different behaviour from sensor to sensor, is even more clear while considering the data of the potential between gold and bronze (Figure 3). The sensors with a good signal, such as the one reported in orange in Figure 3, presented a potential that changed while varying the relative humidity and values always above 50 mV. The ones with a bad signal, instead, often showed values of the potential close to zero. A value of the potential between gold and bronze close to zero means that or there is a short circuit between the two metals or a bad electrical connection between the copper wire and the gold layer. In order to identify the reason of the bad performance of the sensor, it is necessary to consider also the values of the resistance. A very high value of the resistance ( $>1\text{ G}\Omega$ ) would mean a bad electrical connection, a low value, in the other hand could mean a short circuit. It can then be concluded by the trends of the “bad” sensor reported in Figures 3, 4 and 5, that its bad performances most probably had to be ascribed to a non-efficient separation between gold and bronze. All the sensors that presented similar problems were removed and replaced with new ones.



**Figure 3: Potential measurements in OPD laboratory environment for 2 galvanic sensors: in orange sensors with a good signal, in grey a sensor with a bad signal.**

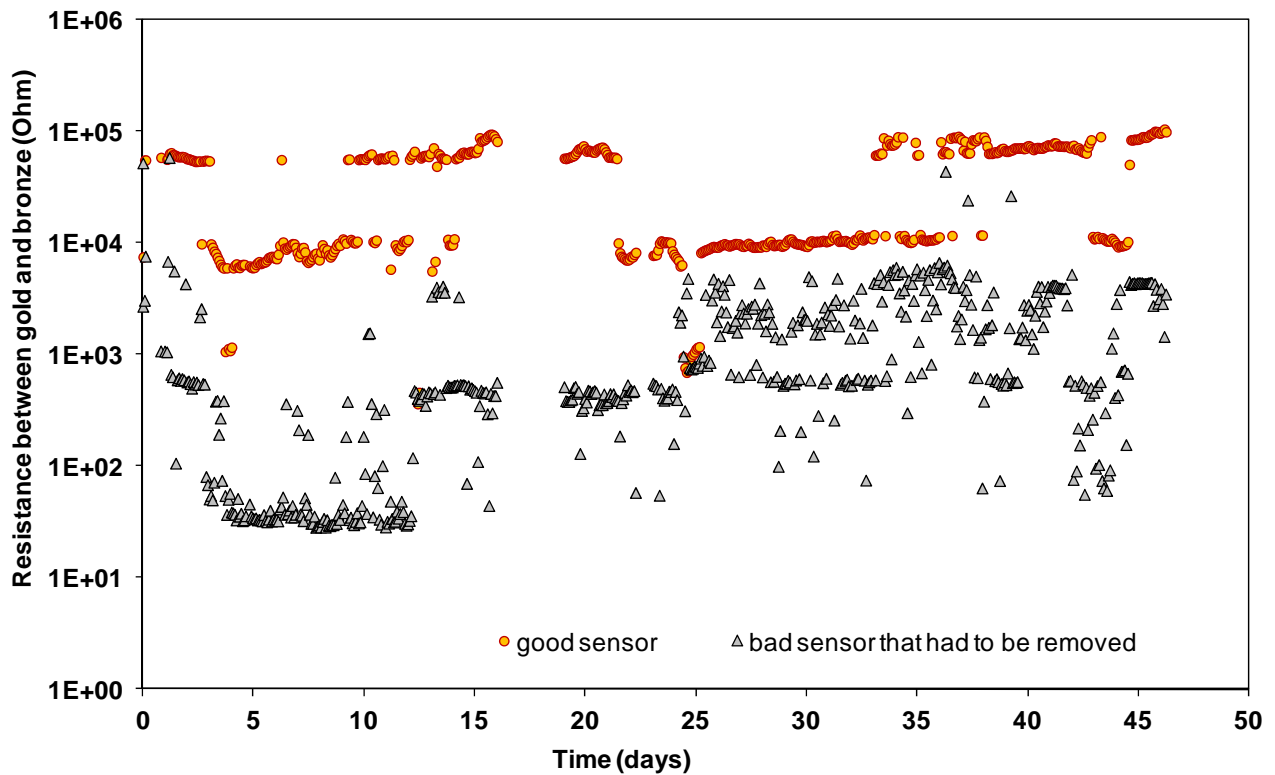


**Figure 4: Resistance measurements in OPD laboratory environment for 2 galvanic sensors: in orange a sensors with a good signal, in grey a sensor with a bad signal.**

At the end of the preconditioning period, the 9 sensors with higher macrocouple current and reactivity (high current density variations correlated with the thermo-hygrometric ones), have been selected to test the three different exposure solutions. Three sensors have been installed in each display solution, together with real parts of the door in order to evaluate the behaviour of the electric parameters and to estimate the corrosion rate.

The trend of the macrocouple current measured for the chosen samples for the two closed showcase can be observed in Figure 5a. The sensors selected for the test in the closed showcase with low relative humidity are coloured in light blue, while the sensors chosen for the showcase purged with nitrogen are coloured in green. In Figure 5b it is reported, in red, the trend of the macrocouple current of the sensors chosen for the exposure in the open showcase.

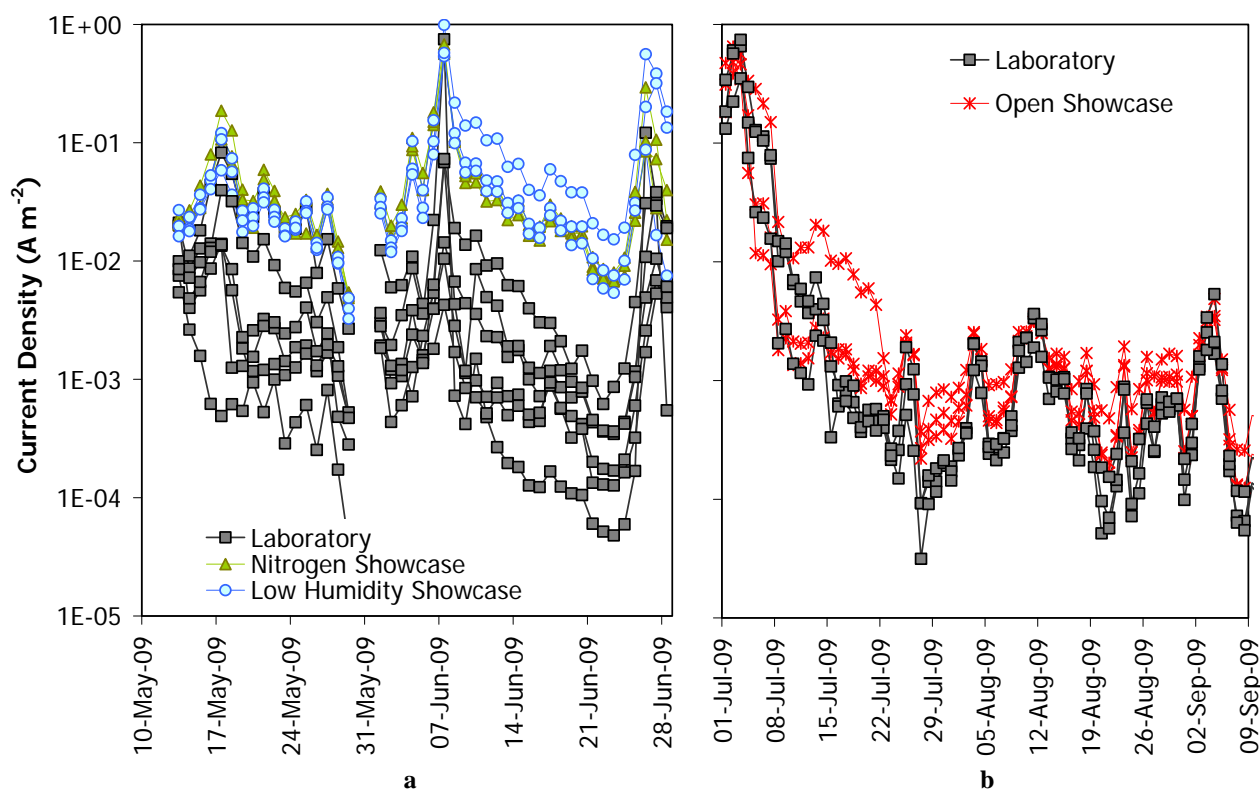


**Figure 5: Average daily value of current density during the preconditioning time before the installation of the sensors into three showcases. The triangles indicate the sensors chosen for the nitrogen showcase. The circles indicate the sensors chosen for the low humidity showcases. The cross indicate the sensors chosen for the monitoring in the open showcase.**

During preconditioning period, a high macrocouple current variability, exceeding more than two orders of magnitude, was recorded, and this variability was interpreted in terms of indoor RH variability. Furthermore it should be notices that three was a lack of reproducibility of the macrocouple current supplied by each sensor. However the trends were very similar and, as it will be discussed later, the variations observed introducing the sensors into the different display option were significantly higher than the variability observed between different sensors.

Some sensors have remained exposed to uncontrolled laboratory conditions as a reference for the duration of the testing period. The daily average values of macrocouple current of these sensors are reported in Figure 6.

Unfortunately, deterioration of the sensors led to a decrease of the average macrocouple current with exposure time. Deterioration mainly consisted in volume variations of the patina, that cause severe damages of the gilding. Therefore, the most deteriorated sensors were periodically replaced by new ones.

Deterioration, consisting in physical degradation of the sensors, resulted in a decreasing corrosion rate with time, as observed in Figure 6. The average decrease of the corrosion rate measured during the entire period of monitoring reaches almost two order of magnitude.

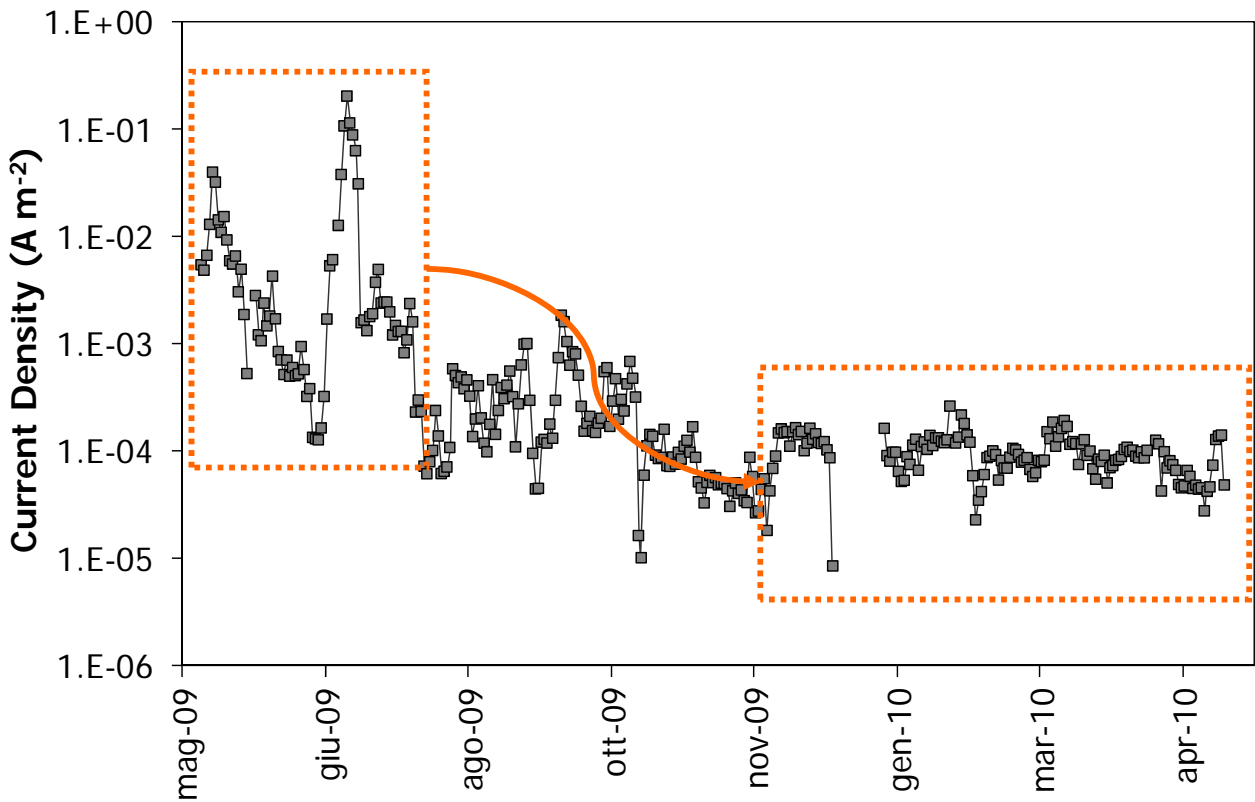


**Figure 6: Average current density as a function of time of the sensors that have remained exposed to uncontrolled laboratory conditions for the duration of the testing period.**

In Figure 7 are reported the daily average values of the macrocouple current of each of 20 sensors monitored for the entire period of the experiment (1 year, from May 2009 to May 2010). As it can be noticed by the graph, a great variability has been observed between the macrocouple current supplied by each sensors. However comparing the values of the sensors exposed in the different relative humidity conditions, it is clear that the value of macrocouple current are significantly different, and that the corrosion rate decreases significantly decreasing the relative humidity, i.e. in the three showcases.

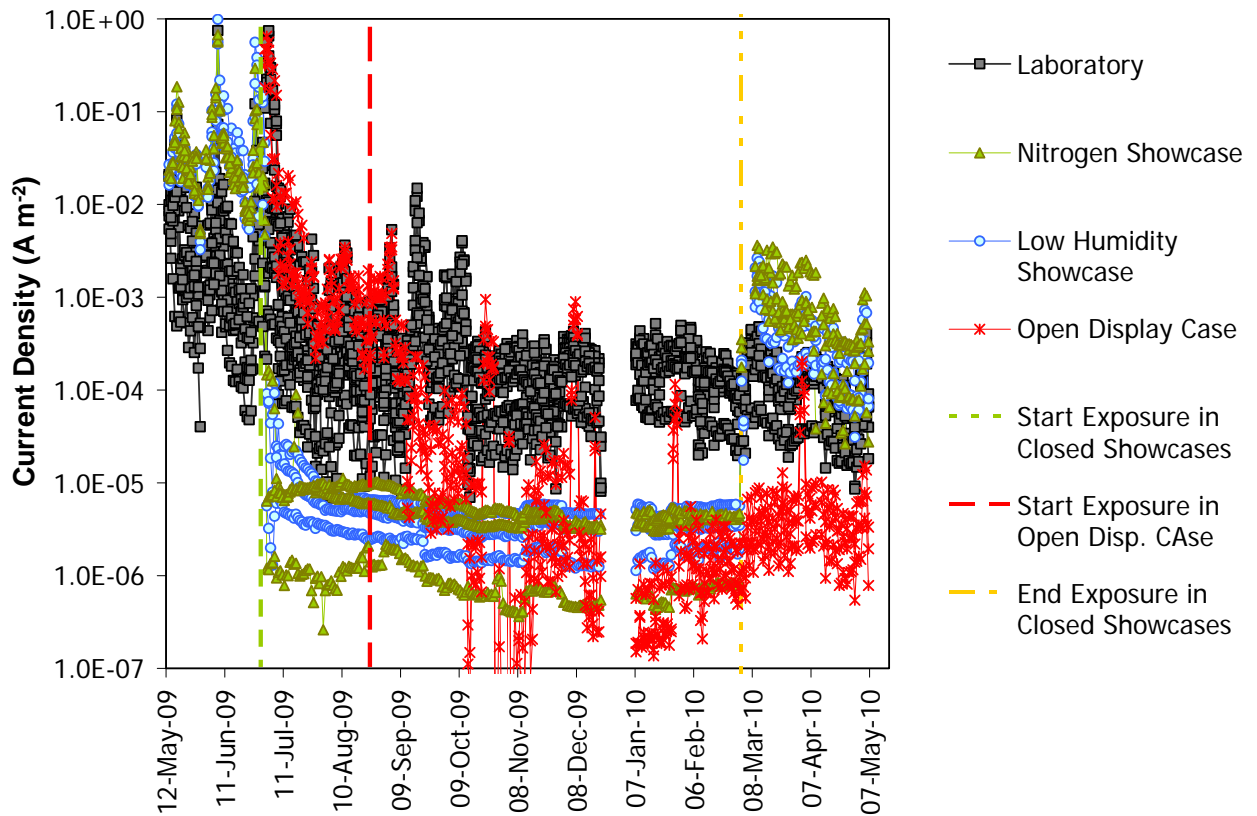


**Figure 7: Current density of all the sensors used for the choice of the optimal display option for the Porta del Paradiso.**

For clarity reasons in the following graphs the average corrosion rate measured for the sensors in the same exposure solution instead of the values of each sensor will be reported.

### 4.2.1 Closed showcases

Figure 8 reports the average values of the corrosion rate of the sensors that were placed in the two closed showcases and of the sensors that remained in the OPD laboratory for all the time. The moment of introduction into the two showcases is indicated by the green dotted vertical line, while the moment of their removal and exposure to the uncontrolled laboratory conditions by the blue one. As previously said the best sensor were chosen to be placed into the two closed showcases. The average corrosion rate during the preconditioning period in the laboratory was about 65  $\mu\text{m}/\text{y}$  and 80  $\mu\text{m}/\text{y}$  for the sensors that were then installed into the nitrogen and low humidity showcases, respectively, with a peak of about 1 mm/y.

As previously mentioned (Paragraph 3.4.1), the sensors were designed to mimic a gilded bronze presenting very unstable corrosion products underneath the gilding layer. The purpose was to reproduce the conditions of the most unstable parts of the doors. The obtained data clearly show that



any part of the door presenting these conditions could suffer quite high corrosion if subject to insufficient environment control, such as the conditions encountered in the OPD laboratory.

As it can be observed in Figure 8, after the introduction of the sensors into the two closed showcases, the corrosion rate was drastically reduced by more than three orders of magnitude. The effect was immediate for the nitrogen showcase and slower for the showcase with low RH. After one month, however, the two sets of sensors showed similar corrosion rate, which continuously decreased with time. After seven months the corrosion rate was as low as 4 nm/y.

In Figure 8, it can be noticed that the sensors revealed to be still really reactive to RH variations at the end of exposure in the closed showcases even after 10 months of monitoring. They recovered quite high corrosion rate values, significantly higher than those of the sensors left under uncontrolled atmosphere in the laboratory. This means that, during their exposure into the closed showcases, they were not subjected to the degradation processes that affected the sensors exposed in the OPD laboratory. Also by visual inspection, they looked unchanged compared to the moment they were introduced into the two closed showcases. However after just few weeks after their removal from the nitrogen showcase, these sensors showed significant deterioration, as it can be noticed in Figure 9. Apparently the very low relative humidity inside the nitrogen showcase (<7%) caused the dehydration of the patina, making it very sensitive and reactive to subsequent RH increases. These phenomena have been further investigated and will be presented in Chapter 4.4.

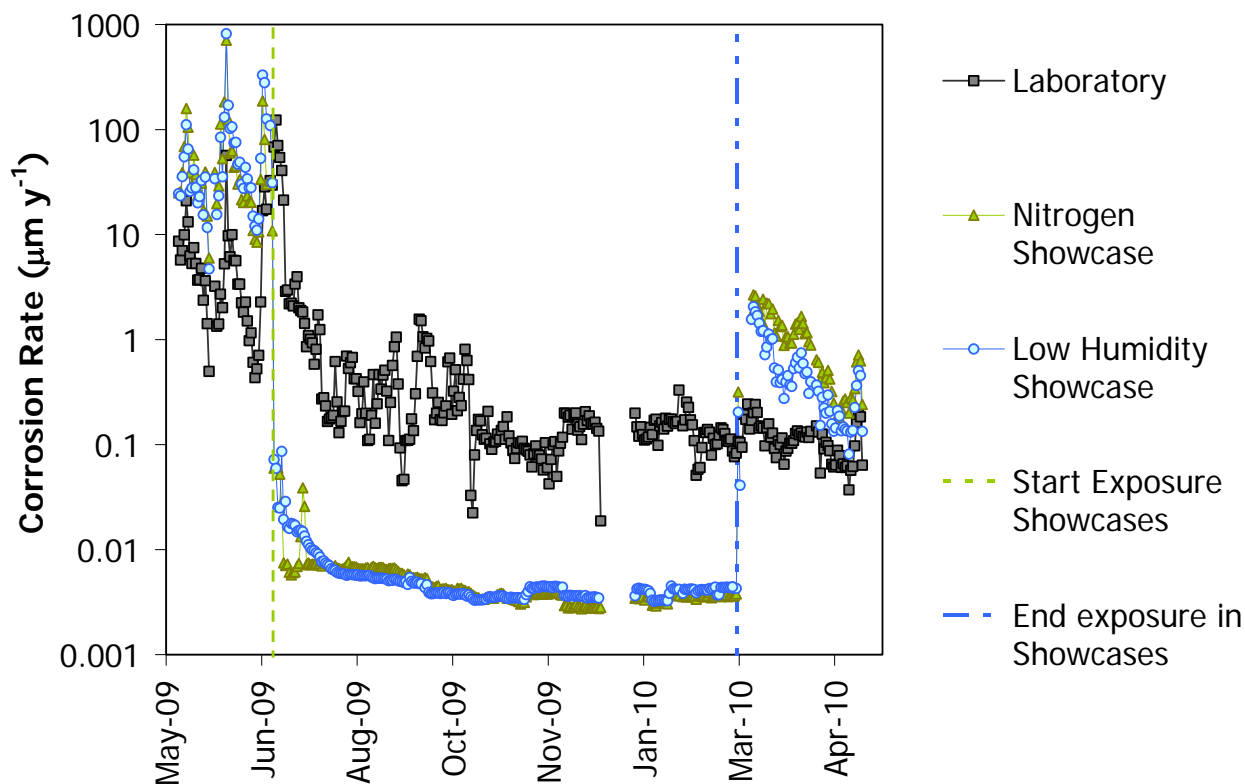
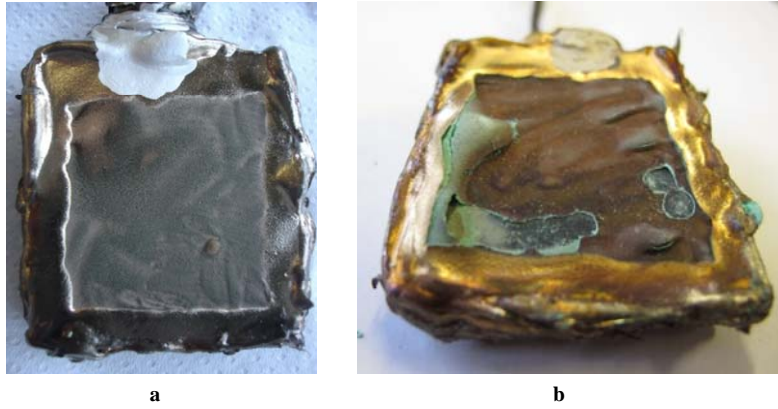


Figure 8: Monitoring of the corrosion rate in the two closed showcases



**Figure 9: “Sensor for the Porta del Paradiso” before the exposure in the closed showcase purged by nitrogen (a) and few weeks after its removal from the showcase and its exposure at the OPD laboratory end of the exposure (b).**

### **4.2.2 Open showcase**

As it can be observed in figure 5b, the sensors that were installed in the open showcase were more deteriorated, possibly due to the longer preconditioning period. These sensors had a reduced capacity (more than 10 times) in their ability to supply macrocouple current compared to the sensors that were placed into the nitrogen-purged and the low RH cases.

As it can be noticed in Figure 10, after the introduction of the sensor into the open showcase, the corrosion rate was reduced by more than one order of magnitude with an average value during the first 10 days of about  $0.1 \mu\text{m}/\text{y}$ . The sudden increase in the corrosion rate in October 2009, is associated with a compressor failure that exposed the sensors to the partially controlled laboratory environment. However, this incident revealed that the sensors respond quickly to RH variations. When the RH inside the open showcase reached values similar to those in the closed showcases, the corrosion rate reached very low values. This values are similar to and sometime lower than the ones of the sensors in the closed cases. It should be reminded, however, that the sensors in the open showcase were originally more deteriorated and their macrocouple current was lower compared with that of the sensors in the closed showcases.

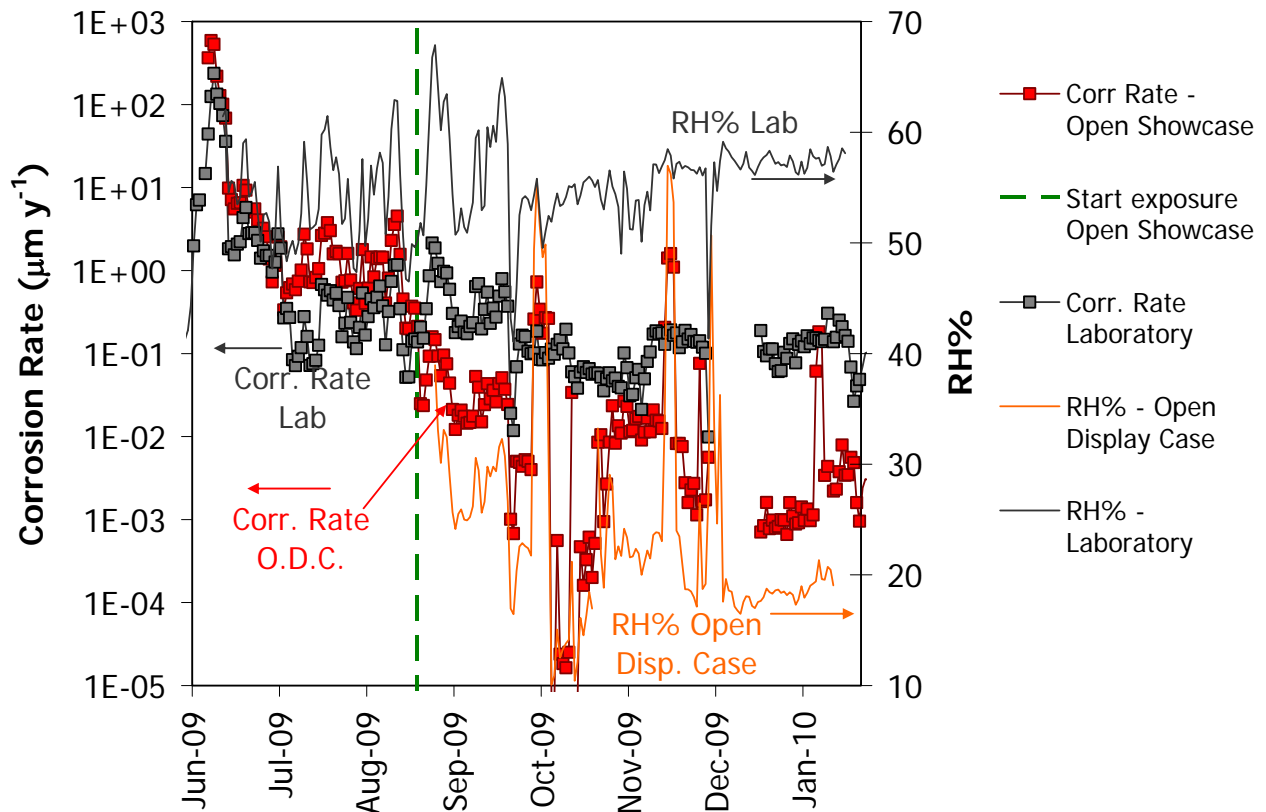


Figure 10: Monitoring of the corrosion rate in the open showcases

### 4.2.3 Final considerations for the choice of the best display solution

At the end of this stage of the research some conclusions could be drawn:

- No significant difference appeared between displaying the Porta del Paradiso in a showcase saturated with nitrogen or in one under low and controlled RH. However, unstable corrosion products are very sensitive to RH fluctuations, even when corrosion is negligible. Furthermore, very low levels of RH may favour the dehydration of the patina, causing embrittlement. The showcase with low RH would be preferable respect to the nitrogen showcase for economical and safety reasons.
- The level of RH obtained in the open showcase significantly reduces the corrosion rate, even though it is definitely less efficient than the other two closed cases. If the efficiency of the open showcase is improved, ensuring a RH level below 20%, it could be considered as protective as the other two closed cases.

#### **4.2.4 Considerations about the performances of the galvanic sensors realised for the study of the Porta del Paradiso**

Based on the presented results, galvanic sensors can be then considered as a powerful tool for the monitoring of corrosion rate of corroded gilded bronzes. However significant improvements are necessary. In particular some modifications are requested to improve the reproducibility of the signal between different sensors and their durability with time. As it will be discussed in Chapter 4.3 the main factors influencing the durability and reproducibility are:

- Continuity and thickness of the gold layer, that influence the durability of the sensors.
- Adhesion of the patina to the substrate, that can cause the loss of the electric signal.
- Thickness and roughness of the artificial patina, that influence both the reproducibility and the durability of the sensors.

A new setup has then been developed and improved sensors realised, as it will be described in the following chapter.

## 4.3 Evaluation of the performance of the “Gold leaf sensors”

As mentioned in the previous chapter, the two main factors that influence the durability and the reproducibility of the galvanic sensors are the gilding process and the patination methodology. The improvements introduced in the new sensors, called “Gold leaf sensors” were previously described in paragraph 3.4.2.

In this chapter the results of the monitoring of the “Gold leaf sensors”, both with chloride rich and brochantite patina, are here reported and discussed. As already described in Paragraph 3.4.3, brochantite ( $\text{Cu}_4\text{SO}_4(\text{OH})_6$ ) has been selected because is a common corrosion product on outdoor bronze surfaces. Only a few tests have been performed, during this work, using sensors with brochantite patina and the results obtained are reported together with the ones for the “Gold leaf sensors” with chloride rich patina.

Since also the very first Gold leaf sensors, named “preliminary gold leaf galvanic sensors” with chloride rich patina (Paragraph 3.4.2.1) already gave good results, some data obtained with these sensor are also reported and discussed.

Between the preliminary gold leaf sensors set up and the definitive there were a few small improvements in the methodology of preparation, that can be summarized as follows (Paragraph 3.4.2.1):

- Thickness of the layer of patina: the quantity of powder of copper salts per  $\text{cm}^2$ , used to obtain the paste, has been decreased from 0.1 to 0.025 g. The powder to water ratio has been decreased from 4 to 1. These two variations permit to obtain a thinner, smoother and consequently more stable layer of patina.
- Gilding methodology: the protocol set up for the preliminary gold leaf sensors was long and complicated. A new and simpler methodology, described in Paragraph 3.4.2, was then established that allows to produce a more continuous and reproducible layer of gold.

The advantage of using a thinner layer of patina is the increased durability of the sensors that still respond very well to relative humidity variations but are mechanically more stable. The improvement introduced by the new methodology of gilding allows to obtain a more continuous layer of gold using an easier procedure. The resistance between gold and bronze depends on the patina thickness and resistivity. The lower the resistance, the higher the macrocouple current and therefore the performances of the sensors should be. The resistivity varies with the relative humidity

and it is one of the main parameter that influences the macrocouple current and therefore the corrosion rate of gilded bronzes.

The modifications introduced in the final procedure are important because permit to obtain, with an easier methodology, more durable sensors . However, the electrical parameters collected do not improve significantly.

The “Gold leaf sensors” have been monitored using the same multi-channel acquisition system KEITHLEY 3706 used for the “Sensors for the Porta del Paradiso”. Unfortunately, due to technical reasons, it was not possible to perform the experiments in climatic chamber, as originally planned. Therefore the tests have been conducted in the uncontrolled laboratory environment.

### 4.3.1 Preliminary gold-leaf galvanic sensors with chloride rich patina

The monitoring of these preliminary gold leaf sensors started in November 2010 and ended in July 2011, with an interruption of about two months between February and April 2011 due to technical issue.

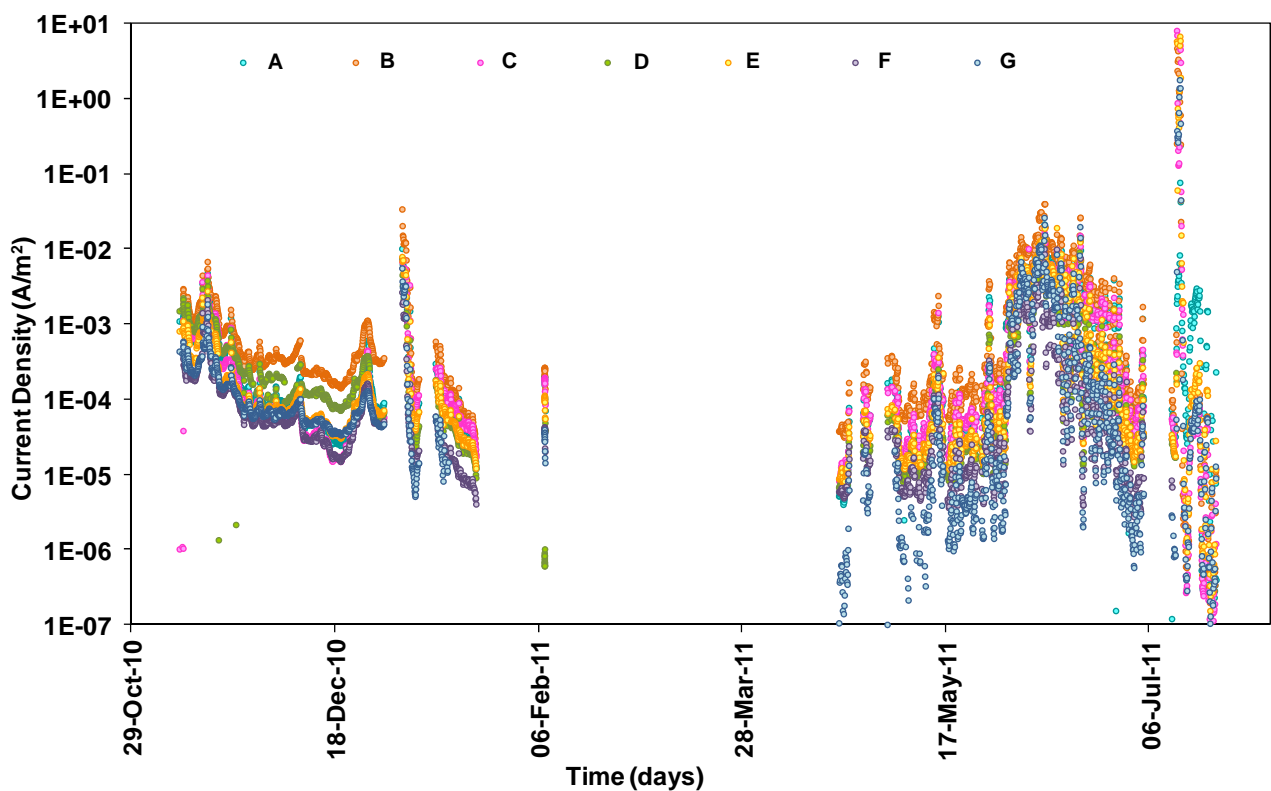
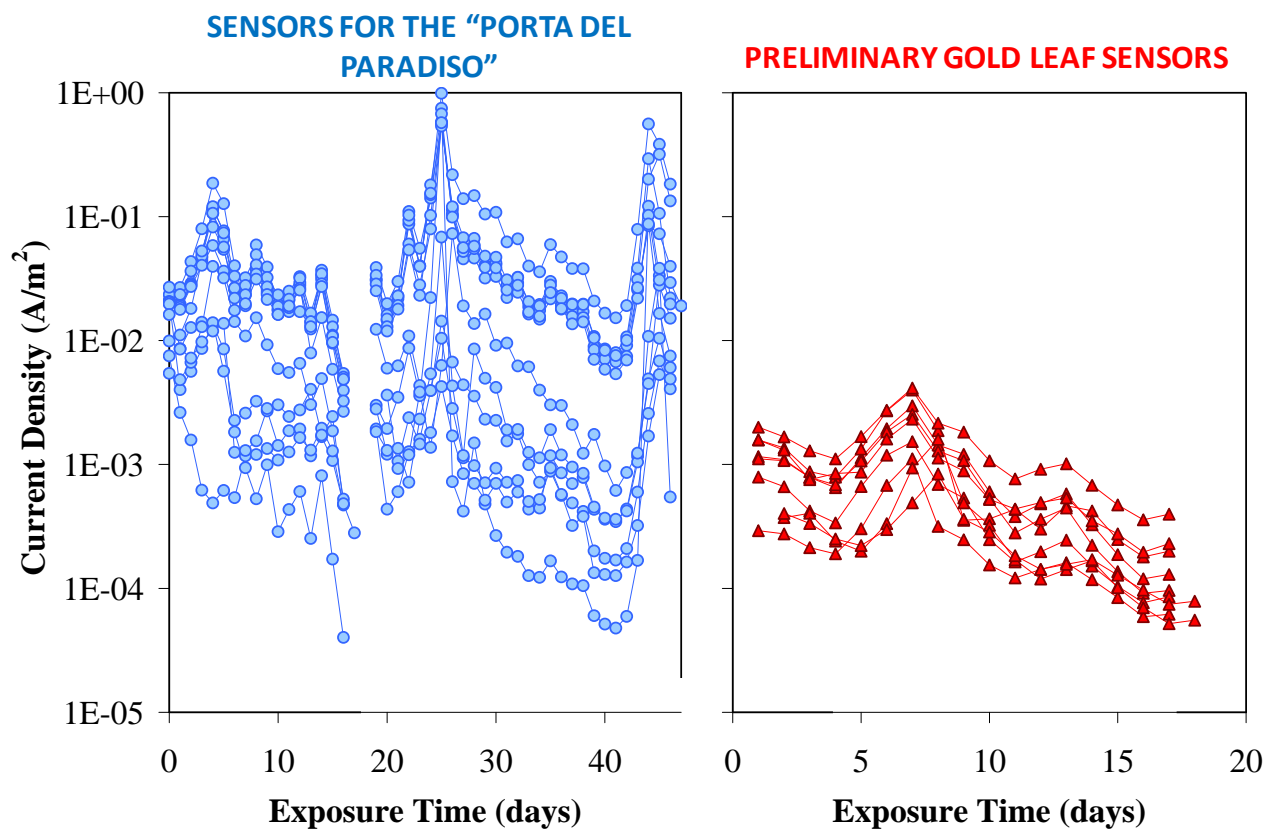


Figure 1: Current density of the preliminary gold leaf galvanic sensors A-G during the entire period of monitoring.

Figure 1 presents the macrocouple current recorded during the whole period of monitoring for all the prepared sensors. As it can be observed, all of the sensors presented a good agreement concerning the macrocouple current. Considering the daily average values of the macrocouple current (Figure 2) it can be noticed that the distribution of the values ranges within one order of magnitude (Figure 2b), which is a great improvement compared to more than two orders of magnitude of the “Sensors for the Porta del Paradiso” (Figure 2a) [1]. The introduced improvements resides in: first of all the higher water/powder ratio used for the preparation of the paste. The paste is therefore more fluid and can be spread in a more uniform way. The thickness of the patina was also reduced from 0.1 to 0.025 g of powder per cm<sup>2</sup>. In addition, the gold leaf allows the realisation of a more continuous gilding layer with a more reproducible roughness and a higher mechanical resistance compared to the sputtered gold.



**Figure 2: Daily average values of the macrocouple current of “Sensors for the Porta del Paradiso” (a) and “Preliminary gold leaf sensors” (b).**

In Figure 1, the values of the macrocouple current of sensors A – G are scattered in a slightly larger range (but still less than two orders of magnitude) during the second period (April – July) respect to the first one (November – January). This is due to a partial degradation of the sensors left in laboratory under uncontrolled environment. It is important to notice that the trend of the macrocouple current variation is quite well correlated for all these sensors. It should be also noticed

that there is not the same decreasing trend that was observed in the case of the “Sensors for the Porta del Paradiso” (Chapter 4.2) and that was due to the degradation of the sensors.

When the monitoring restarted in April 2011, the values of the macrocouple current were more or less the same as those measured at the end of January. This may be due to the fact that in the period January – April the environmental conditions in the laboratory, where the sensors were kept, were quite constant due to the heating system of the laboratory. This is also confirmed by the peak of macrocouple current observed the 3<sup>rd</sup> of January 2011 (Figure 3): in fact, between the 29<sup>th</sup> of December 2010 and the 3<sup>rd</sup> of January, the multimeter stopped and no data are available for those days, but the Department of Chemistry, Material and Chemical Engineering, where the measurements took place, was close in that period and the heating system was turned off. For this reason the sensors were exposed to a higher range of relative humidity variations and followed more the outdoor atmospheric variations. The meteorological data available on the ARPA Lombardia – Servizio Meteorologico Regionale website [2] confirm that two peaks of higher relative humidity were registered in the mornings of 3<sup>rd</sup> and 5<sup>th</sup> of January, and the macrocouple current of the sensors follows exactly the same trend, as noticeable in Figure 3. After the 9<sup>th</sup> of January the heating system was turned on again and the sensors recover more stable values concerning their macrocouple currents. In April the heating system was turned off and the relative humidity of the laboratory was more strongly influenced by the external one. This explains the higher variability of the macrocouple current after April. Unfortunately the laboratory RH values are not available for the period November 2010 – May 2011. The monitoring of the temperature and of the relative humidity, indeed, started at the end of May 2011.



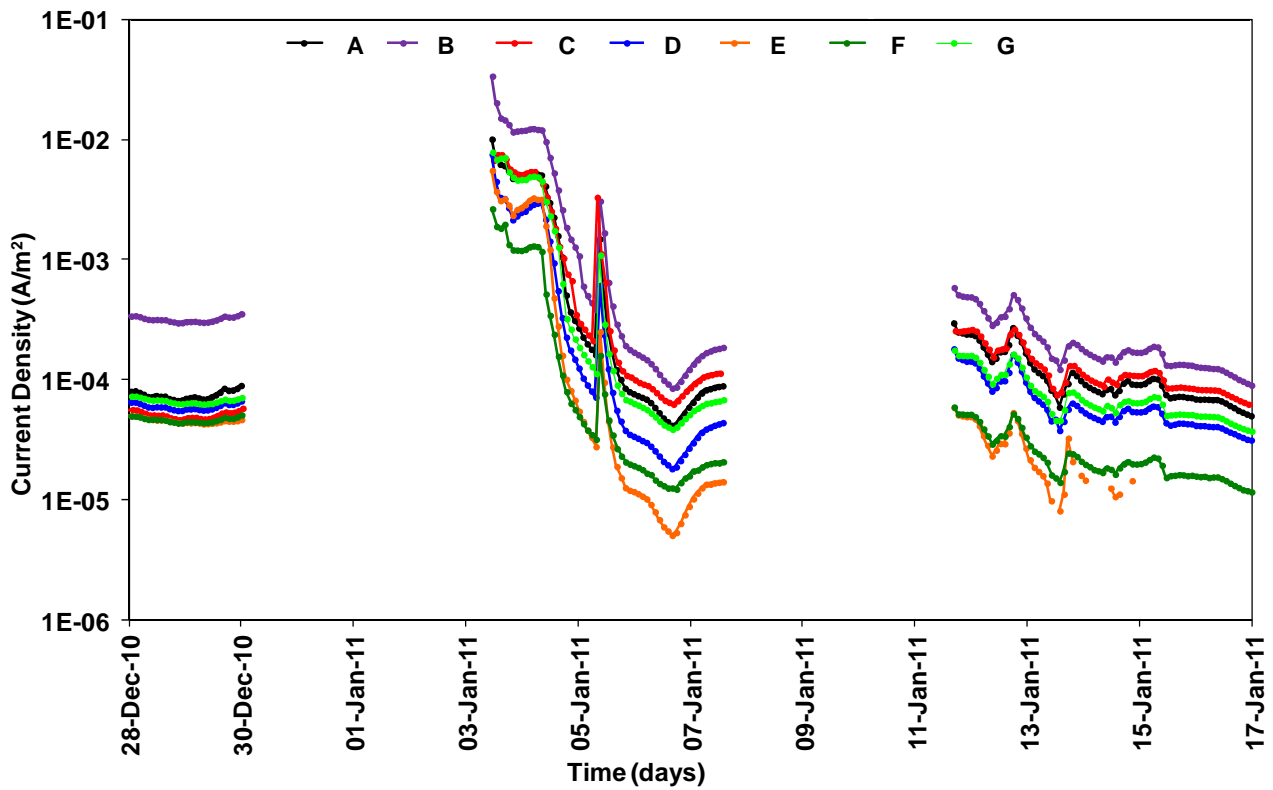


Figure 3: Macrocouple current values in the first days of January 2011.

The reactivity of these sensors was additionally tested in July 2011 by increasing the relative humidity surrounding the galvanic sensors. To this aim, a plastic box presented in Figure 4 was used to confine the environment around the sensors and the relative humidity inside the box was increased up to more than 90% by inserting two beakers full of water.



Figure 4: Setup for the increasing relative humidity experiment.

As observed in Figure 5, the macrocouple current density of the galvanic sensors increased, for the sensors with the higher value (sample B, purple coloured in Figure 5), from  $6 \cdot 10^{-5} \text{ A/m}^2$  to  $4 \text{ A/m}^2$  (more than four orders of magnitude) with the relative humidity; this means that even 10 months after their preparation the reactivity of all the sensors was still very good. At the end of the experiment, the macrocouple current recovered values similar to the one they presented before.

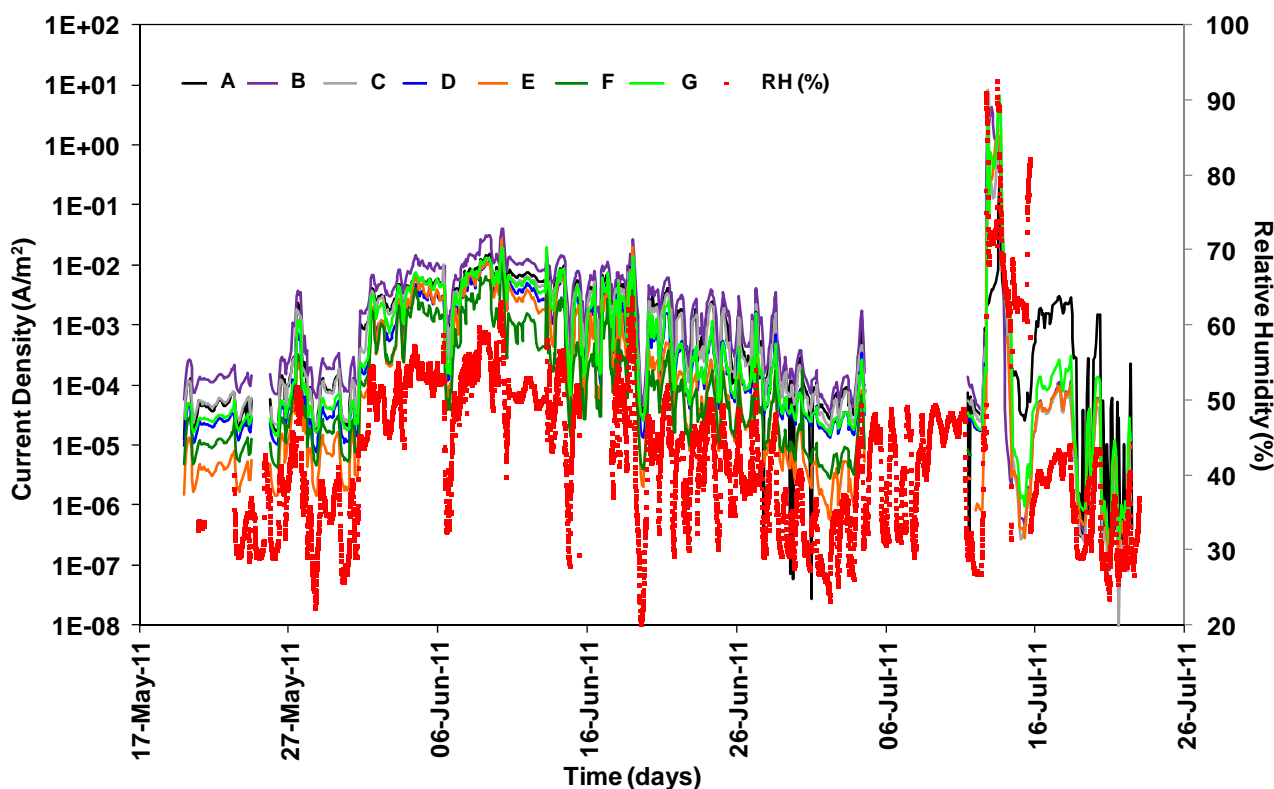
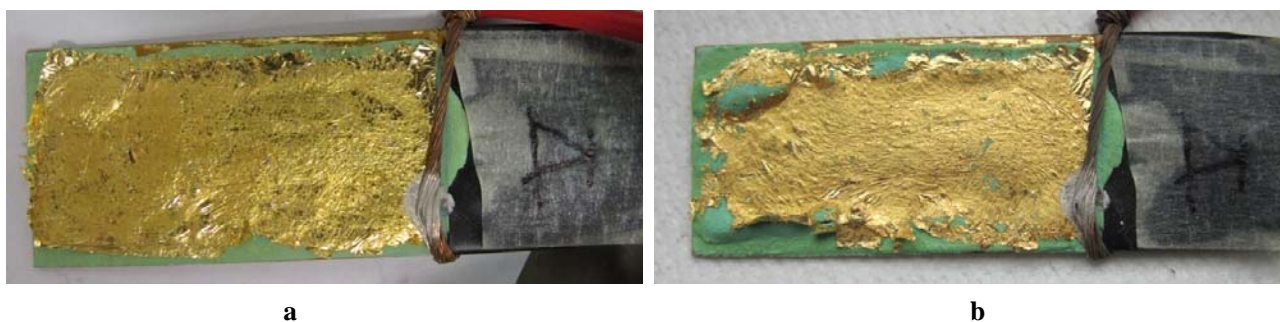


Figure 5: Current density of preliminary gold leaf galvanic sensors A-G for the period April – July.

As it can be noticed by Figure 5, the macrocouple current density is perfectly following the RH variations in the laboratory.

The new methodology applied for the preparation of the preliminary gold leaf galvanic sensors proved to be successful in reducing some deterioration factors highlighted in the “Sensors for the Porta del Paradiso”. In particular, the thinner patina and the gold leaf techniques allow to obtain more durable galvanic sensors with a more reproducible signal. In fact, as can be observed in Figure 6, the sensors did not show any evident sign of deterioration until the “reactivity test” at 90% RH that was performed in the final stage of the monitoring. After that the first signs of deterioration were observed, confirming that high humidity is very dangerous for gilded bronzes contaminated by chlorides (Figure 6).



**Figure 6: “Preliminary gold leaf sensor” before (a) and after (b) the test at 90% of relative humidity.**

Therefore, it can be concluded that the new setup for the realisation of the artificial patina and the subsequent application of the gold leaf are two key steps to obtain sensors of higher quality and reliability.

The reduced thickness of the patina is another crucial parameter for the production of durable galvanic sensors. To this aim, thinner chlorides rich patinas have been realized in the final stage of this research project and the results are reported in the next paragraph.

#### **4.3.2 Gold leaf sensors with chloride rich and brochantite patina**

The sensors prepared and monitored in the last phase of this research project were the “Gold leaf sensors” with a thinner layer of chloride rich patina. Additionally, a more continuous layer of gold was obtained thanks to a new methodology for the application of the gold leaf (Paragraph 3.4.2).

The results of the tests performed on these sensors are satisfactory because the samples are clearly more durable, due to the thinner layer of patina, but at the same time still really reactive to relative humidity variations as it can be noticed in Figure 7.

The chlorides rich patina, as mentioned before, represents the worst and extreme case of corrosion of bronzes artefacts, due to very high content of chlorides. Sensors with patina of different composition have also been realized. Brochantite ( $\text{Cu}_4\text{SO}_4(\text{OH})_6$ ), one of the most common corrosion product on copper alloys in urban environment, has been synthesized and used for the preparation of the patina. An example of macrocouple current of a “Gold leaf sensors with brochantite patina” is reported in orange in Figure 7 and may be compared with the macrocouple current of the sensors prepared with chloride rich patina. One may notice that, even if brochantite is much more stable than chlorides to relative humidity variations, the sensors with brochantite patina follow quite well the change with time of relative humidity. Moreover, the fact that brochantite is chemically more stable than the patinas containing chloride makes the “Gold leaf sensors with brochantite patina” more durable.

Resistance and potential between gold and bronze have been also monitored and are reported in Figures 8 and 9, respectively.

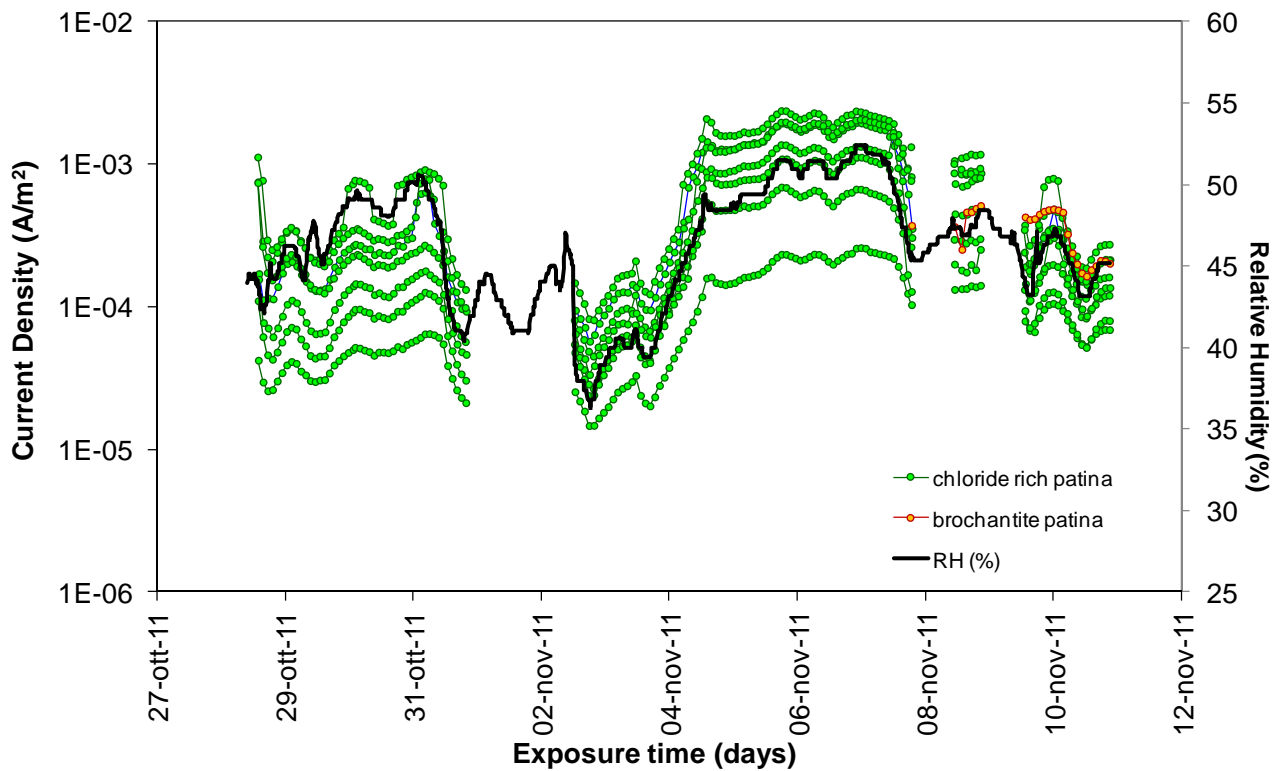


Figure 7: Macrocouple current of the “Gold leaf sensors” with chloride rich and brochantite patina.

Concerning the resistance values reported in Figure 8, as expected, the trend is exactly the opposite of the one exhibited by the macrocouple current when varying the relative humidity: indeed, the resistance decreases when the relative humidity increases.

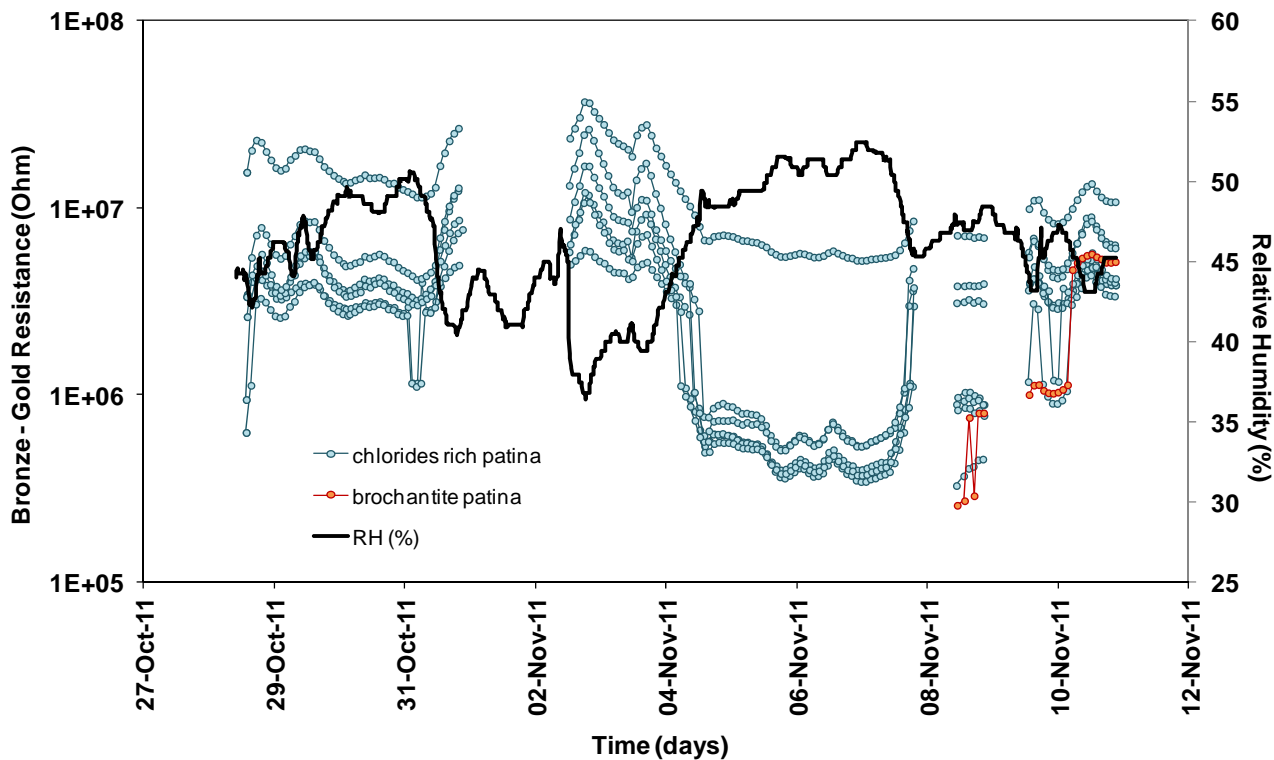


Figure 8: Resistance measurement of the “Gold leaf sensors” with chloride rich and brochantite patina.

Additionally, one may notice in Figure 9 that as it was the case for the current density values, the variation of the potential are in quite good agreement with the variations of the relative humidity.

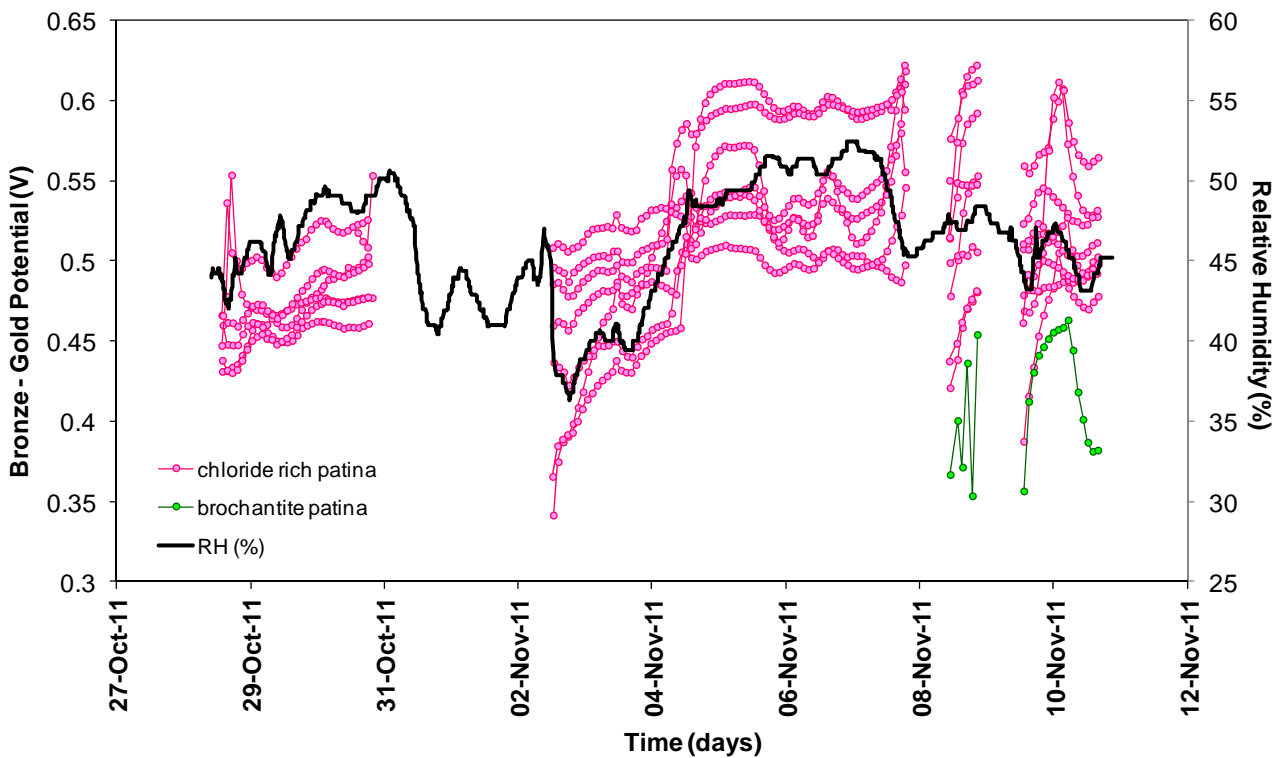
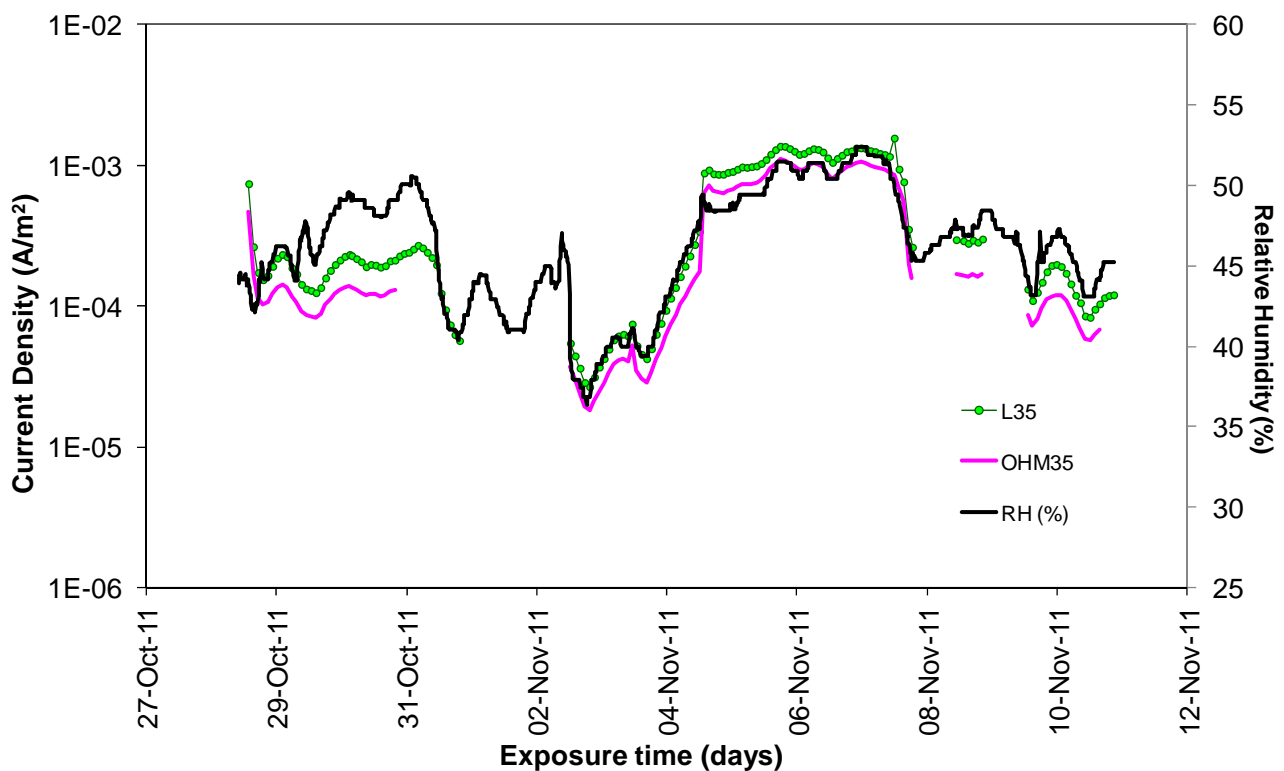


Figure 9: Potential measurement of the “Gold leaf sensors” with chloride rich and brochantite patina.

It was then evaluated for all the sensors how well the recorded values followed the Ohm's law. Figure 10 presents the current density that was measured for the sensor labelled L35 (green line), taken as an example, as well as the value of the current density calculated using Ohm's law. The latter (pink line) was based on the measurements of the potential and the resistance of the sensor. This calculation is only presented here as an example, and was performed in order to check the reliability of the acquired data. Indeed, one may observe that both the current densities, calculated as well as measured, follow exactly the same trend in agreement with relative humidity change in time. Surprisingly, the calculated value is always about 50% lower than the measured one, whereas, the opposite may be expected. Nevertheless, the fact that in the present case, the potential and the resistance are measured at open circuit and the current only after 5 minutes of stabilization may introduce a systematic bias regarding the absolute values. Moreover, at the beginning of the research project, the multimeter was tested with reference cells, in order to estimate the reliability of the measurements: the current and potential measurements did not give rise to significant problems and provided quite reliable values, while the resistance measurements gave less reliable results. Thus, the latter may be responsible for the discrepancy between the measured values and the ones calculated using Ohm's law. This topic was not further investigated in the present work and will be thoroughly analysed in future studies.



**Figure 10: Comparison between the recorded values of current density (green) and the values calculated using Ohm's law (pink).**

The improvement introduced in the “Gold leaf sensors with chloride rich patina” revealed to be quite efficient. The more continuous layer of gold and the thinner patina make the sensors more durable, but still highly reactive to environmental changes. The data obtained by these sensors are in fact well correlated with the variation of relative humidity. The reproducibility of the sensors was as well improved: all of them followed the same trend and the variability between sensors remains approximately within one order of magnitude.

Also the results obtained with the sensors with brochantite patina are encouraging: they revealed to be as reactive as the chloride rich patina to environmental variations. The absence of chlorides, however, makes them more durable. The values of macrocouple current for these sensors are in good agreement with the values of chloride rich patina sensors. Sensors with other patinas can be produced easily according to the corrosion products expected.

## References

- [1] S. Goidanich, L. Brambilla, B. Salvadori, S. Porcinai, A. Cagnini, L. Toniolo, **Galvanic sensors for monitoring corrosion rate of gilded bronzes**, 10<sup>th</sup> International Conference on non-destructive investigations and microanalysis for the diagnostics and conservation of cultural and environmental heritage (Art'11), 13th-15th April 2011, Florence, Italy, E17
- [2] <http://ita.arpalombardia.it/meteo/dati/richieta.asp> Servizio Meteorologico Regionale – Arpa Lombardia

## 4.4 Characteristics and stability of the patinas

During the setup of the best methodology for the preparation of galvanic sensors one of the problems that was highlighted was the stability of the patina. As mentioned before (Chapters 4.2 and 4.3), the behaviour of the patina, in terms of stability, adhesion to the substrate and volume variations, changes with relative humidity values. A common way to prevent the deterioration phenomena, due to changes in volume of patina constituents, and to reduce corrosion rate, is to control microclimate conditions. This solution is only applicable in confined environments.

Since it is well known that lowering the RH leads to a reduced corrosion rate, a very low relative humidity is suggested [1], normally, in the context of the preservation of metallic artefacts that present conservation issues related to the presence of chlorides.

However too low a relative humidity may favour the dehydration of the patina, which may become then brittle and more sensitive to subsequent RH increases.

Some compounds such as nantokite ( $\text{CuCl}$ ) are particularly unstable in the presence of relative humidity variations. It is therefore really important to check their stability and behaviour, during high and low RH cycles. The following compounds, that are naturally presents on copper alloys exposed to the atmosphere, have been subjected to high and low RH cycles with the purpose of evaluating their behaviour and stability: Nantokite ( $\text{CuCl}$ ), Chloride rich patina ( $\text{CuSO}_4 \cdot 5\text{H}_2\text{O} + \text{CuCl}_2 \cdot 2\text{H}_2\text{O} + \text{CuCl}$ ) as well as Brochantite ( $\text{Cu}_4\text{SO}_4(\text{OH})_6$ ).

The first observations concerning the stability of patinas kept under different relative humidity conditions have been carried out at the end of the monitoring of the “Porta del Paradiso” (Chapter 4.2). The patina of the sensors used in the closed showcase purged by nitrogen presented in fact problems of stability after the end of the exposure. After 9 months in the nitrogen showcase with a RH lower than 7% the samples did not show any visible evidence of deterioration. However, already few weeks after their removal from the nitrogen showcase, they showed dramatic deterioration (Figure 1). The degradation observed in these sensors was more severe respect to most of the sensors remained in the laboratory for all the time of exposure. It was evident then that the passage from an environment with really low relative humidity to another one with a higher RH, such as the laboratory of Opificio delle Pietre Dure, can be really dangerous for bronzes with unstable patina such as the sensors realised for the Porta del Paradiso. In addition, it is important to underline that the “cracking” of the patina of these sensors occurred only a few weeks after the end of the test, while during all the period of the monitoring in the nitrogen showcase (9 months) no relevant changes had been noticed. This phenomenon was attributed to the complete dehydration



and subsequent re-hydration of the components of the patina ( $\text{CuCl}$ ,  $\text{CuCl}_2$  and  $\text{CuSO}_4 \cdot 5\text{H}_2\text{O}$ ) (Chapter 4.2).

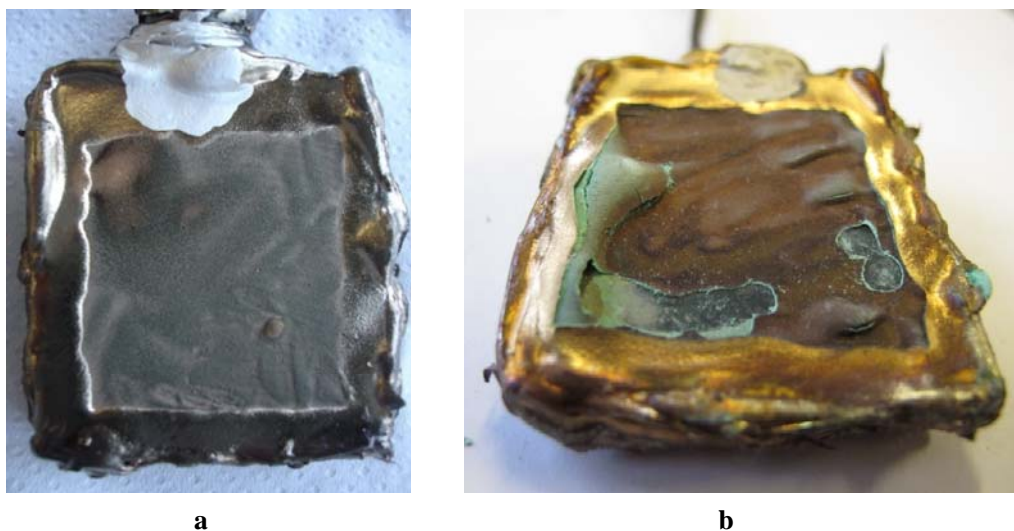


**Figure 1: “Sensor for the Porta del Paradiso” before the exposure in the closed showcase purged by nitrogen (a) and a few weeks after its removal from the showcase and its exposure at the OPD laboratory (b).**

#### **4.4.1 Stability tests on “Gold leaf sensors”**

In order to confirm that the phenomenon observed for the “Sensors for the Porta del Paradiso” was really associated to the loss and gain of water in the patina, another experiment was performed using two “Preliminary Gold leaf sensors” with chloride rich patina. As previously described (Paragraph 3.4.2.1) these sensors differ from the definitive ones mainly for the higher thickness of the patina and Powder/Water ratio.

The two “Preliminary gold leaf sensors” with chloride rich patina were kept for 6 months in a closed desiccator with silica gel. After their removal from the dry environment, no visible change in the patina volume was noticed (Figure 2). Nevertheless, after few weeks under the uncontrolled atmosphere of the laboratory environment, the patina detached from the metallic substrate in several points as it can be observed in Figure 2.

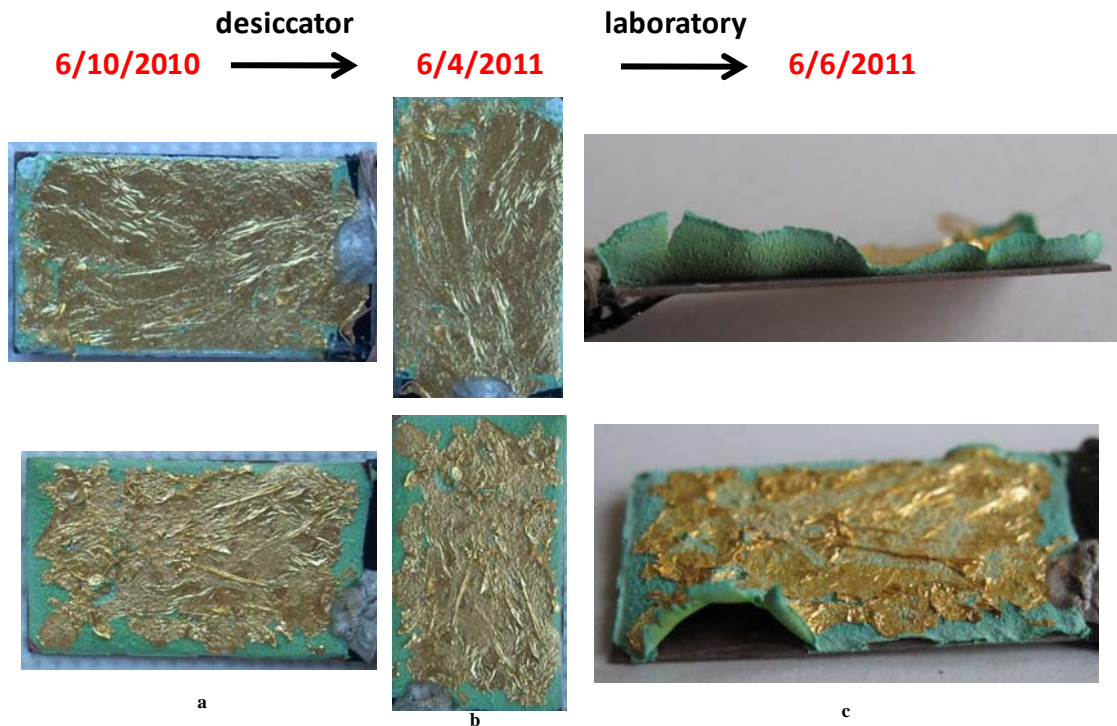


**Figure 2: “Gold leaf sensors” with chloride rich patina before the conditioning in the desiccator with silica gel (a), after the removal from the dry environment (b) and after the exposure in uncontrolled laboratory environment (c).**

The other “Preliminary gold leaf sensors” that have remained for 8 month in the same laboratory did not show significant signs of detachment or deterioration of their patina , as it can be observed in Figure 3.

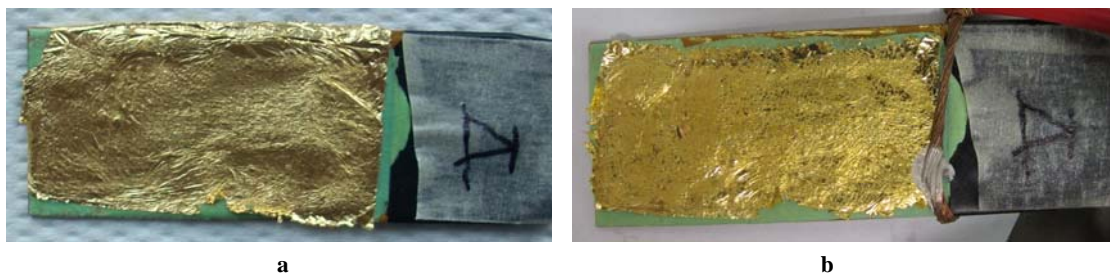


**Figure 3: “Gold leaf sensors” with chloride rich patina at the moment of its preparation (a) and after 8 months of exposure in uncontrolled laboratory environment (b)**

It can then be concluded that a very dry environment (nitrogen or desiccator with low RH) is definitively not the best choice to preserve a corroded metallic artefact. In fact, if the solution of a really dry environment is adopted, the risk is to condemn the artefact to be kept forever in such a dry environment. Unfortunately with increasing the RH, also corrosion rate increases, especially in the presence of chlorides. Therefore the difficult task is to identify for each artefact which is the

optimal level of RH in order to guarantee both the reduction of corrosion processes and the stability of the patina.

Since the stability, during time, of the patina is most probably dependent on the composition of the patina itself, two “Gold leaf sensors”, one with chloride rich patina and one with brochantite patina, were enclosed in a sealed box and kept at about 80% RH for 24 hours. As it can be observed in Figure 4, already after 24 hours, the sensor with chloride rich patina presented volume variations of the patina, while no visible change has been observed for the sensor with brochantite patina (Figure 5).

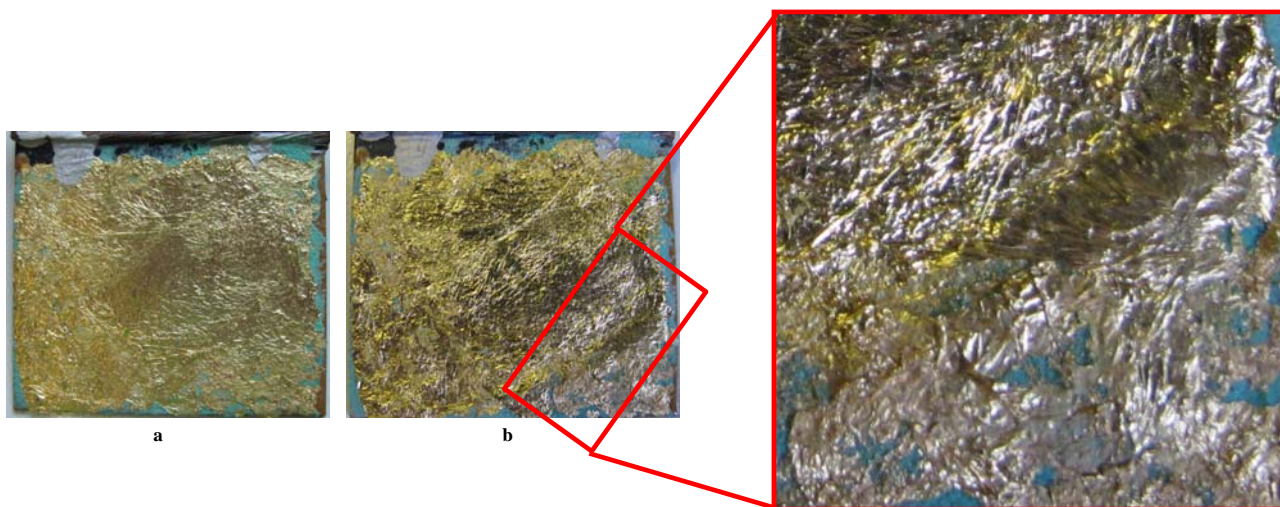


**Figure 4: “Gold leaf sensor” with chloride rich patina before (a) and after (b) the experiment in the sealed box at 80% of relative humidity. On the right magnification of the area in which the variation of volume of the patina is clearly visible.**

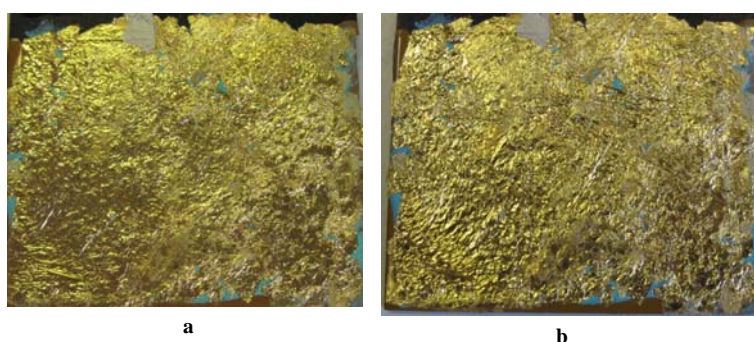


**Figure 5: “Gold leaf sensor” with brochantite patina before (a) and after (b) the experiment in the sealed box at 80% of relative humidity.**

It was already noticed, during the investigation to determine the best methodology for preparation of the sensors, that too high a relative humidity can lead to the “migration” of the chlorides trough

the pores of gold. After this additional experiment it was once more evident that chlorides are the main cause for the volume variations of patinas.

#### **4.4.2 Stability tests on powders of the patinas and of Nantokite**

With the purpose of understanding the transformation to which the patinas constituents are subjected as a consequence of RH variation, some additional tests were performed. The brochantite and the chloride rich patina were prepared and subjected to different RH conditioning. Since Nantokite (CuCl) is considered one of the most dangerous and critical constituents of bronze patinas, some tests were also performed on a pure Nantokite powder. All these powders were subjected to the following environmental conditioning:

- Laboratory environment (average measured relative humidity of 30-40%), except for nantokite.
- Desiccator with silica gel (relative humidity of approximately 5%).
- Closed box with a beaker of water, that keep the relative humidity between 70 and 80%.
- 48 hours in a desiccator with silica gel and then 24 hours in a closed box at 70-80% RH .

Raman analysis was performed on all the samples to address the changes that occur in the samples while varying the relative humidity conditions. Micro-Raman analyses were carried out using a green laser ( $\lambda = 514$  nm, power 20 mWatt, magnification 20x or 50x, time for acquisition 2x20 seconds). At least 3 spectra for each sample were acquired in the spectral range 100–3700  $\text{cm}^{-1}$ . The spectrum of standard mineral of Atacamite was recorded between 100 and 3500  $\text{cm}^{-1}$ .

Raman spectroscopy has been selected as the technique of choice for the monitoring of the behaviour of the patinas exposed to different relative humidity conditions because it allows the analysis without any pre-treatment of the sample and is a non-destructive method. FTIR spectroscopy was not suitable for this purpose, in the presence of high amount of water, such in the case of the nantokite at high relative humidity, as the broad bands of the water molecule vibrations would cover all the other peaks. Furthermore, it was not possible to use analytical techniques that required vacuum, such as XPS or SEM-EDX, because the water contained in the sample would evaporate during the analysis.

##### Nantokite

Nantokite (CuCl) was analysed first, because it revealed to be the compound that is the most sensitive to relative humidity variation. In Figure 6, the aspect of the samples of CuCl exposed to the different environments is reported. Three samples have been analysed for this compound: one kept at low relative humidity (Figure 6a), one kept first 48 hours at low relative humidity and then

48 hours at 70-80% of relative humidity (Figure 6b and 6c) and one kept at high relative humidity (Figure 6d). Unfortunately, for technical reasons, it was not possible to analyse the sample kept at low relative humidity and then at high relative humidity for 24 hours (Figure 6b). Before the exposition and before Raman analysis the samples were accurately grinded and mixed (in the case of “paste-like” samples).

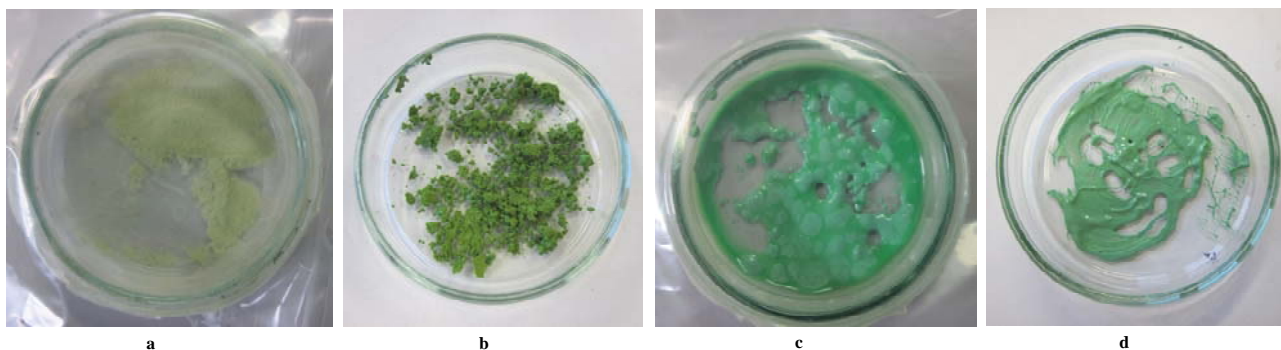


**Figure 6: CuCl kept in dessicator with silica gel (a), CuCl kept in the dessicator and then left at 70-80% of relative humidity for 24 hours (b) and for 48 hours (c), CuCl kept few days at 70-80% of relative humidity (d).**

Raman spectra of samples a, c and d of Figure 6 were recorded and are respectively reported in Figure 7, 8 and 9.

Raman spectra evidenced that the nantokite transforms to atacamite when the relative humidity increases above 70-80%.

The spectrum of nantokite (Figure 7) at low relative humidity (Figure 6a) corresponds very well to the reference spectrum reported in literature [2-4]. The peaks observed are reported in Table 1. It has to be observed, however, that nantokite, as well as other copper(I) compounds, decompose in the presence of water in the atmosphere and additional bands have been observed in the Raman spectrum (such as the  $\nu_{\text{OH}}$  at  $3384 \text{ cm}^{-1}$ ).

In Figure 8 is reported the spectrum of the sample of nantokite kept in low relative environment and then conditioned for 48 hours at 70-80% of relative humidity (Figure 6c), that revealed the partial transformation of the CuCl in atacamite [3]. In that spectrum, the peaks of water are also visible, in particular at approximately  $1630 \text{ cm}^{-1}$  ( $\delta_{\text{H}_2\text{O}}$ ) and over  $3000 \text{ cm}^{-1}$  (enlargement of the peak due to  $\text{H}_2\text{O}$  stretching) [5]. The peaks attributions are reported in Table 1.

The spectrum (Figure 9) of nantokite kept at high relative humidity (Figure 6d), revealed an even more evident transformation of CuCl in atacamite. The peaks of the spectrum correspond to those of atacamite references [3-4, 6]. One may notice that after the analysis the sample were “burnt” in correspondence of the point of measurement due to the laser used for Raman measurement. The peaks of water are not clearly visible because most of the water evaporated during the analysis. The spectrum of the atacamite mineral taken as standard reference is reported in Figure 10.

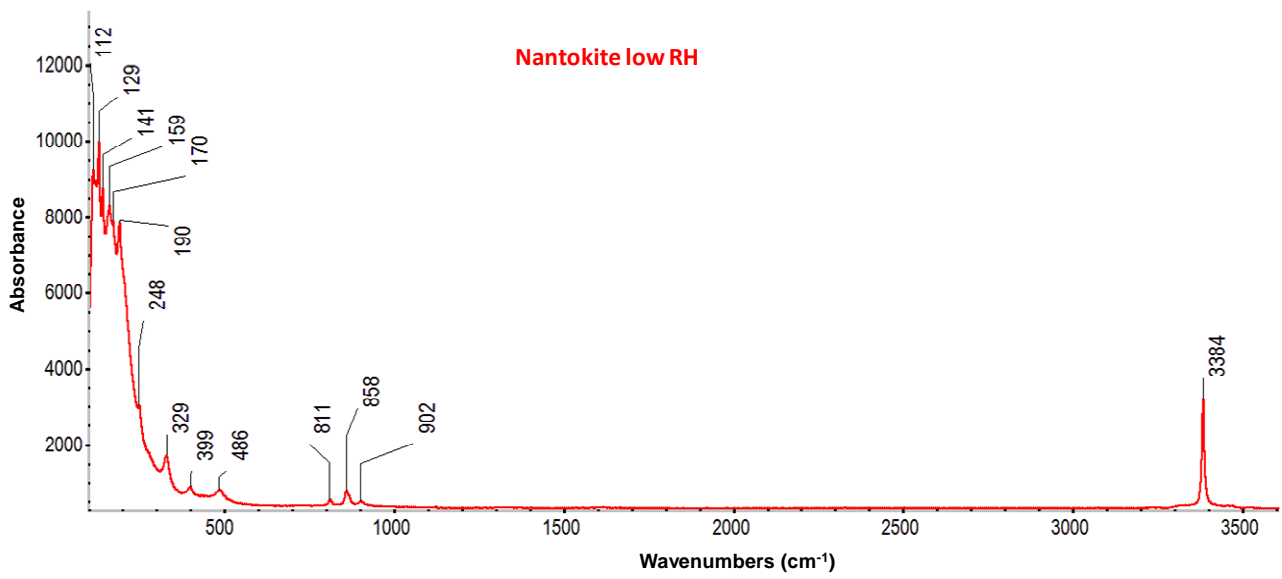


**Figure 7: Raman spectrum of Nantokite at low relative humidity.**

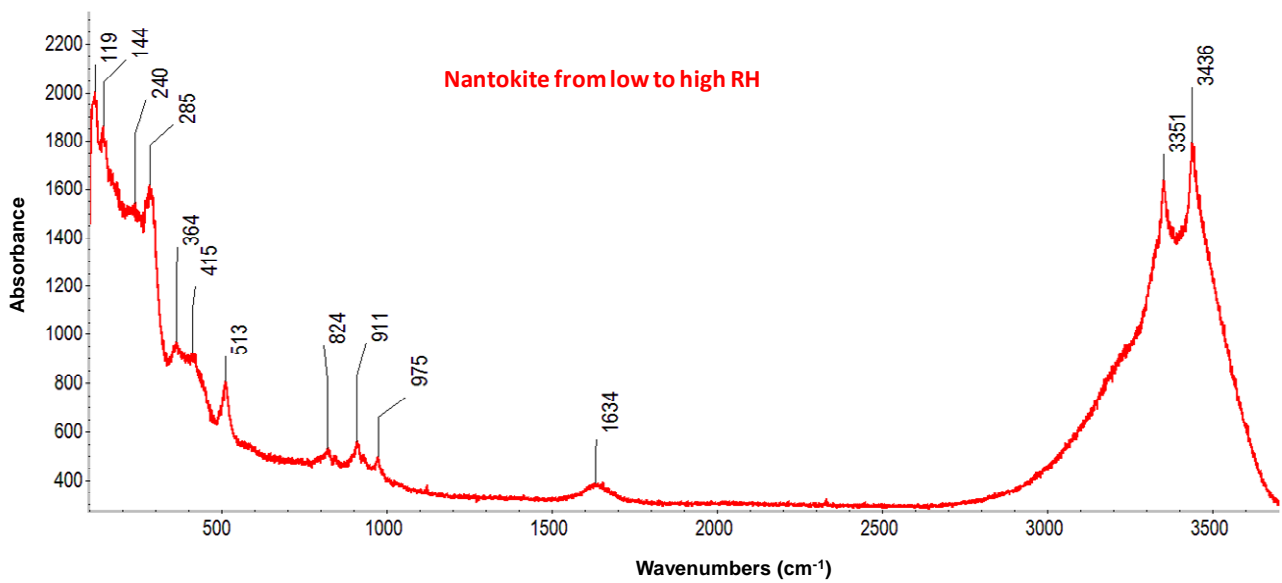


**Figure 8: Raman spectrum of Nantokite first kept at low relative humidity and then at 70-80% of relative humidity for 48 hours.**

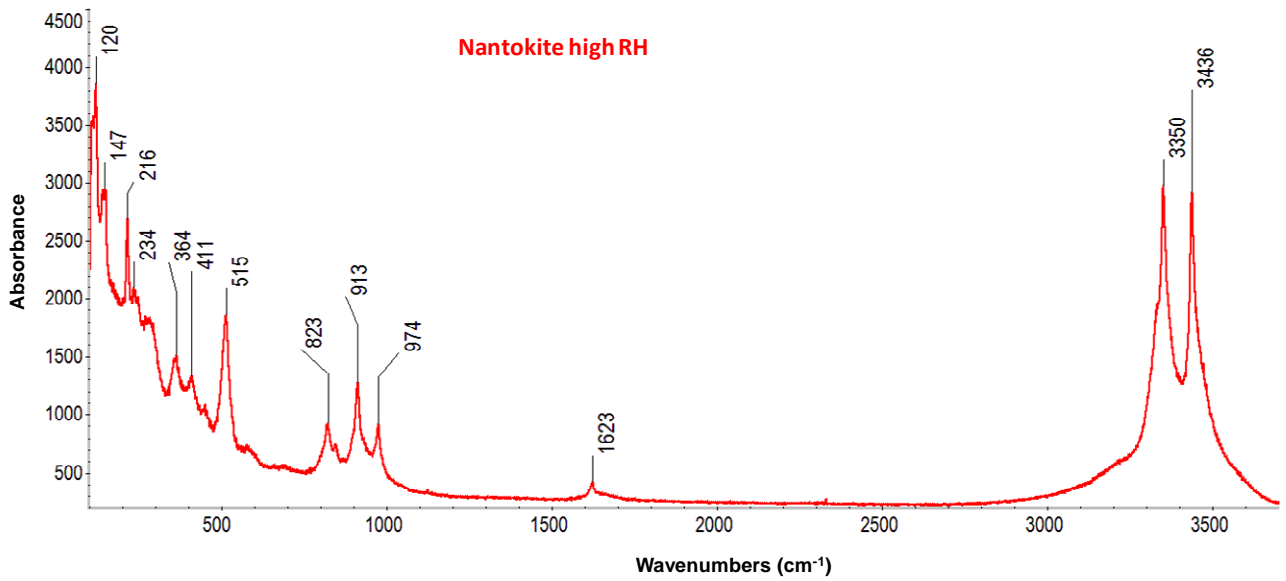


**Figure 9: Raman spectrum of Nantokite at high relative humidity.**

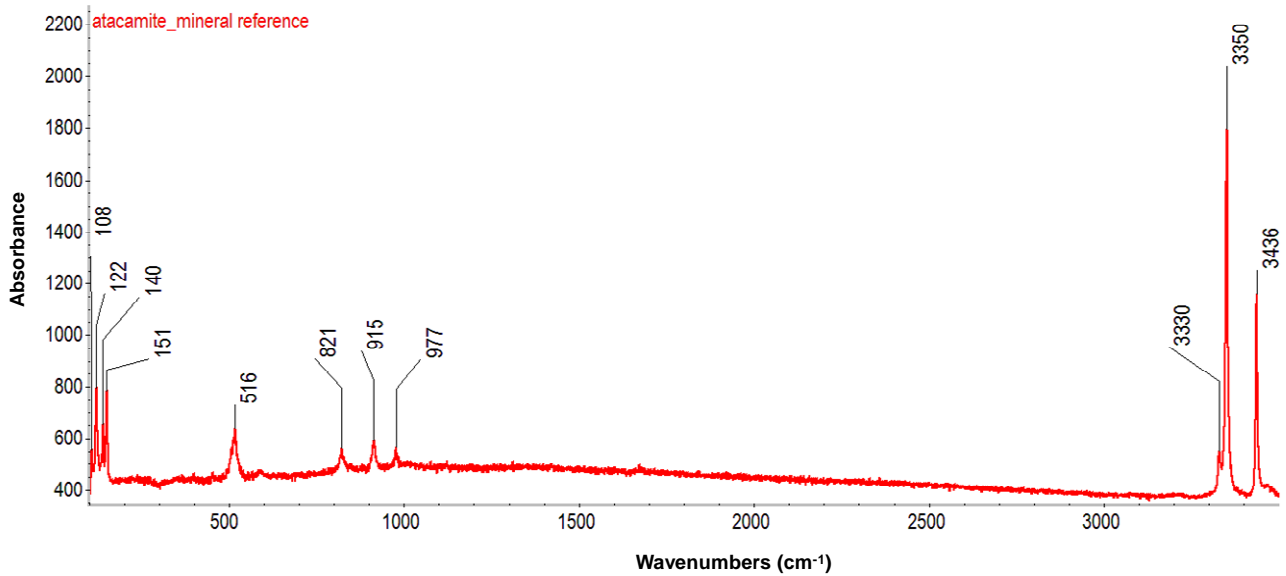


**Figure 10: Raman spectrum of atacamite mineral taken as reference material.**

**Table 1: Peaks attribution of the samples of CuCl analyzed by Raman spectroscopy compared to the atacamite standard reference.**

	<b>Nantokite – low RH</b>	<b>Nantokite – from low to high RH</b>	<b>Nantokite – high RH</b>	<b>Atacamite – mineral reference</b>
V <sub>OH</sub>		3436	3436	<u>3436</u>
	3384			
		3351	3350	<u>3350</u>
				3330 shoulder
δ <sub>H<sub>2</sub>O</sub>		1634	1623	
OH deformations		975	974	977
	902	911	913	915
		824	823	821
	858			
V <sub>CuCl</sub>		513	515	516
	486			
V <sub>CuO</sub>		415	411	
V <sub>CuCl</sub>	399			
		364	364	
	329			
		285	285	
δ <sub>Cl-Cu</sub>	248	240	234	
	190		216	
	170			
	159			151
	141			140
	129	144	147	122
	112	119		108

### Chloride rich patina

The study of the chloride rich patina was more complex, because the samples appeared to be really inhomogeneous at the microscopic scale. The final aspect of the three samples kept under different relative humidity conditions may be observed in Figure 11. The sample maintained at low relative humidity assumed a lighter blue colour compared to the other two, probably due to the dehydration of the chalcantite (CuSO<sub>4</sub>·5H<sub>2</sub>O), while the greener aspect of the patina at high relative humidity is most probably due to the complete transformation of nantokite in atacamite.



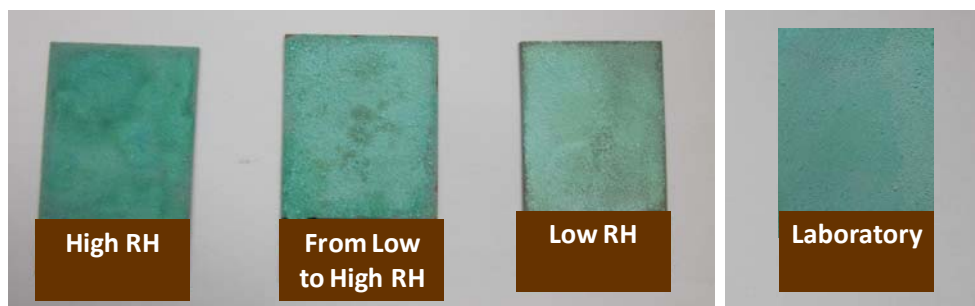


**Figure 11: final aspect of chloride rich patinas conditioned at high relative humidity (left), from low to high relative humidity (centre left), at low relative humidity (centre right) and in laboratory environment (right).**

In all the samples, crystals of different shapes and dimensions have been observed. At least three spectra for every sample, on different crystals have been acquired. The results of these spectroscopic analyses can be summarized as follows (Figures 12 to 17):

- Low relative humidity: the two spectra presented in Figure 12 are rather similar and differ only for the bands at: 217, 513, 820, 917 and 974 (shoulder)  $\text{cm}^{-1}$ , visible only in the spectrum labelled 01 and attributable to the presence of atacamite, together with the bands at 3350 and 3435  $\text{cm}^{-1}$  present in both spectra. The other peaks exhibited in the spectra (248, 432, 588, 619 and 1009  $\text{cm}^{-1}$ ) are attributable to chalcocyanite ( $\text{CuSO}_4$ ), the anhydrous version of copper sulphate. The origin of the two peaks at 480 and 1125  $\text{cm}^{-1}$  remains difficult to confirm in the present set of experiments. These results confirm that at low relative humidity the chalcantite loose the water of hydration.
- From low to high relative humidity (Figure 13): as observed for the nantokite samples, the spectra of this sample are more similar to the sample kept at high relative humidity than to that at low relative humidity (even if the sample was kept at relative humidity 70-80% only for 24 hours), Figure 17. In some locations (spectrum labelled 01 in Figure 13) of the sample the presence of atacamite is clearly evident (148, 516, 911, 3350, 3435  $\text{cm}^{-1}$ ), while in others (spectrum 02 in Figure 13) only the peaks at 3350 and 3435  $\text{cm}^{-1}$  are visible. In both points the following peaks of chalcantite are visible: 202, 281, 462, 611, 983, 1097, 1122, 1145, 3198  $\text{cm}^{-1}$ .
- High relative humidity (Figure 14): the considerations reported for the previous sample are valid also in the case of sample exposed to high relative humidity. In these samples, are visible both atacamite and chalcantite, as it can be observed in Figure 14. The peaks positions are the same as reported above.

As can be noticed in Figure 17, a shift of the strong peak at about 1000  $\text{cm}^{-1}$  (from 1009 to 983  $\text{cm}^{-1}$ ) was observed both in sample “from low to high relative humidity” and the one at high relative humidity respect to the case of the sample at low relative humidity. This shift is

due to the fact that at high relative humidity the copper sulphate is pentahydrate, while at low relative humidity is anhydrous.

- Laboratory environment (Figure 15 and 16): in the patina left in laboratory environment, two different kinds of spectra have been recorded. The first one is rather similar to the spectra of the patina at high relative humidity, in which the peaks of atacamite and chalcantite are clearly visible (Figure 15). The main difference with the samples at high relative humidity is the fact that in this case the presence of atacamite is prevalent. The peaks positions are the same as reported above.

In the second kind of spectra (Figure 16), recorded for needle-shaped, fan-shaped crystals, the peaks typical of eriochalcite ( $\text{CuCl}_2 \cdot \text{H}_2\text{O}$ ) are exhibited: at 110, 212, 236, 409, 697 and  $1622 \text{ cm}^{-1}$ . Atacamite is also present in this sample with peaks at 519, 821, 914, 983, 3350 and  $3435 \text{ cm}^{-1}$ . No crystals with the same shape have been observed in the patina kept in the other environments. Since the powder (mixture of  $\text{CuCl}$ ,  $\text{CuCl}_2 \cdot \text{H}_2\text{O}$  and  $\text{CuSO}_4 \cdot 5\text{H}_2\text{O}$ ) used for the preparation of the sample was always the same, it can be assumed that it is only the laboratory environmental condition (average of 30-40% of relative humidity) that favour the growth of this kind of crystals, due to unreacted  $\text{CuCl}_2 \cdot \text{H}_2\text{O}$ .

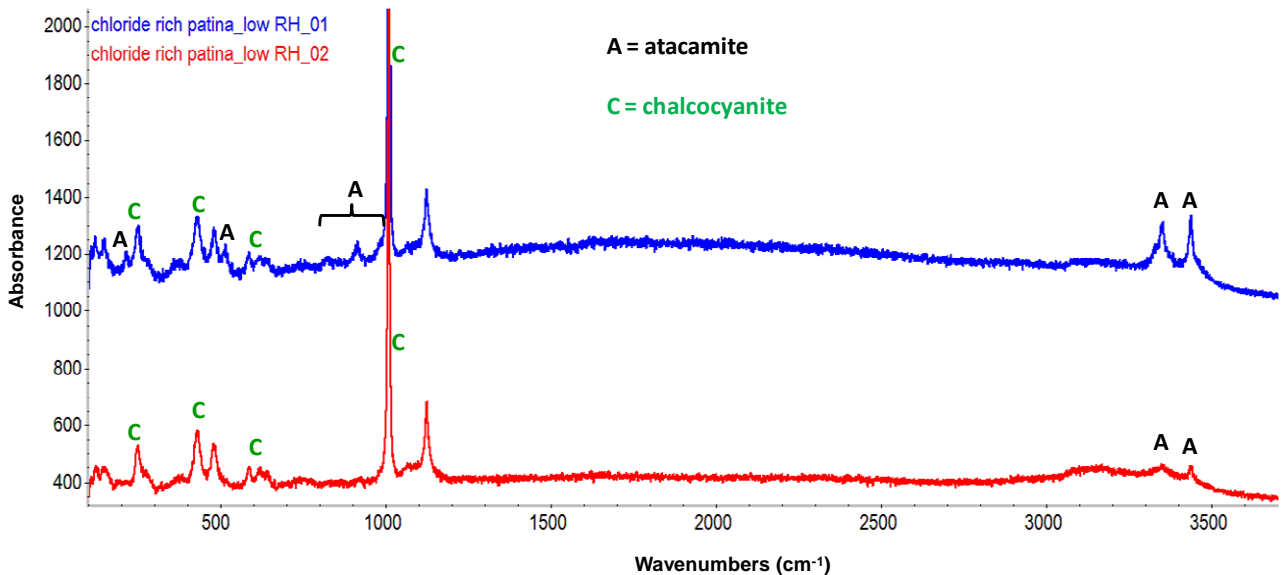


**Figure 12: Raman spectra (two different point of the sample) of chloride rich patina kept at low relative humidity.**

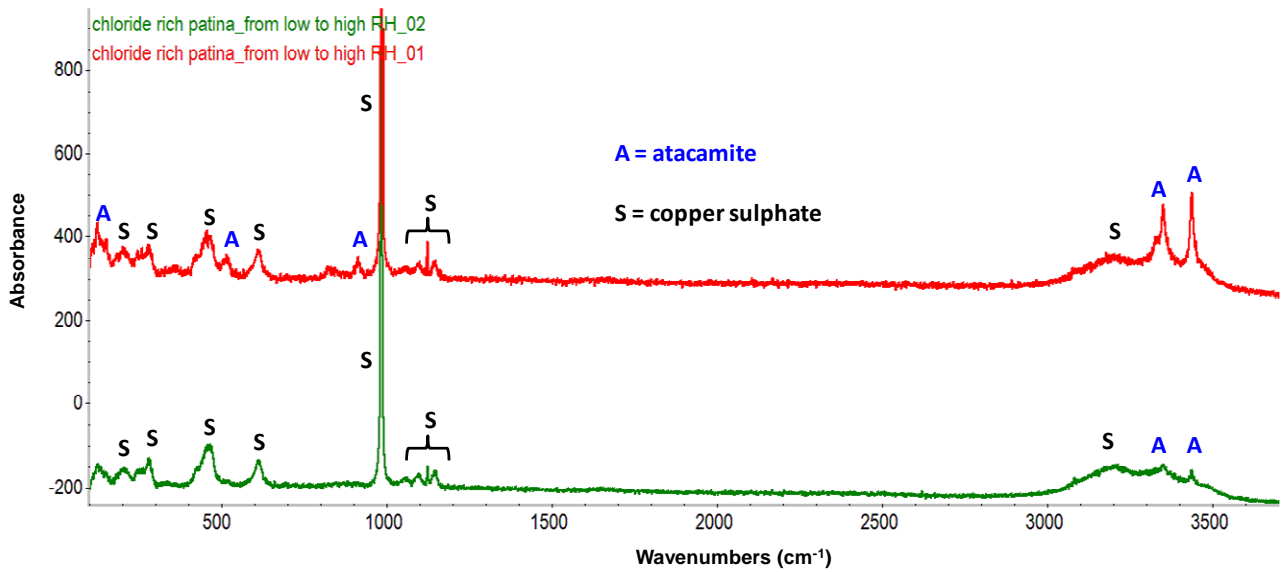


Figure 13: Raman spectra (two different point of the sample) of chloride rich patina kept at low relative humidity and then at high relative humidity for 24 hours.

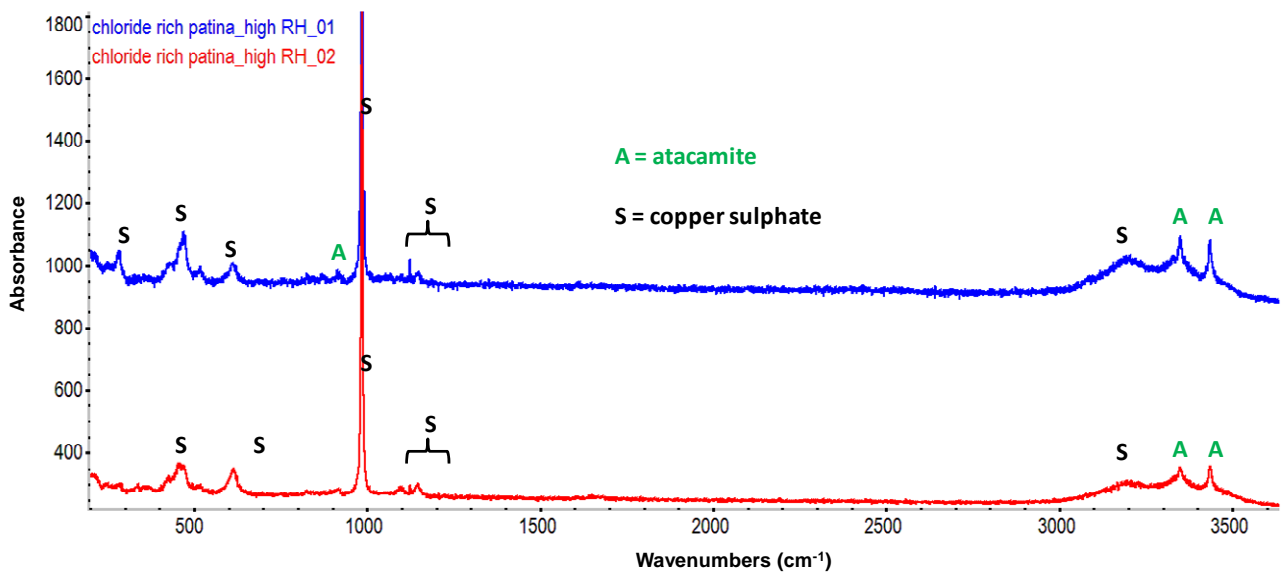


Figure 14: Raman spectra (two different point of the sample) of chloride rich patina kept at high relative humidity.

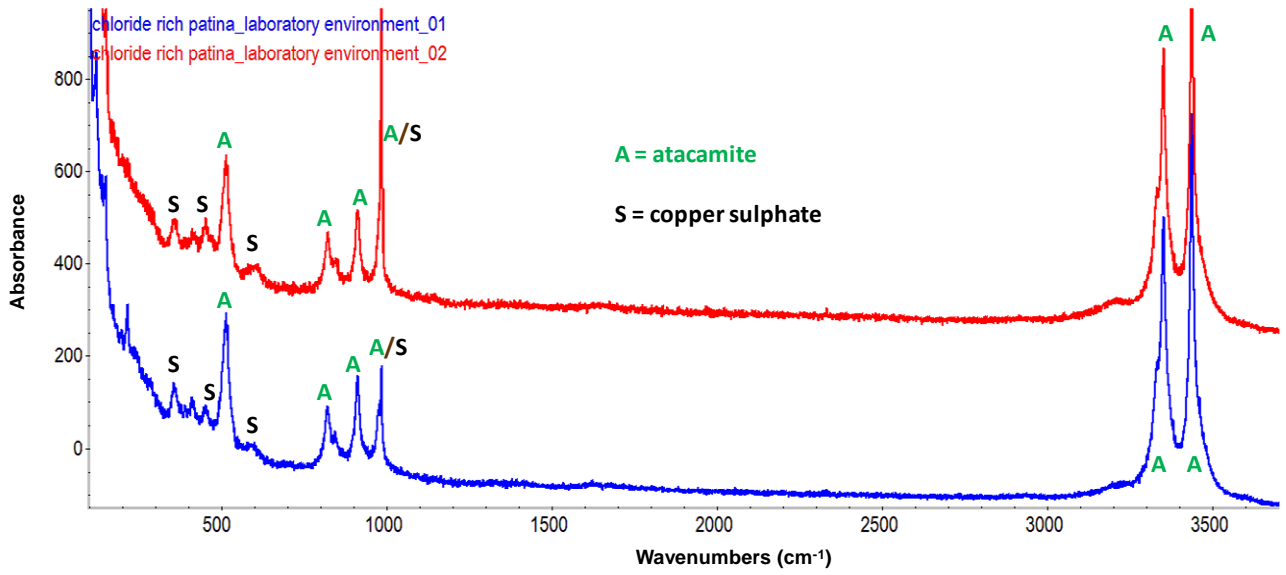


Figure 15: Raman spectra (two different point of the sample) of chloride rich patina in laboratory environment.

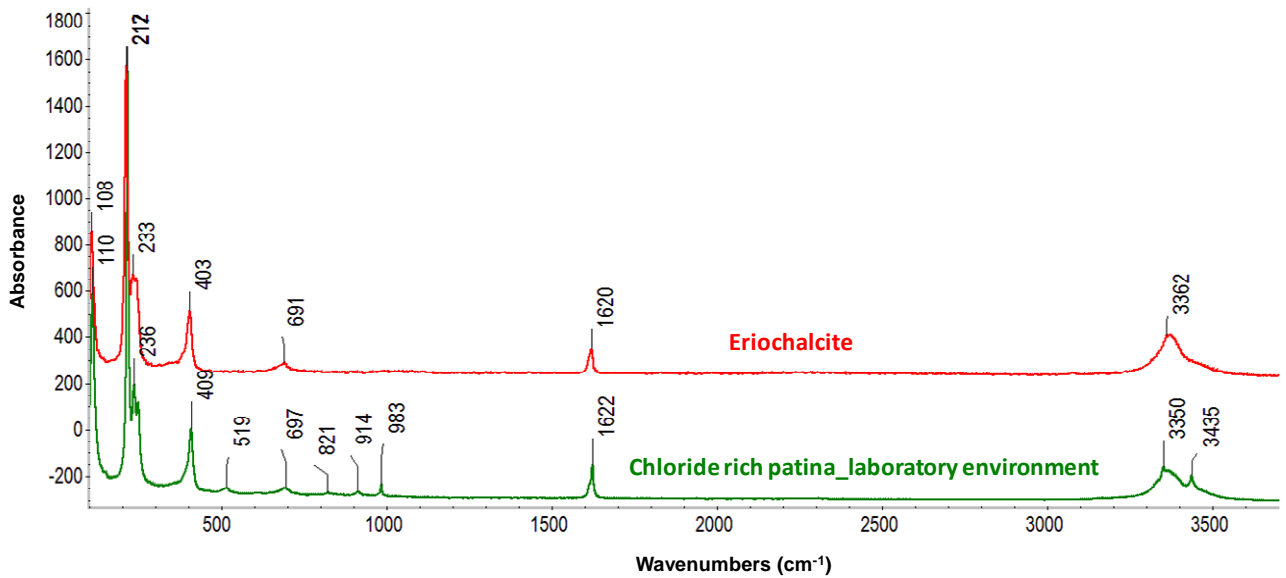
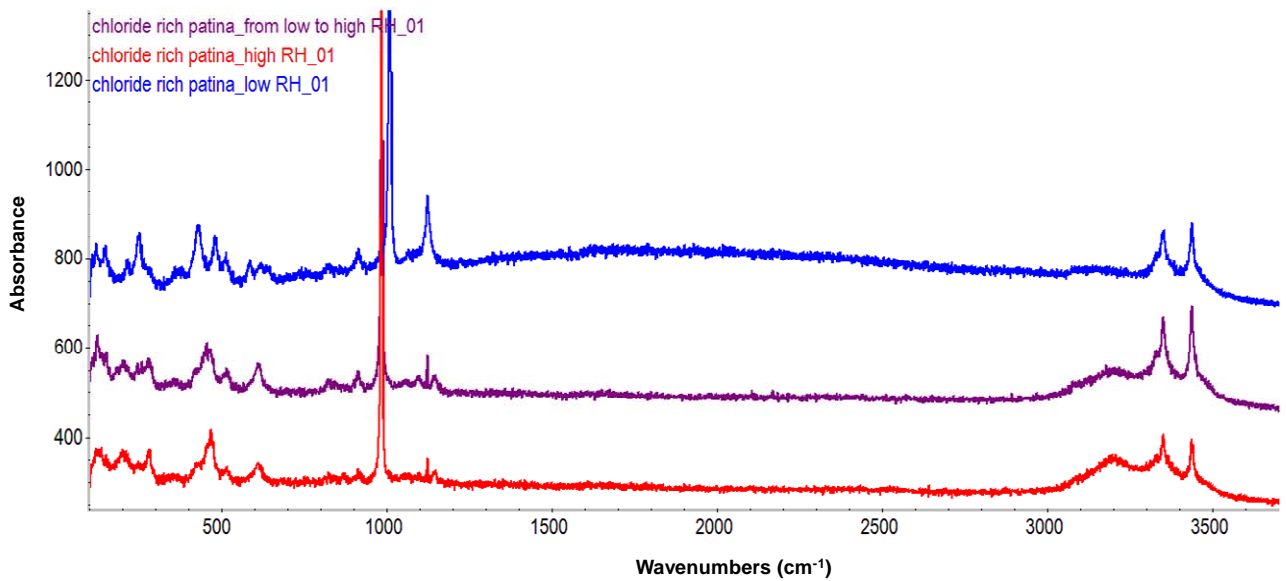


Figure 16: Raman spectrum recorded on a needle-shaped crystal on the chloride rich patina in laboratory environment, compared with eriochalcite Raman spectrum.



**Figure 17: comparison between Raman spectra of chloride rich patina kept at low relative humidity, high relative humidity and first at low relative humidity and then for 24 hours at high relative humidity.**

Brochantite patina

Concerning brochantite patina, no differences between the samples kept in various relative humidity environments have been noticed, either in the general aspect of the patina or in the spectra, as observed in Figure 18. This result confirm that brochantite is stable regarding relative humidity variations. The spectra acquired on brochantite patinas (Figure 19 and 20) correspond to the references found in literature [3-4, 6-7]. The peaks attributions are reported in Table 2.

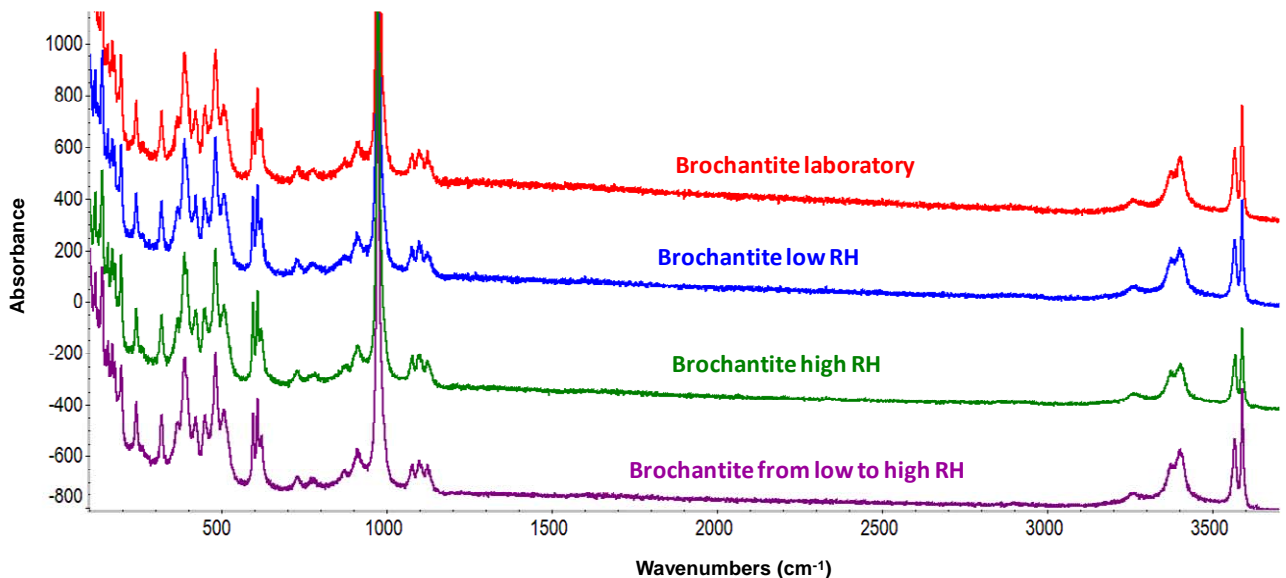


**Figure 18: Comparison between Raman spectra of brochantite patinas in different relative humidity conditions.**

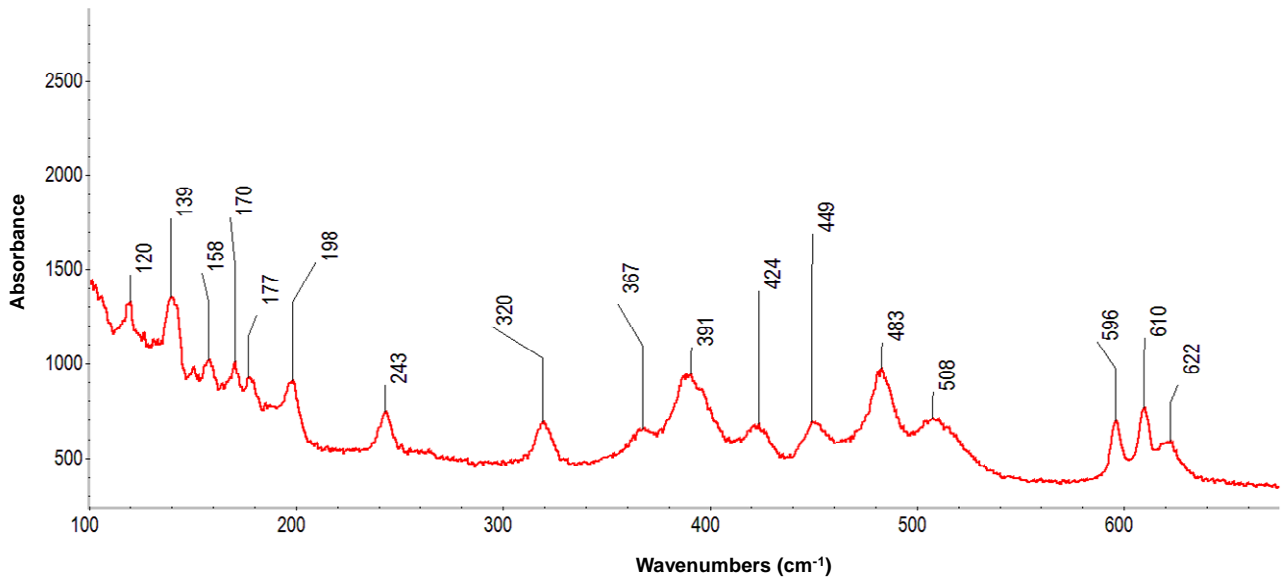


**Figure 19: Raman spectra of brochantite patina – spectral range 100–670  $\text{cm}^{-1}$ .**

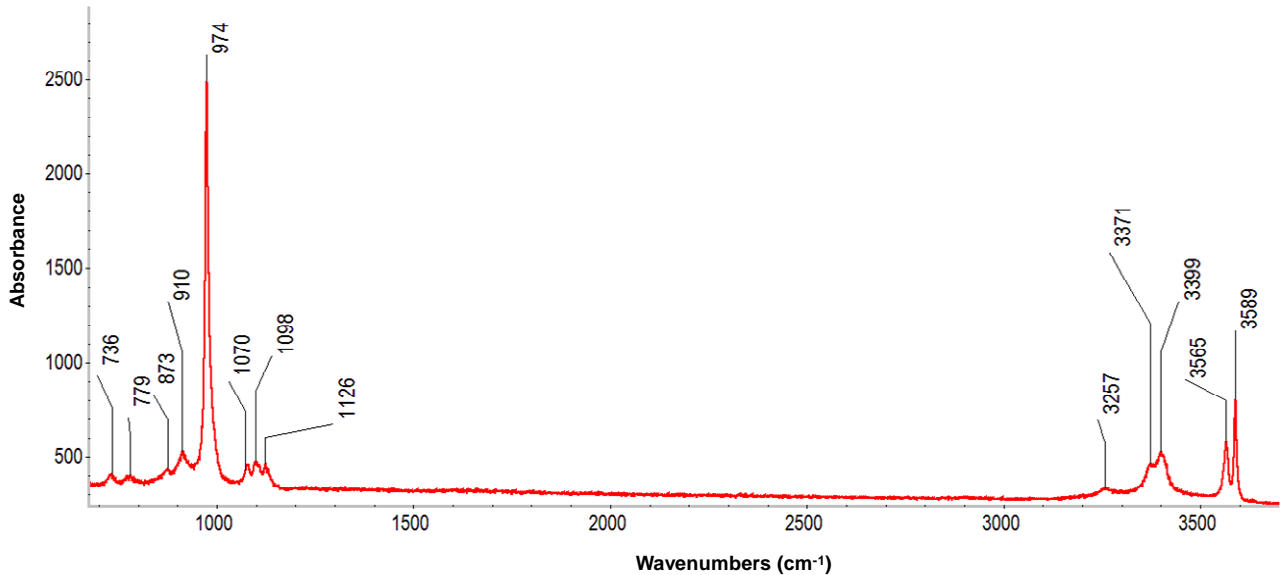


**Figure 20: Raman spectra of brochantite patina – spectral range 670–3700  $\text{cm}^{-1}$ .**

The results of these observations and analysis allow to conclude that the patina chosen for the preparation of galvanic sensors for the monitoring of corrosion rate of gilded bronze is really reactive to relative humidity variations. Extreme relative humidity conditions both too high and too low, can cause chemical modification in the patina and reduce the durability of the sensors. Patinas mainly constituted by brochantite confirmed to be quite stable to relative humidity variations.

**Table 2: Peak attribution of the samples of brochantite patina analyzed by Raman spectroscopy compared to the standard reference.**

	<b>Brochantite – sample analysed</b>	<b>Brochantite – reference [4]</b>
V <sub>OH</sub>	3589	3585
	3565	3563
	3399	3398
	3371	3369
	3257	3252
V <sub>SO4=</sub> asymm	1126	1126
	1098	1097
	1070	1076
V <sub>SO4=</sub> symm	974	974
	910	911
OH deformations	873	872
	779	777
	736	730
$\delta_{\text{SO4=}}$	662	
	610	611
	596	597
V <sub>CuO</sub>	508	506
	483	483
	449	449
	424	429
	391	389
	367	366
	320	319
	243	243
	198	195
	177	177
	170	171
$\delta_{\text{O-Cu-O}}$	158	160
	139	143
	120	123

## References

- [1] Shreir L.L., R.A. Jarman, G.T. Burstein, **Corrosion**, Butterworth Heinemann (1994) Volume 1 section 1.1.
- [2] R.L. Frost, P.A. Williams, J.T. Kloprogge, **Raman spectroscopy of the copper chloride minerals nantokite, eriochalcite and claringbullite** – implications for copper corrosion, *Jahrbuch für Mineralogie*, 10 (2003) 433–445
- [3] V. Hayez, V. Costa, J. Guillaume, H. Terryna, A. Hubina, **Micro Raman spectroscopy used for the study of corrosion products on copper alloys: study of the chemical composition of artificial patinas used for restoration purposes**, *Analyst*, 130 (2005), 550–556
- [4] V. Hayez, **Use of micro-Raman spectroscopy for the study of the atmospheric corrosion of copper alloys of cultural heritage**, PhD Thesis, Vrije Universiteit Brussel, Department of Metallurgy, Electrochemistry and Materials Science (2006)
- [5] J.C. Deak, S.T. Rhea, L.K. Iwaki, D.D. Dlott, **Vibrational energy relaxation and spectral diffusion in water and deuterated water**, *J. Phys. Chem. A*, 104 (2000), 4866–4875
- [6] K. Marušić, H. Otmačić-Ćurković, Š. Horvat-Kurbegović, H. Takenouti, E. Stupnišek-Lisaca, **Comparative studies of chemical and electrochemical preparation of artificial bronze patinas and their protection by corrosion inhibitor**, *Electrochimica Acta* 54 (2009) 7106–7113
- [7] V. Hayez, J. Guillaume, A. Hubin, H. Terryn, **Micro-Raman spectroscopy for the study of corrosion products on copper alloys: setting up of a reference database and studying works of art**, *Journal of Raman Spectroscopy*, 35 (2004), 732–738





## 5. Conclusions

During this PhD work some issues related to the conservation of bronze and gilded bronze artefacts have been addressed. In particular the following aims were pursued:

- Providing quantitative data for the choice of the best display solution for the “Porta del Paradiso”.
- Development of a methodology for the accelerated artificial ageing of gilded bronze specimens.
- Development of galvanic sensors for the monitoring of the corrosion rate of gilded bronzes.
- Preparation of artificial patinas simulating natural corrosion products of copper alloys.
- Evaluation of the stability of the artificial patinas under different environmental conditions.

### Electrochemical artificial ageing of gilded bronzes

Initially, in order to select the best display solution for the “Porta del Paradiso”, the colleagues of the Opificio delle Pietre Dure di Firenze had realised a series of specimens of gilded bronze, with the same alloy and the same gilding technique used for the door. It was then necessary develop a method to artificially age the samples. Several tests were performed in order to define the suitable electrolytic solution and the appropriate current density to be applied. A new methodology was set up that consists in:

- Realisation of tiny incisions of the gilding in order to localize the corrosion in correspondence with the incisions and to obtain a reproducible growth of the corrosion products.
- Immersion of the gilded bronze sample in a solution containing sodium chloride (2 g/L) and sodium sulphate (4 g/L).
- Application of 1 A/m<sup>2</sup> anodic current density for 5 days, followed by 0.1 A/m<sup>2</sup> anodic current density for 2 days.

The method developed allows the growth of corrosion products between the gold and the bronze, in selected areas of the samples. The number and extension of the corroded areas may be adjusted by varying the number and the dimension of the incisions. The obtained result is quite similar to the actual conditions of some parts of the “Porta del Paradiso” both in terms of composition of corrosion product as well as morphology of the corroded areas.

### Selection of the best display option for the “Porta del Paradiso”

Galvanic sensors, i.e. electrochemical cells, simulating corroded gilded bronzes, that allow the obtaining of quantitative data concerning the corrosion rate have been developed and realised for the selection of the best display option for the “Porta del Paradiso”.

The produced sensors have been used for monitoring the corrosion rate at the Opificio delle Pietre Dure laboratories, from May 2009 to May 2010. Three different sections of the artwork created by Lorenzo Ghiberti have been exposed together with three galvanic sensors in three different conditions: a sealed box purged by nitrogen, a sealed box with controlled and low values of relative humidity, and an open showcase with a controlled microclimate in the immediate proximity of the artefact surface.

The galvanic sensors proved to be a very useful tool because the measured macrocouple current between gold and bronze can be correlated, using Faraday’s law, to the corrosion rate. Additionally, they proved to be very reactive to relative humidity variations as it was expected .

By comparing the results of the measured macrocouple current, it was possible to conclude that: there are no significant differences between a showcase saturated with nitrogen or under low and controlled relative humidity. Nevertheless, the sensors kept in the nitrogen environment reveals to be more sensitive and easily damageable in case of subsequent relative humidity increase after the exposure, as a drawback. The open showcase significantly reduces the corrosion rate, but it is less efficient than the other two closed cases. This is mainly due to an insufficient reduction of the relative humidity. If improved, i.e. with a relative humidity constantly maintained below 20%, it could be as protective as the other two closed showcases.

### Development of galvanic sensors for the monitoring of the corrosion rate of gilded bronzes

The results obtained with the galvanic sensors for the selection of the optimal display option of the “Porta del Paradiso” were quite encouraging. However these sensors, presented several problems and they needed to be improved. They presented a very low durability and the values of macrocouple current were not enough reproducible, since the variations between different sensors reached more than two order of magnitude. The reasons for these unsatisfactory performances have been analysed in depth and a new procedure has been developed.

The principal differences of the new sensors were the use of a gold leaf instead of sputtering as a gilding technique and the artificial patina that was thinner and more homogenous. For this reason these samples were named “Gold leaf sensors”. Furthermore the stratigraphy of the preliminary gold leaf galvanic sensors with chloride rich patina, has been modified, by adding a cuprite (copper oxide) layer between the bronze and the patina, to improve the adhesion between the two layers.

The water/powder ratio of the paste has been changed and the quantity of powder per cm<sup>2</sup> has been reduced, in order to obtain a thinner layer of patina. The use of the gold leaf for the gilding allows to obtain a more thick, resistant and uniform layer of gold respect to the sputtering technique.

These sensors proved to be more reproducible since the variability of macrocouple current supplied by each sensor remained in one order of magnitude. Also their durability was significantly increased.

Sensors with patina of different compositions have been realised in order to simulate bronzes that present different conservation conditions. The so-called chloride rich patina represents the case of a very unstable artefact, heavily contaminated by chlorides, such as the “Porta del Paradiso”. The brochantite patina instead should represent a less problematic situation from a conservative point of view. The developed galvanic sensors can be used both for monitoring the corrosion rate of real objects and for testing new conservation or cleaning procedures.

#### Preparation of artificial patinas for the realisation of galvanic sensors

The patina for the realisation of the galvanic sensors had to fulfil a series of important and specific requirements, such as: 1 – composition similar to the real cases, 2 – adequate thickness, 3 – good homogeneity, 4 – good adhesion to the substrate, 5 – adequate electrical resistance.

All along this project, several kind of artificial patination have been tested. Chemical patination and electrochemical patination have been rejected because the patinas obtained were too inhomogeneous and not thick. It was necessary to develop a new methodology that was derived from the so called “applied paste method”. The proposed methodology consists in realising the spreading on the metallic surface of a paste composed by a mixture of selected copper salts. The applied paste method allows to obtain patinas of desired composition and thickness. The patinas obtained have been characterized thoroughly using different analytical techniques to verify their composition.

The artificial patinas prepared have been subsequently used to produce galvanic sensors mimicking corroded gilded bronzes and used to monitor the corrosion rates.

#### Evaluation of the stability of the patinas

As well as its composition, the patina stability is a very important parameter for all bronze artefacts. Quite often, the studies on metallic artefacts focus mainly on the corrosion rates, whereas also the stability of the patina is crucial for the stability of the artwork itself, in particular in the case of gilded bronzes. In this work, the stability of the realised artificial patinas has been tested under different environmental conditions. It has been found that a too low relative humidity may be

dangerous for corroded artworks, in particular in presence of chlorides compounds. The patina, indeed, becomes more brittle and extremely reactive to subsequent relative humidity variations. Moreover it has been found that the thickness of the patina is a crucial parameter for the stability under different conditions of relative humidity.

## ACKNOWLEDGEMENTS

Questi 3 anni sono volati per un certo verso e mi sono sembrati un'eternità per un altro. La mia vita è cambiata parecchio in questo lasso di tempo. Ho conosciuto persone meravigliose, fatto esperienze straordinarie, imparato un milione di cose. Come tutte le esperienze, è giunta alla fine e ho quindi l'opportunità, ancora una volta, di ringraziare le persone che più mi sono state vicine, mi hanno aiutata e supportata.

Un grazie in particolare:

- *Alla dottoressa Paola Fermo, che ha dato il via a questa mia avventura e mi ha sempre sostenuta fino alla fine. Con l'augurio che ci possano essere in futuro altre occasioni per lavorare insieme.*
- *Alla dottoressa Sara Goidanich, per avermi spronata e guidata in questi 3 anni nel mondo della corrosione dei manufatti metallici e per la pazienza dimostrata durante la scrittura di questa tesi.*
- *Alla Professoressa Lucia Toniolo, per avermi accolta nel suo gruppo di ricerca, per avermi dato fiducia e aperto le porte dei suoi laboratori.*
- *Ai colleghi dell'Opificio delle Pietre Dure, per la disponibilità e il supporto tecnico durante il monitoraggio della Porta del Paradiso. E a tutti gli altri colleghi coinvolti nel progetto.*
- *Ai miei compagni di avventura @PoliMi: a Davide in particolare, perché la nostra amicizia va al di là dei meri rapporti di lavoro; a Francesca, perché nonostante le incomprensioni siamo riuscite a sopravvivere nello stesso ufficio per 3 anni; a Margherita, per il suo stile; a Daniela, perché il suo aiuto e la sua simpatia sono stati utilissimi negli ultimi mesi.*
- *A tutto il personale del Politecnico di Milano con cui ho avuto il piacere di lavorare:*
  - *A Luigi Brambilla, per le analisi Raman*
  - *A Dario Picononi per le indagini SEM-EDX*
  - *A Mattia Ronchi per le diffrazioni e la lucidatura dei campioni*
  - *A Mario e Giorgio, per il taglio di innumerevoli lastre di rame e per la costruzione della preziosissima sonda per misure elettrochimiche in situ*
- *Ai colleghi del dipartimento CMC: Alessandro, Andrea, Nicola, Federica, Maria Vittoria, Silvia, Max. Ad Antonello per i consigli preziosissimi sull'ES. Un ringraziamento particolare a Massimo, per le lunghe chiacchierate, lo scambio di strumenti e aiuti, la nichelatura della foglia d'oro... ci vedremo in giro per le strade della Brianza o della Svizzera.*
- *Ai miei compagni di dottorato: a Federica, in particolare, insieme fino alla discussione finale... sono certa che sentirò parlare di te d'oltreoceano; a Luca, dottorando milanese solo d'adozione, per le chiacchierate e le colazioni insieme; a Lena, Marta e a tutti gli altri dottorandi del XXIV ciclo di Scienze Chimiche e Chimica Industriale.*

- *A tutti i tesisti con cui ho avuto il piacere di lavorare: Elisa (2 volte... questo è masochismo!), Michele, Davide, Silvia, Tommaso, Francesca, perché il vostro aiuto è stato prezioso.*
- *Al laboratorio di Paola @UniMi, e in particolare ad Andrea, per le collaborazioni e i continui scambi di opinione che durano ormai da anni e anni... e a tutti quelli che da quel laboratorio sono passati, in particolare, Monia, Francesca, Ugo, Marzia.*
- *A Paola Letardi, per la sua disponibilità, per i consigli fondamentali per la costruzione della sonda per l'ES, per l'entusiasmo che mette nel suo lavoro nonostante tutte le difficoltà di fare ricerca in Italia.*
- *All' ARG, perché dimostra che ci sono ancora "giovani" in Italia entusiasti del loro lavoro di ricerca.*
- *Alla Corale Controcanto, per aver allietato i miei mercoledì sera e per i vari concerti in giro per la Lombardia.*
- *Agli amici "dei cani", Donatella, Patrizia, Paolo, Livio, Raffaella, per le pizzate e le chiacchierate.*
- *Ai miei amici più cari dispersi per il mondo, senza il cui supporto morale sarebbe stato sicuramente molto più difficile arrivare a questo risultato: a Jennifer, perché la nostra amicizia nata per caso è cresciuta fino a diventare quello che è ora... ma ricorda: "Io non parlo con gli sconosciuti"; a Giuseppe, perché riusciamo sempre a trovare il modo di tenerci in contatto e di vederci; a Marzia, per la nostra amicizia che dura ormai da 23 anni (e un bacio a Daniele); a Susi, la mia crucca - romana preferita (e un bacio a Valerio); a Frances, Martin, Natanael, Leah e Ewa, la mia famiglia svedese, perché so che ci sarà sempre un posto per me a casa vostra; a Laura e Francesca, per la nostra amicizia nata tra i banconi del laboratorio; agli amici dottorandi sparsi per l'Europa: Federico, Francesco e Alessandro.*
- *Alla mia famiglia, a 2 e 4 zampe:*
  - *A mia mamma e mio fratello, perché mi supportano e sopportano in ogni situazione.*
  - *Ai miei parenti (in ordine sparso): zia Gigia, zia Donata, zio Maurizio, Anna, Arianna, zia Enrica, Silvia, Chiara, Giulia, Letizia, etc. etc., perché so che posso sempre contare sul loro aiuto.*
  - *A Tara, Smeagol e Lamù, per il loro affetto incondizionato.*
- *Last but not least (for sure)... To Christophe, who came into my life suddenly, and that sustained, supported and cuddled me during the writing of this thesis ... I would not have done it without you!*